Etablierung und Evaluierung eines auf Mikrogeweben basierenden Knochengewebes

Inaugural-Dissertation

zur Erlangung des Doktorgrades
der Mathematisch-Naturwissenschaftlichen Fakultät
der Heinrich-Heine-Universität Düsseldorf

vorgelegt von

Fabian Langenbach
aus Siegburg

Düsseldorf, Juni 2012

aus der Klinik für Mund-, Kiefer- und Plastische Gesichtschirurgie
der Heinrich-Heine Universität Düsseldorf

Gedruckt mit der Genehmigung der
Mathematisch-Naturwissenschaftlichen Fakultät der
Heinrich-Heine-Universität Düsseldorf

Referent: PD Dr. Dr. Jörg Handschel

Korreferent: Prof. Dr. Thomas Klein

Tag der mündlichen Prüfung: 17. Dezember 2012

Die vorliegende Arbeit ist eine

kumulative Dissertation

gemäß § 6 Promotionsordnung der Mathematisch-

Naturwissenschaftlichen Fakultät der Heinrich-Heine-Universität Düsseldorf

zur Verleihung des Grades „Dr. rer. nat.“

Sie besteht aus 6 erschienenen Originalarbeiten, einem eingereichten Übersichtsartikel, einem Übersichtsartikel zur Einordnung der Arbeiten in einen größeren wissenschaftlichen Kontext, einer Zusammenfassung, einer Einleitung sowie einem Fazit und einem Ausblick.

Publikationen zur Dissertation

Die kumulative Dissertation umfasst 6 Originalarbeiten sowie zwei Übersichtsartikel die große Teile der Originalarbeiten mit der Literatur in Zusammenhang bringen. Alle bereits erschienenen Arbeiten sind in internationalen peer reviewed Zeitschriften, mit überdurchschnittlichem Einfluss auf ihrem Themengebiet, erschienen (siehe Deckblätter der jeweiligen Publikation ab Seite 18).

* = gleicher Beitrag zur Publikation; # = korrespondierender Autor

Originalarbeiten:

[1] **Langenbach, F.**, Naujoks, C.#, Kersten-Thiele, P.V., Berr, K., Depprich, R.A., Kubler, N.R., Kogler, G., and Handschel, J. (2010). Osteogenic differentiation influences stem cell migration out of scaffold-free microspheres. Tissue Eng Part A *16*, 759-766.

Mein Anteil an der Publikation: ca. 90% der Versuche und 90% der schriftlichen Arbeit

Impact Factor: 4,636

[2] **Langenbach, F.***, Berr, K.*, Naujoks, C.#, Hassel, A., Hentschel, M., Depprich, R., Kubler, N.R., Meyer, U., Wiesmann, H.P., Kogler, G., and Handschel, J. (2011). Generation and differentiation of microtissues from multipotent precursor cells for use in tissue engineering. Nat Protoc *6*, 1726-1735.

Mein Anteil an der Publikation: ca. 60% der Versuche und 30% der schriftlichen Arbeit

Impact Factor: 8,363

[3] Lammers, L., Naujoks, C.#, Berr, K., Depprich, R., Kubler, N., Meyer, U., **Langenbach, F.**, Luttenberg, B., Kogler, G., Wiesmann, H.P., and Handschel J. (2012). Impact of DAG stimulation on mineral synthesis, mineral structure and osteogenic differentiation of human cord blood stem cells. Stem Cell Res *8*, 193-205.

Mein Anteil an der Publikation: ca. 10% der Versuche und 10% an der schriftlichen Arbeit

Impact Factor: 3,338

[4] Naujoks, C., **Langenbach, F.**#, Berr, K., Depprich, R., Kubler, N., Meyer, U., Handschel, J., and Kogler, G. (2011). Biocompatibility of osteogenic predifferentiated human cord blood stem cells with biomaterials and the influence of the biomaterial on the process of differentiation. J Biomater Appl *25*, 497-512.

Mein Anteil an der Publikation: ca. 70% der Versuche und 20% der schriftlichen Arbeit

Impact Factor: 2,246

[5] **Langenbach, F.**, Naujoks, C.#, Laser, A., Kelz, M., Kersten-Thiele, P., Berr, K., Depprich, R., Kubler, N., Kogler, G., and Handschel, J. (2012). Improvement of the cell-loading efficiency of biomaterials by inoculation with stem cell-based microspheres, in osteogenesis. J Biomater Appl *26*, 549-564.

Mein Anteil an der Publikation: ca. 35% der Versuche und 90% der schriftlichen Arbeit

Impact Factor: 2,246

[6] Handschel, J., Naujoks, C.#, **Langenbach, F.**, Berr, K., Depprich, R.A., Ommerborn, M.A., Kubler, N.R., Brinkmann, M., Kogler, G., and Meyer, U. (2010). Comparison of ectopic bone formation of embryonic stem cells and cord blood stem cells in vivo. Tissue Eng Part A *16*, 2475-2483.

Mein Anteil an der Publikation: ca. 35% der Versuche und 35% der schriftlichen Arbeit

Impact Factor: 4,636

Übersichtsartikel:

[7] **Langenbach, F.**, Naujoks, C.# Berr, K., Smeets, R., Depprich, R., Stamm, T., Schwartz, F., Kubler, N.R. and Handschel, J. (2012). Effects of dexamethasone, ascorbic acid and β-glycerophosphate in the osteogenic differentiation of stem cells. Stem Cells Reviews and Reports. Überarbeitete Version wurde eingereicht

Mein Anteil an der Publikation: ca. 90 % der schriftlichen Arbeit

Impact Factor: 3,766

[8] **Langenbach, F.**, Naujoks, C.# Smeets, R., Berr, K., Depprich, R., Kubler, N.R. and Handschel, J. (2012). Scaffold-free microtissues: differences to monolayer cultures and their potential in bone tissue engineering. Clin Oral Invest. Akzeptiert

Mein Anteil an der Publikation: ca. 90 % der schriftlichen Arbeit

Impact Factor: 2,25

Gesamtsumme der Impact Factor Punkte: 31,481

Inhaltsverzeichnis

Zusammenfassung

Große nicht selbstständig heilende Knochendefekte und kleinere schlecht oder langsam heilende Defekte machen therapeutische Maßnahmen zur Knochenregeneration oder zum Knochenaufbau notwendig. Als Alternative zu klassischen Therapien wird dem osteogenen Tissue Engineering (TE) großes Potential beigemessen. Zur Herstellung von TE-Knochentransplantaten (TEKT) *in vitro* werden in der Regel multipotente Stammzellen in der zweidimensionalen (2D) Zellkultur herangezüchtet und vor der Implantation mit einem geeigneten Gerüst kombiniert. Wachstumsraten, Differenzierungsverhalten und Transkriptionsprofile haben jedoch gezeigt, dass Zellen in dreidimensionalen (3D) Zellkulturen deutlich ähnlichere Eigenschaften verglichen mit Zellen *in vivo* aufweisen. Daher war das Ziel dieser Arbeit die Entwicklung, Analyse und präklinische Anwendung eines TEKT auf Basis von 3D Mikrogeweben (MG) in Kombination mit einem geeigneten Biomaterial.

Multipotente unrestringierte somatische Stammzellen aus humanem Nabelschnurblut wurden zu sphärischen osteogenen MG differenziert, die schneller als 2D Kulturen mineralisierten. Dabei zeigte sich, dass die MG auch ohne die Zugabe von osteogenen Wachstumsfaktoren spontan osteogen differenzierten. Bevor jedoch osteogene MG für das TE verwendet werden konnten, musste sichergestellt werden, dass Zellen aus differenzierten MG in die Umgebung auswachsen können, um zellfreie Bereiche im Gerüst zu kolonisieren. Daher wurden MG einen, zwei drei und fünf Tage osteogenem Medium ausgesetzt und anschließend auf eine Zellkulturoberfläche ausgesetzt. Es zeigte sich, dass mit zunehmender Dauer der osteogenen Vordifferenzierung die Anzahl und die Distanz von auswachsenden Zellen deutlich zurückgingen. Dabei wurde eine optimale osteogene Differenzierung bei gleichzeitiger Erhaltung der Auswuchsfähigkeit für einen Zeitraum von drei Tagen beobachtet. Da die gleichen Effekte auch in Extrazellulärem Matrix (EZM)-Gel bestätigt wurden, lies sich schließen, dass Zellen vermutlich auch *in vivo* in die EZM eindringen können und somit der Besiedelung von Zwischenräumen keine Grenze gesetzt ist [1].

Zwecks der Standardisierung des Herstellungsprozesses, der Bestimmung von Variationsmöglichkeiten in Größe und Kulturdauer, sowie der Etablierung von histologischen und molekularbiologischen Analysemethoden wurde ein detailliertes Protokoll zur osteogenen MG-Kultur erarbeitet. Dabei zeigte sich, dass MG leicht in variablen Größen hergestellt werden können. Wegen gewisser Nachteile in der Spezifizität von Alizarin Rot S und der Von Kossa Färbung zur Detektion des Knochenspezifischen Minerals Hydroxylapatit (HA) wurde ein kommerziell erhältlicher, für die Fluorimetrie entwickelter HA-spezifischer Fluoreszenzfarbstoff für die Histologie adaptiert. Dadurch konnte die Sensitivität der Mineraldetektion in MG sowie in Einzelzellschichten im Vergleich zu herkömmlichen histologische Färbeprotokollen deutlich erhöht werden [2].

Histologische Methoden reichen jedoch für die Bestimmung der genauen Mineralzusammensetzung nicht aus. Mittels Raster- und Transmissions-Elektronenmikroskopie (REM und T EM), Röntgenstrukturanalyse sowie Ramanspektroskopie konnte festgestellt werden, dass sich die Mineralien der osteogen differenzierten (+DAG) und Kontroll-MG (-DAG) signifikant in der Verteilung, Struktur und Zusammensetzung unterschieden. Es fanden sich calcium-defizitäres-HA (CDHA) und amorphes Calciumphosphat (ACP) in den -DAG Geweben und ACP, Octa-Calciumphosphat, (Mg-)Whitlockit, HA und CDHA in den +DAG Geweben. Durch die Zugabe von β-Glycerolphosphat kann es in Kombination mit Apoptose der Zellen zu einer dystrophischen Mineralisierung kommen. Zum Ausschluss falsch positiver Ergebnisse für die Mineralisation konnte mittels TUNEL-Assay die Apoptose von Zellen als Ursache für die Mineralisation ausgeschlossen werden [3].

Um ein geeignetes Biomaterial für das TE zu finden wurden verschiedene Materialien hinsichtlich ihrer Biokompatibilität mit USSC untersucht: multiporöses β-Tricalciumphosphat (β-TCP), uniporöses β-TCP, deproteinierte Spongiosa, demineralisierte Spongiosa (ICBM) und Kollagenschwamm wurden mit Zellen besät und kultiviert. Mittels fluorimetrischer Zellzahlbestimmung und REM konnte ICBM als das Material mit den besten Eigenschaften für die Anhaftung und die Proliferation von USSC bestimmt werden [4].

Daher wurden anschließend ICBM mit MG kombiniert. Durch das Einsetzen von MG in ICBM konnten bis zu 40-mal mehr Zellen auf ein Gerüst gegeben werden als durch Einzelzellbesiedelung möglich gewesen wäre. Zudem konnte ein schneller Auswuchs an Zellen erreicht werden, wodurch in kurzer Zeit Bereiche zwischen den Spongiosabälkchen ausgefüllt wurden [5].

Zur Analyse des osteogenen Potentials von USSC-ICBM- und MG-ICBM-Konstrukten wurden sie in Muskeltaschen auf dem Rücken von Ratten implantiert und die Neubildung von Knochen wurde mittels Computertomographie und Histologie ausgewertet. Das Prinzip der osteogenen Vorbehandlung der Konstrukte basierte dabei auf den Erfahrungen bei den Auswuchsexperimenten. Es zeigte sich ektope Knochenbildung in den USSC-ICBM- und MG-ICBM-Konstrukten, während unbesiedelte ICBM nicht zur Bildung von Kochen beitrugen [6].

Zum besseren Verständnis der Mechanismen in der osteogenen Differenzierung von Stammzellen unter dem Einfluss von Dexamethason (DEX), Askorbinsäure (ASC) und β-Glycerolphosphat (β-GLY), wurde auch eine Literaturstudie angefertigt. Es scheint, dass DEX Stammzellen zur Differenzierung treibt, welche dann dur ch ASC und β-GLY in die Osteogenese gelenkt wird. DEX induziert die osteogene Differenzierung durch eine Hochregulation von TAZ (transcriptional co-activator with PDZ-binding motif), welches mit dem Master Transkriptionsfaktor Runx2 interagiert. Zusätzlich wird die Runx2 Aktivität durch

die DEX-induzierte Hochregulation der Mitogen-aktivierten-Protein-Kinase(MAPK)-Phosphatase (MKP-1) reguliert. ASC trägt zur osteogenen Differenzierung als Ko-Faktor in der Kollagen Typ I Synthese bei, wodurch der Aufbau einer osteogenen EZM und somit die osteogene Differenzierung beschleunigt wird. Das Phosphat in β-GLY wird in HA ($Ca_{10}(PO_4)_6(OH)_2$) eingebaut und dringt zusätzlich in die Zelle ein, wo es durch Phosphorylierung der „Extracellular signal related Kinase (ERK)“ zur Expression von vielen verschiedenen Knochenproteinen beiträgt [7].

Um die oben genannten Arbeiten in den literarischen Kontext des jetzigen Forschungsstandes einzuordnen wurde eine Literaturstudie durchgeführt und ein Review angefertigt. Dabei wurden unter Anderem drei mögliche Ursachen für die beschleunigte und die spontane osteogene Differenzierung der MG ermittelt. Erstens trägt vermutlich der 3D-Kontakt zu EZM-Proteinen zur Differenzierung bei. Dabei übertragen Integrine extrazelluläre Reize mittels fokaler Adhäsionskinase an den MAPK Signalweg, wodurch Runx2 phosphoryliert wird und es zur Expression von osteogenen Proteinen kommt. Ein zweiter Grund ist die hohe Zelldichte innerhalb der MG. Durch den engen Kontakt der Zellen zueinander können parakrine osteogene Faktoren besser zur Osteogenese beitragen als bei vereinzelten Zellen. Drittens führen autokrine BMP2 Signale zu einer verstärkten Osteogenese. Durch die dreidimensionale Kultur von Stammzellen aus dem Knochenmark kommt es sowohl in osteogenem Medium als auch in Kontrollmedium zu einer vielfach höheren BMP2 Expression, die anschließend zu einer erhöhten Expression von Collagen Typ I, Runx2 und weiteren osteogenen Proteinen führt [8].

Zusammenfassend lässt sich sagen, dass osteogene MG verbesserte *in vivo* ähnlichen Bedingungen aufzeigen und ihre schnelle Differenzierung, sowie die präzise Applizierbarkeit bedeutende Vorteile gegenüber 2D Zellkulturen bieten. Mit MG kann die Effizienz bei dem Beimpfen von Gerüsten verbessert und die Anzahl von Zellen im Gerüst deutlich erhöht werden. Darüber hinaus verringern MG sowohl beim Tissue Engineering als auch bei gerüstfreien Zelltherapien die Gefahr des Auswaschens und der ungewünschten Verteilung der Zellen. Mit der Fähigkeit zur ektopen Knochenbildung *in vivo* bilden Kombinationen aus MG und geeigneten Gerüsten wie ICBM einen höchst vielversprechenden Ansatz zur Rekonstruktion von großen Knochendefekten.

Summary

Large bone defects that do not heal spontaneously and smaller slow-healing defects necessitate therapeutic measures for bone regeneration or bone augmentation. As an alternative to classic therapies, osteogenic tissue engineering (TE) is regarded as a promising technology for bone regeneration. As a standard procedure multipotent stem cells are incubated in two-dimensional (2D) cell cultures before they are combined with scaffolds, to form a TE bone graft (TEBG) that is implanted. However, analysis of growth rates, differentiation characteristics and transcription profiles revealed that cells in a 3D-environment have similar properties to cells *in vivo*. Therefore, the aim of the work was the development, analysis and preclinical application of a TEBG based on 3D microtissues (MTs) in combination with a suitable biomaterial.

Multipotent human stem cells from umbilical cord blood (USSC) have been differentiated to spherical osteogenic MTs, which mineralized faster than 2D cell cultures. Moreover, also control microspheres that have been treated without osteoinductive agents mineralized spontaneously. However, prior to the use of MTs for TEBGs, it had to be ensured that cells are able to migrate out of osteogenic differentiated MTs to colonize spaces in the scaffold. For this purpose, MTs were treated for one, two, three and five days with osteogenic medium and afterwards were seeded on a cell culture surface. It was found that with increasing duration of osteogenic predifferentiation the number and distance of outgrowing cells constantly decreased. The optimum duration for an osteogenic predifferentiation, while retaining the ability of cells to migrate out of the MT, was found to be 3 days. Since the same effect was found in extracellular matrix (ECM)-gel, it was concluded that probably also cells *in vivo*, have the ability to migrate into the surrounding and to fill up cell free spaces [1].

In order to standardize the generation process, a detailed protocol for the osteogenic differentiation of MTs cultures was established. This method allowed for defining the variability in size and culture period, as well as for the establishment of histological and molecular biologic analysis. It was found that MTs of variable but defined sizes can be generated. Due to disadvantages in the specificity of alizarin red S and Von Kossa stain for the detection of the bone specific mineral hydroxylapatit, a commercially available hydroxylapatit-specific fluorescent dye was adapted for histology. This method provided higher sensitivity in the mineral detection in MTs and in mono-layers compared to standard histological stains [2].

For the exact determination of the mineral content histological methods are not sufficient and cannot discriminate between dystrophic and bone specific mineralization. Through scanning electron microscopy (SEM), and transmission electron microscopy (TEM), energy dispersive x-ray spectroscopy and Raman spectroscopy, it was found that minerals in

osteogenic differentiated (+DAG) and control MTs (-DAG) differ significantly in their distribution, structure and composition. Calcium-deficient hydroxyapatite (CDHA) and amorphous calciumphosphate (ACP) were found in –DAG-microtissues and ACP, octa-calciumphosphate, (Mg)Whitlockit, CDHA and HA were found in the +DAG-microtissues. Dystrophic mineralization after apoptosis of cells inside the MTs could be excluded by TUNEL-assay [3].

For the identification of a suitable biomaterial for osteogenic tissue engineering, various materials were compared with regard to their biocompatibility with USSC: multiporous β-Tricalciumphosphat, (β-TCP), uniporous β-TCP, deproteinized spongiosa, demineralized spongiosa (ICBM) and collagen sponge were seeded with cells and cultivated. Assay-based fluorimetric cell counting and SEM revealed the best results for attachment and proliferation of USSC on ICBM-scaffolds [4].

As a consequence from these findings, ICBM was combined with MTs. When inoculating ICBM with MTs a 40 fold increased cell number could be integrated in one scaffold, in contrast to inoculation with cell suspensions. During subsequent incubation, a fast outgrowth of cells could be observed, that filled spaces between the trabeculae of the scaffold within two weeks [5].

For the investigation of the osteogenic potential of USSC-ICBM- and MT-ICBM-Scaffolds the constructs were implanted into dorsal muscle bags of immuno-compromised rats, and ectopic bone formation was analyzed by computer-tomography and histology. The procedure of the osteogenic pretreatment was based on the results of the outgrowth experiment. It was found that ectopic bone formation was induced in USSC-ICBM- and MT-ICBM-scaffolds, whereas cell free ICBM did not lead to bone formation [6].

In order to understand the mechanisms behind the osteogenic differentiation of stem cells in response to dexamethasone (DEX), ascorbic acid (ASC) and β-glycerophosphate (β-GLY) a detailed review of the literature was performed. DEX seems to induce the differentiation of stem cells, which is then guided by ASC and β-GLY into osteogenesis. DEX induces differentiation by up-regulating TAZ (transcriptional co-activator with PDZ-binding motif), which interacts with the master osteogenic transcription factor Runx2. Moreover, Runx2 activity is regulated by DEX-induced up-regulation of the mitogen-activated protein kinase (MAPK) phosphatase (MKP-1). ASC contributes to osteogenic differentiation through its role as a co-factor in collagen synthesis, which results in the enhanced assembly of an osteogenic ECM and thereby enhances osteogenic differentiation. The phosphate of β-GLY is incorporated into the bone HA, ($Ca_{10}(PO_4)_6(OH)_2$), and also enters the cell where it phosphorylates extracellular signal related kinase (ERK) leading to the expression of many osteogenic genes [7].

In order to relate the publications resulting from this work to their scientific context the recent literature was reviewed. In doing so, three probable reasons that might be responsible for the improved and spontaneous osteogenic differentiation of MTs were determined. First, a 3D-contact to ECM-proteins seems to contribute to the differentiation. In this process integrins transmit extracellular cues via focal adhesion kinases to the MAPK pathway. This results in the phosphorylation of Runx2 which in turn leads to the expression of osteogenic proteins. A second reason could be the high cell density inside the MTs. Due to the close contacts of the cells to each other paracrine osteogenic factors can better unfold their potential compared to cells in monolayers. Third, autocrine BMP2 signals lead to an accelerated osteogenic differentiation. The 3D culture of bone marrow stem cells results in a strong increase in BMP2 expression in osteogenic and control medium, which is followed by an increase in the expression of collagen type I, Runx2 and other osteogenic proteins [8].

In conclusion, MTs offer improved *in vivo*-like conditions for stem cells than 2D cultures resulting in enhanced osteogenic differentiation. MT technology can ameliorate seeding efficiency of biomaterials and can increase the cell load of a scaffold. Furthermore, microtissues reduce the risk of unwanted cellular distribution and wash out in tissue engineering and scaffold free cell therapy. With their capability of ectopic bone formation MT-ICBM-constructs hold promise for facilitated, accelerated and improved bone regeneration.

1 Einleitung

Große Knochendefekte mindern die Lebensqualität von Patienten meist erheblich. Entweder durch eine funktionelle Beeinträchtigung des Bewegungsapparates oder durch ästhetische Abweichungen im Erscheinungsbild der Person. Die häufigsten Ursachen für Knochendefekte sind Traumata aufgrund von Unfällen oder Rohheitsdelikten, Zysten, Osteoporose und die chirurgische Entfernung von Tumoren. Überschreitet ein Knochendefekt eine bestimmte Größe, heilt der Knochen nicht mehr von selbst und man spricht man von einem „Critical Size Defect (CSD)". Bei einem CSD finden dann bspw. die beiden Defektenden nicht mehr zueinander und in die Lücke wächst Bindegewebe ein.

Als Therapie kommen in solchen Fällen meist autologe Knochentransplantate, zum Beispiel aus der Hüfte, zum Einsatz. Häufig ist jedoch diese konventionelle Therapie für die Regeneration des Knochengewebes nicht möglich, da autologer Knochen nur in begrenzter Menge zur Verfügung steht, oder das Risiko des Entnahme bedingten Eingriffs inklusive möglicher späterer Komplikationen zu hoch ist (Sasso et al., 2005). Die Alternative zu autologen Knochen bietet die Verwendung von Biomaterialien allogenen, xenogenen oder alloplastischen Ursprungs. Solche Biomaterialien, auch als Knochenersatzmaterialien oder KEM bezeichnet, können eingesetzt werden um den Knochen zu ersetzen oder die Regeneration des Knochens zu unterstützen. Die Verwendung von KEM kann auch bei Defekten notwendig werden bei denen kein CSD vorliegt. Durch Zahnverlust kommt es, ins besondere im Alter, zu einer Atrophie des Kieferknochens. Durch fehlende Zähne fehlen dem Kieferknochen mechanische Reize, die für eine Erhaltung der Knochensubstanz notwendig sind. Die Verankerung von Implantaten für den Zahnersatz ist in einem solchen Kiefer ohne einen vorherigen Knochenaufbau (Augmentation) oft nicht möglich.

Die festen Bestandteile des Knochens bestehen aus der Kompakta und der Spongiosa. Die Kompakta ist nach dem Zahnschmelz die härteste Struktur des Körpers. Sie gibt die Form des Knochens vor und schütz das Knochenmark. Im Inneren des Knochens geht die Kompakta in die Spongiosa über. Die Spongiosa ist ein dreidimensionales Geflecht von Bälkchen, welche Kräfte, die auf den Knochen einwirken, verteilen. Entsprechend der Belastung unterliegt die Anzahl der Bälkchen und die stärke deren Vernetzung einem ständigen Umbau. Dabei nimmt die Stärke der Spongiosa in Abhängigkeit der Belastung zu oder auch ab. Bei der Herstellung eines KEM orientiert man sich idealerweise an der Struktur des Knochens. Dabei wird in der Regel versucht die spongiöse Struktur des Knochens nachzubilden. Denn diese bietet nicht nur ideale mechanische Eigenschaften, sondern auch Porengrößen die das Einwachsen von Zellen und Blutgefäßen ermöglicht. Daher liegt die Verwendung von aufbereitetem autologen oder xenogenen Knochen nahe; jedoch gilt es dabei die beste Aufbereitungsmethode zu finden. Die vielfältigen gewünschten

Eigenschaften wie Biokompatibilität, Resorbierbarkeit und Osseointegration bis hin zu anwenderbezogenen Eigenschaften wie Modellierbarkeit und Fixierbarkeit durch den Operateur, macht die Suche nach einem perfekten Material schwierig.

Auch wenn ein KEM all diese Eigenschaften hat, dauert ab einer bestimmten Größe die Besiedelung des KEM mit osteogenen Zellen aus der Umgebung zu lange. Außerdem ist eine vollständige Besiedelung mit osteogenen Zellen oft nicht möglich, weil diese in Konkurrenz zu einwachsendem Bindegewebe stehen. In solchen Fällen bieten sich unterstützende Zelltherapien an, bei denen Stammzellen mit einem osteogenen Potential zum Einsatz kommen. Als vielversprechende Therapie werden daher *ex vivo* generierte Knochengewebe angesehen die mittels osteogenem „Tissue Engineering" hergestellt werden (Meyer et al., 2006). Durch die Verwendung von Gerüsten, Zellen und Wachstumsfaktoren können mittels „Tissue Engineering" erzeugte knochenähnliche Gewebe (TEKG) erzeugt werden (Petite et al., 2011).

Stammzellen sind aus verschiedenen Geweben isolierbar und werden aufgrund ihrer Plastizität und hohen Teilungsfähigkeit als vielversprechende Kandidaten für das osteogene Tissue Engineering angesehen. Jedoch gibt es nur wenige Zellarten mit der Fähigkeit zur Bildung von heterotopem Knochen und viele Stammzellarten mit der Fähigkeit zur Bildung von mineralisiertem Gewebe. Viele Studien zeigen, dass nur skelettale Stammzellen aus dem Knochenmark und unrestringierte somatische Stammzellen aus dem Nabelschnurblut (USSC) eine hämatopoetische Mikroumgebung und Knochen *in vivo* bilden können (Kogler et al., 2004; Robey, 2011). Dagegen gibt es nur wenige Beweise für die Unterstützung der Hämatopoese durch multipotente Stammzellen von anderen Orten als aus dem Knochenmark (wie z.B. Fettgewebe und Zahnpulpa) (Bianco et al., 2008; Robey, 2011). Darüber hinaus führt der Zusatz von β-GLY bei vielen Zellen zu einer dystrophischen Mineralisierung, bei der Mineral gebildet wird, das nicht wie im Knochen üblich an Kollagenstrukturen gebunden ist (Bonewald et al., 2003). Zellen, die gar nicht fähig zu einer osteogenen Differenzierung sind, erzeugen dabei knochenuntypisches Mineral welches andere Calcium/Phosphat Verhältnisse aufweist, andere Mineralisationseigenschaften hat und dadurch auch weniger hart und Widerstandsfähig ist als Hydroxylapatit. Wenn in solchen Fällen eine einfache histologische Färbung zur Detektion von Mineral durchgeführt wird, werden viele falsch positive Ergebnisse für eine osteogene Differenzierung erzielt. Findet man für solche Zellen dann noch positive Ergebnisse für eine chondrogene und adipogene Differenzierung, werden sie fälschlicherweise als mesenchymale Stammzellen beschrieben.

Die embryonale Knochenbildung (Ossifikation) wird unterschieden in desmale und enchondrale Ossifikation. Die meisten Knochen werden durch enchondrale Ossifikation gebildet. Dabei entwickeln sich aus mesenchymalen Stammzellen Knorpelvorläuferzellen. Im

nächsten Schritt hypertrophieren die Vorläuferzellen und differenzieren zu Chondrozyten. Anschließend beginnen die Zellen mit einer rapiden Zellteilung und der Sekretion einer knorpelspezifischen EZM. In der darauffolgenden Phase stoppt die Proliferation und die Zellen nehmen dramatisch an Volumen zu, wodurch sie zu hypertrophen Chondrozyten werden. Die großen Chondrozyten verändern dann durch Sekretion von Collagen Typ X und Fibronektin die EZM und bereiten sie dadurch auf die Mineralisation vor. Nachdem dann die hypertrophen Chondrozyten durch Apoptose absterben, sprossen Blutgefäße in die Matrix ein. Zusätzlich wandern Osteoblasten ein, die dem Perichondrium entstammen und sich aus mesenchymalen Stammzellen entwickelt haben. Die Osteoblasten beginnen dann mit dem Aufbau einer knochenspezifischen EZM worauf die Mineralisierung der Matrix folgt (Chung et al., 2004; Mackie et al., 2011).

Aus der desmalen Knochenbildung entstehen nur die flachen Knochen des Kopfes und das Schlüsselbein. Sie zeichnet sich durch die direkte Knochenbildung ohne zwischenzeitliche Bildung von Knorpel aus. Die mesenchymalen Zellen, die für die Bildung der desmalen Ossifikation verantwortlich sind, entstammen dem Neuralrohr und bilden zu Beginn der Ossifikation mittels Proliferation und Kondensation kompakte Knochenknötchen (bone nodules). Viele dieser Zellen differenzieren zu Osteoblasten und starten mit der Sekretion einer knochenspezifischen EZM. Diese EZM, auch als Osteoid bezeichnet, kann Calciumphopsphate binden und wird dadurch mineralisiert. Manche der Osteoblasten werden dann in die Matrix eingebaut und werden zu Osteozyten. Die Anhäufung von knöcherner EZM wird als Knochenspikula bezeichnet und wird durch die fortschreitende Sekretion von Osteoid durch Osteoblasten immer größer. Irgendwann stoßen die Knochenspikulae aneinander und es bildet sich ein Trabekel. Durch die fortschreitende Vergrößerung stoßen dann auch die Trabekel zusammen und es bildet sich Geflechtknochen (Chung et al., 2004; Kubota and Takigawa, 2011; Mina, 2001). Die osteogene Differenzierung von Stammzellen *in vitro* bildet zu großen Teilen die desmale Ossifikation nach (Gawlitta et al., 2010). Auch hier kommt es ohne Bildung von Knorpel zunächst zu einer Kondensation der Zellen. Darauf folgen die Produktion einer EZM und deren Mineralisierung und damit die Bildung von Knochenknötchen. Durch die Einschränkungen der 2D Kultur können sich jedoch die weiteren Schritte der desmalen Ossifikation nicht vollziehen.

Eine Spezies- und gewebespezifische extrazelluläre Matrix (EZM) spielt eine wichtige Rolle im Tissue Engineering. Denn die EZM interagiert mit anhaftenden Zellen, wobei sie spezifische Zellfunktionen beeinflusst, gleichzeitig aber von diesen Zellen beeinflusst und remodelliert wird (Abbott, 2003). Zellen in 3D Kulturen haben verständlicherweise mehr Kontakt zur EZM als Zellen in 2D Kulturen, bei denen ein großer Teil ihrer Fläche dem Medium exponiert ist. Darüber hinaus haben Zellen in 3D eine höhere Proliferationsrate als

Zellen in Einzelzellschichten und ihre Differenzierung entspricht der *in vivo* besser (Cukierman et al., 2001). Zu guter Letzt ähnelt das Expressionsprofil von Zellen in 3D dem von Zellen *in vivo* viel stärker als dem von Zellen in 2D. Folglich werden 3D Kulturen mit einer natürlichen selbsthergestellten EZM als eine vielversprechende Alternative im Tissue Engineering angesehen. Aufgrund dieser Ergebnisse wurden verschiedene 3D Zellkultur-Systeme für multipotente Stammzellen und osteoblastäre Zellen entwickelt. In verschiedenen Studien stellten sich im Vergleich zu 2D Kulturen deutlich bessere Ergebnisse bei der osteogenen Differenzierung heraus (Boehrs et al., 2008; Burns et al., 2010; Kale et al., 2000; Muraglia et al., 2003; Tortelli and Cancedda, 2009; Trojani et al., 2005).

Die Herstellung von *in vitro* generierten Knochenkonstrukten basiert meist auf dem Beimpfen eines geeigneten Biomaterials in der statischen Zellkultur, um den Zellen die Möglichkeit zur Anhaftung an das Material zu geben. Meist haften sich dann einzelne Zellen an die Oberflächen der Gerüste. Obwohl das Gerüst dreidimensional ist, entspricht die Situation jeder einzelnen Zelle auf den vielen Oberflächen des Gerüstes oft mehr der Situation in Einzelzellschichten als in 3D Geweben. Erst wenn die Zellen in mehreren Schichten übereinander wachsen und mit anderen Zellen zusammenstoßen kann von einem Gewebe gesprochen werden. Daher bietet das Beimpfen von Gerüsten mit mehrschichtigen Zellverbünden oder Mikrogeweben eine vielversprechende Alternative zum Beimpfen mit Zellsuspensionen.

Meist erfolgt nach dem Beimpfen die Kultivierung mit osteoinduktiven Mediumzusätzen entweder in der statischen Zellkultur oder im Bioreaktor. Die Verwendung von Bioreaktoren ist insbesondere dann wichtig, wenn große Gerüste mit kleinen Porengrößen verwendet werden, bei denen mit einer eingeschränkten Diffusion von Nährstoffen zu rechnen ist. Für kleinere Gerüste ist ein Bioreaktor oft nicht notwendig und aus wirtschaftlichen Gründen auch nicht gewünscht. Wird kein Bioreaktor verwendet, muss jedoch darauf geachtet werden, dass durch das Zellwachstum die Diffusion immer weiter eingeschränkt wird.

Auf Basis der oben beschriebenen Informationen, wurde in diesem Projekt versucht, ein KEM, kombiniert mit 3D Mikrogeweben, zu etablieren und dessen Eignung für die Knochenregeneration zu evaluieren. Die folgenden Originalarbeiten sind entsprechend der Projektentwicklung sortiert.

2 Referenzen zur Einleitung

Abbott, A. (2003). Cell culture: biology's new dimension. Nature *424*, 870-872.
Bianco, P., Robey, P.G., and Simmons, P.J. (2008). Mesenchymal stem cells: revisiting history, concepts, and assays. Cell Stem Cell *2*, 313-319.
Boehrs, J., Zaharias, R.S., Laffoon, J., Ko, Y.J., and Schneider, G.B. (2008). Three-dimensional culture environments enhance osteoblast differentiation. J Prosthodont *17*, 517-521.
Bonewald, L.F., Harris, S.E., Rosser, J., Dallas, M.R., Dallas, S.L., Camacho, N.P., Boyan, B., and Boskey, A. (2003). von Kossa staining alone is not sufficient to confirm that mineralization in vitro represents bone formation. Calcif Tissue Int *72*, 537-547.
Burns, J.S., Rasmussen, P.L., Larsen, K.H., Schroder, H.D., and Kassem, M. (2010). Parameters in three-dimensional osteospheroids of telomerized human mesenchymal (stromal) stem cells grown on osteoconductive scaffolds that predict in vivo bone-forming potential. Tissue engineering Part A *16*, 2331-2342.
Chung, U.I., Kawaguchi, H., Takato, T., and Nakamura, K. (2004). Distinct osteogenic mechanisms of bones of distinct origins. J Orthop Sci *9*, 410-414.
Cukierman, E., Pankov, R., Stevens, D.R., and Yamada, K.M. (2001). Taking cell-matrix adhesions to the third dimension. Science *294*, 1708-1712.
Gawlitta, D., Farrell, E., Malda, J., Creemers, L.B., Alblas, J., and Dhert, W.J. (2010). Modulating endochondral ossification of multipotent stromal cells for bone regeneration. Tissue Eng Part B Rev *16*, 385-395.
Kale, S., Biermann, S., Edwards, C., Tarnowski, C., Morris, M., and Long, M.W. (2000). Three-dimensional cellular development is essential for ex vivo formation of human bone. Nat Biotechnol *18*, 954-958.
Kogler, G., Sensken, S., Airey, J.A., Trapp, T., Muschen, M., Feldhahn, N., Liedtke, S., Sorg, R.V., Fischer, J., Rosenbaum, C*., et al.* (2004). A new human somatic stem cell from placental cord blood with intrinsic pluripotent differentiation potential. J Exp Med *200*, 123-135.
Kubota, S., and Takigawa, M. (2011). The role of CCN2 in cartilage and bone development. J Cell Commun Signal *5*, 209-217.
Mackie, E.J., Tatarczuch, L., and Mirams, M. (2011). The skeleton: a multi-functional complex organ. The growth plate chondrocyte and endochondral ossification. Journal of Endocrinology *211*, 109-121.
Meyer, U., Wiesmann, H.P., Berr, K., Kubler, N.R., and Handschel, J. (2006). Cell-based bone reconstruction therapies-principles of clinical approaches. Int J Oral Maxillofac Implants *21*, 899-906.
Mina, M. (2001). Regulation of mandibular growth and morphogenesis. Crit Rev Oral Biol Med *12*, 276-300.
Muraglia, A., Corsi, A., Riminucci, M., Mastrogiacomo, M., Cancedda, R., Bianco, P., and Quarto, R. (2003). Formation of a chondro-osseous rudiment in micromass cultures of human bone-marrow stromal cells. J Cell Sci *116*, 2949-2955.
Petite, H., Vandamme, K., Monfoulet, L., and Logeart-Avramoglou, D. (2011). Strategies for improving the efficacy of bioengineered bone constructs: a perspective. Osteoporos Int *22*, 2017-2021.
Robey, P.G. (2011). Cell sources for bone regeneration: the good, the bad, and the ugly (but promising). Tissue Eng Part B Rev *17*, 423-430.
Sasso, R.C., LeHuec, J.C., and Shaffrey, C. (2005). Iliac crest bone graft donor site pain after anterior lumbar interbody fusion: a prospective patient satisfaction outcome assessment. J Spinal Disord Tech *18 Suppl*, S77-81.
Tortelli, F., and Cancedda, R. (2009). Three-dimensional cultures of osteogenic and chondrogenic cells: a tissue engineering approach to mimic bone and cartilage in vitro. Eur Cell Mater *17*, 1-14.
Trojani, C., Weiss, P., Michiels, J.F., Vinatier, C., Guicheux, J., Daculsi, G., Gaudray, P., Carle, G.F., and Rochet, N. (2005). Three-dimensional culture and differentiation of human osteogenic cells in an injectable hydroxypropylmethylcellulose hydrogel. Biomaterials *26*, 5509-5517.

3 Publikationen der Dissertation

3.1 Osteogenic differentiation influences stem cell migration out of scaffold-free microspheres

Langenbach, F., Naujoks, C.[#], Kersten-Thiele, P.V., Berr, K., Depprich, R.A., Kubler, N.R., Kogler, G., and H andschel, J. (2010). Osteogenic differentiation influences stem cell migration out of scaffold-free microspheres. Tissue Eng Part A *16*, 759-766.

Impact Factor: 4,636

Durchschnittlicher Impact Faktor des Forschungsgebietes:

- Cell & Tissue Engineering:
    - 3,388; Rang 5 von 13 Zeitschriften

- Cell Biology:
    - 3,376; Rang 57 von 178

Mein Anteil an der Publikation:

- Versuche: 90%
- schriftliche Arbeit: 90%

TISSUE ENGINEERING: Part A
Volume 16, Number 2, 2010
© Mary Ann Liebert, Inc.
DOI: 10.1089/ten.tea.2009.0131

Osteogenic Differentiation Influences Stem Cell Migration Out of Scaffold-Free Microspheres

Fabian Langenbach, M.Sc.,[1] Christian Naujoks, M.D.,[1] Pia V. Kersten-Thiele,[1] Karin Berr, Ph.D.,[1] Rita A. Depprich, M.D., D.D.S.,[1] Norbert R. Kübler, M.D., D.D.S., Ph.D.,[1] Gesine Kögler, Ph.D.,[2] and Jörg Handschel, M.D., D.D.S., Ph.D.[1]

Complete bone regeneration of critical-size defects frequently fail because of the use of acellular bone substitutes and because of partially negative influences of artificial scaffolds. However, the supply of cells to critical-size defects is essential for the regeneration. Therefore, engineered scaffold-free tissues, with outgrowing cells that fill up spaces in the bony defect, are promising candidates for bone regeneration approaches. Here, we demonstrate such a scaffold-free tissue construct (microspheres) that, if osteogenic differentiated, mineralizes while maintaining the capability to let cells grow out of the united cell structure. A superior outgrowth capability of microspheres composed of human cord blood-derived unrestricted somatic stem cells compared with murine embryonic stem cells was found and a time-dependent reduction in outgrowth was evident *in vitro*. Even after 5 days of osteoinduction and strong mineralization, the cells migrate out of the microsphere. As migration of cells out of unrestricted somatic stem cell microspheres was also found in extracellular matrix gel, we suggest that cells would migrate also *in vivo*. Thus, microspheres could serve as the scaffold and the source of osteogenic cells in future bone regeneration approaches. Further, microspheres permit the precise administration of large amount of cells into an area of interest.

Introduction

Bone defects that are caused by tumor resection, trauma, or infections may exceed sizes that make self-healing of the bone impedimental or impossible. Usually, artificial materials, such as polymers, metals, and ceramics, or tissue transplants, such as autologous bone, are used for the reconstruction of bone.[1–4] However, all these attempts have their inherent disadvantages, such as problems in biocompatibility and mismatches with the biological complexity at the molecular level of artificial materials as well as comorbidity of autologous bone.[5] Tissue engineering approaches could overcome these difficulties.

In tissue engineering the cultivation of autologous or human leukocyte antigen (HLA)-matched cells, with or without scaffolds, is used to grow implantable tissues. The screening for a suitable scaffold is one big challenge in tissue engineering. Scaffolds should be biodegradable, nontoxic, biocompatible, nonimmunogenic, and surgical fixable. Further, it should mimic the internal and external bone geometry and support osteogenesis and cell attachment. As all these criteria are difficult to meet, and in addition, as sophisticated material science has to be developed further to match the biological complexity at the molecular level,[6] approaches that renounce the use of scaffolds are promising.

The lack of a species- and tissue-specific extracellular matrix (ECM) is another facet in tissue engineering. The ECM contains proteins, such as elastin, laminin, and collagen, which are responsible for the tissue-specific mechanical properties. Among the mechanical function, the ECM interacts with attaching cells by triggering specific cellular function, while being influenced by these cells.[7] This is supported by the finding that biomembranes that consist of compartments of the ECM, namely collagen, increase cellular proliferation, whereas polytetrafluoroethylene membranes do not.[8]

Cellular receptors, particularly a family of proteins called the integrins, determine how the cells interpret biochemical cues from their surrounding area[7] in this process. Cells in three-dimensional (3D) cultures exert higher proliferation rates than cells in monolayer cultures, and their differentiation more closely resembles that seen *in situ*.[9,10] In addition to differences in cellular proliferation rates, cells are able to change their shape and behavior upon specific cell signals,

Department for [1]Oral and Maxillofacial Surgery and [2]Transplantation Diagnostics and Cell Therapeutics, Heinrich-Heine University Hospital of Duesseldorf, Duesseldorf, Germany.

An abstract of this work was submitted to the 19th International Conference on Oral and Maxillofacial Surgery and was published in the Conference Journal.

only when they are cultured in 3D.[11] Further, the gene expression profile of cells in 3D is much closer to the expression of cells *in vivo* than profiles of cells in two-dimensional (2D) cultures.[12]

Therefore, 3D cultures with matrices that resemble the natural ECM are regarded as an upcoming alternative in skeletal tissue engineering. According to Kelm and Fussenegger,[13] advances in microtissue production have highlighted the potential of scaffold-free cell aggregates in maintaining tissue-specific functionality, supporting seamless integration of implants into host tissues, and providing complex feeder structures for difficult-to-differentiate cell types. Further, these tissues are amenable to therapeutic and phenotype-modulating interventions. An alternative to the widespread methods used for microtissue engineering, that is, cultivation in shake flasks, gyratory shakers, and roller bottles or on nonadhesive surfaces, centrifugation-based compression, maintenance in cell culture inserts, or gravity-enforced assembly of microspheres in hanging drops, is the microsphere technology.[10,14,15] These microspheres consist of cells that self-assemble on a concave surface in a microsphere assembly bioreactor that consists of hydrogel-coated 96-well plate.

Numerous cell lines that can be used for skeletal tissue engineering approaches *in vitro* are available, ranging from human osteoblast-like cell lines, for example, SAOS-2[16,17] over primary human osteoblasts to mesenchymal stem cells. Even though experiments with these kinds of cells may produce promising results, the reproducibility of such approaches in the human body will fail because of immunoincompatibility. The use of HLA-matched cells for tissue engineering approaches could overcome this problem. Unrestricted somatic stem cells (USSCs) that are isolated from human umbilical cord blood and HLA characterized at the Jose Carreras Stammzellbank (Düsseldorf, Germany) were shown to be multipotent.[18] As USSCs are able to differentiate toward the osteogenic lineage, these cells are used in this work. To compare USSCs with a cell line that definitely is able to differentiate toward the osteogenic lineage, murine embryonic stem cells (ESCs) are used.

To use microspheres for bone healing approaches, the characteristics of microsphere development need to be determined. When microspheres are implanted into bone defects the question arises how the cells of a microsphere would behave. Whether cells would sprout out of the microsphere or get arrested in it needs to be evaluated, as it is important for the regeneration of the affected tissue. Spaces between microsphere implants need to be colonized and vascularized by cells. Because of limited migration capacities of host cells into a large defect area, implanted cells have to perform the host cells' task. Therefore, it was evaluated in this work whether cells sprout out of microspheres under osteoinductive conditions on tissue culture plates.

We could demonstrate that the outgrowth distance from microspheres remarkably declines if the microspheres are treated with osteoinductive medium for a longer time. It was found that this reduction correlates with the incorporation and production of ECM proteins. Further, mineralization of the microspheres was strong after 1 week with osteoinductive medium but also became evident without osteoinduction.

Because of a superior outgrowth capability of USSCs compared with ESCs in 2D cultures, we only used USSCs to analyze the outgrowth in a 3D model. To prove whether the results obtained in outgrowth experiments on tissue culture plates could be approximated to an *in vivo* situation, a migration experiment in an ECM gel (Geltrex™, Invitrogen, Karlsruhe, Germany, hESC-qualified reduced growth factor basement membrane matrix) was performed. Also in ECM gel, the USSCs migrated out of the microspheres, even after 5 days of osteogenic induction. In some cases even the pass through the gel is retraceable by a gap in the matrix. Therefore, we suggest that migration of cells out of USSC microspheres is also possible *in vivo*, and that osteogenic microspheres are promising candidates for bone regeneration approaches.

Materials and Methods

Culture of cells and assembly of microspheres

USSCs were kindly provided by Gesine Kögler (José Carreras Stammzellbank, Heinrich-Heine-University, Germany). USSCs were isolated from cord blood, with informed consent of the mother, as described by Kögler *et al.*[18] Briefly, Ficoll (Biochrom, Berlin, Germany) gradient centrifugation was used to isolate the mononuclear cell fraction. Cells were plated at $5–7\times10^6$ cells/mL on T25 culture flasks (Costar, Vitaris, Baar, Switzerland) in low-glucose DMEM (Cambrex, East Rutherford, NJ), supplemented with 30% fetal calf serum, dexamethasone (10^{-7} M; Sigma-Aldrich, Munich, Germany), penicillin (100 U/mL; Grünenthal, Aachen, Germany), streptomycin (100 mg/mL; Hefa-Pharma, Werme, Germany), and ultraglutamine (2 mM; Cambrex). Later, during the expansion of cells, the dexamethasone was left out in the medium. The cells were incubated in a humidified atmosphere at 37°C in 5% CO_2. The cells were split when confluence reached 80%, by detaching the cells with 0.25% trypsin (Lonza, Basel, Switzerland) and replating them at a ratio 1:3.

Feeder-independent ESCs were kindly provided by K. Pfeffer (Institute for Microbiology, Heinrich-Heine-University, Germany). The cells were derived from the inner cell mass of blastocysts extracted from C57BL/6 mice and were tested to be positive for the stem cell markers Pouf1 (alias Oct4) and Foxd3.[19] The cells were cultured in DMEM (Gibco, Invitrogen, Karlsruhe, Germany) supplemented with penicillin (100 U/mL; Grünenthal), streptomycin (100 mg/mL; Hefa-Pharma), ultraglutamine (2 mM; Cambrex), 2-mercaptoethanol (500 mM; Gibco), leukemia inhibitory factor (1000 U/mL; Chemicon), and 15% fetal calf serum. The cells were split every 2nd day, and the medium was changed every day by detaching the cells with 0.25% trypsin (Pan Biotech, Aidenbach, Germany).

USSCs or ESCs were detached from the plate, centrifuged and resuspended in normal growth medium (1×10^6 Cells/mL). The microsphere assembly bioreactor was prepared by filling 60 μL of solution consisting of 2% agarose in DMEM (without any supplements) in 96-well plates. In each well, including solidified hydrogel, 180 μL of cell suspension was added, and the cultures were incubated overnight. Because of the concave surface of the hydrogel (caused by capillary actions), the cells congregate in the center of the well and form a sphere within 1 day. The old medium is replaced by 160 μL of control medium or control medium containing 100 nM dexamethasone, 50 μM ascorbic acid, and 10 mM β-glycerolphosphate (DAG; all from Sigma, Sigma-Aldrich, Mumich, Germany) and was once more changed

after 3 days. After 1, 2, 3, or 5 days the microspheres were taken out of the 96-well plates and were transferred to a Petri dish for a washing step with phosphate-buffered saline. For histology, the microspheres were fixed in formalin (4%) until further procession.

For measurement of the outgrowth distances, the microspheres were treated with 0.25% trypsin for 10 min and were then placed in the center of wells of a 24-well tissue culture plate (Corning, Vitaris, Baar, Switzerland) containing 500 µL normal growth medium. The microspheres attached to the tissue culture plate surface and were incubated for 5 days.

In an additional 3D outgrowth experiment, USSC microspheres were seeded in matrix gel after 1, 3, and 5 days osteoinduction. For this approach, 500 µL Geltrex (hESC-qualified reduced growth factor basement membrane matrix) was added into the wells of a 24-well plate. Before the gel solidified, one microsphere was placed in the center of each well into the gel, thereby avoiding the sticking of the microsphere to the bottom of the well to make sure that the sphere is completely surrounded by the gel. After the gel was solidified (30 min incubation at 37°C), 500 µL normal growth medium was added on top. Pictures were taken after 5 days of incubation at 37°C.

Histology

Formalin-fixed microspheres were dehydrated in increasing concentrations of ethanol and were embedded in paraffin. Sections (5 µm) were mounted on superfrost slides, deparaffinized with xylol, and rehydrated in decreasing ethanol concentrations. To stain collagen, a main compartment of the ECM, the sections were stained according to Masson Goldner. Briefly, nuclei were stained with Weigerts hematoxylin for 20 min, cytoplasm was stained red with azophloxin solution as well as tungstophosphoric acid orange G solution, and connective tissue was stained with light green SF solution. Evaluation of the outgrowth distance on chamber slides was performed after staining with Mayer's Hemalarm for 3 min and with eosin for 2 min. Mineralization of the microspheres after 5 days of incubation was performed by staining with alizarin red solution (2%). After dehydration, the sections as well as the microspheres on the chamber slides were embedded in entellan (Merck, Darmstadt, Germany) and were investigated with bright field microscopy.

Statistics

The outgrowth distances were evaluated by measuring the distances from the centers of the microspheres to the most distant cells at predefined angles. For each microsphere, eight angles were evaluated, with each angle being 45° apart from the next. Angles for four to six microspheres were evaluated for each experimental parameter in three independent experiments. For the calculation of significances with the Student's *t*-test, groups with at least 96 single values were compared with each other.

Results

It was investigated whether induction with osteogenic growth medium, containing DAG, has an influence on the capability of cells to migrate out of microspheres. USSCs were used because they are capable of osteogenic differentiation and can be HLA characterized and, in addition, their use does not raise ethical questions. Murine ESCs were used because they are pluripotent and can differentiate into every cell type of the body, including osteogenic cells.

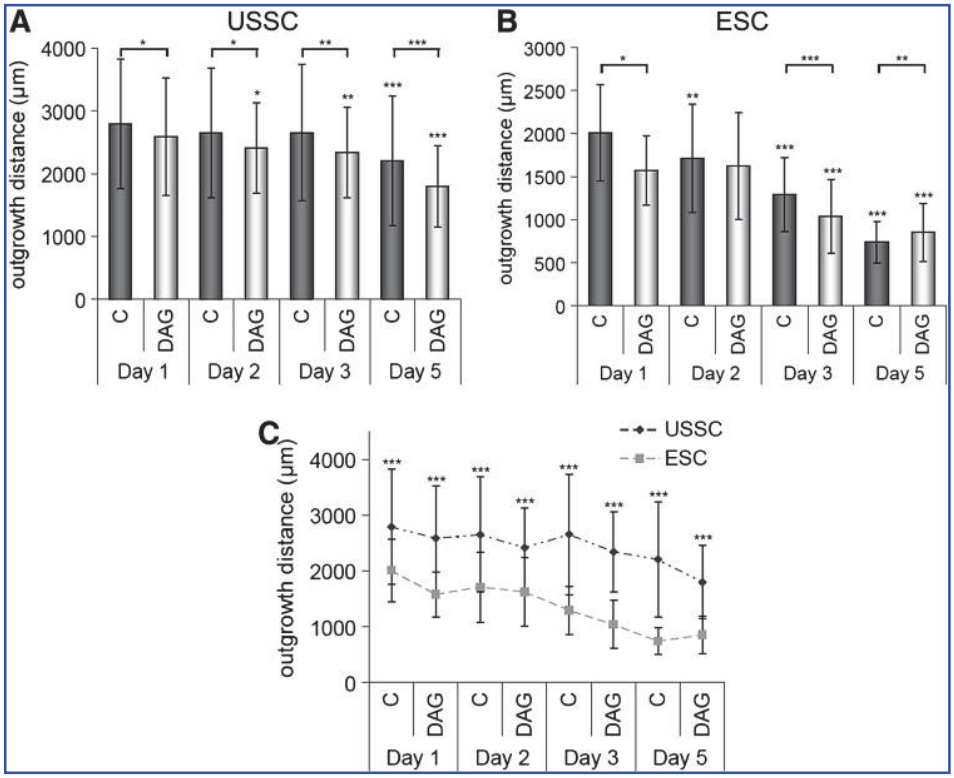

FIG. 1. Incubation time-dependent decrease in outgrowth distances of cells from microspheres. (**A–C**) Mean values ± standard deviation of three independent experiments are shown. (**A, B**) Student's *t*-test was used to calculate *p*-values (*$p < 0.05$, **$p < 0.005$, and ***$p < 0.0005$) for comparison with the respective values of day 1. Further significances between DAG-treated and control microspheres are shown. (**A**) Decrease in outgrowth distances of USSCs during incubation with or without DAG. (**B**) Decrease in outgrowth distances of ESCs during incubation with or without DAG. (**C**) Significant lower outgrowth distances of ESC compared with USSCs. USSCs, unrestricted somatic stem cells; ESC, embryonic stem cells; DAG, 100 nM dexamethasone, 50 µM ascorbic acid, and 10 mM β-glycerolphosphate.

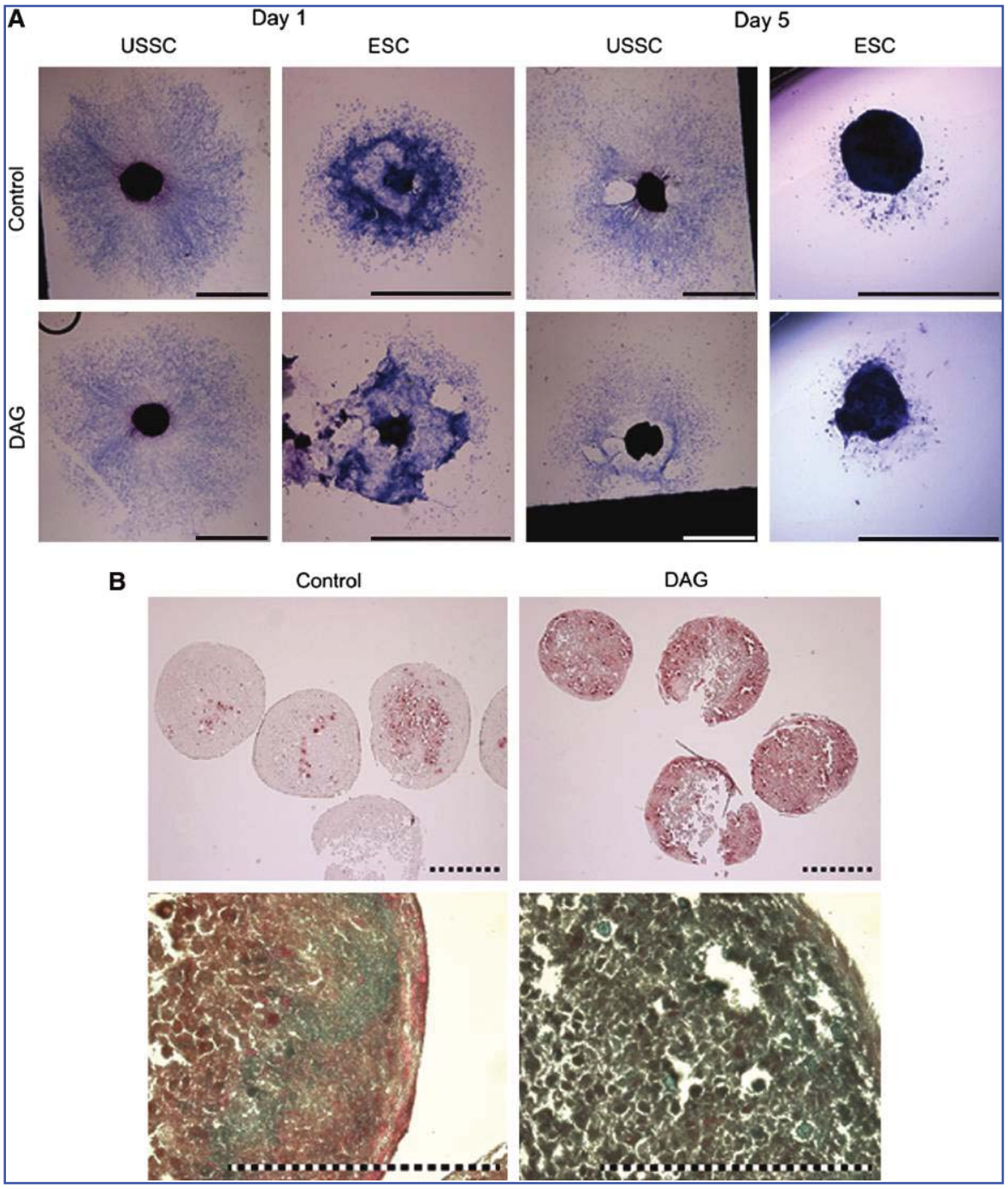

FIG. 2. Effects of DAG treatment on microspheres. (**A**) Microspheres were incubated with (lower lane) or without DAG (upper lane) and were stained with Hemalarm/eosin (scale bars 2 mm). (**B**) Alizarin red S staining (upper lane) and Masson Goldner staining (lower lane) of USSC microspheres, incubated with or without DAG for 5 days. Calcium is stained dark (upper lane); extracellular matrix is green and cytoplasm is red after staining according to Masson Goldner (scale bars = 500 μm). Color images available online at www.liebertonline.com/ten.

Osteogenic induction decreases the outgrowth distances of USSCs from microspheres

A time-dependent reduction in the outgrowth distances of USSCs was found during treatment with and without osteoinductive medium (Figs. 1A and 2A). Incubation of the microspheres with osteoinductive medium (DAG) resulted in statistically significant (evaluated by Student's *t*-test) decreased outgrowth distances after 2 days ($p < 0.05$), 3 days ($p < 0.005$), and 5 days ($p < 0.0005$) when compared with day 1 (Fig. 1A). After 1-day DAG treatment, the cells grew out to 2568 μm (±936 μm), whereas after 5 days the distance

declined to 1796 μm (±652 μm). In addition to the time-dependent reduction in outgrowth distances a DAG-induced reduction compared with controls was significant at all observed times. Hence, the treatment with DAG results in a reduction of the USSC microsphere capacity to let cells migrate into the surrounding area.

Osteogenic induction decreases the outgrowth distances of ESCs from microspheres

Also, ESC microspheres showed incubation time-dependent decreases in outgrowth distances (Figs. 1B and 2A). In contrast to the outgrowth distance of USSCs from microspheres, there is no time-dependent reduction after 2 days of incubation with osteoinductive medium; however, after 3 and 5 days the decreases are tremendous ($p < 0.0005$) (Fig. 1B). In this process, the outgrowth distance of cells from the DAG-treated ESC microspheres decreased from 1547 μm (±403 μm) to 850 μm (±333 μm) at day 5. Just like the USSC microspheres, also the outgrowth distances of cells from ESC microspheres were influenced by DAG treatment (Fig. 1B). However, after 5 days of incubation, a higher outgrowth was observed for the DAG-treated group. The reason for this may be a reduction in size of the control microspheres after 5 days.

Outgrowth distances of ESCs from microspheres are tremendously shorter than that of USSCs

At every observation time (days 1, 2, 3, and 5) the outgrowth distances of cells from ESC microspheres were significantly lower compared with cells from USSC microspheres (Fig. 1C). After 5 days of incubation with or without DAG, USSCs grew to 1796 μm (±652 μm) and 2203 μm (±1030 μm) out of the microsphere, whereas ESCs migrated only to 850 μm (±333 μm) and 738 μm (±243 μm) out of the spheres. Hence, the capability of USSCs to grow out of microspheres is superior to ESCs. As the ESC microspheres failed in the outgrowth experiment, they do not seem to be suitable for tissue regeneration approaches in which the cells have to migrate out of the scaffold (the microsphere). Therefore, only USSCs were further characterized and analyzed.

DAG treatment increases ECM assembly and calcium incorporation of USSC microsphere

Sections (3 μm) of microspheres were stained according to Masson Goldner to detect collagen in the ECM. A significant difference in the proportion of the microsphere that was stained green by light green SF can be detected between those microspheres which were treated for 5 days with or without DAG (Fig. 2B). After 5 days with DAG the microsphere was stained by light green SF to a great extent. Consequently, ECM pervades the complete microsphere in case of foregoing osteoinductive conditions but not under standard conditions. To detect calcium in the microsphere sections, alizarin red S was used. The control microspheres were stained very weak at some spots in the center of the microsphere, whereas those which were treated with DAG were intensively red stained. Consequently, DAG induces the microspheres to incorporate calcium within 5 days of incubation.

Cells migrate out of USSC microspheres and into ECM gel after osteogenic induction

For the investigation whether outgrowth of cells out of USSCs could be approximated to the situation *in vivo*, osteogenically differentiated microspheres were incubated in reduced growth factor basement membrane matrix gel (Geltrex). Both control microspheres, incubated in normal growth medium, and osteogenically differentiated microspheres let the cells migrate into the matrix after each incubation time. In Figure 3A it is shown that after osteogenic differentiation for 1, 3, and 5 days, the cells could be detected after further incubation for 5 days in the gel matrix. Thus, it is evident that the cells are capable of migrating through the gel. This is also supported by the finding that the movement of the cells through the matrix seems to be retraceable. One can observe a gap in the uniform gel matrix between the cell and the microsphere (Fig. 3B).

Discussion

Usually, in bone regeneration, surgeons used natural or synthetic substrates, which had limited success because they provided a scaffold that can be invaded only by bone-forming bioactive cells.[20,21] Thus, only small defects could be treated by implanting those materials.[22] A main challenge in the regeneration of large bone defects is the adequate supply of the tissue with osteoblasts. Therefore, biomaterial scaffolds loaded with mesenchymal stem cells were used in various studies, including different sizes of animals and ranging from non-resorbable ceramics to biodegradable corral, with the result of a superior regeneration capacity of bioengineered bone compared with the regeneration capacity of scaffolds alone.[23–26] However, as this method relies also on the choice of a biomaterial that fulfills many of the required characteristics, even this method was not optimal. In our work it was shown that the cells dissolve out of the cellular meshwork of microspheres and spread out into the surrounding area. It was found that the longer the microspheres are incubated in the assembly bioreactor, the outgrowth distances get smaller. When the microspheres were incubated with osteoinductive medium the outgrowth was suppressed. But even after 5 days of DAG treatment of the microspheres, the USSCs grew out to about 1.8 mm (±0.65 mm). At this time the microspheres already incorporated huge amounts of calcium. Probably, the incorporation of calcium and the accumulation of ECM molecules could be the reason for the decreased outgrowth distance of the DAG-treated group. Further, it is possible that osteogenic differentiation has an effect on the proliferation of the cells.

Because of their mineralization, microspheres can be considered as a scaffold and a source for cells with osteogenic potential. Further, microsphere technology provides an easy method for the administration of large cell numbers on accurately defined places in the tissue. Also, the precise placement into biomaterials with sponge-like structures and pores or spaces with sizes of the microspheres, that is, insoluble collagenous bone matrix (ICBM), seems possible.

It was found that the outgrowth distances from microspheres of ESCs were much smaller than USSCs. After 5 days of osteoinduction, the outgrowth distance of USSCs was more than twice as that of ESCs. Thus, ESCs do not seem to be suitable for microsphere-based tissue regeneration approaches. Further, USSCs are more easily accessible and

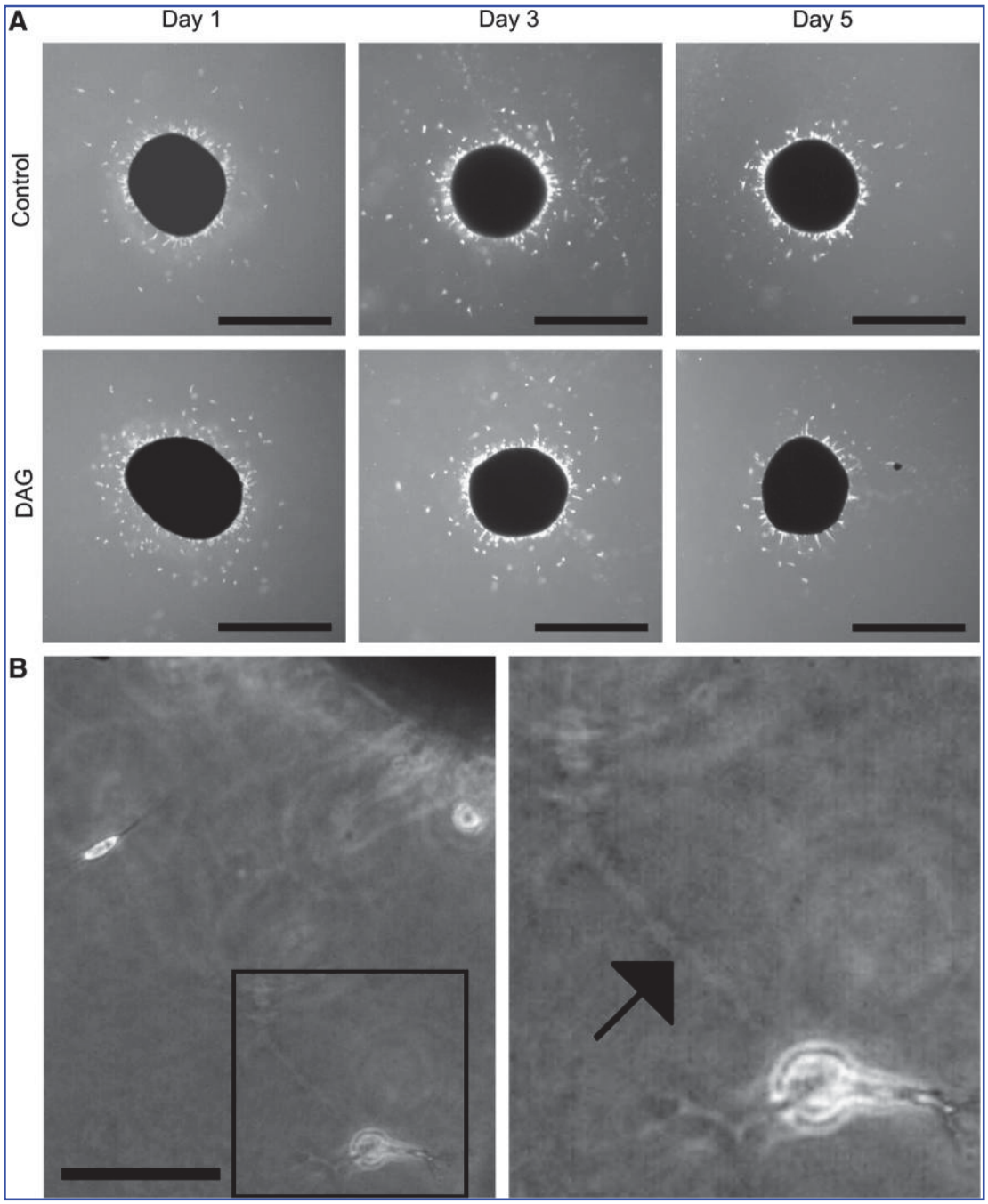

FIG. 3. Outgrowth of cells out of USSC microspheres in extracellular matrix gel (Geltrex). (**A**) Microspheres were incubated with (lower lane) or without DAG (upper lane) for 1, 3, or 5 days and were then placed in Geltrex for 5 days (scale bars = 1 mm). (**B**) Magnification of a single cell of a USSC microsphere after 3 days of differentiation and 5 days of further incubation. The trace of the cell in the gel matrix is visible as a gap (arrow) in the uniform matrix (scale bar = 0.1 mm).

routinely HLA matched after their isolation, and their use does not raise ethical concerns.[18]

The use of 2D cell cultivation is widespread and popular, although it is known that cells behave different when they are cultivated in 3D. Weaver and colleagues demonstrated that antibodies against the cell surface receptor β1 integrin completely changed the behavior of cancerous breast cells when they were grown in 3D.[11] The major cause for these differences is the interaction between ECM and integrins on the cell surface. The integrins (comprised of α and β subunits) bind ECM proteins, signal bidirectionally across the plasma membrane, exert an impact at the level of gene expression, and influence many important cell behaviors, that is, cell proliferation, migration, and survival.[27–29]

Here, we demonstrated that microspheres secrete collagen, which is a major compartment of the ECM, within a few days. In accordance with the findings of Aubin,[30] collagen production is enhanced when cells were treated with osteoin-

ductive conditions. Interestingly, also these microspheres that were not treated with osteoinductive medium began to produce collagen. One reason may be a spontaneous differentiation of the cells toward the osteogenic lineage, resulting in the expression of collagen type I. However, the more likely reason is the formation of ECM. This process was already observed in confluent fibroblastic cell cultures in which fibrillogenesis leads to the accumulation of a thick matrix.[31]

The differentiation potential of USSCs and ESCs toward the osteogenic lineage is well known and was verified by our working group and by Kögler and colleagues.[18,32] Calcium deposition in the microspheres was detected after a few days of osteoinduction and after 1 week without induction. This spontaneous calcium incorporation of control microspheres may be a result of collagen type I binding induced osteogenesis. According to Kundu *et al.*,[33] the *de novo* synthesis and deposition of ECM proteins by mesenchymal stem cells alters the chemical identity of polymeric substrate, stimulates changes in integrin expression profiles, and thereby alters signaling pathways to influence osteogenesis. Cell adhesion to collagen type I have been shown to induce the activity of the mitogen-activated protein kinase cascade, which appears to play a critical role in the osteogenic differentiation of osteoblastic cells by activating the Runx2/CBFA-1 transcriptional activator.[34,35]

Microspheres do become osteogenic after short time and could contribute to structural rigidity of the affected tissue. The fact that USSCs are able to contribute to the structural rigidity of bone was corroborated by the findings of our group (paper, in preparation), using scaffold–cell implants in rat. Bovine ICBM scaffolds (0.1 cm^3) were seeded with USSCs or ESCs, underwent osteogenic differentiation for 3 days, and were implanted into muscle pockets in the back of immunocompromized rats [Rowett nude rats (RNU)]. After 1 week postoperation, no mineralization could be detected by computed tomography scan and histological staining in any group. However, after 4 months, strong mineralization was found in the USSC group, whereas in the ESC group no mineralization could be detected. The combination of ICBM scaffolds and USSCs led to bone formation in immunocompromized rats and is therefore a promising therapeutic approach. Nevertheless, the use of ICBM or any other animal- or donor-derived tissue or tissue compartment harbors the danger of immunorejection. The approach described in our study, however, renounces the use of an artificial scaffold. The renouncement of any artificial scaffold may reduce unpredictable risks, for example, influence on cell differentiation by the scaffold.

Microspheres provide an easy method for the administration of large amounts of osteogenically predifferentiated cells into accurately defined areas of interest. However, for the regeneration of critical-size bone defects, microspheres have to mineralize and also maintain the potential to let cells migrate into the surrounding area to fill up spaces. In this study, it was emphasized that the outgrowth of cells from USSC microspheres was superior to the outgrowth from ESC microspheres. So USSC microspheres, with their superior outgrowth distances and advantageous inherent characteristics (good accessibility and no ethical objections) compared with ESC microspheres, were further analyzed regarding their potential to contribute to bone regeneration approaches. We could show that even after 5 days of osteoinduction and strong mineralization of the USSC microsphere, the cells migrate out of the united structure into the surrounding area. The decline in the outgrowth distances was found to be dependent on the osteogenic induction and the incubation time. Alizarin red staining of histological sections revealed that after 5 days of osteogenic differentiation, a strong mineralization was evident. Further, the accumulation of the ECM molecule, collagen, was strongly enhanced in the osteogenically differentiated microspheres. Beside its key role in the ECM, collagen is a main compartment of bone. So the microspheres, with the accumulation of collagen and their mineralization, exhibit two main attributes of bone. As in the outgrowth experiments on tissue culture plates the cells do not have to cope with a physiological barrier, like ECM or basement membrane, the microspheres were exposed to conditions that resemble best the *in vivo* conditions. We found that cells from osteogenically predifferentiated microspheres were able to penetrate ECM gels *in vitro*. Therefore, osteogenically differentiated microspheres with outgrowing cells that can fill up spaces in the bony defect are promising candidates for bone regeneration approaches. Further, microspheres permit the transplantation of more cells compared with cell suspensions or gels and guaranty that the transplanted cells stay at the place of interest.

Acknowledgments

Fabian Langenbach was supported by a DFG grant (HA 3228/2-1). The authors are thankful to Prof. Dr. G. Kögler, José Carreras Stammzellbank of the Heinrich-Heine-University, Düsseldorf, Germany, for providing USSCs, and to Prof. Dr. K. Pfeffer, Institute for Microbiology at the Heinrich-Heine-University Düsseldorf, for providing the murine ESCs.

Disclosure Statement

No competing financial interests exist.

References

1. Frenkel, G., and Niederdellmann, H. Use of compact aluminum oxide ceramics for reconstruction of the temporomandibular joint. Quintessenz **26,** 37, 1975.
2. Leake, D.L., and Habal, M.B. Craniofacial contour defect reconstruction with a dacron/urethane composite: an alloplastic tray for bone induction fabrication and application. J Biomed Mater Res **10,** 555, 1976.
3. Niwa, H., Miyazaki, J., and Smith, A.G. Quantitative expression of Oct-3/4 defines differentiation, dedifferentiation or self-renewal of ES cells. Nat Genet **24,** 372, 2000.
4. Pochon, J.P., and Klöti, J. Cranioplasty for acquired skull defects in children—a comparison between autologous material and methylmethacrylate 1974–1990. Eur J Pediatr Surg **1,** 199, 1991.
5. Yazar, S., Lin, C., and Wei, F. One-stage reconstruction of composite bone and soft-tissue defects in traumatic lower extremities. Plast Reconstr Surg **114,** 1457, 2004.
6. Navarro, M., Michiardi, A., Castaño, O., and Planell, J.A. Biomaterials in orthopaedics. J R Soc Interface **5,** 1137, 2008.
7. Abbott, A. Cell culture: biology's new dimension. Nature **424,** 870, 2003.
8. Kasaj, A., Reichert, C., Götz, H., Röhrig, B., Smeets, R., and Willershausen, B. *In vitro* evaluation of various bioabsorbable and nonresorbable barrier membranes for guided tissue regeneration. Head Face Med **4,** 22, 2008.

9. Cukierman, E., Pankov, R., Stevens, D.R., and Yamada, K.M. Taking cell-matrix adhesions to the third dimension. Science **294,** 1708, 2001.
10. Handschel, J.G.K., Depprich, R.A., Kübler, N.R., Wiesmann, H., Ommerborn, M., and Meyer, U. Prospects of micromass culture technology in tissue engineering. Head Face Med **3,** 4, 2007.
11. Weaver, V.M., Petersen, O.W., Wang, F., Larabell, C.A., Briand, P., Damsky, C., and Bissell, M.J. Reversion of the malignant phenotype of human breast cells in three-dimensional culture and *in vivo* by integrin blocking antibodies. J Cell Biol **137,** 231, 1997.
12. Sivaraman, A., Leach, J.K., Townsend, S., Iida, T., Hogan, B.J., Stolz, D.B., Fry, R., Samson, L.D., Tannenbaum, S.R., and Griffith, L.G. A microscale *in vitro* physiological model of the liver: predictive screens for drug metabolism and enzyme induction. Curr Drug Metab **6,** 569, 2005.
13. Kelm, J.M., and Fussenegger, M. Microscale tissue engineering using gravity-enforced cell assembly. Trends Biotechnol **22,** 195, 2004.
14. Mello, M.A., and Tuan, R.S. High density micromass cultures of embryonic limb bud mesenchymal cells: an *in vitro* model of endochondral skeletal development. In Vitro Cell Dev Biol Anim **35,** 262, 1999.
15. Edwall-Arvidsson, C., and Wroblewski, J. Characterization of chondrogenesis in cells isolated from limb buds in mouse. Anat Embryol (Berl) **193,** 453, 1996.
16. Fogh, J., Fogh, J.M., and Orfeo, T. One hundred and twenty-seven cultured human tumor cell lines producing tumors in nude mice. J Natl Cancer Inst **59,** 221, 1977.
17. Rodan, S.B., Imai, Y., Thiede, M.A., Wesolowski, G., Thompson, D., Bar-Shavit, Z., Shull, S., Mann, K., and Rodan, G.A. Characterization of a human osteosarcoma cell line (Saos-2) with osteoblastic properties. Cancer Res **47,** 4961, 1987.
18. Kögler, G., Sensken, S., Airey, J.A., Trapp, T., Müschen, M., Feldhahn, N., Liedtke, S., Sorg, R.V., Fischer, J., Rosenbaum, C., Greschat, S., Knipper, A., Bender, J., Degistirici, O., Gao, J., Caplan, A.I., Colletti, E.J., Almeida-Porada, G., Müller, H.W., Zanjani, E., and Wernet, P. A new human somatic stem cell from placental cord blood with intrinsic pluripotent differentiation potential. J Exp Med **200,** 123, 2004.
19. Baharvand, H., Ashtiani, S.K., Taee, A., Massumi, M., Valojerdi, M.R., Yazdi, P.E., Moradi, S.Z., and Farrokhi, A. Generation of new human embryonic stem cell lines with diploid and triploid karyotypes. Dev Growth Differ **48,** 117, 2006.
20. Damien, C.J., and Parsons, J.R. Bone graft and bone graft substitutes: a review of current technology and applications. J Appl Biomater **2,** 187, 1991.
21. Shors, E.C. Coralline bone graft substitutes. Orthop Clin North Am **30,** 599, 1999.
22. Logeart-Avramoglou, D., Anagnostou, F., Bizios, R., and Petite, H. Engineering bone: challenges and obstacles. J Cell Mol Med **9,** 72, 2005.
23. Kadiyala, S., Young, R.G., Thiede, M.A., and Bruder, S.P. Culture expanded canine mesenchymal stem cells possess osteochondrogenic potential *in vivo* and *in vitro*. Cell Transplant **6,** 125, 1997.
24. Bruder, S.P., Kurth, A.A., Shea, M., Hayes, W.C., Jaiswal, N., and Kadiyala, S. Bone regeneration by implantation of purified, culture-expanded human mesenchymal stem cells. J Orthop Res **16,** 155, 1998.
25. Bruder, S.P., Kraus, K.H., Goldberg, V.M., and Kadiyala, S. The effect of implants loaded with autologous mesenchymal stem cells on the healing of canine segmental bone defects. J Bone Joint Surg Am **80,** 985, 1998.
26. Kon, E., Muraglia, A., Corsi, A., Bianco, P., Marcacci, M., Martin, I., Boyde, A., Ruspantini, I., Chistolini, P., Rocca, M., Giardino, R., Cancedda, R., and Quarto, R. Autologous bone marrow stromal cells loaded onto porous hydroxyapatite ceramic accelerate bone repair in critical-size defects of sheep long bones. J Biomed Mater Res **49,** 328, 2000.
27. Hervy, M., Hoffman, L., and Beckerle, M.C. From the membrane to the nucleus and back again: bifunctional focal adhesion proteins. Curr Opin Cell Biol **18,** 524, 2006.
28. Schmidhauser, C., Casperson, G.F., Myers, C.A., Sanzo, K.T., Bolten, S., and Bissell, M.J. A novel transcriptional enhancer is involved in the prolactin- and extracellular matrix-dependent regulation of beta-casein gene expression. Mol Biol Cell **3,** 699, 1992.
29. Schwartz, M.A., and Assoian, R.K. Integrins and cell proliferation: regulation of cyclin-dependent kinases via cytoplasmic signaling pathways. J Cell Sci **114,** 2553, 2001.
30. Aubin, J.E. Advances in the osteoblast lineage. Biochem Cell Biol **76,** 899, 1998.
31. Beacham, D.A., Amatangelo, M.D., and Cukierman, E. Preparation of extracellular matrices produced by cultured and primary fibroblasts. Curr Protoc Cell Biol 10.09.07, 2007.
32. Handschel, J., Berr, K., Depprich, R.A., Kübler, N.R., Naujoks, C., Wiesmann, H., Ommerborn, M.A., and Meyer, U. Induction of osteogenic markers in differentially treated cultures of embryonic stem cells. Head Face Med **4,** 10, 2008.
33. Kundu, A.K., Khatiwala, C.B., and Putnam, A.J. Extracellular matrix remodeling, integrin expression, and downstream signaling pathways influence the osteogenic differentiation of mesenchymal stem cells on poly(lactide-co-glycolide) substrates. Tissue Eng A **15**, 273, 2009.
34. Xiao, G., Jiang, D., Thomas, P., Benson, M.D., Guan, K., Karsenty, G., and Franceschi, R.T. MAPK pathways activate and phosphorylate the osteoblast-specific transcription factor, Cbfa1. J Biol Chem **275,** 4453, 2000.
35. Franceschi, R.T., and Xiao, G. Regulation of the osteoblast-specific transcription factor, Runx2: responsiveness to multiple signal transduction pathways. J Cell Biochem **88,** 446, 2003.

Address correspondence to:
Fabian Langenbach, M.Sc.
Department of Oral and Maxillofacial Surgery
Heinrich-Heine University Hospital of Duesseldorf
Moorenstr. 5
40225 Duesseldorf
Germany

E-mail: fabian.langenbach@med.uni-duesseldorf.de

Christian Naujoks, M.D.
Department of Oral and Maxillofacial Surgery
Heinrich-Heine University Hospital of Duesseldorf
Moorenstr. 5
40225 Duesseldorf
Germany

E-mail: christian.naujoks@med.uni-duesseldorf.de

Received: February 25, 2009
Accepted: September 21, 2009
Online Publication Date: November 4, 2009

3.2. Generation and differentiation of microtissues from multipotent precursor cells for use in tissue engineering

Langenbach, F.*, Berr, K.*, Naujoks, C.#, Hassel, A., Hentschel, M., Depprich, R., Kubler, N.R., Meyer, U., Wiesmann, H.P., Kogler, G., and Handschel, J (2011). Generation and differentiation of microtissues from multipotent precursor cells for use in tissue engineering. Nat Protoc *6*, 1726-1735.

Impact Factor: 8,363

Durchschnittlicher Impact Faktor des Forschungsgebietes:

- Biochemical Research Methods:
    - 2,340; Rang 4 von 71

Mein Anteil an der Publikation:

- Versuche: 60%
- schriftliche Arbeit: 30%

PROTOCOL

Generation and differentiation of microtissues from multipotent precursor cells for use in tissue engineering

Fabian Langenbach[1,5], Karin Berr[1,5], Christian Naujoks[1], Andrea Hassel[1], Michael Hentschel[1], Rita Depprich[1], Norbert R Kubler[1], Ulrich Meyer[2], Hans-Peter Wiesmann[3], Gesine Kögler[4] & Jörg Handschel[1]

[1]Department of Oral and Maxillofacial Surgery, Heinrich Heine University Medical Center, Düsseldorf, Germany. [2]MKG Münster, Münster, Germany. [3]Institute for Materials Science, Technische Universität Dresden, Dresden, Germany. [4]Institute for Transplantation Diagnostics and Cell Therapeutics, Heinrich Heine University Medical Center, Düsseldorf, Germany. [5]These authors contributed equally to this work. Correspondence should be addressed to C.N. (christian.naujoks@med.uni-duesseldorf.de).

Published online 13 October 2011; doi:10.1038/nprot.2011.394

This protocol describes an effective method for the production of spherical microtissues (microspheres), which can be used for a variety of tissue-engineering purposes. The obtained microtissues are well suited for the study of osteogenesis *in vitro* when multipotent stem cells are used. The dimensions of the microspheres can easily be adjusted according to the cell numbers applied in an individual experiment. Thus, microspheres allow for the precise administration of defined cell numbers at well-defined sites. Here we describe a detailed workflow for the production of microspheres using unrestricted somatic stem cells from human umbilical cord blood and adapted protocols for the use of these microspheres in histological analysis. RNA extraction methods for mineralized microtissues are specifically modified for optimum yields. The duration of running the complete protocol without preparatory cell culture but including 2 weeks of microsphere incubation, histological staining and RNA isolation is about 3 weeks.

© 2011 Nature America, Inc. All rights reserved.

INTRODUCTION

This protocol describes a stepwise procedure for the generation, differentiation and analysis of spherical microtissues from human umbilical cord blood stem cells[1–3]. In the literature, these constructs are also known as cellular spheres, spheroids, multicellular bodies or microspheres; the latter term will be used for the remainder of this protocol. In contrast to former protocols for the generation of spheroids, e.g., for drug testing in tumor biology[4–6], our focus has been on differentiation and the analytical methods needed for the determination of the level of differentiation. The number of cells used for microsphere formation in our protocol lies in a range up to 120-fold higher than the numbers of cells used in drug screen protocols, such as those of Friedrich *et al.*[7]. This results in different treatment of the cultures; although general drug screen tests rely on the stability of a cell type (e.g., tumor cell lines), we recommend generating spheres consisting of viable cells for differentiation into new cell types. Microspheres can serve as a means of differentiation and transfer in a single approach.

The cells used to generate microspheres in this protocol are multipotent human unrestricted somatic stem cells (USSCs), isolated from umbilical cord blood. Microspheres generated from USSCs are particularly well suited for the study of osteogenesis *in vitro*; however, this protocol is also suitable for the generation of microspheres from other cell types, such as embryonic stem cells (ESCs), as previously shown by our group[3], or mesenchymal stem cells (MSCs). Microspheres distinguish themselves by sharing more characteristic features with native tissue than monolayer cultures. Intercellular contacts as well as cell-matrix interactions in microspheres more closely resemble *in vivo* conditions. A previous finding of our group that further highlights the potential of microspheres for the study of osteogenesis *in vitro* is the ability of USSC-derived microspheres to differentiate spontaneously into osteogenic tissues[1,3]. In contrast to monolayer cultures, a three-dimensional (3D) approach accounts for the specific requirements of cells regarding mechanical as well as nutritional aspects present in natural bone. Other studies have revealed that MSCs can also differentiate into osteogenic tissue in a process dependent on the interaction of cells with extracellular matrix proteins such as collagen type I and vitronectin[8]. On the basis of these results, it has been hypothesized that contact of USSCs with extracellular matrix proteins may have a major role in spontaneous differentiation[1,3]. Another trigger for osteogenic differentiation may be the high cell density inside microspheres. In fact, several studies have shown that osteogenic differentiation is restricted or inhibited during cell proliferation, and that higher seeding densities result in increased bone formation *in vivo*[1,3,9]. In addition, expression of runt-related nuclear transcription factor 2 (RUNX2), an osteogenic master regulator, and osteonectin (secreted protein, acidic and rich in cysteine (SPARC)), were found to be upregulated as a consequence of higher cell densities[1,3,10].

Over the last decade 3D cell culture approaches have become increasingly important. The differentiation of cells in 3D cultures shares more features with *in situ* conditions, and cells in 3D cultures reach higher proliferation rates than do cells in monolayer cultures[11–13]. Furthermore, it has been shown that only cells cultured in 3D systems show changes in shape and behavior as a consequence of their ability to respond to specific cell signals[14]. Moreover, gene expression profiles of cells grown in 3D cultures show higher correlation in their gene expression profiles with cells grown *in vivo* compared with those from cells grown in 2D cultures[15]. Extracellular matrices (ECMs) contain various proteins, such as laminins, elastins and collagens, which have major roles in maintaining the mechanical stability of tissues. In cell culture experiments, interactions of ECMs with attaching cells lead to crosstalk between extracellular and intracellular signaling pathways, closely resembling the situation *in vivo*[11]. Receptor molecules belonging to the integrin family serve as mediators of these signals between

ECMs and the associated cellular response[11]. As species- and tissue-specific ECMs are not readily available for cell culture experiments, there is a growing demand for cells that are able to produce their own compatible matrices.

Different approaches have been developed to enable the production of 3D tissues for tissue engineering[11,13,16]. Specific methods for microtissue production include the formation of agglomerates by centrifugation for cartilage engineering[17,18], the establishment of embryoid bodies using either the hanging drop method[19–21] or nonadherent plane culture surfaces, and the production of microtissues using gyratory shakers or spinner flasks for the study of tumor biology[4,22]. For the study of osteogenesis in 3D cultures in this protocol, we use a method for the production of spherical microtissues (i.e., microspheres) that takes advantage of the potential of cells to self-assemble into spheres on nonadherent, concave culture surfaces[1–3,23].

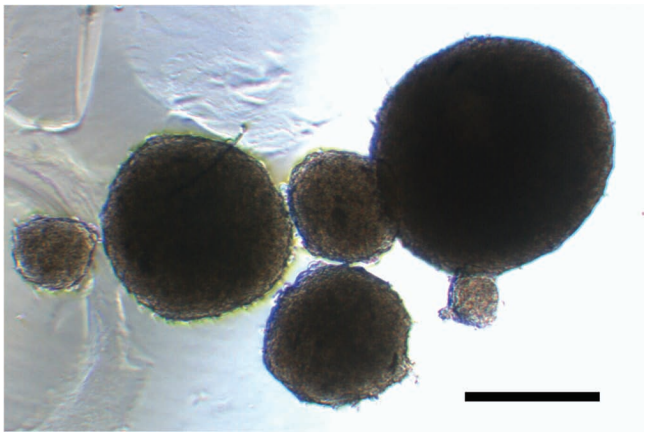

Figure 1 | Microspheres of different sizes. Microspheres consist of 500, 1,000, 2,500, 5,000, 10,000 or 20,000 cells. Scale bar, 500 μm.

Development of the protocol

In general, the method used here is based on the inability of cells to adhere to concave surface profiles of culture vessels. This method takes advantage of the tendency of an aqueous solution to form a meniscus in the culture vessel by adhesion to the wall of the well. On the concave surface of either hydrogel-coated 96-well plates[1,3,7] or round-bottomed nonadhesive well plates[23], plated cells will aggregate in the center of the wells[24]. Thus, the general principle of this method is comparable to the preparation of spheres from hanging drops. In both cases, a curved surface is essential. However, the main advantage of the method used in this protocol, compared with hanging drop protocols, lies in simplified plate handling. This is further supported by the findings of Hildebrandt *et al.*[25], who demonstrated that the cultivation of human MSCs in 96-well nonadhesive plates allows for efficient production of homogenous cellular aggregates compared with rotation culture and hanging drop technique. Both hydrogel-supported cultures and cultures grown in round-bottomed plates are less prone to loss through sudden movements than are hanging drop cultures, and they can safely be handled by laboratory workers with less experience in maintaining spheroids.

The method used here is suitable for the generation, osteogenic differentiation and analysis of cellular microspheres of various sizes. In previous experiments[1,3] from our group, cellular spheres created from 1.8×10^5 cells were characterized, and the suitability of this method for the generation of smaller microspheres has also been shown (**Fig. 1**). Other groups have produced smaller microspheres, ranging from several hundred cells to 1×10^4 cells[23]. We use a range of initial cell densities from 1×10^4 up to 1.8×10^5 cells per microsphere, with diameters from 150 μm to 1.0 mm. This size variability is important for microspheres, which will be implanted in scaffold pores for *in vivo* use (e.g., in an insoluble collagenous bone matrix (ICBM) scaffold; see **Supplementary Fig. 1** (refs. 2,23)). Microsphere dimensions can be readily adjusted by choosing the appropriate initial number of cells per well. However, maximum microsphere size is restricted by nutritional supply limitations. Aside from the research focus of stem cell–based microspheres, one difference from other protocols[7] is the concentration of the agarose used to coat wells in which the microspheres are grown. We use a 2% (wt/vol) agarose solution, resulting in an increased gel strength. Good gel stability is important for further culture of the spheres. The high gel strength in our protocol makes the agarose less prone to damage during medium change when a pipette tip comes in contact with the surface of the gel.

For the osteogenic differentiation, standard growth medium is supplemented with dexamethasone to promote osteogenic differentiation, ascorbic acid to support collagen synthesis and β-glycerol phosphate to provide a source of phosphate for the mineralization[26,27]. For histological evaluation of microsphere differentiation, the frequently used technique is alizarin red S staining. However, as this stain detects not only calcium in calcium phosphate but also calcium-binding proteins and proteoglycans[28], a second staining method is used that specifically stains hxdroxyapatite. For this purpose, we describe how to modify the protocol of a commercial hydroxyapatite-specific fluorescence dye staining kit. Changes in gene transcription profiles of differentiating stem cells can be investigated through the analysis of mRNA expression levels. For optimum yields, protocols for the extraction of mRNA should be adapted to the requirements of specific tissues. The specific properties of mineralized tissues are taken into account in the description of extraction methods for RNA; we use TRIzol instead of column-based RNA extraction kits, which may get clogged with calcium phosphate particles. Subsequently, RNA cleanup is necessary in order to remove residual TRIzol, proteins or other contaminants.

Applications of the method

Although microspheres have been used for several decades, their use for tissue engineering has only recently gained more importance. Spheres are used in various tissue-engineering approaches of different research areas. Cardiac myocytes are reaggregated to spheroids and examined for their response to the influence of electromagnetic fields[29]. Spheroids consisting of reaggregated hepatocytes are used in a model system of an artificial liver[30]. Moreover, interactions of membranes with microspheres consisting of periodontal fibroblasts are investigated in biocompatibility studies[31]. In microspheres, a faster accumulation of triglycerides is detectable during adipogenesis compared with the rates found in two-dimensional cultures[32]. Aggregation of MSCs into spheroids enhances their anti-inflammatory properties[33], and microvessel formation *in vivo* is achieved by the use of spheroids[34]. Microspheres are successfully used in chondrogenic tissue engineering where the secretome and chondrogenic potential of spheres consisting of MSC from umbilical cord blood is analyzed[35]. Cocultures of

© 2011 Nature America, Inc. All rights reserved.

articular chondrocytes and bone marrow MSCs in microspheres are applied to investigate stable neocartilage formation[36]. Recent unpublished findings of our group indicate that microspheres of *in vitro* expanded articular chondrocytes have substantial positive impact on the healing of cartilage defects *in vivo* (**Supplementary Fig. 2**). In addition to these multiple tissue-engineering approaches, applications in developmental biology are described. Here spheroid cultures are applied as model systems for the differentiation of ESCs. Conley *et al.*[37] suggest that embryoid bodies recapitulate various aspects of early development and are capable of triggering developmental programs for the induction of all three germ layers. Therefore, embryonic body formation has been used as an initial step in several studies intending to differentiate ES cells into specific cell types.

A key role of 3D spheroid culture methods in osteogenic tissue engineering was demonstrated by Wang *et al.*[38] by substantially improving differentiation efficiency through the use of spheroid-based approaches. Microspheres allow for the precise administration of defined cell numbers to any site on a porous scaffold or surface, while at the same time enabling the creation of any desired seeding pattern. In previous work from our group, insoluble collagenous bone matrix scaffolds implanted with microspheres have been shown to mediate ectopic bone formation upon implantation in rat muscle bags, whereas scaffolds implanted without cells did not lead to bone formation[2]. In this study, the reproducibility and robustness of bone tissue engineered using microspheres and ICBM scaffolds was also demonstrated; 1 month after implantation of microsphere-ICBM constructs in 30 immunocompromised rats, a mean volume of mineralization of 151.3 ± 15 mm^3 was measured by computer tomographic scans. With the help of microspheres, cell numbers that can be added to biomaterials exceed by far the numbers in current applications relying on the applications of cell suspensions. Furthermore, microspheres offer several advantages for cell delivery without a scaffold. Because of their larger size, microspheres are not as susceptible to washout as single cells, and, because of increased ECM production, they are substantially more adhesive than monolayer cultures or single cells[39,40].

Limitations of the method

Limitations of the method are that the cell line used must be able to develop toward the desired lineage and the supplements used must be able to initiate differentiation processes; therefore, the protocol must be adapted to the specific situation in each experiment. This protocol is not restricted to cord blood cells, as long as the cells used fulfill the above-mentioned requirements. In general, any cell population that is able to retain its specific features under the conditions of this protocol and that is able to differentiate into desired lineages should be suitable. To date, the described method of microsphere formation has been set up only for the production of small batches. For high-throughput or automated production, problems with losing microspheres during medium change may occur. With the use of multichannel pipettes the workload of producing microspheres can be reduced. A further limitation of the method lies in the relatively large cell numbers that are needed for the production of the spheres. This makes the initial cell culture time consuming and expensive. The technology may have different outcomes when using different cell lines, requiring adaptations for mass production.

MATERIALS

REAGENTS

- USSCs: cryopreserved (obtained from the group of G. Kögler, José Carreras Cord Blood Bank, Düsseldorf, Germany) ! CAUTION Adhere to all relevant ethical guidelines when working with human tissues. Ensure that informed consent is obtained from donors or their legal guardians.
- Agarose (Biozyme, cat. no. 840100)
- Alizarin red S (1,2-dihydroxy-anthraquinone; Sigma-Aldrich, cat. no. A5533-25G) ! CAUTION It is an irritant (R: 36/37/38); wear suitable protective clothing.
- Ascorbic acid (Sigma-Aldrich, cat. no. A5960) ▲ CRITICAL Protect ascorbic acid from light and contact with metals, as it will be readily oxidized.
- Chloroform (VWR Merck, cat. no. 22711.324) ! CAUTION It is harmful (R: 22-38-40-48/20/22); wear dust mask, eye shield and gloves.
- Dexamethasone (Sigma-Aldrich, cat. no. D8893) ! CAUTION It is an irritant (R: 43); wear eye shield and gloves.
- Disodium tetraborate, anhydrous (VWR Merck, cat. no. 1.06306.0250) ! CAUTION It is toxic (R60-61); avoid exposure, wear dust mask, eye shield and gloves.
- DMEM (Lonza, cat. no. BE707-12F)
- Distilled water, DNase/RNase free (Gibco, cat. no. 01977-035)
- Entellan (VWR Merck, cat. no. 1.07961.0100) ! CAUTION It is harmful (R: 10-20/21); avoid contact with eyes and skin, wear gloves.
- Ethanol ACS (Merck, cat. no. 1.00983.2511) ! CAUTION It is flammable.
- Denatured ethanol ! CAUTION It is flammable.
- Fetal calf serum (FCS; Pan, cat. no. 2602-P290310)
- Formalin (Merck, cat. no. 1.00496.5000) ! CAUTION It is harmful (R: 20/21/22-40-43); avoid contact with eyes and skin, wear gloves.
- Hydrochloric acid (Roth, cat. no. 4625.1) ! CAUTION It is corrosive (R: 34-37); wear protective gloves and eye shield, and work under a fume hood.
- Isopropyl alcohol (Merck, cat. no. 1.09634.2511) ! CAUTION It is flammable and an irritant (R: 11-36-67); avoid eye and skin contact.
- L-Glutamine (Biochrom AG, cat. no. K0283)
- Masson-Goldner trichrome staining kit (Merck, cat. no. 1.00485.0001)
- OsteoImage mineralization assay (Lonza, cat. no. PA-1503)
- Paraffin (Merck, cat. no. 1.07337.1000)
- Phosphate-buffered saline (PBS; Gibco, cat. no. 14190-169)
- Penicillin-streptomycin (Biochrom AG, cat. no. A2213)
- Roti-MountFluor care DAPI (Roth, cat. no. HP20.1)
- TRIzol reagent (Invitrogen, cat. no. 15596-026) ! CAUTION It is toxic and corrosive (R: 23/24/25-32-34-48/20/21/22-52/54-68); avoid contact with skin and eyes, wear suitable protective clothing, gloves and eye/face protection.
- Trypsin (2.5%, Lonza, cat. no. BE17-160E) ! CAUTION It is harmful (R: 36/37/38-42); wear suitable protective clothing and gloves.
- Weigert's iron hematoxylin kit (Merck, cat. no. 1.15973.0001)
- Xylene (Merck, cat. no. 1.08685.2500) ! CAUTION It is an irritant (R: 10-20/21-38); avoid contact with eyes.
- β-Glycerol phosphate (Sigma-Aldrich, cat. no. G9891) ! CAUTION Avoid contact with eyes and skin.
- β-Mercaptoethanol (Bio-Rad, cat. no. 1610710) ! CAUTION It is toxic and dangerous for the environment (R: 22-23/24-34-51/53); avoid contact with eyes and skin, wear suitable clothing and an eye shield. Dispose of it properly.
- RNeasy MinElute cleanup kit (Qiagen, cat. no. 74204)

EQUIPMENT

- Gassed incubator (Heraeus, model: Cytoperm 2; http://thermoscientific.com/wps/portal/ts/products/detail?navigationId=L10468&categoryId=81876&productId=12703809)

© 2011 Nature America, Inc. All rights reserved.

- Gassed incubator (Heraeus, model: HERAcell 240; http://www.djblabcare.co.uk/djb/product/2243/Incubators-51019557-Heraeus_HERAcell_240)
- Drying oven (Universal oven, Memmert, model: UNB 400; http://www.memmert.com/en/products/universal-oven/universal-ovens-models/models/UNB-400/)
- Sliding microtome (Leica, model: SM 2000 R; http://www.leica-microsystems.com/products/total-histology/sectioning/sliding-microtomes/details/product/leica-sm2000-r/)
- Safety cabinet (VWR, Heraeus, model: Herasafe KS15)
- Centrifuge (Heraeus, model: Multifuge 1 S-R; http://www.heraeuscentrifuge.co.uk/multifuge1sr.html)
- Fluorescence microscope (Leica, model: DM5000B; http://www.leica-microsystems.com/products/light-microscopes/life-science-research/fluorescence-microscopes/details/product/leica-dm5000-b/)
- Software (Leica Application Suite; http://www.leica-microsystems.com/products/microscope-software/imaging-software/details/product/leica-application-suite/)
- Fluorescence camera (Leica, model: DFC420C; http://www.leica-microsystems.com/products/microscope-cameras/life-science/details/product/leica-dfc420-c/)
- Inverted microscope (Leica, model: DM IL LED; http://www.leica-microsystems.com/products/light-microscopes/life-science-research/inverted-microscopes/details/product/leica-dm-il-led/)
- pH meter (HANNA instruments, model: pH 211; http://www.hanna-de.de/produits.asp?langue=de&famille=3&type=7&modele=382)
- Water bath (neoLab, model: WBS30; http://www.neolab.de/nshopartdetails.do?kgrpId=4521)
- Solution basin (Biozyme, cat. no. 675002)
- Microtome blades (low-profile blades, Leica, cat. no. 819)
  ! CAUTION Handle with care to avoid danger of incised wounds.
- Embedding cassettes (Neolab, cat. no. 7-0013)
- Charged slides (SuperFrost Plus, VWR, cat. no. 631-0449)
- Cell pestles, DNase/RNase free (VWR, cat. no. 431-0094)
- Sterile filter (GV Filter unit 0.22 µm; MILLEX cat. no. SLGU033RS)
- Filter paper (Grade 589/2, ashless; Whatman, cat. no. 10300106)
- Multichannel pipette (Biohit, Model M100 and M300)
- Glassware (Duran)
- Parafilm (Pechiney)
- Microcentrifuge tubes (Eppendorf, cat. no. 022363204)
- Reagent tubes (50 ml, BD Falcon, cat. no. 352070)
- Cell culture flask (75 cm^2, Greiner BioOne, Cellstar, cat. no. 658 175)
- 96-well plates (Greiner BioOne, Cellstar, cat. no. 655 180)
- Spectrophotometer

REAGENT SETUP

Growth medium Combine DMEM (68%, vol/vol), 30% (vol/vol) FCS (heat inactivated for 30 min at 56 °C), 1% (vol/vol) penicillin-streptomycin and 1% (vol/vol) L-glutamine. Growth medium can be stored for 1 month at 4 °C in the dark.

FCS Before use, FCS needs to be inactivated. Incubate for 30 min in a water bath at 56 °C. Inactivated FCS can be aliquotted in desired portions and stored for 2 months at −20 °C.

Trypsin (2.5%, vol/vol) Combine trypsin (10%, vol/vol) (2.5%) and 90% (vol/vol) PBS. This solution is stable for several months at 4 °C.

Dexamethasone solution (50 µM) Dissolve 10 mg dexamethasone in 10 ml of absolute ethanol ACS. This dexamethasone/ethanol solution can be stored at −80 °C for several months. Add 1 ml of dexamethasone/ethanol solution to 49 ml of growth medium. This solution is stable for 1 week at 4 °C.

Ascorbic acid solution (50 mM) Dissolve 880 mg of ascorbic acid in 100 ml of PBS. Pass the solution through a sterile filter into two sterile 50-ml reaction tubes. If protected from light, this solution is stable up to 4 weeks at 4 °C. **▲ CRITICAL** If its color changes to yellow, discard the solution.

β-Glycerol phosphate solution (1 M) Weigh out 5.6 g of β-glycerol phosphate and fill up to 20 ml with PBS. Pass the solution through a sterile filter into a sterile 50-ml reaction tube. This solution is stable for 1 week at 4 °C. **▲ CRITICAL** β-Glycerol phosphate takes up volume. First, add 10 ml of PBS and let β-glycerol phosphate dissolve completely before filling up to 20 ml.

Dexamethasone, ascorbic acid and β-glycerol phosphate (DAG) medium Growth medium is supplemented with 100 nM dexamethasone solution, 50 µM ascorbic acid and 10 mM β-glycerol phosphate. Transfer 40 ml of growth medium into a 50-ml reaction tube and add 80 µl dexamethasone solution (50 µM), 40 µl ascorbic acid solution (50 µM) and 400 µl β-glycerol phosphate solution (1.00 M). If protected from light, this solution is stable for 1 week at 4 °C.

Ethanol dilutions If not stated otherwise, ethanol dilutions are prepared with 99.5% (vol/vol) denatured ethanol and distilled water. Ethanol dilutions used for RNA isolation are prepared with ethanol ACS and DNAse/RNase-free water (distilled water). In tightly shut flasks these solutions are stable for several months at room temperature (RT; 22–23 °C).

RLT/β-mercaptoethanol buffer (RNeasy MinElute cleanup kit) This buffer is composed of 1% (vol/vol) β-mercaptoethanol and 99% (vol/vol) buffer RLT (from RNeasy MinElute cleanup kit). This solution is stable for 1 month when stored at RT.

Buffer RPE (RNeasy MinElute cleanup kit) This buffer is composed of buffer RPE concentrate (20%, vol/vol) and 80% (vol/vol) ethanol ACS 100% (vol/vol). This solution must be freshly prepared.

OsteoImage wash buffer Mix wash buffer stock solution (10%, vol/vol) and 90% (vol/vol) distilled water. This solution must be freshly prepared.

OsteoImage staining reagent Mix OsteoImage staining reagent (1%, vol/vol) and 99% (vol/vol) staining reagent dilution buffer. This solution must be freshly prepared.

Alizarin red S solution (2%, wt/vol) Dissolve 2 g of alizarin red S in 100 ml of distilled water. Use a pH meter to adjust the pH value to 4.5 by adding 1 M hydrochloric acid and checking constantly. This solution is stable for several months at RT. If the pH has changed over storage time, discard the solution and freshly prepare.

Weigert's iron hematoxylin kit Mix 100 ml of solution A with 100 ml solution of B prior to use. This solution must be freshly prepared.

Masson-Goldner trichrome staining kit Prepare 800 ml of 1% (vol/vol) acetic acid by diluting 10% (vol/vol) acetic acid to 1:10. This solution is stable for several weeks at RT in a tightly shut laboratory flask. Note: Azophloxin solution and tungstophosphoric acid orange G solution are ready-to-use components of this kit.

Tris-HCl (10 mM, pH 8) Dissolve 0.121 g of Tris in 100 ml of DNase/RNase-free water and adjust the pH value to 8 with 1 M HCl. This solution is stable for several weeks at 4 °C.

PROCEDURE

Thawing the cells ● TIMING 1 h

1| Take cryopreserved MSCs (e.g., USSC) out of liquid nitrogen, thaw the cells at 37 °C in a water bath and wash with a tenfold volume of growth medium (see REAGENT SETUP) to dilute the DMSO; centrifuge at 470*g* for 7 min at 4 °C. We recommend plating out 2 million cells and distributing them into three 75-cm^2 cell culture flasks, each containing 15 ml of growth medium. Make sure to resuspend the cells completely by pipetting up and down because remaining cell clumps will build very dense cell clusters in culture. This confluence of cells can start up a differentiation process.

▲ CRITICAL STEP To avoid fungal and bacterial contamination whenever exposing cells and solutions to air, work under sterile conditions by using a flow hood.

? TROUBLESHOOTING

© 2011 Nature America, Inc. All rights reserved.

PROTOCOL

2| Place the plates into a gassed incubator (37 °C, 5% CO_2, 20% O_2) and allow the cells to attach.

3| Exchange the medium 12–24 h after plating because dead cells and their degradation products may inhibit cell growth. Subsequently, change the complete medium twice a week using growth medium warmed to 37 °C.

Splitting cells ● TIMING 1 h

4| When a cell confluence of 90% is reached, remove the medium with a pipette and wash the cells once with 15 ml of PBS. Remove the PBS, add 15 ml of fresh PBS and incubate for 7 min at 37 °C. This step is essential for gentle detachment of the cells because residual FCS may inhibit trypsin activity.

5| Remove the PBS and add 7 ml of 0.25% (vol/vol) trypsin solution (see REAGENT SETUP) and incubate for 8 min at 37 °C. Before proceeding to the next step, observe the cells with an inverted microscope. If a considerable portion of the cells has not yet detached from the flask, the incubation time can be extended up to 10 min.
? TROUBLESHOOTING

6| Transfer 8 ml of growth medium to the cell suspension to inhibit the trypsin solution, and then rinse the bottom of the flask by pipetting the suspension up and down.

7| Transfer the cells into a 50-ml reaction tube and centrifuge at 470*g* for 7 min at 4 °C.

8| Resuspend the cell pellet with growth medium and split the cells at a ratio of 1:4. Cultivate cells to a number of at least 3×10^6 cells for the generation of 15 microspheres intended for mRNA isolation and histology. Ten microspheres (1.8×10^6 cells) will be needed for the isolation of 3–6 µg of total RNA, and five microspheres (9×10^5 cells) will be needed for histological analyses. We recommend preparing some microspheres in excess, as microspheres may get lost during cell culture or sample embedding.

Preparing USSC microspheres ● TIMING 24 h

9| Add 2 g of agarose to 100 ml of DMEM in a 200-ml glass bottle and autoclave for 20 min at 115 °C and 210 kPa; let the solution cool down to 70 °C.
! CAUTION Protect your skin against the hot glass bottle.

10| Pipette 60 µl of the liquid into each well of a 96-well plate using a multichannel pipette and a solution basin.
▲ CRITICAL STEP Make sure to pipette the correct volume into the wells. Work in accordance with the recommendations of the pipette manufacturer for handling viscous solutions. Work quickly to avoid solidification of the solution in the bottle before you have finished dispensing.

11| Let the agarose solution in the wells solidify and cool down for 1 h. Meanwhile, detach the cultivated cells from Step 8 as described in Steps 4–7, by applying trypsin solution after rinsing with PBS. Count the cells and adjust the cell concentration to 1×10^6 cells per ml using growth medium.

12| Pipette 180 µl of this suspension per well into an agarose-coated 96-well plate from Step 10, omitting the marginal wells, and then incubate the plate at 37 °C with 20% O_2 and 5% CO_2. After 24 h, the microspheres will have reached sufficient stability for further processing.
▲ CRITICAL STEP In long-term culture, the marginal wells may dry out or the concentration of the liquid within may be changed because of evaporation.

Osteogenic differentiation of USSC microspheres ● TIMING 14 d

13| Substitute the growth medium after 24 h with DAG medium (see REAGENT SETUP) or normal growth medium (e.g., serving as an untreated control). We recommend adjusting the volume of a single-channel pipette to 160 µl to remove the old medium. When adding fresh medium, add 165 µl to each well to compensate for losses from evaporation. Exchange growth medium every second day.

Harvesting microspheres ● TIMING 10 min

14| Use a 5-ml pipette to harvest the microspheres.
▲ CRITICAL STEP We advise against using a single-channel pipette with a 1,000-µl tip because the shear force that develops during adsorption may damage the microspheres.

© 2011 Nature America, Inc. All rights reserved.

15| Take up at least 15 microspheres per sample and transfer them into a 1.5-ml microcentrifuge tube.

16| Remove most of the remaining medium carefully and wash the microspheres once with PBS. Transfer ten microspheres for RNA isolation and five microspheres for histology to separate microcentrifuge tubes.
■ **PAUSE POINT** The microspheres can be deep-frozen at −80 °C and stored for several months before RNA extraction (Step 17A), or they can be fixed with 4% (vol/vol) formalin for histological methods (Step 17B).
! **CAUTION** Work under a fume hood for protection against the evaporating formalin.

RNA extraction or analysis of microspheres ● TIMING variable; up to 3 d
17| The microspheres can be used for RNA extraction (option A) or analyzed by histological methods (option B):
(A) RNA extraction ● TIMING ~3 h
(i) *Isolation of total RNA from microspheres with TRIzol reagent*. Take the microspheres out of the −80 °C freezer, place them on ice and grind the cold cells with a sterile cell pestle.
! **CAUTION** Work under a fume hood for protection against evaporating TRIzol and chloroform.
▲ **CRITICAL STEP** While isolating or working with RNA, make sure to follow general advice to avoid RNase contamination.
(ii) Add 0.5 ml TRIzol reagent into the microcentrifuge tube, mix by pipetting up and down and incubate for 5 min at RT.
(iii) Add 80 µl of chloroform, shake the tubes gently by inverting several times and incubate for 3 min at RT.
(iv) Centrifuge for 15 min at 12,000*g* at 4 °C and transfer the upper (aqueous) phase into a fresh 1.5-ml tube.
▲ **CRITICAL STEP** Make sure not to disturb the phase separation. This may lead to contamination of the upper, aqueous phase with the lower phase containing proteins and DNA.
(v) Transfer 200 µl of isopropyl alcohol into the tube with the aqueous phase containing the RNA, mix well by pipetting up and down and incubate for 10 min at RT.
(vi) Centrifuge for 10 min at 12,000*g* at RT, discard the supernatant and wash the pellet with 200 µl of 75% (vol/vol) ethanol.
(vii) Centrifuge for 5 min at 7,500*g* at RT and carefully remove the supernatant.
▲ **CRITICAL STEP** It is useful to keep the position in which the tubes are put into the centrifuge in mind, as the pellet sometimes is hard to see after centrifugation.
(viii) Let the remaining alcohol evaporate and dissolve the pellet in 40 µl of DNase/RNase-free water by incubating for 10 min at 56 °C.
▲ **CRITICAL STEP** Do not let the pellet dry completely, as it will be very difficult to dissolve afterwards.
■ **PAUSE POINT** Samples can be stored at −80 °C for at least 1 month.
(ix) *Concentration and purification of RNA with the Qiagen RNeasy MinElute cleanup kit*. Add 60 µl of DNase/RNase-free water to adjust the sample volume to 100 µl.
! **CAUTION** Work under a fume hood for protection against evaporating β-mercaptoethanol.
(x) Add 350 µl of buffer RLT/β-mercaptoethanol (see REAGENT SETUP) to the sample and mix well by pipetting up and down.
(xi) Add 250 µl of ethanol and mix again.
▲ **CRITICAL STEP** Do not work on ice. Components of the buffers may precipitate.
(xii) Take an RNeasy MinElute spin column fitted to a 2 ml collection tube and transfer the whole sample volume onto its membrane.
(xiii) Centrifuge for 15 s at 8,000*g* at RT and discard the flow-through.
! **CAUTION** As the flow-through contains buffer RLT, which can form highly reactive compounds with peroxides (e.g., hydrogen peroxide), make sure peroxides and acidic solutions are not discarded in the same waste container.
(xiv) Place the RNeasy MinElute spin column into a new collection tube, add 500 µl of buffer RPE (see REAGENT SETUP), centrifuge at 8,000*g* for 15 s at RT and discard the flow-through.
(xv) Add 500 µl of 80% (vol/vol) ethanol onto the RNeasy MinElute spin column and centrifuge for 2 min at 8,000*g* at RT.
▲ **CRITICAL STEP** When removing the spin column from the collection tube, be sure not to carry over ethanol by bringing the spin column into contact with the flow-through.
(xvi) Put the RNeasy MinElute spin column into a new collection tube and centrifuge it at full speed for 5 min with an open lid. The opened lid allows the ethanol to flow through the column completely.
(xvii) Put the RNeasy MinElute spin column into a new collection tube and add 14 µl of RNase-free water. Centrifuge for 1 min at full speed at RT. The final sample volume will be 12 µl because 2 µl will remain on the membrane.
▲ **CRITICAL STEP** Make sure you pipette the water directly onto the top of the column.
(xviii) Assess the purity of the RNA by diluting 1 µl of the RNA with 99 µl of 10 mM Tris-HCl (pH 8) (see REAGENT SETUP) and measure the 260 nm/280 nm and 260 nm/230 nm optical density (OD) ratios with a spectrophotometer. High RNA quality has a 260 nm/280 nm ratio of >2 and a 260 nm/230 nm ratio of >1.8. As the absorption maximum of proteins is 280 nm, a low 260/280 ratio is an indicator of protein contamination.

© 2011 Nature America, Inc. All rights reserved.

PROTOCOL

■ **PAUSE POINT** Samples can be stored at −80 °C or immediately processed.
? TROUBLESHOOTING

(B) Histological analysis ● TIMING ~2 h to up to 2–3 d

(i) *Fixation and embedding in paraffin for histological studies.* Cut two sheets of wetted filter paper into shape; use one to line the bottom of a paraffin embedding cassette and place the microspheres (from Step 16) on it. Cover them with a second sheet and close the cassette.

(ii) Fix the microspheres in 4% (vol/vol) buffered formalin overnight.

(iii) Put the cassette with the microspheres into a beaker and wash the samples with running tap water for 1 h.

(iv) Put the cassette with the microspheres into a beaker filled with 50% (vol/vol) ethanol and incubate for 1 h at RT. Repeat this step with 70% (vol/vol) ethanol, 90% (vol/vol) ethanol, 96% (vol/vol) ethanol, isopropanol and then twice with xylene.

(v) Incubate the microspheres twice in liquid paraffin for 1 h at 60 °C.
! CAUTION Protect your skin from the hot paraffin.

(vi) Place a small amount of fresh liquid paraffin into a prewarmed embedding form and transfer the microspheres into the embedding form using prewarmed tweezers or a pipette; allow the microspheres to sink down. Cover the embedding mold with the lower part of the embedding cassette and fill it up with paraffin. Put the embedding mold on ice until the paraffin is solidified.

© 2011 Nature America, Inc. All rights reserved.

BOX 1 | HISTOLOGICAL STAINING OPTIONS

For general information on cellular and extracellular structures, choose Masson-Goldner trichrome staining; to show hydroxyapatite mineral, perform an OsteoImage stain; and for information on calcium-rich regions, apply the Alizarin red S stain.

Masson-Goldner trichrome staining

1. Incubate the slides for 5 min in Weigert's iron hematoxylin solution (see REAGENT SETUP).
! CAUTION Wear gloves to protect your skin from the staining solutions.
2. Rinse for 3 min in running tap water.
3. Incubate for 30 s in 1% (vol/vol) acetic acid.
4. Incubate in azophloxin solution (in Masson-Goldner staining kit) for 10 min at RT and immediately transfer for 30 s to 1% (vol/vol) acetic acid.
5. Incubate for 1 min at RT in tungstophosphoric acid orange G solution (in Masson-Goldner staining kit) and immediately transfer for 30 s to 1% (vol/vol) acetic acid (see REAGENT SETUP).
6. Incubate for 2 min at RT in light-green SF solution (in Masson-Goldner staining kit). Immediately rinse for 30 s in 1% (vol/vol) acetic acid.
7. Dehydrate the sections by incubating them in 70% (vol/vol) ethanol for 5 s, 96% (vol/vol) ethanol for 5 s and in absolute ethanol for 2 min.
▲ CRITICAL STEP Make sure not to let the slides sit for too long in low-percentage alcohols, as these will wash out the light-green SF.
8. Incubate twice for 5 min in xylene and place one drop of Entellan directly onto the section; carefully put a cover glass onto it and let it dry.
9. Place the slide under a bright-field microscope at appropriate magnification (100–200-fold) to assess the staining of each specimen. Collagen is stained with the light-green SF dye, cytoplasm appears red and nuclei are stained black.

OsteoImage staining

1. Rinse the slides with OsteoImage wash buffer (see REAGENT SETUP) and transfer 100 µl of OsteoImage staining reagent (see REAGENT SETUP) to each section on the slides. Cover the slides with Parafilm to ensure even distribution of the staining reagent.
2. Incubate for 30 min at RT while protecting the slides from light. Afterward, discard the supernatant by shaking it off the slides.
3. Wash three times with 200 µl OsteoImage wash buffer for 5 min protected from light.
4. Cover the slides with one drop of Roti-Mount and carefully lay a cover slip on the slides. Roti-Mount is a mounting medium that includes a DNA-specific dye (DAPI).
5. Observe the fluorescence of the OsteoImage reagent with a fluorescence microscope using an excitation wavelength of 492 nm and the blue-stained nuclei at an excitation wavelength of 355 nm.

Alizarin red S staining

1. Incubate the slides for 2 min in alizarin red S solution at RT.
2. Rinse the slides with distilled water until no more color drains out of the sections.
3. Dehydrate the slides by putting them in 70% (vol/vol), 96% (vol/vol) and absolute ethanol for 3 min each and twice in xylene for 5 min. Afterwards, cover them with Entellan as described above in this box (step 8; Masson-Goldner trichrome staining).
4. Examine stained sections under a bright-field microscope (magnification 100–200-fold) to asses the staining of each specimen. Calcium-rich regions appear dark red.
? TROUBLESHOOTING

(vii) *Preparation of sections for staining.* Use single-use blades to cut 4-µm-thick sections with a paraffin microtome.
(viii) Carefully place the sections on the surface of a 37 °C prewarmed water bath for flattening. Collect two sections per charged slide.
(ix) Place sections in a drying oven for 20 min at 70 °C and leave them overnight at 56 °C.
▲ **CRITICAL STEP** This step is important, as it increases the affinity of the section to the slide during further treatment.
(x) Incubate the slides twice for 5 min in xylene, for 3 min in ethanol, for 3 min in 70% (vol/vol) ethanol and for 3 min in distilled water. Continue with histological staining options as described in **Box 1**.

? TROUBLESHOOTING

Troubleshooting advice can be found in **Table 1**.

TABLE 1 | Troubleshooting table.

Step	Problem	Possible reason	Solution
1	Low numbers of living cells and high content of cell debris in the medium after thawing the cells	Diluting the thawed cell suspension with a tenfold amount of fresh medium took too long	Immediately dilute the thawed cells after thawing
5	Cells do not detach with trypsin	Poor batch of trypsin Trypsin has expired Cells are differentiated	Use a higher concentration of trypsin (2×) Use a freshly prepared trypsin dilution Use a new cell culture
17A(xviii)	Low RNA quality in terms of 260/280 and 260/230 ratios	Separation of the phases in Step 17A(iv) was not appropriate	Repeat RNA cleanup
	No or low RNA	You may have lost the RNA pellet RNases may have degraded the RNA	Repeat the RNA isolation Make sure to follow the guidelines for working with RNA
Box 1	Fractures in the microsphere sections	Paraffin embedding was not appropriate	Increase incubation times in alcohol and paraffin
		Microtome blade is not sharp enough	Use a new blade
	Weak fluorescence signal in the OsteoImage-stained microspheres	The fluorescence was bleached out	Protect the sample slides from light

© 2011 Nature America, Inc. All rights reserved.

● TIMING

Steps 1–3, Thawing cells: ~1 h
Steps 4–8, Splitting cells: ~1 h
Steps 9–12, Preparing the microspheres: 24 h
Step 13, Osteogenic differentiation of the microspheres: 14 d
Steps 14–16, Harvesting the microspheres: 10 min
Step 17A(i–viii), Isolation of RNA from microspheres: 1.5 h
Step 17A(ix–xviii), Concentration and purification of RNA: 1.5 h
Step 17B(i–vi), Embedding of microspheres: 1.5 h
Step 17B(vii–ix), Preparation of the sections: 2–3 d
Step 17B(x), Deparaffinization and rehydration of the slides: ~20 min
Box 1, Masson-Goldner trichrome staining: 30 min
Box 1, OsteoImage: 1 h
Box 1, Alizarin red S staining: 30 min

ANTICIPATED RESULTS

One day after seeding cells on hydrogel-coated 96-well plates as described above, microspheres will spontaneously form in the central cavity. These microspheres will appear as a uniformly shaped cell mass (**Fig. 1**). At that point they will have sufficient stability to withstand manipulations, such as medium changes or transfers to other vessels. For vessel transfer, the

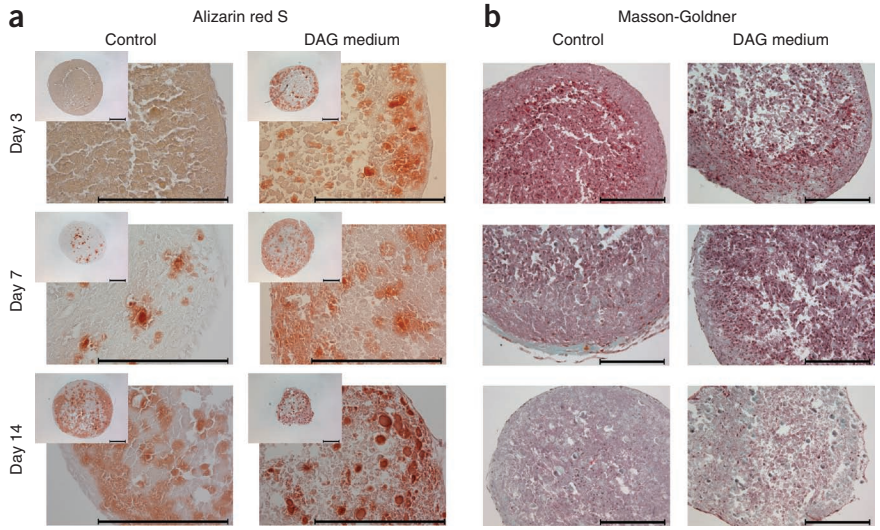

Figure 2 | Histological stains of microsphere sections after 3, 7 and 14 d of differentiation. Differentiation is shown with DAG medium and without DAG (control). (**a**) Alizarin red S (Image acquisition: inserted images exposure time 29.3 ms, large images exposure time 70 ms) binds to calcium-rich regions, resulting in a strong dark-red staining. Calcium is the principal component of hydroxyapatite, therefore a positive staining with alizarin red S serves as an indicator of mineralization processes. (**b**) Masson-Goldner (Image acquisition: exposure time 25.4 ms) staining; the light-green SF dye in the Masson-Goldner staining binds to collagen, which is the predominant molecule of the nonmineralized portion of bone that is built up by osteoblasts. Detection of collagen by light-green SF is an indicator for early differentiation processes of stem cells into osteoblasts. Scale bars, 200 μm.

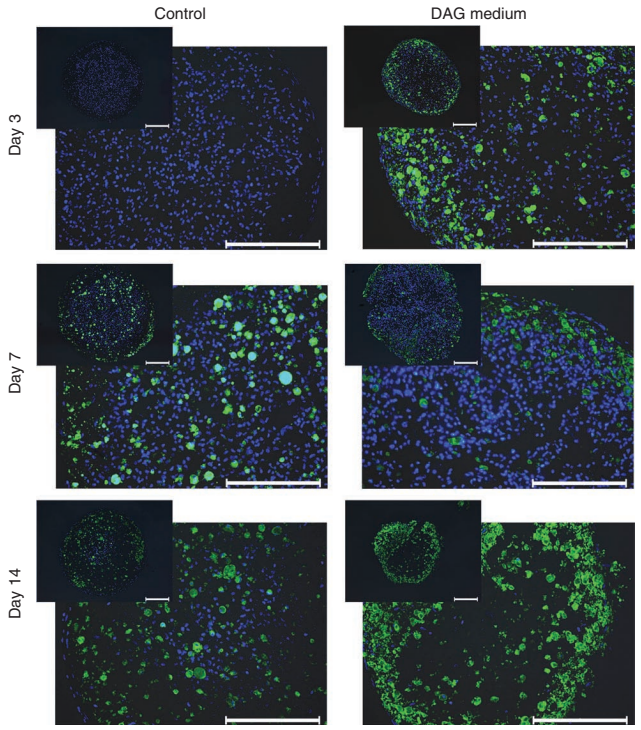

Figure 3 | Fluorescent stain (OsteoImage) of microsphere sections after 3, 7 and 14 d of differentiation. Differentiation is shown with DAG medium and without DAG (control). Cell nuclei appear blue (4,6-diamidino-2-phenylindole (DAPI)), mineralized areas are green. The OsteoImage dye specifically binds to hydroxyapatite and therefore is more sensitive than Alizarin red S, which binds to calcium. Blue (DAPI exc: 355 nm, em: 460 nm) and green (fluorescein isothiocyanate exc: 492 nm, em: 530 nm). Exposure time for DAPI is 250 ms in the inserted images and 205 ms in the large images. Exposure time for green fluorescence is 205 ms in the inserted images and 154 ms in the large pictures. Bright-field exposure time is 10 ms in both magnifications. Overlays were created with 100% signal intensity of the DAPI signal, 130% of the green fluorescence signal and 45% of the bright-field signal. Scale bars, 200 μm.

constructs should be collected with sufficiently large pipette tips. When the microspheres are cultured in osteogenic medium, mineralized areas can be readily detected in the peripheral zone of the microsphere after 3 d (**Figs. 2a** and **3**). The proportion of mineralized area increases with ongoing supplementation of the medium with DAG. In this process, the microspheres mineralize from the periphery to the center of the sphere. If microspheres are not subjected to osteogenic medium, mineralization is initiated in the center of the microsphere and becomes detectable after 7 d (**Figs. 2a** and **3**). Expected RNA concentrations after isolation from ten microspheres (1.8×10^5 cells each) with TRIzol and further purification using the RNeasy kit range from 0.24 to 0.46 μg μl^{-1}, leading to a total yield of 2.83–5.48 μg RNA in 12 μl (**Table 2**). An optimum purity of the RNA is indicated by a 260 nm/280 nm OD ratio between 1.9 and 2.1 and a 260 nm/230 nm OD ratio above 1.8.

TABLE 2 | Typical yields of RNA from a batch of ten microspheres.

	Day 4		Day 7	
	Concentration (μg μl^{-1})	Total RNA yield[a] (μg)	Concentration (μg μl^{-1})	Total RNA yield[a] (μg)
Control spheres	0.35	4.24	0.46	5.48
Spheres + DAG	0.37	4.51	0.24	2.83

[a]12 μl of RNA.

© 2011 Nature America, Inc. All rights reserved.

Note: Supplementary information is available via the HTML version of this article.

ACKNOWLEDGMENTS We thank M. Hölbling for technical assistance. We also thank the group of G. Kögler (José Carreras Cord Blood Bank) for providing USSCs. F.L. was supported by a Deutsche Forschungsgemeinschaft (DFG) grant (HA 3228/2-1).

AUTHOR CONTRIBUTIONS F.L. and A.H. performed the majority of the experiments and wrote the manuscript, K.B. supervised the project and wrote the manuscript. U.M. and H.-P.W. established the method. J.H. and C.N. supervised the project and adapted the protocol for USSCs and ESCs. M.H. performed the microscopy, R.D. supported data analysis. N.R.K. administered the project and G.K. provided the cells.

COMPETING FINANCIAL INTERESTS The authors declare no competing financial interests.

Published online at http://www.natureprotocols.com/.
Reprints and permissions information is available online at http://www.nature.com/reprints/index.html.

© 2011 Nature America, Inc. All rights reserved.

1. Langenbach, F. *et al.* Improvement of the cell-loading efficiency of biomaterials by inoculation with stem cell-based microspheres, in osteogenesis. *J. Biomater. Appl.*, published online, doi:10.1177/088532821 0377675 (6 September 2010).
2. Handschel, J. *et al.* Comparison of ectopic bone formation of embryonic stem cells and cord blood stem cells *in vivo*. *Tissue Eng. Part A* **16**, 2475–2483 (2010).
3. Langenbach, F. *et al.* Osteogenic differentiation influences stem cell migration out of scaffold-free microspheres. *Tissue Eng. Part A* **16**, 759–766 (2010).
4. Kunz-Schughart, L.A., Kreutz, M. & Knuechel, R. Multicellular spheroids: a three-dimensional *in vitro* culture system to study tumour biology. *Int. J. Exp. Pathol.* **79**, 1–23 (1998).
5. Mueller-Klieser, W. Multicellular spheroids. A review on cellular aggregates in cancer research. *J. Cancer Res. Clin. Oncol.* **113**, 101–122 (1987).
6. Santini, M.T. & Rainaldi, G. Three-dimensional spheroid model in tumor biology. *Pathobiology* **67**, 148–157 (1999).
7. Friedrich, J., Seidel, C., Ebner, R. & Kunz-Schughart, L.A. Spheroid-based drug screen: considerations and practical approach. *Nat. Protoc.* **4**, 309–324 (2009).
8. Kundu, A.K., Khatiwala, C.B. & Putnam, A.J. Extracellular matrix remodeling, integrin expression, and downstream signaling pathways influence the osteogenic differentiation of mesenchymal stem cells on poly(lactide-co-glycolide) substrates. *Tissue Eng. Part A* **15**, 273–283 (2009).
9. Holy, C.E., Shoichet, M.S. & Davies, J.E. Engineering three-dimensional bone tissue *in vitro* using biodegradable scaffolds: investigating initial cell-seeding density and culture period. *J. Biomed. Mater. Res.* **51**, 376–382 (2000).
10. Bitar, M. *et al.* Effect of cell density on osteoblastic differentiation and matrix degradation of biomimetic dense collagen scaffolds. *Biomacromolecules* **9**, 129–135 (2008).
11. Abbott, A. Cell culture: biology's new dimension. *Nature* **424**, 870–872 (2003).
12. Handschel, J.G. *et al.* Prospects of micromass culture technology in tissue engineering. *Head Face Med.* **3**, 4 (2007).
13. Cukierman, E., Pankov, R., Stevens, D.R. & Yamada, K.M. Taking cell-matrix adhesions to the third dimension. *Science* **294**, 1708–1712 (2001).
14. Weaver, V.M. *et al.* Reversion of the malignant phenotype of human breast cells in three-dimensional culture and *in vivo* by integrin blocking antibodies. *J. Cell Biol.* **137**, 231–245 (1997).
15. Sivaraman, A. *et al.* A microscale *in vitro* physiological model of the liver: predictive screens for drug metabolism and enzyme induction. *Curr. Drug Metab.* **6**, 569–591 (2005).
16. Kelm, J.M. & Fussenegger, M. Microscale tissue engineering using gravity-enforced cell assembly. *Trends Biotechnol.* **22**, 195–202 (2004).
17. Estes, B.T., Diekman, B.O., Gimble, J.M. & Guilak, F. Isolation of adipose-derived stem cells and their induction to a chondrogenic phenotype. *Nat. Protoc.* **5**, 1294–1311 (2010).
18. Kafienah, W., Al-Fayez, F., Hollander, A.P. & Barker, M.D. Inhibition of cartilage degradation: a combined tissue engineering and gene therapy approach. *Arthritis Rheum.* **48**, 709–718 (2003).
19. Keller, G.M. *In vitro* differentiation of embryonic stem cells. *Curr. Opin. Cell Biol.* **7**, 862–869 (1995).
20. Potter, S.W. & Morris, J.E. Development of mouse embryos in hanging drop culture. *Anat. Rec.* **211**, 48–56 (1985).
21. Wobus, A.M., Wolf, E. & Beier, H.M. Embryonic stem cells and nuclear transfer strategies. Present state and future prospects. *Cells Tissues Organs* **166**, 1–5 (2000).
22. Kelm, J.M., Timmins, N.E., Brown, C.J., Fussenegger, M. & Nielsen, L.K. Method for generation of homogeneous multicellular tumor spheroids applicable to a wide variety of cell types. *Biotechnol. Bioeng.* **83**, 173–180 (2003).
23. Burns, J.S., Rasmussen, P.L., Larsen, K.H., Schroder, H.D. & Kassem, M. Parameters in three-dimensional osteospheroids of telomerized human mesenchymal (stromal) stem cells grown on osteoconductive scaffolds that predict *in vivo* bone-forming potential. *Tissue Eng. Part A* **16**, 2331–2342 (2010).
24. Meyer, U. & Wiesmann, H.P. *Bone and Cartilage Engineering* (Springer-Verlag, 2006).
25. Hildebrandt, C., Buth, H. & Thielecke, H. A scaffold-free *in vitro* model for osteogenesis of human mesenchymal stem cells. *Tissue Cell* **43**, 91–100 (2011).
26. Jaiswal, N., Haynesworth, S.E., Caplan, A.I. & Bruder, S.P. Osteogenic differentiation of purified, culture-expanded human mesenchymal stem cells *in vitro*. *J. Cell Biochem.* **64**, 295–312 (1997).
27. Kogler, G. *et al.* A new human somatic stem cell from placental cord blood with intrinsic pluripotent differentiation potential. *J. Exp. Med.* **200**, 123–135 (2004).
28. Bonewald, L.F. *et al.* von Kossa staining alone is not sufficient to confirm that mineralization *in vitro* represents bone formation. *Calcif. Tissue Int.* **72**, 537–547 (2003).
29. Daus, A.W., Goldhammer, M., Layer, P.G. & Thielemann, C. Electromagnetic exposure of scaffold-free three-dimensional cell culture systems. *Bioelectromagnetics* **32**, 351–359 (2011).
30. Nyberg, S.L. *et al.* Rapid, large-scale formation of porcine hepatocyte spheroids in a novel spheroid reservoir bioartificial liver. *Liver Transpl.* **11**, 901–910 (2005).
31. Berahim, Z., Moharamzadeh, K., Rawlinson, A. & Jowett, A.K. Biological Interaction of 3d periodontal fibroblast spheroids with collagen-based and synthetic membranes. *J Periodontol.* **82**, 790–797 (2011).
32. Miyagawa, Y. *et al.* A microfabricated scaffold induces the spheroid formation of human bone marrow-derived mesenchymal progenitor cells and promotes efficient adipogenic differentiation. *Tissue Eng. Part A* **17**, 513–521 (2011).
33. Bartosh, T.J. *et al.* Aggregation of human mesenchymal stromal cells (MSCs) into 3D spheroids enhances their antiinflammatory properties. *Proc. Natl Acad. Sci. USA* **107**, 13724–13729 (2010).
34. Laib, A.M. *et al.* Spheroid-based human endothelial cell microvessel formation *in vivo*. *Nat. Protoc.* **4**, 1202–1215 (2009).
35. Arufe, M.C. *et al.* Analysis of the chondrogenic potential and secretome of mesenchymal stem cells derived from human umbilical cord stroma. *Stem Cells Dev.* **20**, 1199–1212 (2011).
36. Giovannini, S. *et al.* Micromass co-culture of human articular chondrocytes and human bone marrow mesenchymal stem cells to investigate stable neocartilage tissue formation *in vitro*. *Eur. Cell Mater.* **20**, 245–259 (2010).
37. Conley, B.J., Young, J.C., Trounson, A.O. & Mollard, R. Derivation, propagation and differentiation of human embryonic stem cells. *Int. J. Biochem. Cell Biol.* **36**, 555–567 (2004).
38. Wang, W. *et al.* 3D spheroid culture system on micropatterned substrates for improved differentiation efficiency of multipotent mesenchymal stem cells. *Biomaterials* **30**, 2705–2715 (2009).
39. Kelm, J.M. *et al.* A novel concept for scaffold-free vessel tissue engineering: self-assembly of microtissue building blocks. *J. Biotechnol.* **148**, 46–55 (2010).
40. Kelm, J.M. & Fussenegger, M. Scaffold-free cell delivery for use in regenerative medicine. *Adv. Drug Deliv. Rev.* **62**, 753–764 (2010).

3.3 Impact of DAG stimulation on mineral synthesis, mineral structure and osteogenic differentiation of human cord blood stem cells

Lammers, L., Naujoks, C.[#], Berr, K., Depprich, R., Kubler, N., Meyer, U., **Langenbach, F.**, Luttenberg, B., Kogler, G., Wiesmann, H.P., and Handschel, J (2012). Impact of DAG stimulation on mineral synthesis, mineral structure and osteogenic differentiation of human cord blood stem cells. Stem Cell Res *8*, 193-205.

Impact Factor: 3,338

Durchschnittlicher Impact Faktor des Forschungsgebietes:

- Cell & Tissue Engineering:
    - 3,388; Rang 8 von 13 Zeitschriften
- Biotechnology and Applied Microbiology:
    - 1,874; Rang 37 von 160 Zeitschriften
- Cell Biology:
    - 3,376; Rang 88 von 178 Zeitschriften

Mein Anteil an der Publikation:

- Versuche: 10%
- schriftliche Arbeit: 10%

Stem Cell Research (2012) 8, 193–205

Available online at www.sciencedirect.com

SciVerse ScienceDirect

www.elsevier.com/locate/scr

Impact of DAG stimulation on mineral synthesis, mineral structure and osteogenic differentiation of human cord blood stem cells ☆

Lydia Lammers [a, 1], Christian Naujoks [b,*, 1], Karin Berr [b], Rita Depprich [b], Norbert Kübler [b], Ulrich Meyer [b], Fabian Langenbach [b], Beate Lüttenberg [a], Gesine Kögler [c], Hans-Peter Wiesmann [d], Jörg Handschel [b]

[a] *Department of Cranio- and Maxillofacial Surgery, University of Münster, Waldeyerstr. 30, 48149 Münster, Germany*
[b] *Department of Cranio- and Maxillofacial Surgery, Heinrich Heine University of Düsseldorf, Moorenstr. 5, 40225 Düsseldorf, Germany*
[c] *Institute for Transplantation Diagnostics and Cell Therapeutics Heinrich Heine University of Düsseldorf, Moorenstr. 5, 40225 Düsseldorf, Germany*
[d] *Institute for Material Science, University of Dresden, Helmholtzstr. 7, 01062 Dresden, Germany*

Received 11 April 2011; received in revised form 19 July 2011; accepted 27 September 2011
Available online 8 October 2011

Abstract It remains unexplored in what way osteogenic stimulation with dexamethasone, ascorbic acid and β-glycerol phosphate (DAG) influences the process of mineralization, the composition and structure of the assembled mineral. Therefore, we analyzed and characterized biomineralization in DAG-stimulated and unstimulated 3D human unrestricted somatic stem cell (USSC) cultures. Microspheres were analyzed by histological staining, scanning electron microscopy (SEM), semi-quantitative energy-dispersive X-ray spectroscopy (EDX), quantitative wavelength-dispersive X-ray spectroscopy (WDX), transmission electron microscopy (TEM), selected area electron diffraction (SAED) and Raman spectroscopy.
Mineral material was detected by SEM and histological staining in both groups, and showed structural differences. DAG influenced the differentiation of USSCs and the formation, structure and composition of the assembled mineral. SEM showed that cells of the +DAG spheres exhibited morphological signs of osteoblast-like cells. EDX and WDX confirmed a Ca–P mineral in both groups. Overall, the mineral material found showed structural similarities to the mineral substance of bony material.
© 2011 Elsevier B.V. All rights reserved.

☆ We confirm that no prior or duplicate publication or submission elsewhere of any part of the work has taken place.

* Corresponding author at: Department of Cranio- and Maxillofacial Surgery, Heinrich Heine University of Düsseldorf, Moorenstr. 5, 40225 Düsseldorf, Germany. Fax: +49 211 81 18877.
E-mail address: christian.naujoks@med.uni-duesseldorf.de (C. Naujoks).

[1] Contributed equally.

1873-5061/$ - see front matter © 2011 Elsevier B.V. All rights reserved.
doi:10.1016/j.scr.2011.09.004

Introduction

By definition, the process of synthesizing mineralized structures performed by creatures via inorganic solid states is called biomineralization. In general, a distinction is made between "biologically induced mineralization" and "biologically controlled mineralization". In the first process a mineral is formed as a side-product or an end-product of cellular metabolism and interaction of the cells with the environment (Lowenstam, 1981). This procedure results in heterogeneous minerals. In contrast, the second process leads to very complex structured intra- or extracellular minerals with specific properties such as bone or dentin.

It is also well known that the inorganic share of biominerals in mammals formed by the abovementioned processes mainly consists of calcium phosphate (Ca–P), which is chemically the same as hydroxyl apatite (HA) (LeGeros, 2001; Dorozhkin and Epple, 2002). However, there are differences between biominerals and HA regarding the Ca/P ratios, for example, caused by Ca deficits (LeGeros, 1991). In addition, the process of biomineralization can be physiological or pathological (LeGeros, 2001). Pathological mineral formation can be seen when excessive cell growth takes place, for instance, in tumors (Skinner, 2000, 2005). In this case, dead cells disintegrate, release phosphate and, due to a higher concentration of Ca, exceed the solubility product in the extracellular space and precipitation takes place (Skinner, 2005).

During the formation of minerals alongside collagen fibers, in vivo osteoblasts primarily form an extracellular matrix (ECM) consisting of collagen and proteoglycane, followed by a restructuring of the proteins at so-called "active sides" (Hohling et al., 1995, 1997; Plate et al., 1998; Wiesmann et al., 1993, 2005).

Another hypothesis for the process of mineralization concentrates on the appearance of matrix vesicles (MV). According to this hypothesis cells emit MVs into the extracellular space (Barckhaus et al., 1981; Bonucci, 1981) via exocytosis. It is suggested that a selective ion pump regulates ion deposition, the concentration of polymers and the pH value in the MVs (Wuthier, 1977). Depending on the state of the MVs, precipitation/mineralization takes place.

Weiner et al. observed another process of mineralization using precursor Ca–P minerals (Weiner and Lowenstam, 1989). The formation of these precursor minerals is kinetically favorable compared to the direct formation of HA (Mann, 2001). The existence of these precursor minerals has been verified by different working groups; in particular, amorphous calcium phosphate (ACP), di-calcium phosphate (DCP) and octa-calcium phosphate (OCP) have been detected (LeGeros, 2001; Wuthier et al., 1985).

It is generally accepted that the formation of minerals in a stem cell culture indicates an ostoblastic differentiation of the stem cells (Buttery et al., 2001; zur Nieden et al., 2003). Furthermore, it has been shown that the addition of dexamethasone, β-glycerol phosphate and ascorbic acid to the culture medium seems to trigger the osteogenic differentiation of various stem cells (e.g. mesenchymal stem cells (MSC) and embryonic stem cells (ESC)) (Bielby et al., 2004; Handschel et al., 2008; Jaiswal et al., 1997; Kogler et al., 2004; Pittenger et al., 1999). In a previous study, we were able to show that osteogenic stimulation with DAG exceeds the stimulation with BMP-2 in ESCs (Handschel et al., 2008). The mineral-inductive potential of ESCs was also demonstrated in a previous animal study in rats, and ESCs were able to promote ectopic bone formation in vivo when they were used with demineralized bone (Kahle et al., 2010).

A few years ago a promising stem cell source was established by Kögler and colleagues (Kogler et al., 2004; Kögler, 2009). These stem cells were derived from umbilical cord blood, have the ability to develop into mesodermal, endodermal and ectodermal cells and were subsequently termed human unrestricted somatic stem cells (USSCs). These CD45- and HLA class II-negative stem cells display proliferative capacity in vitro without spontaneous differentiation. It is possible to expand the cells to 10^{15} cells without losing multipotency. In vitro, a differentiation into osteoblasts, chondroblasts, hematopoietic and neural cells is possible using specific stimuli (Kogler et al., 2004). In a previous study, we were able to show that stimulation with DAG leads to mineralization even in vivo (Handschel et al., 2010). Compared to the ESCs, the USSCs do not show any immunological rejection and have fewer ethical and legal restrictions. So the USSCs are much closer to clinical practice than the ESCs, e.g. hematopoietic cells from cord blood are already used in the therapy of hematopoietic and genetic disorders (Benito et al., 2004).

Loss of bone due to tumor surgery or trauma is still a clinical challenge in modern reconstructive surgery. The repair of bone defects still poses a significant problem for many clinicians. Modern cell-based bone reconstruction techniques may offer new therapeutic opportunities for the repair of bone damaged by disease or injury. Generally, the combination of scaffolds, bioactive factors, and living cells provides a surgically implantable product for use in tissue regeneration and functional restoration (Handschel et al., 2009; Tuan et al., 2003; Vacanti and Vacanti, 1994). Yet, there is still controversy concerning the use of artificial scaffolds contra the sole use of a natural matrix. Therefore, a new approach with so-called microsphere technology has been invented to overcome these problems by avoiding the need for scaffolds. Technically, cells are dissociated and the dispersed cells are then re-aggregated into cellular spheres. Importantly, since the newly formed tissue is devoid of any artificial material, it more closely resembles the in vivo situation (review in Handschel et al., 2007).

Apparently, it is generally accepted that the addition of DAG to the culture medium stimulates the osteogenic differentiation of stem cells (Jaiswal et al., 1997; Bourne et al., 2004). However, most of the studies neglected to analyze the minerals formed and the process of mineralization. The aim of this study was to analyze the process of mineralization and to characterize the mineral formed using histological staining, scanning electron microscopy (SEM), energy-dispersive diffraction analysis (EDX), wavelength dispersive diffraction analysis (WDX), transmission electron microscopy (TEM) with selected area diffraction analysis (SAED), Raman spectroscopy and an apoptosis assay. Because of the abovementioned advantages of the USSCs compared to other stem cells and the results of our previous studies, we decided to use USSCs. In order to simulate the in vivo situation more closely, we used the 3D microsphere culture technique.

Results

Histological staining

Differences between the (+) and (−) DAG groups regarding the quantity and distribution of mineral material in the spheres at a certain time of cultivation were detected. Fig. 1 shows spheres stained with toluidine blue and counterstained with alizarin red from the (+) and (−) DAG groups. On day 3, both groups showed a dense cellular matrix. While this dense cellular matrix did not change during the course of the experiment in the −DAG group, the cells of the +DAG group became more and more bulked up. The +DAG group showed earlier mineral deposition in the spheres (day 3) compared to the −DAG group (day 7) and there were differences in the distribution of the minerals. The mineralization of the −DAG group started in the center and was homogenously distributed over the cross-sectional area of the spheres after 21 days of cultivation. In contrast, the +DAG spheres showed mineralization beginning at the border region of the spheres. Even after 28 days, no distribution over the whole spheres could be observed. Higher magnification of a −DAG sphere showed that there were large round formations or agglomerations of mineral material composed of smaller granular or globular mineralized structures (Fig. 1e). Furthermore, some of the larger rounded mineral formations showed cavities containing cellular material.

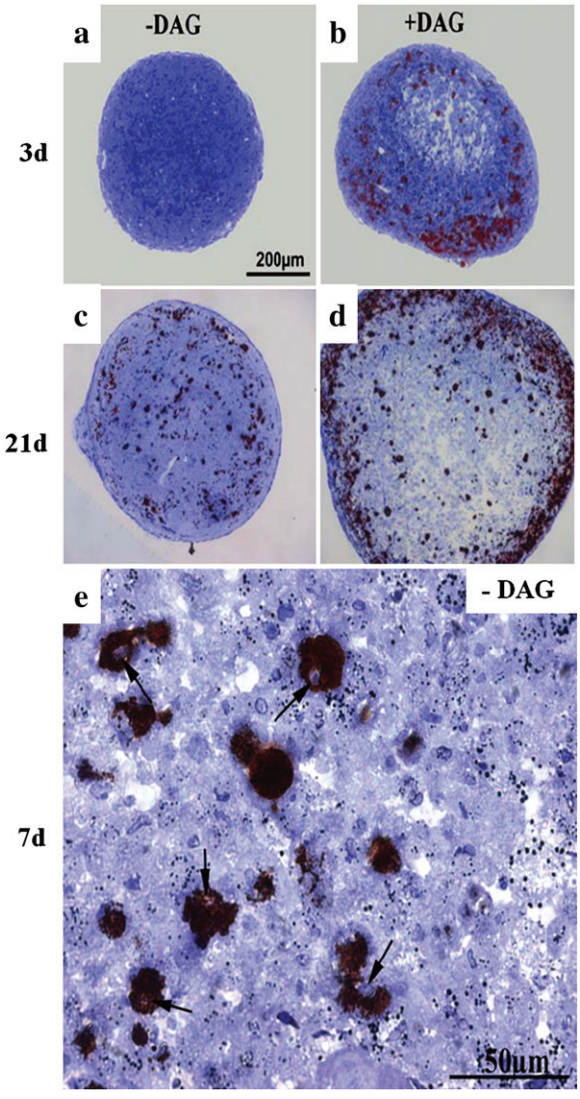

Figure 1 Spheres stained with toluidine blue and alizarin red after 3 (a, b) and 21 (c, d) days of cultivation with and without DAG. Note the different distribution of the mineralization and the differences in cell density, especially on day 21. Section e is an image of a sphere on day 7, −DAG, at a higher magnification. Note the granular or globular mineralized structures as well as the bigger mineral formations found in the −DAG group.

Field emission scanning electron microscopy (FESEM)

The FESEM pictures showed no morphological differences between the two groups on day 7. The spheres were small and the cells appeared elliptical with a fibroblast-like morphology. Except for a newly generated plain and compact surface of the spheres, no cell-morphological changes appeared in the −DAG group after 28 days of cultivation. In contrast, cells of the +DAG group showed a low density and a cuboidal, osteoblast-like morphology after 28 days (Fig. 2). Overall, spheres of the +DAG group seemed to increase in size during incubation compared to the −DAG group.

Mineralization on the surface area of the spheres

In both groups, mineralization on the exterior area of the microspheres appeared after 14 days of cultivation, whereas there were quantitative disparities between the two groups (Fig. 3a, b). The +DAG group exhibited greater amounts of mineral material than the −DAG group and after 28 days the whole surfaces of +DAG spheres were almost covered. In contrast, even after 28 days, there were hardly any minerals visible on the surface of the −DAG group (Fig. 3c, d). But this does not mean that there was no mineralization in the −DAG spheres. Fig. 3c shows a sphere after 28 days, opened during preparation so that a look inside the sphere was possible. It can be seen that mineral material had formed inside the spheres. At a higher magnification the mineral substance looked like globular structures of different sizes lying between the cells and it seemed to be connected to the extracellular matrix (Fig. 4). Fig. 4c indicates that there is an association between the mineral and the collagen fibers of the ECM. Furthermore, it seemed that the mineral globular structures agglomerated with each other to form larger mineral formations.

Mineralization in the interior of the spheres

In contrast to the mineralization on the exterior area of the spheres, mineralization in the center started in both groups after only a few days. Once again, there were the same quantitative differences between the two groups after 7 days of cultivation, as described above. The +DAG group formed a greater amount of mineral substance compared to the −DAG group. After 14 days of incubation, it seemed that the differences in mineral quantity between the two groups were diminished (Suppl. 1a, b). Still, the distribution of the mineral was

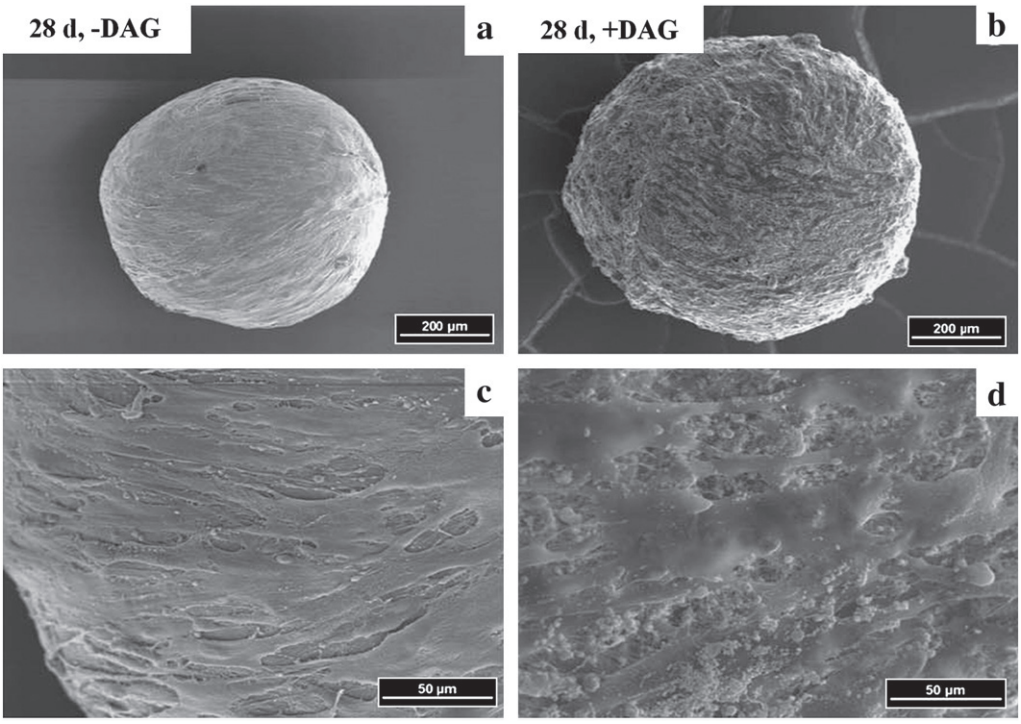

Figure 2 SE-image of the spheres after 28 days of cultivation, −DAG (a, c) and +DAG (b, d). Compared to the −DAG group the morphology of the +DAG group has changed to a cuboid, osteoblast-like morphology.

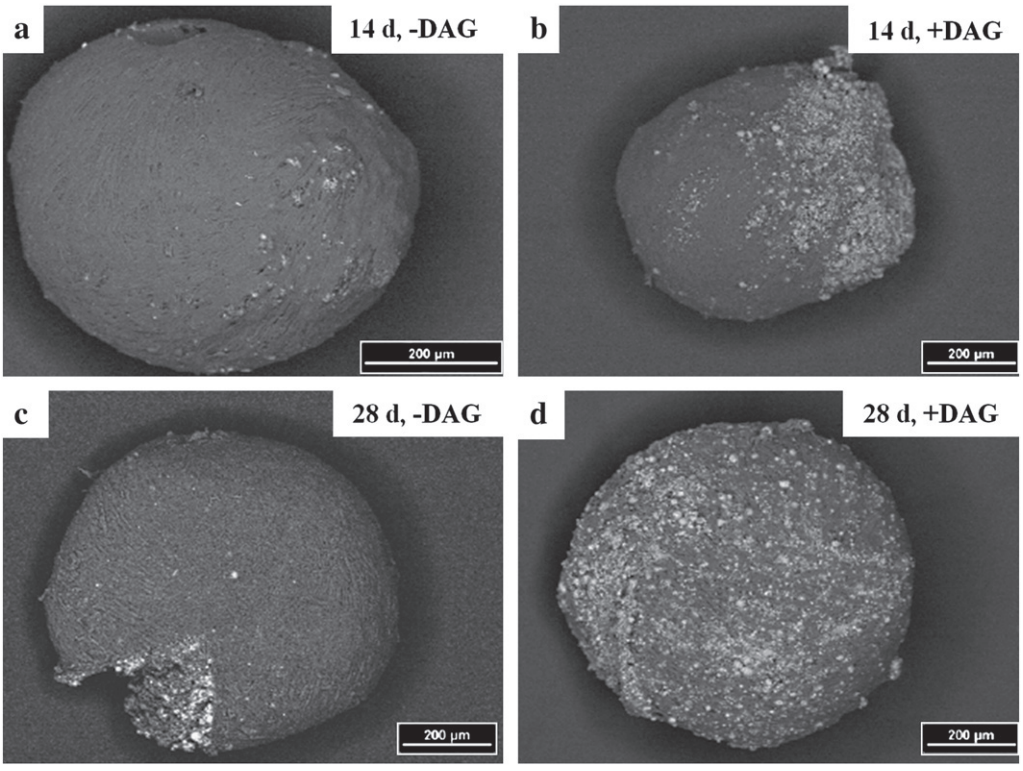

Figure 3 BSE-images of the mineralization on the surface area after 14 and 28 days of cultivation with and without DAG. Note the quantitative differences between the −DAG (left column) and +DAG (right column) groups. Image c provides a view of an opened sphere from the −DAG group, indicating mineralization in the center of the sphere.

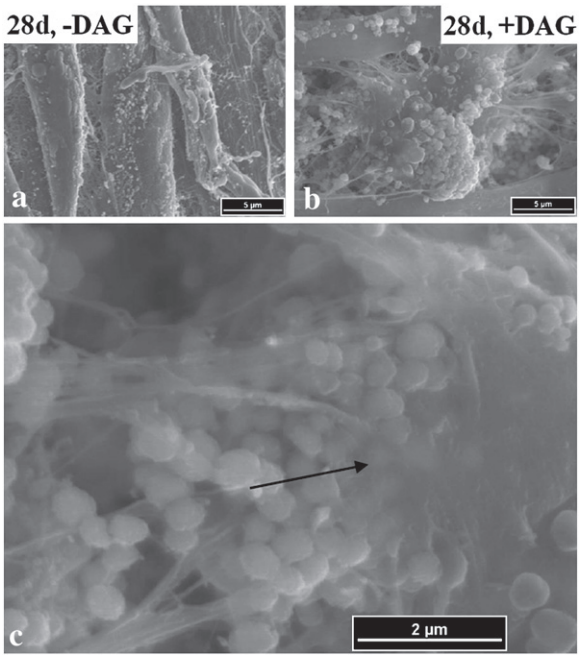

Figure 4 SE-image of spheres after 28 days of cultivation without (a) and with (b) DAG. The higher magnification in c shows a globular mineral substance associated with collagen fibers of the ECM in the +DAG group.

different between the groups. The −DAG spheres showed a nearly homogenous distribution of the mineral substance over the whole cross-sectional area of the sphere, whereas in the +DAG group mineralization predominantly took place at the boundary areas. Higher magnifications showed that the size of the minerals formed differed between the groups. Whereas the +DAG group showed at least a few large, agglomerative mineral globules, the −DAG group showed very small individual globules. After 28 days of cultivation, both groups showed intense mineralization (Suppl. 1c, d). In the center of the +DAG group, loosely arranged cells without signs of mineralization were observed. The areas of the mineral substance had diameters of between 5 and 25 µm (average diameter of 10 µm) and showed, as already mentioned in the histological results, round cavities with no mineral material inside these areas.

EDX and WDX mineral analysis

The following data are based on 134 analysis points of mineralized areas of the −DAG and +DAG groups on days 3, 14, 21 and 28. The EDX analysis showed high peaks for calcium, phosphate and oxygen. Both groups showed a small, but significant magnesium peak. Small amounts of sodium, sulfur and chlorine were also observed in both groups. The Ca/P ratios of both groups lay between 1.1 and 1.6 (1.4 mean). Over the whole period of this study, the Ca/P ratios of the −DAG group were higher than the ratios of the +DAG group (Fig. 5b). Even though there was a tendency for the Ca/P ratios to decrease over time in both groups, the −DAG group showed a increased ratio on day 21. In contrast, the Ca/P ratio in the +DAG group declined constantly after day 14 (Fig. 5b). The amount of Ca and P in the substance increased over the time period of the experiment in both groups until day 21 and declined on day 28. Even though the −DAG group showed higher levels of Ca and P on days 14 and 21, the amount of both in the substance were equal between the groups after 28 days (Fig. 5a).

As mentioned above, there was a slight peak in Mg in the EDX analysis of both groups. The calculated percentage of the fraction of Mg in the substance increased slightly with time in both groups (Fig. 5c). Whereas, the increase in the Mg fraction in the −DAG group continued until day 14, the Mg fraction in the +DAG group increased throughout the entire experiment (Fig. 5d).

In order to evaluate the EDX analysis data, a WDX analysis for specimens of the +DAG and −DAG groups, as well as of standard hydroxyl apatite, was performed. No significant differences in the percentage fractions on Ca and P in the substance were found between both groups. The WDX analysis was able to prove the trend of decreasing Ca/P ratios in the +DAG group even though the ratio on day 7 was slightly higher in the +DAG group. Compared to standard HA, the Ca fraction in the samples of both groups was lower. In addition, WDX substantiated the EDX findings regarding the increase in the Mg fraction in the mineral material (Fig. 5d).

Transmission electron microscopy with selected area electron diffraction

The morphological and crystal structures of the formed mineral samples from days 4 and 14 (of both groups) were investigated with TEM and SAED. In contrast to the −DAG group with no signs of mineralization on day 4, small mineralized areas were detected in the +DAG group (Fig. 6a, b). At higher magnifications it could be seen that the crystallites were unordered (Fig. 6b). In both groups, mineralization was detectable after 14 days. However, the mineral substance in the −DAG group had a more microcrystalline structure and was more compact compared to the +DAG group (Fig. 6c, d). In addition, the +DAG group showed that the mineral resembled a dendritic growth.

By day 4, the SAED patterns of the mineral substance already showed a few diffuse ring formations in the +DAG group (Fig. 7a). After 14 days the minerals of both groups showed a more or less well-defined SAED pattern, but rings in the +DAG group already showed more clearly defined reflexes than the −DAG group (Fig. 7b, c). The patterns of the −DAG and +DAG groups were very similar to an SAED pattern of bone mineral, as the comparison with a diffraction pattern of rat bone shows (Fig. 7d).

Raman spectroscopy

Raman spectroscopy was also used to analyze the mineral material. In both groups, the spectra showed a symmetrical, maximum peak at around 960 cm^{-1}, which is in agreement with the presence of HA because reference spectra in the literature (Crystal Sleuth Program) and the collected spectra of the HA standard with different embedding materials showed a maximum peak at 961 cm^{-1} (Suppl. 2).

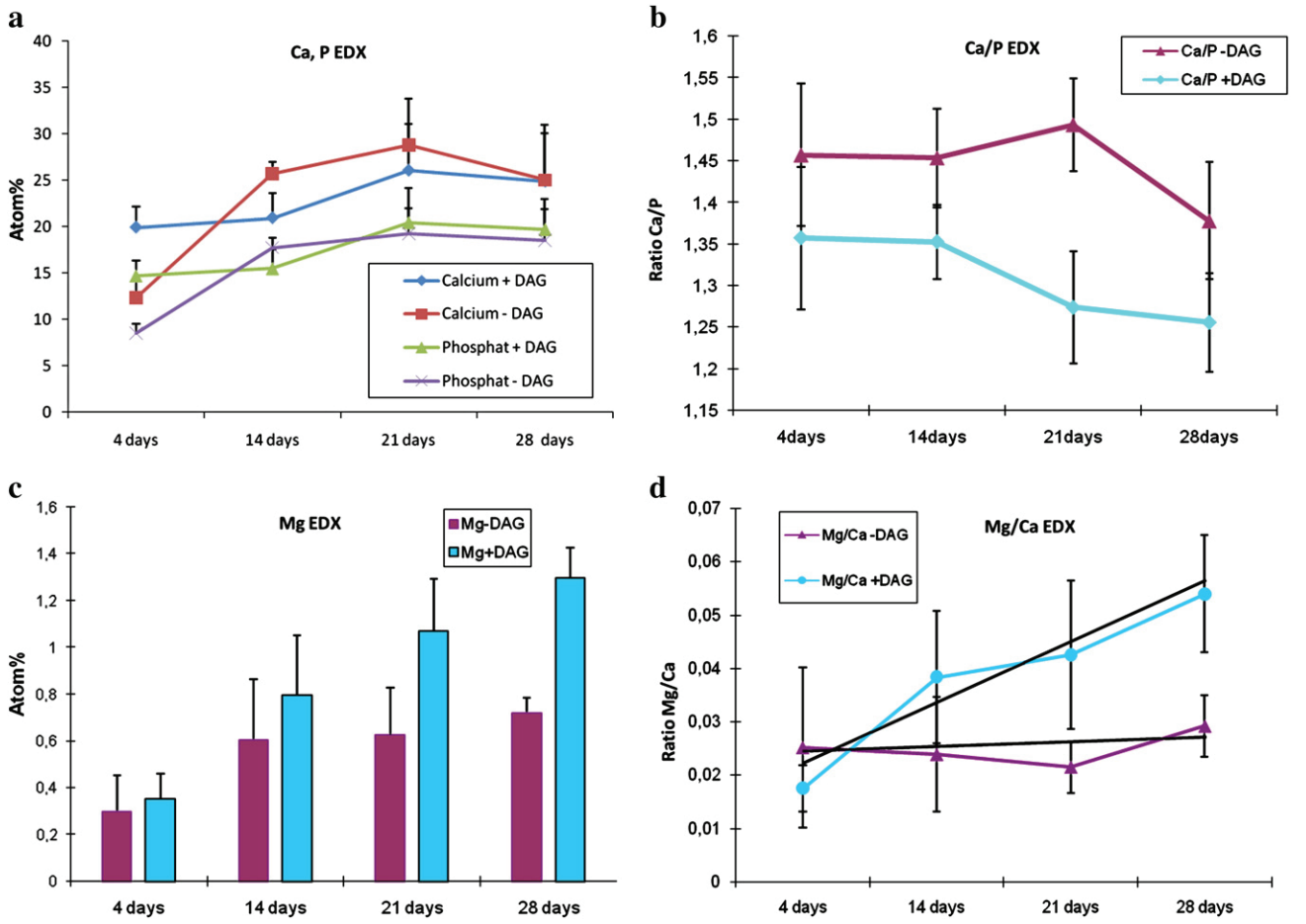

Figure 5 (a) EDX substance fractions of Ca and P over the time period of the experiment in both groups. (b) Calculated Ca/P ratio of the +and −DAG groups over the time period of the experiment. Note the earlier decline after day 14 in the +DAG group. (c) EDX substance fraction of Mg over the time period of the experiment in both groups. (d) Calculated Mg/Ca ratio of the + and −DAG groups over the time period of the experiment.

At early points throughout cultivation of the +DAG group the 960 cm^{-1} peak seemed to show a small shoulder that became more defined with time. The shoulder of the +DAG group may represent additional underlying peaks.

Apoptosis assay

No signs of apoptosis were observable in either group after 3 and 7 days of cultivation. After 14 days, a very slight rate of apoptosis was detectable in the +DAG group. However, on days 21 and 28 no quantitative differences were found when both groups were compared to each other and to the results of day 14 (Suppl. 3).

Discussion

The FESEM analysis of the spheres in this study verified a morphological development of the cells to cuboidal, osteoblast-like cells after 28 days, especially in the +DAG group. According to different workgroups, the morphological changes towards an osteoblast-like appearance and the mineralization are regarded as indicators of osteoblastic differentiation (Bielby et al., 2004; Handschel et al., 2008; Jaiswal et al., 1997; Pittenger et al., 1999; Jager et al., 2004; Vats et al., 2005). Toluidine blue and alizarin red staining demonstrated that mineralization occurred in the spheres of both groups, with and without the supplementation of DAG (dexamethasone, ascorbate, β-glycerophosphate). Despite these similarities, several differences between the two groups were observed by analyzing the histological staining, for example regarding the time point of the beginning of mineralization, the quantity of minerals formed and the distribution the mineralization within the spheres.

The distribution of the mineral substance was more homogenous in the −DAG group, and in this group the mineral material formed had a more microcrystalline structure compared to the +DAG group. Furthermore, in the +DAG group, smaller mineral globules merged to form to larger aggregations of the mineral substance and an association was observed between the mineral material and the collagen fibers of the ECM. Interestingly, no differences were detected between the groups regarding the quantity of mineralization after 21 days of cultivation.

All of these facts may be signs of an acceleration of mineralization due to the DAG in the spheres. A possible reason for the differences in the distribution of mineral formation

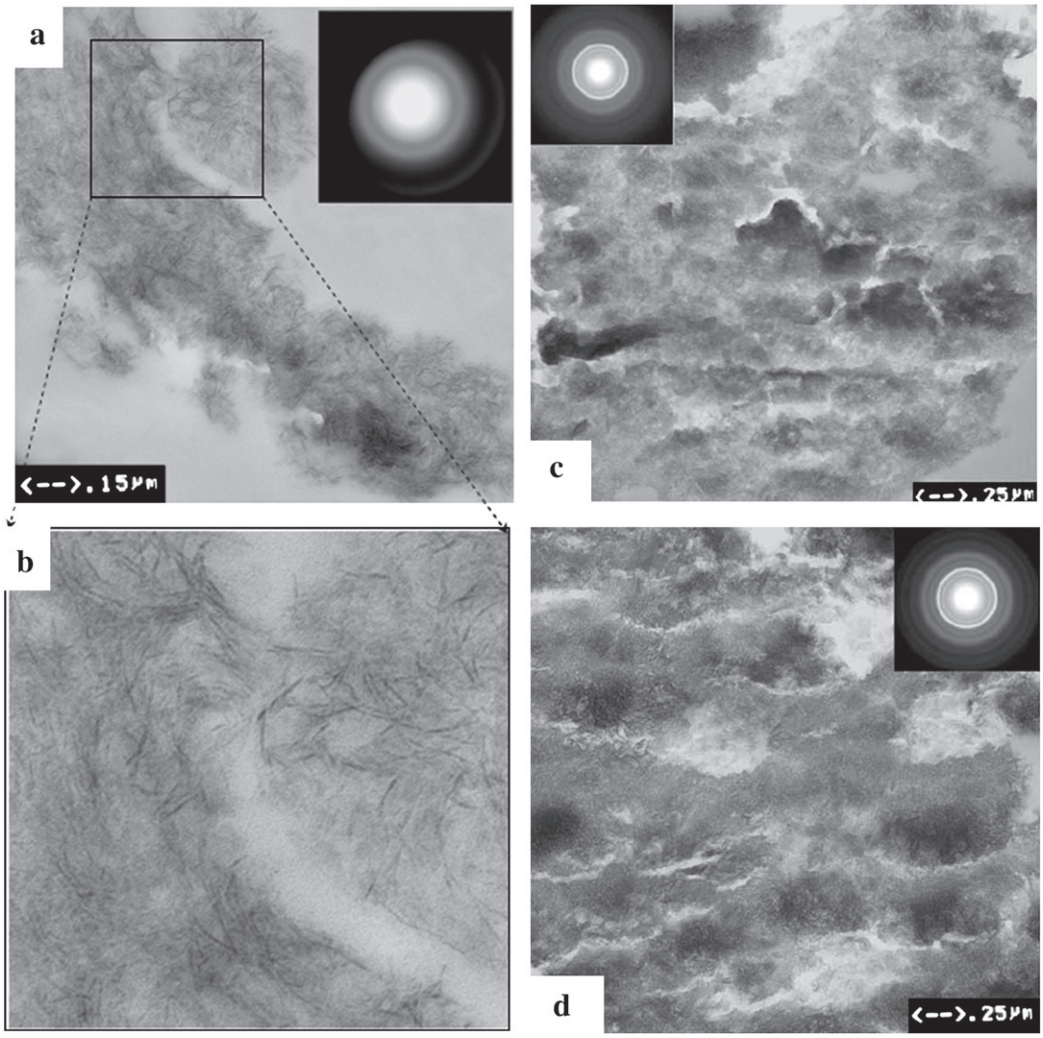

Figure 6 Transmission electron microscopy of the +DAG group after 14 days. Note the scorching crystallites embedded in a matrix (b). The mineral substance detected in the −DAG group after 14 days (c) looked more compact and microcrystalline compared to the +DAG group (d).

may be a simple problem of diffusion. Only the outer cell layers of the spheres were in direct contact with the ambient medium and were therefore exposed to a higher concentration of DAG compared to the inner cells. Consequently, only the outer cells could become stimulated by DAG and mineralization started earlier and was more pronounced in these cells. In addition, previously published results of our work showed that cell migration out of USSC microspheres is reduced by prolonged osteogenic induction (DAG) over time (Langenbach et al., 2010).

Following the fact that mineral material was present even in spheres of the −DAG group in this study there must be further factors that trigger the process of mineralization. It is well known that osteogenic differentiation occurs subsequently to proliferation and therefore high seeding densities of cells are suggested to support osteogenic differentiation. Wilson and colleagues demonstrated that higher seeding densities resulted in increased bone formation in vivo and that during cell proliferation osteogenic differentiation was restricted or inhibited (Wilson et al., 2002). Furthermore, high cell seeding densities led to a higher proportion of osteocalcin-positive tissue compared to low seeding densities (Holy et al., 2000). Additionally, as a consequence of high cell densities, both expression of the important osteogenic regulatory factor RUNX2 (runt related nuclear transcription factor 2) and transcription of osteonectin (secreted protein, acidic, cystein rich — SPARC) were upregulated in vitro (Bitar et al., 2008). The presence of mineral material even in the −DAG group spheres of this study may be caused by high cell densities in the centers of these spheres which may lead to osteogenic differentiation of these cells. Another reason for the spontaneous differentiation may lie in the communication between the cells and the interaction between the cells and the extracellular matrix (Langenbach et al., 2010). Cells interact with the ECM via integrins, which span the plasma membrane. These integrins provide binding sites for ECM proteins like collagen type I and they signal bi-directionally across the plasma membrane, thereby influencing many important cellular processes, such as proliferation, migration and gene expression (Hervy et al., 2006; Schwartz and Assoian, 2001). The de novo synthesis and deposition of ECM proteins by mesenchymal

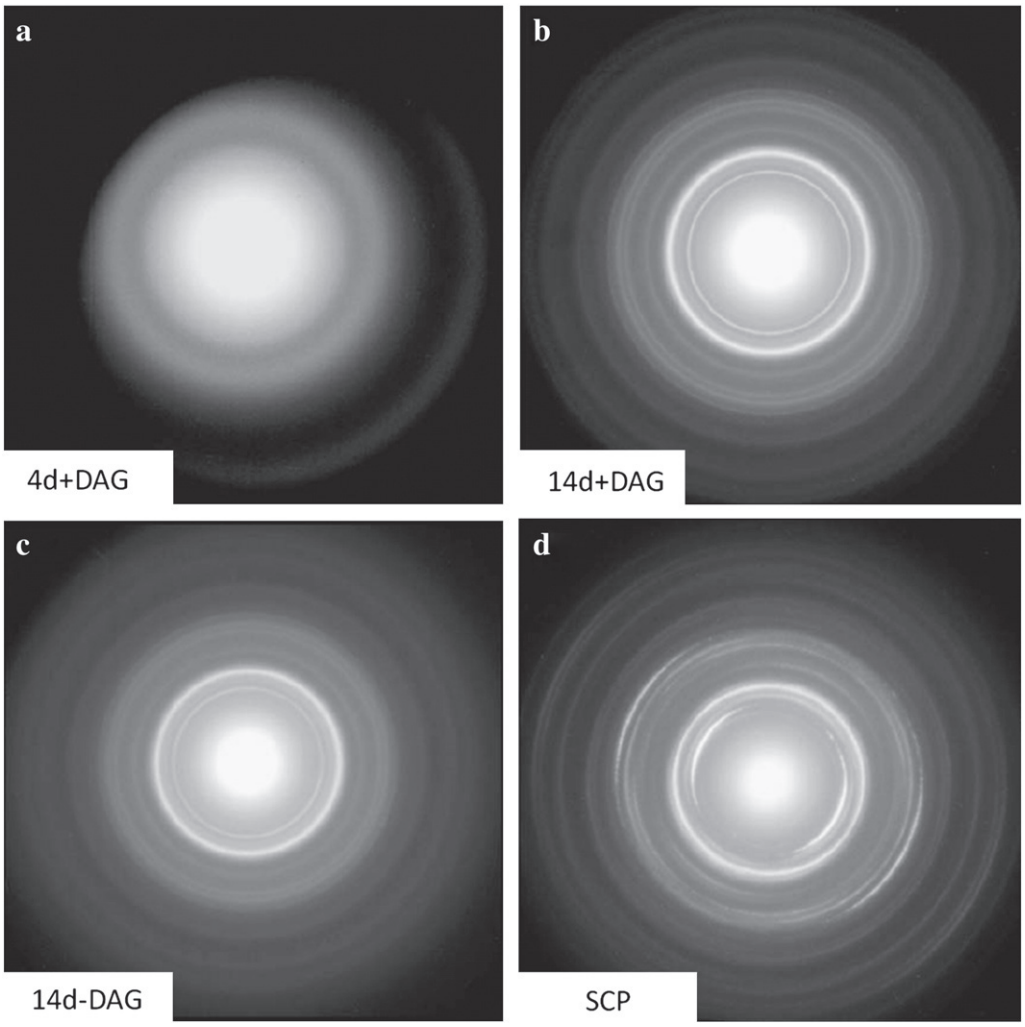

Figure 7 Selected area electron diffraction patterns of mineralized areas of the +DAG group after 7 (a) and 14 (b) days as well as after 14 days in the −DAG group (c). Note the reflexes of the patterns developing over time in both groups. The SAED pattern of the mineral material at day 14 and a diffraction pattern of a rat calotte reveal structural similarities (d).

stem cells were shown to change the chemical identity of substrate materials, as well as integrin expression and signal transduction, and they were also shown to influence osteogenesis (Kundu et al., 2009). The mitogen-activated protein kinase (MAPK) cascade plays a critical role in osteogenic differentiation by activating the RUNX2 transcription activator (Xiao et al., 2000; Franceschi and Xiao, 2003). Salasnyk and colleagues demonstrated that the adhesion to collagen type I and vitronectin is sufficient for inducing osteogenic differentiation by mesenchymal stem cells. In this process, upon ECM molecules, the focal adhesion kinase (FAK) pathway is activated, which in turn phosphorylates the extracellular signal-related kinase (EKR), which then regulates RUNX2 transcription. Our group was able to show the importance of different ECM proteins such as osteonectin and collagen type I in the osteogenic differentiation of USSCs (Naujoks et al., 2011). In addition, in another experiment by our workgroup, the expression of osteonectin, a matrix-associated protein influencing the synthesis of ECM proteins (Bradshaw et al., 2003), and the expression of collagen type I by DAG-stimulated USSCs on different biomaterials were investigated (Naujoks et al., 2011). We found an increased expression of osteonectin on collagen type I sponges compared to other biomaterials. The expression of these matrix proteins may prove the osteogenic differentiation of USSCs.

In contrast to the above, the loose cell network in the +DAG group that was observed via histological staining may be a sign of reduced cell vitality. It is well known that cell death often leads to mineralization that is not combined with the formation of bone (Kirsch, 2006). Inorganic phosphate and glucocorticoids were thought to trigger apoptosis (Meleti et al., 2000; Boyan et al., 2000; Adams et al., 2001; Giachelli, 2005; Weinstein et al., 1998). However, the apoptosis assay performed in the present study showed no signs of apoptosis over the whole period of the experiment, so that a correlation between mineralization and apoptosis in this case was unlikely.

The characterization and identification of the minerals formed were not possible from histological staining or FESEM analysis, nor could the influence of DAG stimulation on the structure of the mineral material be analyzed.

According to LeGeros et al., a mineral can be characterized by its lattice structure and chemical composition (LeGeros, 1991). The EDX analysis showed that the mineral

material formed mainly consisted of the elements Ca, P and O, providing evidence that the formed mineral was a Ca–P mineral. Furthermore, the spectra showed qualitative similarities to HA spectra (Cheng and Pritzker, 1983; Cheng et al., 1983). But quantitatively, the spectra showed significant differences to the standardized HA and between both groups. There are a lot of different calcium phosphates and each has its specific Ca/P ratio, as proven by other workgroups (LeGeros, 2001; Cheng et al., 1983). Hence, the different Ca/P ratios compared to HA may indicate the presence of different calcium phosphates in the formed mineral. Due to the Ca/P ratios observed (1.1 to 1.4 +DAG/1.3 to 1.6 −DAG), the presence of amorphous Ca–P (ACP), octacalcium phosphate (OCP) and calcium-deficient hydroxyl apatite (CDHA) could be assumed. Different workgroups supposed that Ca–P minerals can follow precursor minerals such as OCP, brushite and monetit (LeGeros, 2001; Lagier and Baud, 2003). The fact that in the present study there were different Ca/P ratios not only between the groups but also in the chronological order of the minerals may be an indicator of the presence of different minerals as well as different stages in the development of these minerals. The fact that there was no continuous increase in the ratio over time in both groups seems to refute this hypothesis. In particular, the +DAG group showed a decrease in the Ca/P ratio after 14 days.

A possible source for other detected elements (Na, Cl, S, Mg) could be the organic matrix of the cells, the embedding material or the medium. The occurrence of different stages of minerals, intermediate stages of minerals or substitution processes may account for the quantitative differences found (Wiesmann et al., 1993).

It is well known that biominerals often differ from the stoichiometric formula because ions in the crystallite lattice may be substituted by others (LeGeros, 2001). In the present study, the EDX analysis in both groups showed a significant peak in Mg; thus, Mg was potentially substituted for Ca, leading to the lower Ca/P ratios over the time period of the experiment. This was confirmed by WDX analysis, indicating that Mg was part of the mineral formed in both groups. The portion of Mg in the mineral increased over time whereas the portion of Ca decreased in the WDX analysis of the +DAG group. In the −DAG group, a minor increase in Mg and a lower Mg/Ca ratio was detected compared to the +DAG group. It seems that DAG amplified the substitution of Mg for Ca during the process of mineralization, although in both groups a substitution of Mg for Ca took place, as already reported by others (Bigi et al., 1996; Wiesmann et al., 1997). A possible source of Mg may be the cultivation medium. The question arises as to why there were differences in the Mg integration between the +DAG and −DAG groups. There was probably a quantitative lack of Ca caused by the accelerated mineralization in the +DAG group, leading to a substitution by Mg.

However, the possibility that changes in the elements could have been caused by the preparation of the samples (Wiesmann et al., 1993; Plate et al., 1992) or by mechanical–physical ascendancies, which may lead to measuring errors, cannot be excluded. In particular, the fact that the analyzed minerals were very small suggests that parts of the surrounding tissue were analyzed as well as the mineral, leading to higher P concentrations and therefore lower Ca/P ratios.

In order to analyze and identify the obtained mineral, additional Raman spectroscopy was performed (Putnis, 1992). It is known that calcium phosphate minerals show a characteristic peak at 960 cm^{-1} (Koutsopoulos, 2002; Sauer et al., 1994). All of the samples analyzed in the present study showed a strong peak at 960 cm^{-1}, and so this suggests that the minerals formed in both groups belonged to a group of calcium phosphates. A more detailed differentiation would be possible by analyzing the varying lengths of linkage between phosphate and oxygen (Sauer et al., 1994). A comparison of the spectra collected with regard to the two groups and cultivation days as well as with standard HA embedded in different materials showed that the mineral formed is structurally similar to hydroxyl apatite. The spectra collected from the +DAG group showed a maximum peak of 960 cm^{-1} with a shoulder. The shoulder could represent additional peaks such as ACP (945–952 cm^{-1}), OCP (955–957 cm^{-1}) and HA (960–963 cm^{-1})(Freeman et al., 2001). In contrast, the spectra collected from the −DAG group showed an asymmetric but wider peak at 960 cm^{-1}. The widening of the peak in the −DAG group could have resulted from a minor order in the crystallite lattice (Sauer et al., 1994; Freeman et al., 2001). Wopenka and co-workers analyzed human bone regarding this mineral with Raman spectroscopy and were able to show that, besides HA, other minerals were also present within the bone (Wopenka and Pasteris, 2005).

These findings correlate with the results of the TEM, indicating a more nanocrystalline or amorphous mineral in the −DAG group.

Characterization of the mineral formed by TEM and SAED showed a great similarity to bone mineral. Therefore, the abovementioned results are not contrary to the findings in the SAED that the mineral formed was very similar to the pattern of a human calotte. Due to the fact that bone mineral is mainly composed of HA (Wiesmann et al., 1998), one can expect that the mineral formed exhibited an apatite-like structure. Dorozhkin and co-workers showed that the physiological mineral of mammals is not only composed of pure apatite but also of CDHA, OCP, CAP and brushite (Dorozhkin and Epple, 2002). Both these facts and the results of the EDX and WDX analyses in the present study suggest that the mineral formed was similar to the mineral in bone, but that may have been composed of different mineral phases. However, a definite statement regarding the structure of the mineral analyzed with SAED is difficult because of the limitations of these methods. For example, a possible irradiation of minerals existing in only minor amounts and an overlap of the reflexes of similar minerals in the SAED pattern have to be considered.

However, the combination of these results with the results of the EDX and WDX supports the abovementioned hypothesis that the mineral formed showed structural similarities to bone and that it mainly consisted of CDHA, OCP, CAP and HA.

The SAED pattern also demonstrated a development of the mineral with the formation of more defined reflexes over time. This may be suggestive of a development from a more or less amorphous mass to a more crystalline mineral in both groups, as shown by others (Bonar et al., 1985). In contrast to the −DAG group, the mineral that formed earlier in the +DAG group was more crystalline. The diffuse ring formation pattern without defined reflexes at the beginning of the experiment underlines the hypothesis for the existence

of amorphous mineral phases during formation of the mineral substance.

The results of the TEM together with those from SAED provide evidence of an accelerated growth rate of the mineral in the +DAG group. It is well known that a fast growth of a mineral leads to directed growth for energetic reasons (Mann, 2001; Brown, 1962; Suvorova and Buffat, 2001), leading to thin, elongated crystallites (Mann, 2001; Arnold et al., 2001).This permits the reverse conclusion that the thin, elongated crystallites observed by TEM reflected an accelerated growth rate of the mineral in the +DAG group. These findings correlate with the SAED of these mineral substances, also giving indications of an accelerated growth rate in the +DAG group in the more defined reflection patterns. In contrast, the results of the SAED and TEM of the −DAG group indicate a slower, perhaps more physiological, growth rate. This means that the mineralization in the +DAG group did not only start at an earlier point in time but also that the growth of the minerals was accelerated.

In summary, the EDX and WDX analyses of Ca/P ratios showed that the minerals formed in the osteogenically stimulated group (+DAG) and the control group (−DAG) were a type of calcium phosphate but not a pure HA. Furthermore, TEM and SAED revealed that the mineral formed in both groups showed similarities to bone mineral, which is almost an HA. It seems that there were different levels of mineral formation in the two groups. The low Ca/P ratio in both groups, the microcrystalline appearance, the diffuse reflexes in the SAED and the wide peak in Raman spectroscopy lead to the assumption that the first minerals formed had an amorphous fraction. Considering all these results, it seems that the mineral of the −DAG group mainly consisted of calcium-deficient HA (CDHA) with an amorphous mineral fraction (ACP). The mineral formed in the +DAG group mainly consisted of ACP, OCP, Mg whitlockite, CDHA and HA.

Both groups showed mineralization patterns, indicating that mineralization itself is not induced by DAG only. However, the results of this study also show that DAG leads to certain differences regarding the quantity and quality of mineralization.

Materials and methods

Culture of USSCs

Unrestricted somatic stem cells (USSCs) were kindly provided by the José Carreras stem cell bank (Heinrich-Heine University of Düsseldorf, Germany). The cells were isolated from cord blood with informed consent of the mother and afterwards isolated and cultivated in accordance with a standardized protocol published by Kogler et al. (2004). Briefly, Ficoll (Biochrom) gradient centrifugation was used to isolate the mononuclear cell fraction. Cells were plated out at $5–7\times10^6$ cells/mL on T25 culture flaks (Costar) in low glucose DMEM (Cambrex), supplemented with 30% FCS, dexamethasone (10^{-7} M; Sigma-Aldrich), penicillin (100 U/mL; Grünenthal), streptomycin (100 mg/mL; Hefa-pharm) and ultraglutamine (2 mM; Cambrex). Later on in the expansion of the cells, dexamethasone was left out of the medium. The cells were incubated in a humidified atmosphere at 37 °C in 5% CO_2. When confluency reached 80%, the cells were split by detaching the cells with 0.25% trypsin (Lonza) and re-plating them in at a ratio of 1:3. The medium was changed every day.

Stimulation of osteogenic differentiation and preparation of USSC microspheres

As mentioned, the USSC spheres were prepared using the microsphere culture technique. Therefore, a 60 μL solution consisting of 2% agarose in DMEM (without any supplements) was poured into each slot of a 96-well plate and left until hardened. The USSCs were detached from the plates, centrifuged and re-suspended in normal growth medium (1 million cells/mL). Then, a 180 μL cell suspension containing 180,000 cells was added on top of the solidified agarose gel and the cultures were incubated overnight. Due to the non-adhesive properties of the gel, the cells congregated in the center of the well and formed a sphere. A 160 μL volume of the medium was changed every second day.

After 3 days, 0.1 μM dexamethasone, 50 μM ascorbic acid and 10 mM β-glycerolphosphate (all from Sigma) were added to the normal growth medium (+DAG group) to achieve osteogenic pre-differentiation according to previously published works (Buttery et al., 2001; Bielby et al., 2004; Chaudhry et al., 2004; Depprich et al., 2008). A control group of USSC microspheres was cultured without DAG-mediated osteogenic stimulation (−DAG group). Subsequently, the spheres were cultured for 3, 7, 14, 21 and 28 days with a medium change every other day.

Histological staining

In order to improve the handling of the spheres they were first placed into a HistoGel® (Richard Allen Scientific, KNr.HG-4000-012). Afterwards, the samples were fixed in 4% paraformaldehyde and after dehydration in increasing alcohol concentrations they were embedded in paraffin. Slides were made using a Leica Microtome RM L155. The 1–3 μm thick slides produced were deparaffinized and stained. Furthermore, araldite-embedded spheres were sectioned into thin slices and stained. Both araldite and paraffin-embedded spheres were stained with toluidine blue and alizarine red, as mentioned in the literature. Briefly, after staining with toluidine blue the slides were counterstained with alizarin red (a mixture of 0.5 g alizarin red and 5 mL 0.28% NH3 with 45 mL distilled water (pH: 6.4)). The slides were incubated in xylene before finally being covered with entellan.

Critical point drying and preparation of the specimens for SEM

Due to the small diameter of the spheres a container was used to avoid a loss of spheres. After pipetting each sphere into a CellSafe biopsy (Leica Microsystems), the edges of the container were agglutinated. Thus, safe critical point drying could be performed without crushing or losing the spheres. Then the samples were fixed with 4% glutaraldehyde, washed with 0.1 M PBS and dehydrated in increasing concentrations of alcohol (30 min in 30, 50, 70, 90, 96% ethanol, and 100% isopropanol). The critical point drying procedure was performed following the instructors protocol. During this procedure subsequently isopropanol was substituted

for CO_2. After drying, the specimens were directly placed onto a carbon pad of a SEM holder (Cambridge). The specimens were sputtered with platinum for morphological analysis and with carbon for the EDX analysis. In order to get a view of the inner part of the spheres, some specimens were cut through the middle with a razor blade. Furthermore, for quantitative analysis, some specimens were embedded in a polymer (EPOfix®, Struers) in accordance with the manufacturer's instructions. In addition, inorganic standards of hydroxyl apatite (Bio-RAD) and calcium pyrophosphate (ChemPur) were embedded in EPOfix® to analyze the influence of the specimen preparations on the results.

Preparation of the specimens for TEM

The spheres were fixed with 2.5% glutaraldehyde and then synchronously with osmium and aldehyde for cell-morphology analysis. First, the specimens were washed three times with 0.1 M PBS for 10 min, then dehydrated in increasing alcohol concentrations (50, 70, 90, 96, 100%; 30 min each step) and transferred to propylene oxide. Afterwards, they were transferred to pure araldite by using intermediate ratios of mixtures (100% propylene oxide, 2/1 propylene oxide/araldite, 1/1, 1/2, 100% araldite). In order to harden the araldite, the specimens were kept at 42 °C for 24 h and afterwards they were sectioned with a microtome (Ultracut S, Reichert). For morphological studies, ultrathin sections were stained with osmium tetroxide (OsO_4). For ultrastructural assessment of the mineral substances no staining was performed and water contact during preparation, particularly sectioning, was reduced to a minimum in order to avoid mineral dissolution or redistribution.

Preparation of specimens for Raman spectroscopy

Normally, special fixing is not necessary for Raman spectroscopy. Paraffin-embedded samples, deparaffinized samples and araldite-embedded samples were used for the spectroscopy investigations. Paraffin slides were sectioned into 5 μm slides and araldite into 3 μm slides so that slides were thick enough for penetration of the laser. Reference spectra were taken of the EPOfix® embedded standards of hydroxyl apatite (Bio-RAD) and calcium pyrophosphate (ChemPur), and of the pure standards simply placed onto a glass holder.

Field emission scanning electron microscopy (FESEM)

In order to further analyze mineralization, scanning electron microscopy was performed by a JEOL 6300F (0.5–20 kV) equipped with an energy-dispersive X-ray detector (EDX, Oxford Inca). The pictures were processed using AnalySIS software (Olympus Soft Imaging Solutions, Münster). In order to obtain information about the morphology, the cellular matrix and the mineral on the surface of the spheres, an acceleration voltage of 1–5 kV was applied and secondary electrons (SE) were detected. An acceleration voltage of 10 kV was used for backscattered electrons (BSE) to gain a good material contrast. Semi-quantitative (EDX) analysis was performed with an acceleration voltage of 10 kV in order to have the optimum excitation energy for a range of elements. The EDX analyses were performed with INCA software. An interim analysis of the prepared standards was performed to avoid measuring errors.

Transmission electron microscopy with selected area diffraction analysis (SAED)

Samples were prepared as described above and examined in a transmission electron microscope (TEM) (EM902; Zeiss, Germany) operated at an acceleration voltage of 80 kV. The SAEDs were collected using a 1 μm aperture to select mineralized areas. Analysis of the diffraction patterns and calculation of the lattice interspaces were performed in accordance with Bragg's law. A comparison of the collected data with the lattice interspaces of different Ca–P minerals in the ASTM register (American Society for testing materials, data 1967 (e.g. HA = ASTM No. 9–432, 1967)) was made.

Raman spectroscopy

The Raman spectra were produced and collected with a confocal Jobin Yvon HR800 Raman spectrometer using an Nd-YAG (532 nm) laser running at a power of 8.5 mW with a 1000 μm aperture. The time for measurement of each spectrum was 2×30 s. The data were analyzed using Cristal Sleuth software (RRUFF Project) and compared to spectra gained from self-prepared standards of pure HA (BioRAD) on glass slides or epoxy resin-embedded and polished HA and calcium pyrophosphate (Chempur, Karlsruhe, Germany), and also to spectra from natural minerals in the program library. In order to exclude the influence of the embedding materials on the analysis, spectra of all of the embedding materials used were recorded.

Wave-length dispersive X-ray spectroscopy

For wavelength-dispersive X-ray spectroscopy (WDX) analysis the samples were embedded in Struers EPOfix®. The polished blocks were then examined using a JEOL JXA 8900 electron microprobe operated at an accelerating voltage of 15 kV and a probe current of 435×10^{-9} A. Processing of the data was performed using AnalySIS software (Olympus Soft Imaging Solutions, Münster).

Apoptosis assay

A DNA fragmentation analysis (DNA fragmentation kit III, Promocell, Germany) for the detection of apoptotic cells in the samples was used according to the manufacturer's instructions. Briefly, slices of the spheres were deparaffinized, rehydrated in decreasing ethanol concentration steps (100%, 95%, 85%, 70% and 50%), washed with PBS and fixed in 4% formaldehyde/PBS. A 20 μg/mL volume of proteinase K solution was applied for 5 min at room temperature, followed by another washing and fixing step with PBS, and then they were placed in 4% formaldehyde/PBS. After incubation with DNA Labeling Solution, the staining solution was applied for 60 min at 37 °C. The slides were washed twice with Rinse Buffer and incubated with propidium

iodide/RNase A solution for 30 min. Analysis was performed with fluorescence microscopy using a Leica DM5000B.

Supplementary materials related to this article can be foundonline at doi:10.1016/j.scr.2011.09.004.

References

Adams, C.S., Mansfield, K., Perlot, R.L., Shapiro, I.M., 2001. Matrix regulation of skeletal cell apoptosis. Role of calcium and phosphate ions. J. Biol. Chem. 276, 20316–20322.

Arnold, S., Plate, U., Wiesmann, H.P., Stratmann, U., Kohl, H., Hohling, H.J., 2001. Quantitative analyses of the biomineralization of different hard tissues. J. Microsc. 202, 488–494.

Barckhaus, R.H., Krefting, E.R., Althoff, J., Quint, P., Hohling, H.J., 1981. Electron-microscopic microprobe analysis on the initial stages of mineral formation in the epiphyseal growth plate. Cell Tissue Res. 217, 661–666.

Benito, A.I., Diaz, M.A., Gonzalez-Vicent, M., Sevilla, J., Madero, L., 2004. Hematopoietic stem cell transplantation using umbilical cord blood progenitors: review of current clinical results. Bone Marrow Transplant. 33, 675–690.

Bielby, R.C., Boccaccini, A.R., Polak, J.M., Buttery, L.D., 2004. In vitro differentiation and in vivo mineralization of osteogenic cells derived from human embryonic stem cells. Tissue Eng. 10, 1518–1525.

Bigi, A., Gandolfi, M., Koch, M.H., Roveri, N., 1996. X-ray diffraction study of in vitro calcification of tendon collagen. Biomaterials 17, 1195–1201.

Bitar, M., Brown, R.A., Salih, V., Kidane, A.G., Knowles, J.C., Nazhat, S.N., 2008. Effect of cell density on osteoblastic differentiation and matrix degradation of biomimetic dense collagen scaffolds. Biomacromolecules 9, 129–135.

Bonar, L.C., Lees, S., Mook, H.A., 1985. Neutron diffraction studies of collagen in fully mineralized bone. J. Mol. Biol. 181, 265–270.

Bonucci, E., 1981. Mechanisms of localization and increase of metastases in bone tissue. Radiol. Med. 67, 243–247.

Bourne, S., Polak, J.M., Hughes, S.P., Buttery, L.D., 2004. Osteogenic differentiation of mouse embryonic stem cells: differential gene expression analysis by cDNA microarray and purification of osteoblasts by cadherin-11 magnetically activated cell sorting. Tissue Eng. 10, 796–806.

Boyan, B.D., Schwartz, Z., Boskey, A.L., 2000. The importance of mineral in bone and mineral research. Bone 27, 341–342.

Bradshaw, A.D., Graves, D.C., Motamed, K., Sage, E.H., 2003. SPARC-null mice exhibit increased adiposity without significant differences in overall body weight. Proc. Natl. Acad. Sci. U. S. A. 100, 6045–6050.

Brown, W.E., 1962. Crystallographic and chemical relations between octacalcium phosphate and hydroxylapatite. Nature 196, 1050–1055.

Buttery, L.D., Bourne, S., Xynos, J.D., Wood, H., Hughes, F.J., Hughes, S.P., Episkopou, V., Polak, J.M., 2001. Differentiation of osteoblasts and in vitro bone formation from murine embryonic stem cells. Tissue Eng. 7, 89–99.

Chaudhry, G.R., Yao, D., Smith, A., Hussain, A., 2004. Osteogenic cells derived from embryonic stem cells produced bone nodules in three-dimensional scaffolds. J. Biomed. Biotechnol. 2004, 203–210.

Cheng, P.T., Pritzker, K.P., 1983. Solution Ca/P ratio affects calcium phosphate crystal phases. Calcif. Tissue Int. 35, 596–601.

Cheng, P.T., Pritzker, K.P., Kandel, R.A., Reid, A., 1983. Analytical scanning and transmission electron microscopy and X-ray microdiffractometry of calcium pyrophosphate dihydrate crystal deposits in tissues. Scan. Electron Microsc. 369–377.

Depprich, R., Zipprich, H., Ommerborn, M., Mahn, E., Lammers, L., Handschel, J., Naujoks, C., Wiesmann, H.P., Kubler, N.R., Meyer, U., 2008. Osseointegration of zirconia implants: an SEM observation of the bone-implant interface. Head Face Med. 4, 25.

Dorozhkin, S.V., Epple, M., 2002. Biological and medical significance of calcium phosphates. Angew. Chem. Int. Ed. Engl. 41, 3130–3146.

Franceschi, R.T., Xiao, G., 2003. Regulation of the osteoblast-specific transcription factor, Runx2: responsiveness to multiple signal transduction pathways. J. Cell. Biochem. 88, 446–454.

Freeman, J.J., Wopenka, B., Silva, M.J., Pasteris, J.D., 2001. Raman spectroscopic detection of changes in bioapatite in mouse femora as a function of age and in vitro fluoride treatment. Calcif. Tissue Int. 68, 156–162.

Giachelli, C.M., 2005. Inducers and inhibitors of biomineralization: lessons from pathological calcification. Orthod. Craniofac. Res. 8, 229–231.

Handschel, J.G., Depprich, R.A., Kubler, N.R., Wiesmann, H.P., Ommerborn, M., Meyer, U., 2007. Prospects of micromass culture technology in tissue engineering. Head Face Med. 3, 4.

Handschel, J., Berr, K., Depprich, R.A., Kubler, N.R., Naujoks, C., Wiesmann, H.P., Ommerborn, M.A., Meyer, U., 2008. Induction of osteogenic markers in differentially treated cultures of embryonic stem cells. Head Face Med. 4, 10.

Handschel, J., Simonowska, M., Naujoks, C., Depprich, R.A., Ommerborn, M.A., Meyer, U., Kubler, N.R., 2009. A histomorphometric meta-analysis of sinus elevation with various grafting materials. Head Face Med. 5, 12.

Handschel, J., Naujoks, C., Langenbach, F., Berr, K., Depprich, R., Ommerborn, M., Kubler, N., Brinkmann, M., Kogler, G., Meyer, U., 2010. Comparison of ectopic bone formation of embryonic stem cells and cord blood stem cells in vivo. Tissue Eng Part A. 16 (8), 2475–2483.

Hervy, M., Hoffman, L., Beckerle, M.C., 2006. From the membrane to the nucleus and back again: bifunctional focal adhesion proteins. Curr. Opin. Cell Biol. 18, 524–532.

Hohling, H.J., Arnold, S., Barckhaus, R.H., Plate, U., Wiesmann, H.P., 1995. Structural relationship between the primary crystal formations and the matrix macromolecules in different hard tissues. Discussion of a general principle. Connect. Tissue Res. 33, 171–178.

Hohling, H.J., Arnold, S., Plate, U., Stratmann, U., Wiesmann, H.P., 1997. Analysis of a general principle of crystal nucleation, formation in the different hard tissues. Adv. Dent. Res. 11, 462–466.

Holy, C.E., Shoichet, M.S., Davies, J.E., 2000. Engineering three-dimensional bone tissue in vitro using biodegradable scaffolds: investigating initial cell-seeding density and culture period. J. Biomed. Mater. Res. 51, 376–382.

Jager, M., Sager, M., Knipper, A., Degistirici, O., Fischer, J., Kogler, G., Wernet, P., Krauspe, R., 2004. In vivo and in vitro bone regeneration from cord blood derived mesenchymal stem cells. Orthopade 33, 1361–1372.

Jaiswal, N., Haynesworth, S.E., Caplan, A.I., Bruder, S.P., 1997. Osteogenic differentiation of purified, culture-expanded human mesenchymal stem cells in vitro. J. Cell. Biochem. 64, 295–312.

Kahle, M., Wiesmann, H.P., Berr, K., Depprich, R.A., Kubler, N.R., Naujoks, C., Cohnen, M., Ommerborn, M.A., Meyer, U., Handschel, J., 2010. Embryonic stem cells induce ectopic bone formation in rats. Biomed. Mater. Eng. 20, 371–380.

Kirsch, T., 2006. Determinants of pathological mineralization. Curr. Opin. Rheumatol. 18, 174–180.

Kögler, G., 2009. The unrestricted somatic stem cell (USSC) from Cord blood for regenerative medicine. In: Meyer, U., Meyer, T., Handschel, J., Wiesmann, H.P. (Eds.), Fundamentals of Tissue Engineering and Regenerative Medicine. Springer-Verlag, Berlin, Heidelberg, pp. 167–176.

Kogler, G., Sensken, S., Airey, J.A., Trapp, T., Muschen, M., Feldhahn, N., Liedtke, S., Sorg, R.V., Fischer, J., Rosenbaum, C., Greschat, S., Knipper, A., Bender, J., Degistirici, O., Gao, J., Caplan, A.I., Colletti, E.J., Almeida-Porada, G., Muller, H.W., Zanjani, E., Wernet, P., 2004. A new human somatic stem cell from

placental cord blood with intrinsic pluripotent differentiation potential. J. Exp. Med. 200, 123–135.

Koutsopoulos, S., 2002. Synthesis and characterization of hydroxyapatite crystals: a review study on the analytical methods. J. Biomed. Mater. Res. 62, 600–612.

Kundu, A.K., Khatiwala, C.B., Putnam, A.J., 2009. Extracellular matrix remodeling, integrin expression, and downstream signaling pathways influence the osteogenic differentiation of mesenchymal stem cells on poly(lactide-co-glycolide) substrates. Tissue Eng. Part A 15, 273–283.

Lagier, R., Baud, C.A., 2003. Magnesium whitlockite, a calcium phosphate crystal of special interest in pathology. Pathol. Res. Pract. 199, 329–335.

Langenbach, F., Naujoks, C., Kersten-Thiele, P.V., Berr, K., Depprich, R.A., Kubler, N.R., Kogler, G., Handschel, J., 2010. Osteogenic differentiation influences stem cell migration out of scaffold-free microspheres. Tissue Eng. Part A 16, 759–766.

LeGeros, R.Z., 1991. Calcium phosphates in oral biology and medicine. Monogr. Oral Sci. 15, 1–201.

LeGeros, R.Z., 2001. Formation and transformation of calcium phosphates: relevance to vascular calcification. Z. Kardiol. 90 (Suppl. 3), 116–124.

Lowenstam, H.A., 1981. Minerals formed by organisms. Science 211, 1126–1131.

Mann, S., 2001. Biomineralization: Principles and Concepts in Bioorganic Materials Chemistry. Oxford University Press, United States.

Meleti, Z., Shapiro, I.M., Adams, C.S., 2000. Inorganic phosphate induces apoptosis of osteoblast-like cells in culture. Bone 27, 359–366.

Naujoks, C., Langenbach, F., Berr, K., Depprich, R., Kubler, N., Meyer, U., Handschel, J., Kogler, G., 2011. Biocompatibility of osteogenic predifferentiated human cord blood stem cells with biomaterials and the influence of the biomaterial on the process of differentiation. J. Biomater. Appl. 25, 497–512.

Pittenger, M.F., Mackay, A.M., Beck, S.C., Jaiswal, R.K., Douglas, R., Mosca, J.D., Moorman, M.A., Simonetti, D.W., Craig, S., Marshak, D.R., 1999. Multilineage potential of adult human mesenchymal stem cells. Science 284, 143–147.

Plate, U., Hohling, H.J., Reimer, L., Barckhaus, R.H., Wienecke, R., Wiesmann, H.P., Boyde, A., 1992. Analysis of the calcium distribution in predentine by EELS and of the early crystal formation in dentine by ESI and ESD. J. Microsc. 166, 329–341.

Plate, U., Arnold, S., Stratmann, U., Wiesmann, H.P., Hohling, H.J., 1998. General principle of ordered apatitic crystal formation in enamel and collagen rich hard tissues. Connect. Tissue Res. 38, 149–157 discussion 201–145.

Putnis, A., 1992. Introduction to Mineral Sciences. Cambridge University Press, Cambridge.

Sauer, G.R., Zunic, W.B., Durig, J.R., Wuthier, R.E., 1994. Fourier transform Raman spectroscopy of synthetic and biological calcium phosphates. Calcif. Tissue Int. 54, 414–420.

Schwartz, M.A., Assoian, R.K., 2001. Integrins and cell proliferation: regulation of cyclin-dependent kinases via cytoplasmic signaling pathways. J. Cell Sci. 114, 2553–2560.

Skinner, H.C.W., 2000. Minerals and human health. In: Vaughan, D.J., Wogelius, R.A. (Eds.), Environmental Mineralogy. EoÈtvoÈs University Press, Budapest, pp. 383–412.

Skinner, H.C.W., 2005. Mineralogy of bone. In: Selinus, O. (Ed.), Essentials of Medical Geology: Impacts of the Natural Environment on Public Health. Academic Press, pp. 667–693.

Suvorova, E.I., Buffat, P.A., 2001. Electron diffraction and high resolution transmission electron microscopy in the characterization of calcium phosphate precipitation from aqueous solutions under biomineralization conditions. Eur. Cell. Mater. 1, 27–42.

Tuan, R.S., Boland, G., Tuli, R., 2003. Adult mesenchymal stem cells and cell-based tissue engineering. Arthritis Res. Ther. 5, 32–45.

Vacanti, C.A., Vacanti, J.P., 1994. Bone and cartilage reconstruction with tissue engineering approaches. Otolaryngol. Clin. North. Am. 27, 263–276.

Vats, A., Bielby, R.C., Tolley, N.S., Nerem, R., Polak, J.M., 2005. Stem cells. Lancet 366, 592–602.

Weiner, S., Lowenstam, H.A., 1989. On Biomineralization. Oxford University Press, p. 324.

Weinstein, R.S., Jilka, R.L., Parfitt, A.M., Manolagas, S.C., 1998. Inhibition of osteoblastogenesis and promotion of apoptosis of osteoblasts and osteocytes by glucocorticoids. Potential mechanisms of their deleterious effects on bone. J. Clin. Invest. 102, 274–282.

Wiesmann, H.P., Plate, U., Hohling, H.J., Barckhaus, R.H., Zierold, K., 1993. Analysis of early hard tissue formation in dentine by energy dispersive X-ray microanalysis and energy-filtering transmission electron microscopy. Scanning Microsc. 7, 711–718.

Wiesmann, H.P., Tkotz, T., Joos, U., Zierold, K., Stratmann, U., Szuwart, T., Plate, U., Hohling, H.J., 1997. Magnesium in newly formed dentin mineral of rat incisor. J. Bone Miner. Res. 12, 380–383.

Wiesmann, H.P., Chi, L., Stratmann, U., Plate, U., Fuchs, H., Joos, U., Hohling, H.J., 1998. Sutural mineralization of rat calvaria characterized by atomic-force microscopy and transmission electron microscopy. Cell Tissue Res. 294, 93–97.

Wiesmann, H.P., Meyer, U., Plate, U., Hohling, H.J., 2005. Aspects of collagen mineralization in hard tissue formation. Int. Rev. Cytol. 242, 121–156.

Wilson, C.E., Dhert, W.J., Van Blitterswijk, C.A., Verbout, A.J., De Bruijn, J.D., 2002. Evaluating 3D bone tissue engineered constructs with different seeding densities using the alamarBlue assay and the effect on in vivo bone formation. J. Mater. Sci. Mater. Med. 13, 1265–1269.

Wopenka, B., Pasteris, J.D., 2005. A mineralogical perspective on the apatite in bone. Mater. Sci. Eng., C 25, 131–143.

Wuthier, R.E., 1977. Electrolytes of isolated epiphyseal chondrocytes, matrix vesicles, and extracellular fluid. Calcif Tissue Res. 23, 125–133.

Wuthier, R.E., Rice, G.S., Wallace Jr., J.E., Weaver, R.L., LeGeros, R.Z., Eanes, E.D., 1985. In vitro precipitation of calcium phosphate under intracellular conditions: formation of brushite from an amorphous precursor in the absence of ATP. Calcif. Tissue Int. 37, 401–410.

Xiao, G., Jiang, D., Thomas, P., Benson, M.D., Guan, K., Karsenty, G., Franceschi, R.T., 2000. MAPK pathways activate and phosphorylate the osteoblast-specific transcription factor, Cbfa1. J. Biol. Chem. 275, 4453–4459.

zur Nieden, N.I., Kempka, G., Ahr, H.J., 2003. In vitro differentiation of embryonic stem cells into mineralized osteoblasts. Differentiation 71, 18–27.

3.4 Biocompatibility of osteogenic predifferentiated human cord blood stem cells with biomaterials and the influence of the biomaterial on the process of differentiation.

Naujoks, C., **Langenbach, F.**[#], Berr, K., Depprich, R., Kubler, N., Meyer, U., Handschel, J., and Kogler, G. (2011). Biocompatibility of osteogenic predifferentiated human cord blood stem cells with biomaterials and t he influence of the biomaterial on the process of differentiation. J Biomater Appl *25*, 497-512.

Impact Factor: 2,246

Durchschnittlicher Impact Faktor des Forschungsgebietes:

- Biomedical Enginnering:
    - 1,579; Rang 22 von 70 Zeitschriften

- Materials Science, Biomaterials:
    - 2,246; Rang 13 von 25 Zeitschriften

Mein Anteil an der Publikation:

- Versuche: 70%
- schriftliche Arbeit: 20%

Journal of Biomaterials Applications
http://jba.sagepub.com/

Biocompatibility of Osteogenic Predifferentiated Human Cord Blood Stem Cells with Biomaterials and the Influence of the Biomaterial on the Process of Differentiation

Christian Naujoks, Fabian Langenbach, Karin Berr, Rita Depprich, Norbert Kübler, Ulrich Meyer, Jörg Handschel and Gesine Kögler

J Biomater Appl 2011 25: 497 originally published online 5 March 2010
DOI: 10.1177/0885328209358631

The online version of this article can be found at:
http://jba.sagepub.com/content/25/5/497

Published by:
SAGE
http://www.sagepublications.com

Additional services and information for *Journal of Biomaterials Applications* can be found at:

Email Alerts: http://jba.sagepub.com/cgi/alerts

Subscriptions: http://jba.sagepub.com/subscriptions

Reprints: http://www.sagepub.com/journalsReprints.nav

Permissions: http://www.sagepub.com/journalsPermissions.nav

Citations: http://jba.sagepub.com/content/25/5/497.refs.html

>> Version of Record - Jan 13, 2011

Proof - Mar 5, 2010

What is This?

Downloaded from jba.sagepub.com at Universitats-Landesbibliothek on October 28, 2011

Biocompatibility of Osteogenic Predifferentiated Human Cord Blood Stem Cells with Biomaterials and the Influence of the Biomaterial on the Process of Differentiation

CHRISTIAN NAUJOKS, FABIAN LANGENBACH,* KARIN BERR, RITA DEPPRICH, NORBERT KÜBLER, ULRICH MEYER AND JÖRG HANDSCHEL
Department for Cranio- and Maxillofacial Surgery, Heinrich-Heine-University Düsseldorf, Moorenstr. 5, 40225 Düsseldorf, Germany

GESINE KÖGLER
Institute for Transplantation Diagnostics and Cell Therapeutics, Heinrich-Heine-University Düsseldorf, Moorenstr. 5 40225 Düsseldorf, Germany

ABSTRACT: Modern cell-based bone reconstruction therapies offer new therapeutic opportunities and tissue engineering represents a more biological-oriented approach to heal bone defects of the skeleton. Human unrestricted somatic stem cells (USSCs) derived form umbilical cord blood offer new promising aspects e.g., can differentiate into osteogenetic cells. Furthermore these cells have fewer ethical and legal restrictions compared to embryonic stem cells (ESCs). The purpose of this study was to evaluate the compatibility of osteogenic pre-differentiated USSCs with various biomaterials and to address the question, whether biomaterials influence the process of differentiation of the USSCs. After osteogenic differentiation with DAG USSCs were cultivated with various biomaterials. To asses the biocompatibility of USSCs the attachment

*Author to whom correspondence should be addressed.
E-mail: fabian.langenbach@med.uni-duesseldorf.de

0885-3282/11/05 0497–16 $10.00/0 DOI: 10.1177/0885328209358631
© The Author(s), 2011. Reprints and permissions:
http://www.sagepub.co.uk/journalsPermissions.nav

Downloaded from jba.sagepub.com at Universitats-Landesbibliothek on October 28, 2011

and the proliferation of the cells on the biomaterial were measured by a CyQUANT® assay, the morphology was analyzed by scanning electron microscopy and the influence of the gene expression was analyzed by real time PCR. Our results provide evidence that insoluble collagenous bone matrix followed by β-tricalciumphosphate is highly suitable for bone tissue engineering regarding cell attachment and proliferation. The gene expression analysis indicates that biomaterials influence the gene expression of USSCs. These results are in concordance with our previous study with ESCs.

KEY WORDS: biocompatibility, bone tissue engineering, gene expression, scaffold, scanning electron microscopy, stem cell.

INTRODUCTION

Bone defects of the cranio- and maxillofacial skeletal system can occur congenital or can be originated by manifold causes like trauma, tooth loss, infection, age depending atrophy of the jaw, and tumor resection. To achieve a sufficient quality of life it is necessary to regenerate or reconstruct these bony defects in order to recover aesthetic and functional aspects of the *stomathognatic system*. Despite the substantial progress in field of tissue engineering the use of autologous bone grafts, especially in patients with alterations of the tissue caused by radiotherapy[1], is still the gold standard [2,3] for tissue repair even though there is significant morbidity from donor site procedures and quantitative limitations [4–6]. Modern cell-based bone reconstruction therapies may offer new therapeutic opportunities and tissue engineering represents a more biological-oriented approach to heal tissue defects [7]. By using cells, scaffolds, and growth factors, the three-fold model of tissue engineering, a specialized tri-dimensional tissue is grown *in vitro* and can be implanted into the bone defect [8]. Different types of scaffolds, growth factors and cell sources – alone [9–14] or in various combinations with bioactive cytokines like bone morpheogenetic protein (BMP)-7, BMP-2, or BMP-2-mutants [15–17] – have been applied for development of bioartificial bone tissues [18–20].

Whereas transfer of the patient's own tissue as an *in situ* stimulation relies on autologous cells, extracorporal tissue engineering and genetic engineering can be done with a wide variety of cells in different stages of cell differentiation and maturation including autologous cells as well as allogenic and xenogenic cells. [21–23].

It has been shown by various investigators that embryonic stem cells (ESCs), representing pluripotent embryonic precursor cells, can differentiate under selective culture conditions into osteogenic cells [24–26]. The most common way to initiate osteogenetic differentiation in stem

Downloaded from jba.sagepub.com at Universitats-Landesbibliothek on October 28, 2011

cells is to supplement the medium with dexamethasone, ascorbic acid, and β-glycerolphosphate [26–28]. For this reason in the presented study we performed osteogenic predifferentiation of the USSCs by the supplementation of DAG to the medium. An advantage of using ESCs instead of tissue-derived progenitor cells is that ESCs are immortal and could potentially provide an unlimited supply of differentiated osteoblasts and osteoprogenitor cells for transplantation. In contrast the proliferative, self-renewal and differentiation capacity of cells derived from the adult tissue decreases with age [29,30]. In a previous animal study in rats, the osteoinductive potential of ESCs was demonstrated. ESCs were able to promote ectopic bone formation *in vivo* when they were used with demineralized bone (insoluble collagenous bone matrix, ICBM) [31].

Recently, a new promising stem cell source was established by Kögler and co-workers [32]. Human unrestricted somatic stem cells (USSCs), a multipotent cell line derived from cord blood, also have the ability to differentiate into osteogenetic cells. Moreover, compared to the ESCs the USSCs do not show any immunological rejection. Hematopoetic differentiated cells from cord blood are already used in the therapy of hematopoetic and genetic disorders [33]. In addition, we could show that USSCs can perform an osteogenic differentiation and format hydroxyl apatite in micromass culture technology [34] in a previous study (data not shown, paper in progress). Due to these facts and the above-mentioned disadvantages of ESCs we analyzed the biocompatibility of USSCs with biomaterials in the presented study.

Beside the cells the scaffold is another important field of tissue engineering. There are high demands on an ideal scaffold like cytocompatibility with the cells and biodegradability. Furthermore, the scaffold should support the attachment and proliferation of the cells and may be remodeled by the cells themselves. To date, several different bone substitutes have been studied as scaffold material for applications in tissue engineering [20]. Deproteinized bovine bone (Bio Oss®), β-tricalciumphosphate (β-TCP) (Cerasorb®), multiporose β-TCP (Cerasorb M®), collagen (Resorba®), and ICBM are commonly used scaffold materials. In a previous study, we analyzed the cytocompatibility of ESCs and the influence of the biomaterial on the differentiation of the cells on these biomaterials. We were able to show that ICBM followed by β-TCP is most suitable for bone tissue engineering regarding cell attachment and proliferation as well as the influence on the phenotype of the cells [35].

Despite the fact that scaffolds as well as the extracellular matrix have both direct and indirect influence on cells and their behavior, e.g., the rate of proliferation and gene expression profile, common approaches to engineer bone *ex vivo* are based on a combination of

Downloaded from jba.sagepub.com at Universitats-Landesbibliothek on October 28, 2011

cells and scaffolds [36]. There is still controversy concerning the use of artificial scaffolds compared to natural matrix because the physico-chemical properties of the biomaterials influence the proliferation and the gene expression of the cells [12,18,19]. On this account, we analyzed the influence of the biomaterial on the process of differentiation of USSCs by the gene expression profile.

Summarized our previous results regarding ESCs and USSCs as well as the findings of the literature conducted us to evaluate the compatibility of pre-differentiated USSCs with various biomaterials and to address the question whether biomaterials influence the process of differentiation of the USSCs.

MATERIALS AND METHODS

Culture of USSCs with Biomaterials

USSC were kindly provided by the José Carrereas Stammzellbank, Heinrich-Heine-University Düsseldorf, Germany. The cells were isolated from cord blood with informed consent of the mother, isolated, and cultivated according to a standardized protocol published by Kögler et al. [32]. Briefly, Ficoll (Biochrom) gradient centrifugation was used to isolate the mononuclear cell fraction. Cells were plated out at 5 to 7×10^6 cells/mL on T25 culture flaks (costar) in low glucose DMEM (Cambrex), supplemented with 30% FCS, dexamethasone (10^{-7} M; Sigma-Aldrich), penicillin (100 U/mL; Grünenthal), streptomycin (100 mg/mL; Hefa-pharm), and ultraglutamine (2 mM; Cambrex). Later on in the expansion of the cells, the dexamtehasone was left out of the medium. Cells were incubated in a humidified atmosphere at 37°C in 5% CO_2. The cells were split when confluency reached 80%, by detaching the cells with 0.25% trypsin (Lonza) and re-plating at ratio 1 : 3. After proliferation of the cells the osteogenic pre-differentiation was performed by addition of 0.1 μM dexamethasone, 50 μM ascorbic acid, and 10 mM β-glycerolphosphate (all from Sigma) to the normal growth medium according to previous published works [26,27,37,38]. After 3 days of osteogenic predifferentiation 200,000 cells suspended in 300 μL medium were seeded on each biomaterial-disk and cultured under the above-mentioned standardized conditions without DAG for 24 h in a 48-well-plate. The biomaterial disks were put into medium for 24 h before seeding them with cells. To standardize the surface of the specimen for each biomaterial a specimen-disk of 0.5 cm thickness and 1 cm diameter was used. After 24 h the disks were conveyed to a 6-well-plate to minimize the influence of cells that were not bound to

Downloaded from jba.sagepub.com at Universitats-Landesbibliothek on October 28, 2011

the biomaterial. Half of the specimen was analyzed at this time (day 1) of cultivation by CyQUANT®-assay reflecting the attachment of the cells on the different biomaterials. The second half of the specimen was cultured under the above mentioned conditions without DAG for 7 days. Medium change was performed every second day. On day 7 the second half of the specimen was analyzed by CyQUANT®-assay representing the proliferation of the cells on the biomaterial. Furthermore scanning electron microscopy was performed for morphological analysis of the specimen. In order to analyze the influence of the biomaterial on the osteogenic gene expression profile of the cells, real time PCR was carried out analyzing the gene expression profile. The following biomaterials were used: deproteinized bovine bone (Bio Oss® Fa. Geistlich Pharma AG, Wolhusen, Switzerland), β-TCP (Cerasorb®, Cerasorb M®, Fa. Curasan AG, Kleinostheim, Germany), collagen (RESORBA®, Fa. Resorba Wundversorgung GmbH + Co. KG, Nürnberg, Germany), and ICBM produced in our laboratory.

Preparation of ICBM

One centimetre thick slices of bovine femur spongiosa were defatted by three washing steps (24 h each) with chloroform–methanol solution (3 : 1; Merck). After a washing step in aqua destillata for 30 min the slices were bleached with H_2O_2 (Merck) for 15 min and washed again in aqua destillata. Washing the slices three times 90 min in 0.5 M HCl (Merck) was used for demineralization. Disks with a diameter of 10 mm and a height of 5 mm were cut and incubated in 4 M Guanidin-HCl/ 50 mM Tris-HCl (pH 7.0) (Merck) for 16 h at 4°C. The slices were incubated with 50 mM Tris-HCl (pH 7.0)/0.15 M NaCl (Merck) for 4 h at 4°C and washed once again with aqua destillata for 30 min.

Attachment-/Proliferation Assay

To assess the attachment and proliferation of the cells on the various biomaterials the CyQUANT® assay was used (CyQUANT Cell Proliferation Assay Kit®, Fa. Invitrogen, Karlsruhe, Germany). The CyQUANT® cell proliferation assay is a highly sensitive, fluorescence-based microplate assay for determining numbers of cultured cells. The assay employs CyQuant GR dye, which produces a large fluorescence enhancement upon binding to cellular nucleic acids that can be measured using standard fluorescein excitation (485 nm) and emission (535 nm) wavelengths. The fluorescence emission of the dye-nucleic acid complexes correlates linearly with the cell number over a large range

Downloaded from jba.sagepub.com at Universitats-Landesbibliothek on October 28, 2011

using a wide variety of cell types. Under the recommended assay conditions, the readouts of the experiments lay well within the detection limits. The assay was performed as previously described[39]. Between 8000 and 63,000 cells were analyzed per biomaterial disc.

PCR

To determine the influence of the biomaterials on the gene expression pattern of the USSCs, quantitative real time PCR was used. Because osteogenic differentiation was the main focus, genes were selected, which are known to play a key role in osteogenic cells. Total RNA was isolated from specimens using the RNeasy Mini Kit (Quiagen, Hilden, Germany) according to the manufacturer's instructions. For cDNA synthesis 800 ng total RNA was used as a template with Superscript II (Invitrogen, Paisley, UK) and OligodT-Primers (Peqlab, Erlangen, Germany). A total of 1 μL cDNA (dilution 1 : 10) was used for amplification performed with specific primers (Fa. MWG-Biotech AG, Ebersberg, Germany) for collagen type I (forward primer: 5′-AAGGGGTCTTCCTGGTGAAT-3′ and reverse primer: 5′-GGGGTACCACGTTCTCCTC-3′), alkaline phosphatase (forward primer: 5′-AAGGCTTCTTCTTGCTGGTG-3′ and reverse primer: 5′-GCCTAACCCTCATGATGTCC-3′) GAPDH (forward primer: 5′-CAATGAATACGGCTACAGCAAC-3′ and reverse primer: 5′-AGGGAGATGCTCAGTGTTGG-3′) and osteonectin (forward primer: 5′-GTGCAGAGGAAACCGAAGAG-3′ and reverse primer: 5′-TGTTTGC AGTGGTGGTTCTG-3′). For quantitative real time PCR the iCycler Thermal Cycler Base (Fa. Bio-Rad Labortatories GmbH, Munich, Germany) and qPCR MasterMix, No Rox, #RT-QP2X-03NR Eurogentec, Cologne, Germany, were used. The increase in reaction products during PCR was monitored by measuring the increase in fluorescence caused by the binding SYBR® Green to double-stranded DNA accumulating during PCR cycles. Reaction mixtures were set up as suggested by the manufacturer. Threshold cycle values of target genes were standardized against GAPDH expression and normalized to expression in cultures of USSCs which were cultured under the same conditions but had no contact to any biomaterial. This control group was differentiated for 3 days with osteogenic medium similar to the cells with contact to a biomaterial. All real time experiments in this study have been performed in accordance with to the publication of Pfaffl [40]. We have applied the mathematical model given there to eliminate deviations due to sample preparation. In order to apply this model, it is necessary to choose a reference gene (e.g., GAPDH) for calculating relative expression levels. Differences were statistically analyzed by the $2^{-\Delta\Delta Ct}$ method, a

Downloaded from jba.sagepub.com at Universitats-Landesbibliothek on October 28, 2011

convenient way to analyze the relative changes in gene expression from real-time quantitative PCR experiments. In this method, the expression of a target gene in a specific sample is normalized to the expression of the house keeping gene GAPDH ($\Delta Ct_{\text{target gene}} = Ct_{\text{target gene}} - Ct_{\text{house keeping gene}}$) and is then compared to the normalized expression of a control group. The complete equation to calculate the relative change in gene expression is $2^{-\Delta\Delta Ct} = (Ct_{\text{target gene}} - Ct_{\text{house keeping gene}})_{\text{Sample}} - (Ct_{\text{target gene}} - Ct_{\text{house keeping gene}})_{\text{Control}}$.

SCANNING ELECTRON MICROSCOPY

For Scanning electron microscopy (SEM) the biomaterial discs were fixed for 3 h with 2.5% glutaraldehyde in 0.1 M PBS (pH = 7.3) and subsequently washed in 0.1 M PBS for 30 min three times. The samples were dehydrated in increasing concentrations of acetone (from 50% to 100%, 10% steps). After critical point drying using CO_2 as transitional fluid (Bal-Tec Dryer CPD-030,) the specimens were sputter-coated with gold and observed in SEM (REM S 3000, Hitachi).

RESULTS

The biocompatibility of human USSCs on biomaterials was assessed by the attachment and the proliferation of the cells on the different materials. Furthermore, the influence of the biomaterial on the process of differentiation of the cells was monitored by an analysis of osteogenic gene expression profile. Morphological analysis of the USSCs was performed with SEM. USSCs are multipotent cell line that would be expected to be able to form bone cells and facilitate extracorporal tissue engineering of bone.

The number of cells on the biomaterial assessed by CyQUANT® assay on day one represents the attachment of USSCs on the biomaterial whether the cell count on day 7 reflects the proliferation of the cells on the biomaterial. The attachment and the proliferation of cells on biomaterials can be equalized with the biocompatibility of the biomaterial. ICBM and Cerasorb M® showed the highest cell count on day one revealing that the USSCs show better attachment on these two biomaterials compared to the other. The Influence of the biomaterial on the attachment was tested by ANOVA and showed a high statistical significance (Figure 1(a) and (b)). Cerasorb M® and ICBM showed no significant difference regarding the attachment. Interestingly, the proliferation of the cells from day 1 to day 7 only took place on ICBM and Cerasorb® and not on Cerasorb M®. The Influence of the biomaterial

Downloaded from jba.sagepub.com at Universitats-Landesbibliothek on October 28, 2011

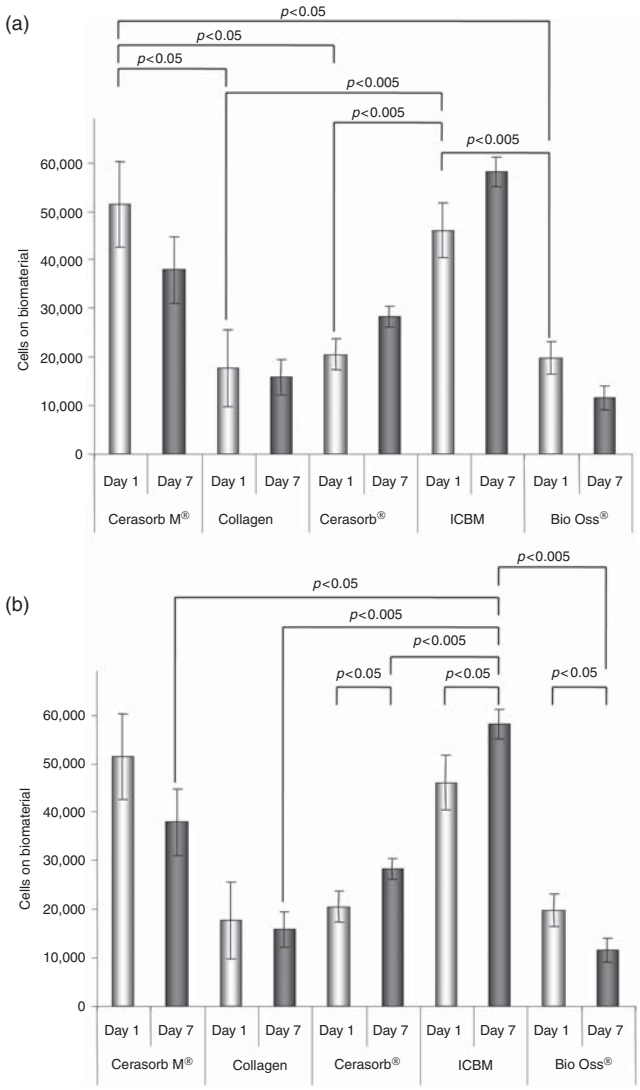

Figure 1. Relative attachment and proliferation values. Shown are the means of the CyQUANT® assay on day 1 and 7 which are a relative measure for attachment or the proliferation of the cells on the biomaterial. ANOVA analysis determined the biomaterial specific differences as statistically significant. (a) ICBM and Cerasorb M® showed a significant better attachment of USSCs compared to Collagen, Cerasorb® and Bio Oss®. (b) Cerasorb® and ICBM show a significant increase of the cell count reflecting a good cell proliferation. Bio Oss® showed a significant decrease of the cell count. Note that on Cerasorb M® the cell count decreases even if this reached no statistical significance. ICBM showed the highest total cell count after 7 days of proliferation.

Downloaded from jba.sagepub.com at Universitats-Landesbibliothek on October 28, 2011

on the proliferation was tested by ANOVA and showed a high statistical significance regarding the increase on ICBM and Cerasorb. All other biomaterials including Cersorb M showed a decrease of the cell count to day seven, but these findings reached statistical significance only on Bio Oss® (Figure 1(c)). On day 7 ICBM showed the highest cell number compared to all other biomaterials. This difference is highly statistically significant compared to all other biomaterials (Figure 1(d)).

The CyQUANT® results were confirmed with SEM. On Bio Oss no cells were observable, whereas on all other biomaterials a layer of cells was visible. The USSCs had direct contact to the biomaterial. An invasion of the cells in the pores of the biomaterial could only be detected

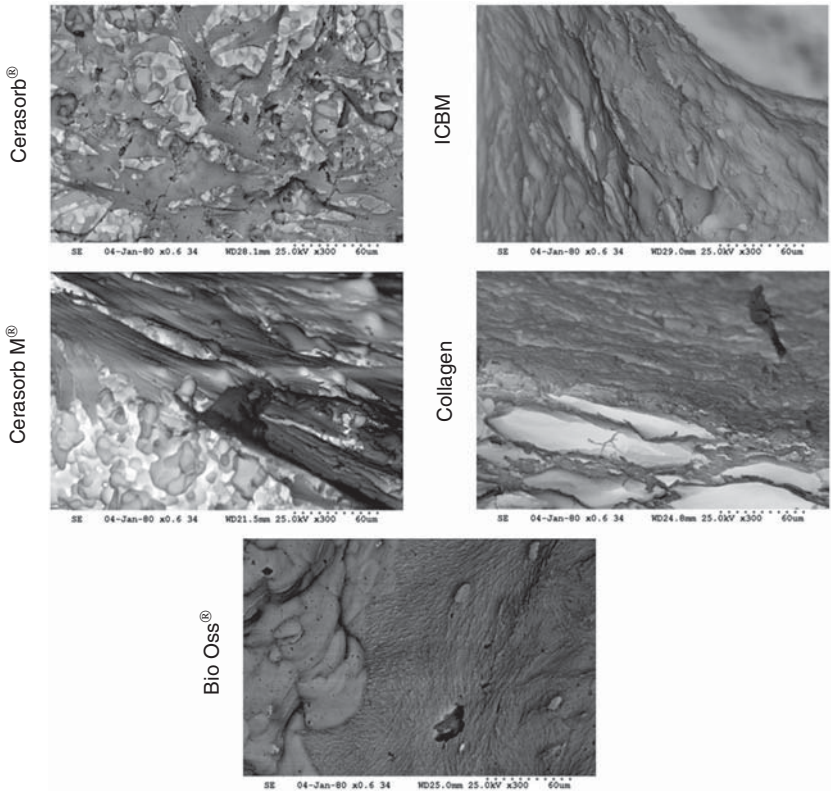

Figure 2. SEM of biomaterials with USSCs. On Bio Oss® there are hardly any cells observable. The other biomaterials show a layer of cells. Morphologically, the cells do not show the characteristics of undifferentiated USSCs but rather of mesenchymal cells and they seem to be in close attachment to each other. An invasion of the cells into the pores is only observable on ICBM.

Downloaded from jba.sagepub.com at Universitats-Landesbibliothek on October 28, 2011

on ICBM. It seems that the pore size of both tricalciumphosphate materials and the collagen is too small to be invaded. Especially on Cerasorb M®, ICBM and Collagen the cells did not show the morphological characteristics of undifferentiated USSCs but rather of mesenchymal cells (Figure 2). The cells showed a cubic, flattened appearance and seemed to be in close attachment to each other like an epithelial layer. Compared to the other biomaterials especially on ICBM a particularly dense cell layer with a close attachment to each other has been formed. In addition the cells on ICBM resemble most closely to the phenotype of osteoblasts.

The gene expression analysis showed varying results. The gene expression levels of the analyzed osteogenic markers varied on every biomaterial so that every biomaterial generated a specific gene expression pattern. Interestingly, also the gene expression pattern varies between the two β-TCP (Cerasorb®, Cerasorb M®) scaffolds. The highest levels of collagen I and osteonectin were seen on Cerasorb M® and Collagen (Figure 3). In conformance with the previous results with ESCs and the CyQUANT® analysis, the RNA content on Bio Oss® was not sufficient for generating cDNA and real time PCR analysis.

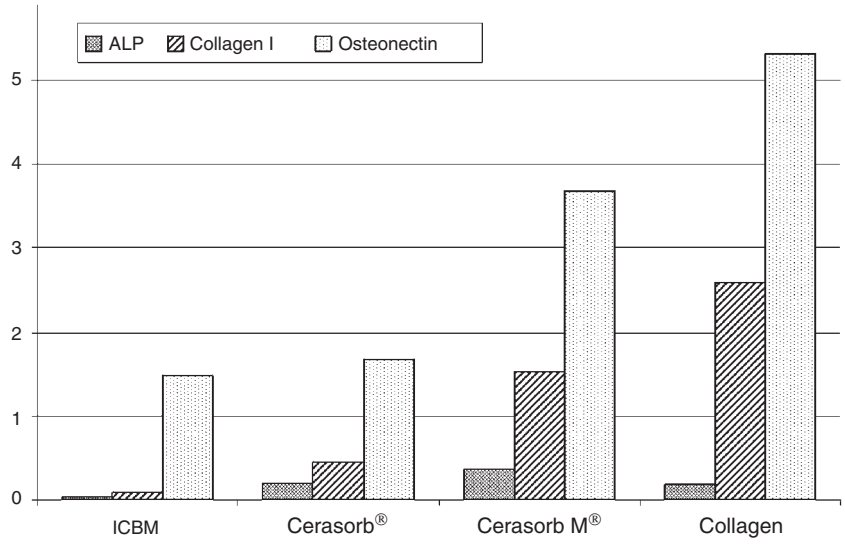

Figure 3. Gene expression analysis. Shown are the multiple of gene expression levels compared to the culture of USSCs without contact to any biomaterial. ▩ expression of alkaline phosphatase; ▨ expression of collagen I; ⁘ expression of osteonectin. Note: On Bio Oss® no values are detectable.

Downloaded from jba.sagepub.com at Universitats-Landesbibliothek on October 28, 2011

DISCUSSION

Besides growth factors, the two main folds of bone tissue engineering are the scaffolds with their material specific properties and the chosen cell line. The USSCs are a promising cell source for tissue engineering of bone. In this study, it has been shown that there are remarkable differences in the compatibility of USSCs with biomaterials. In addition, these biomaterials apparently influence the gene expression profile of the USSCs.

The biocompatibility of different biomaterials and USSCs was evaluated by vital cells on day 1 and day 7 after cell-application analyzed with a fluorescence based microplate assay (CyQUANT® assay). Compared to other assays which detect ATP, the CyQUANT® assay had a lower suspectibility of the intracellular DNA content compared to the ATP concentration measured by other assays. Thus this assay is more sensitive leading to a high correlation between the measured concentration and the cell number in the CyQUANT® assay [39].

The results of the CyQUANT® assay show impressively that after 7 days the highest number of living cells appeared on the demineralized bone (ICBM). The difference to the other biomaterials reached high statistical significance. Even if there were no differences between ICBM and Cerasorb M® regarding the attachment of the cells, the proliferation of the cells only took place on ICBM and not on Cerasorb M®. These findings underline that the USSCs show the best attachment on ICBM; furthermore, they proliferate best on ICBM compared to the other materials. In addition, the SEM analysis supports theses findings. A close correlation between proliferation assay and SEM in compatibility testing was also detected by other authors [41]. On the biomaterials, the cells have lost their spheroidal shape, which is characteristic for USSCs, and are attached to the scaffolds by their pseudopods. Thus these cells resemble osteoblast-like cells. However, regarding the gene expression, which does not reflect osteoblast-like expression patterns, this cell shape could also resemble mesenchymal (stem) cells. These results correlate with previously published results from our work regarding the biocompatibility of ESCs on different biomaterials [35].

Biocompatibility of biomaterials are influenced by the tridimensional topography and the physico-chemical properties of the material surface [19]. Many studies that have demonstrated that osteoblasts are very sensible to the gross topography of the surface of a biomaterial [42–44]. According to the structure of the surface, cells adapt with their orientation, migration and attachment kinetics [45–47]. The porosity of the material is one of the major properties that affects the structure of

Downloaded from jba.sagepub.com at Universitats-Landesbibliothek on October 28, 2011

the surface and should be about 100 μm [48]. Regarding the macropores ICBM has the highest porosity and the largest pores of the materials tested in this study. The pores are interconnected to each other and thus may improve bone formation. These geometric properties may have a positive effect on the formation of bone [49]. This is, however, obvious since ICBM is a natural product made of bovine bone, whereas the products of Cerasorb and collagen are synthetic constructs that try to meet the biological properties. The size of the pores may also be the reason for the differences regarding the proliferation of the cells between Cerasorb® and Cerasorb M®. These materials are both made of β-TCP and only differ in the size of the pores.

Furthermore, the physico-chemical properties of the materials may influence the behavior of the cells. Interestingly, ICBM, which consists primarily of collagen type I, provides the best conditions for the cell attachment and proliferation. Various studies support these findings and could prove that the attachment of osteoblasts in the first hours mainly depends whether the surface of the material is similar to proteins [43,50]. These authors have described that the highest number of mesenchymal stem cells was found on biomaterials with a high content of collagen. The fact that ICBM has by far the highest portion of collagen may be an adequate explanation for the best biocompatibility of ICBM.

Regarding the attachment of cells Turhani et al. showed recently that the attachment on Bio Oss® is worse compared to peptid P15 coated hydroxylapatite. Furthermore, the presented results of this study are in coexistence with the results of Petrovic and co-workers [51], which could show significant higher proliferation and attachment of cells on biomaterials with large fraction of collagen compared to materials with less or without collagen. In the presented study ICBM showed the highest fraction of collagen apart from the collagen sponge (RESORBA®). The fact that RESORBA® has significantly smaller pores compared to the ICBM, may be a possible explanation for the reduced proliferation of the cells compared to the ICBM. Furthermore, it may be possible that ICBM contains relicts of growth factors which could extend the osteogenic stimulation of the cells [15].

Regarding the gene expression we observed very different expression patterns depending on the biomaterial. This means that the biomaterial does affect the gene expression. However, the underlying reasons are not known. These findings are in concordance with our previous results regarding the ESCs [35].

In conclusion, ICBM is highly suitable for bone tissue engineering with USSCs regarding cell proliferation and phenotype. However, this does not infer that this biomaterial induces ostogenic differentiation.

Downloaded from jba.sagepub.com at Universitats-Landesbibliothek on October 28, 2011

That might provide new options in the therapy of periodontal bone defects or bone loss due to trauma, tooth loss, and atrophie. Furthermore, we could demonstrate that the biomaterial influences the osteogenic differentiation of the cells.

ACKNOWLEDGMENTS

Fabian Langenbach is supported by a grant of Deutsche Forschungsgemeinschaft (DFG) (HA 3228/2-1). The work of Prof. Kögler is supported by the DFG grant KO2119/6-1.

REFERENCES

1. Prott, F.J., Handschel, J., Micke, O., Sunderkotter, C., Meyer, U. and Piffko, J. Long-term Alterations of Oral Mucosa in Radiotherapy Patients, *Int. J. Radiat. Oncol. Biol. Phys.*, 2002: **54**: 203–210.
2. Pretorius, J.A., Melsen, B., Nel, J.C. and Germishuys, P.J. A Histomorphometric Evaluation of Factors Influencing the Healing of Bony Defects Surrounding Implants, *Int. J. Oral Maxillofac. Implants*, 2005: **20**: 387–398.
3. Damien, C.J. and Parsons, J.R. Bone Graft and Bone Graft Substitutes: A Review of Current Technology and Applications, *J. Appl. Biomater.*, 1991: **2**: 187–208.
4. Suh, J.D., Sercarz, J.A., Abemayor, E. et al. Analysis of Outcome and Complications in 400 Cases of Microvascular Head and Neck Reconstruction, *Arch. Otolaryngol. Head Neck Surg.*, 2004: **130**: 962–966.
5. Sasso, R.C., LeHuec, J.C. and Shaffrey, C. Iliac Crest Bone Graft Donor Site Pain After Anterior Lumbar Interbody Fusion: A Prospective Patient Satisfaction Outcome Assessment, *J. Spinal. Disord. Tech.*, 2005: **18**: S77–81.
6. Youdas, J.W., Wood, M.B., Cahalan, T.D. and Chao, E.Y. A Quantitative Analysis of Donor Site Morbidity After Vascularized Fibula Transfer, *J. Orthop. Res.*, 1988: **6**: 621–629.
7. Meyer, U., Wiesmann, H.P., Berr, K., Kubler, N.R. and Handschel, J. Cell-based Bone Reconstruction Therapies-Principles of Clinical Approaches, *Int. J. Oral Maxillofac. Implants*, 2006: **21**: 899–906.
8. Naujoks, C., Depprich, R. and Handschel, J. Aktueller Stand Des Osteogenen Tissue Engineerings, *Zahnärztliche Mitteilungen*. (Review), 2008: **98**: 2688–2695.
9. Handschel, J., Wiesmann, H.P., Stratmann, U., Kleinheinz, J., Meyer, U. and Joos, U. TCP is Hardly Resorbed and not Osteoconductive in a Non-loading Calvarial Model, *Biomaterials*, 2002: **23**: 1689–1695.
10. Cohen, S.R., Holmes, R.E., Meltzer, H.S., Levy, M.L. and Beckett, M.Z. Craniofacial Reconstruction with a Fast Resorbing Polymer: A 6- to 12-month Clinical Follow-up Review, *Neurosurg. Focus*, 2004: **16**: E12.

Downloaded from jba.sagepub.com at Universitats-Landesbibliothek on October 28, 2011

11. Holmes, R.E., Cohen, S.R., Cornwall, G.B., Thomas, K.A., Kleinhenz, K.K. and Beckett, M.Z. MacroPore Resorbable Devices in Craniofacial Surgery, *Clin. Plast. Surg.*, 2004: **31**: 393–406.
12. Kasaj, A., Reichert, C., Gotz, H., Rohrig, B., Smeets, R. and Willershausen, B. In Vitro Evaluation of Various Bioabsorbable and Nonresorbable Barrier Membranes for Guided Tissue Regeneration, *Head Face Med.*, 2008: **4**: 22.
13. Thaller, S.R., Hoyt, J., Borjeson, K., Dart, A. and Tesluk, H. Reconstruction of Calvarial Defects with Anorganic Bovine Bone Mineral (Bio-Oss) in a Rabbit Model, *J. Craniofac. Surg.*, 1993: **4**: 79–84.
14. Velich, N., Nemeth, Z., Hrabak, K., Suba, Z. and Szabo, G. Repair of Bony Defect with Combination Biomaterials, *J. Craniofac. Surg.*, 2004: **15**: 11–15.
15. Kubler, N.R., Wurzler, K.K., Reuther, J.F., Sieber, E., Kirchner, T. and Sebald, W. Effect of Different Factors on the Bone Forming Properties of Recombinant BMPs, *Mund Kiefer Gesichtschir.*, 2000: **4**: S465–S469.
16. Terheyden, H., Knak, C., Jepsen, S., Palmie, S. and Rueger, D.R. Mandibular Reconstruction with a Prefabricated Vascularized Bone Graft Using Recombinant Human Osteogenic Protein-1: An Experimental Study in Miniature Pigs. Part I: Prefabrication, *Int. J. Oral Maxillofac. Surg.*, 2001: **30**: 373–379.
17. Depprich, R., Handschel, J., Sebald, W., Kubler, N.R. and Wurzler, K.K. Comparison of the Osteogenic Activity of Bone Morphogenetic Protein (BMP) Mutants, *Mund Kiefer Gesichtschir.*, 2005: **9**: 363–368.
18. Meyer, U., Joos, U. and Wiesmann, H.P. Biological and Biophysical Principles in Extracorporal Bone Tissue Engineering. Part I, *Int. J. Oral Maxillofac. Surg.*, 2004: **33**: 325–332.
19. Meyer, U., Joos, U. and Wiesmann, H.P. Biological and Biophysical Principles in Extracorporal Bone Tissue Engineering. Part III, *Int. J. Oral Maxillofac. Surg.*, 2004: **33**: 635–641.
20. Wiesmann, H.P., Joos, U. and Meyer, U. Biological and Biophysical Principles in Extracorporal Bone Tissue Engineering. Part II, *Int. J. Oral Maxillofac. Surg.*, 2004: **33**: 523–530.
21. Handschel, J., Wiesmann, H.P., Depprich, R., Kubler, N.R. and Meyer, U. Cell-based Bone Reconstruction Therapies–Cell Sources, *Int. J. Oral Maxillofac. Implants*, 2006: **21**: 890–898.
22. Puricelli, E., Ulbrich, L.M., Ponzoni, D. and Filho, J.J. Histological Analysis of the Effects of a Static Magnetic Field on Bone Healing Process in Rat Femurs, *Head Face Med.*, 2006: **2**: 43.
23. Yamaguchi, M., Hirayama, F., Murahashi, H. et al. Ex Vivo Expansion of Human UC Blood Primitive Hematopoietic Progenitors and Transplantable Stem Cells Using Human Primary BM Stromal Cells and Human AB Serum, *Cytotherapy*, 2002: **4**: 109–118.
24. Heng, B.C., Cao, T., Stanton, L.W., Robson, P. and Olsen, B. Strategies for Directing the Differentiation of Stem Cells into the Osteogenic Lineage In Vitro, *J. Bone Miner. Res.*, 2004: **19**: 1379–1394.
25. zur Nieden, N.I., Kempka, G., Rancourt, D.E. and Ahr, H.J. Induction of Chondro-, Osteo- and Adipogenesis in Embryonic Stem Cells by Bone

Downloaded from jba.sagepub.com at Universitats-Landesbibliothek on October 28, 2011

Morphogenetic Protein-2: Effect of Cofactors on Differentiating Lineages, *BMC Dev. Biol.*, 2005: **5**: 1.

26. Chaudhry, G.R., Yao, D., Smith, A. and Hussain, A. Osteogenic Cells Derived from Embryonic Stem Cells Produced Bone Nodules in Three-dimensional Scaffolds, *J. Biomed. Biotechnol.*, 2004: 203–210.
27. Bielby, R.C., Boccaccini, A.R., Polak, J.M. and Buttery, L.D. In Vitro Differentiation and In Vivo Mineralization of Osteogenic Cells Derived from Human Embryonic Stem Cells, *Tissue Eng.*, 2004: **10**: 1518–1525.
28. Handschel, J., Berr, K., Depprich, R.A. et al. Induction of Osteogenic Markers in Differentially Treated Cultures of Embryonic Stem Cells, *Head Face Med.*, 2008: **4**: 10.
29. D'Ippolito, G., Schiller, P.C., Ricordi, C., Roos, B.A. and Howard, G.A. Age-related Osteogenic Potential of Mesenchymal Stromal Stem Cells from Human Vertebral Bone Marrow, *J. Bone Miner. Res.*, 1999: **14**: 1115–1122.
30. Quarto, R., Thomas, D. and Liang, C.T. Bone Progenitor Cell Deficits and the Age-associated Decline in Bone Repair Capacity, *Calcif. Tissue Int.*, 1995: **56**: 123–129.
31. Kahle, M., Wiesmann, H.P., Berr, K. et al. Ectopic Bone Formation with Embryonic Stem Cells in Rats, *Int. J. Artif. Organs*, 2009 (under review).
32. Kogler, G., Sensken, S., Airey, J.A. et al. A new Human Somatic Stem Cell from Placental Cord Blood with Intrinsic Pluripotent Differentiation Potential, *J. Exp. Med.*, 2004: **200**: 123–135.
33. Benito, A.I., Diaz, M.A., Gonzalez-Vicent, M., Sevilla, J. and Madero, L. Hematopoietic Stem cell Transplantation Using Umbilical Cord Blood Progenitors: Review of Current Clinical Results, *Bone Marrow Transplant.*, 2004: **33**: 675–690.
34. Handschel, J.G., Depprich, R.A., Kubler, N.R., Wiesmann, H.P., Ommerborn, M. and Meyer, U. Prospects of Micromass Culture Technology in Tissue Engineering, *Head Face Med.*, 2007: **3**: 4.
35. Handschel, J., Berr, K., Depprich, R. et al. Compatibility of Embryonic Stem Cells with Biomaterials, *J. Biomater. Appl.*, 2008: **23**: 549–560.
36. Meyer, U. and Wiesmann, H.P. (2005). *Bone and Cartilage Tissue Engineering*, Heidelberg, Berlin, Tokyo, New York, Springer.
37. Buttery, L.D., Bourne, S., Xynos, J.D. et al. Differentiation of Osteoblasts and In Vitro Bone Formation from Murine Embryonic Stem Cells, *Tissue Eng.*, 2001: **7**: 89–99.
38. Depprich, R., Zipprich, H., Ommerborn, M. et al. Osseointegration of Zirconia Implants: An SEM Observation of the Bone-implant Interface, *Head Face Med.*, 2008: **4**: 25.
39. Jones, L.J., Gray, M., Yue, S.T., Haugland, R.P. and Singer, V.L. Sensitive Determination of Cell Number Using the CyQUANT Cell Proliferation Assay, *J. Immunol. Methods*, 2001: **254**: 85–98.
40. Pfaffl, M.W. A New Mathematical Model for Relative Quantification in Real-time RT-PCR, *Nucleic Acids Res.*, 2001: **29**: e45.
41. Bandyopadhyay-Ghosh, S., Reaney, I.M., Brook, I.M., Hurrell-Gillingham, K., Johnson, A. and Hatton, P.V. In Vitro Biocompatibility of Fluorcanasite Glass-ceramics for Bone Tissue Repair, *J. Biomed. Mater. Res. A.*, 2006: **80**: 175–183.

Downloaded from jba.sagepub.com at Universitats-Landesbibliothek on October 28, 2011

42. Dalby, M.J., Di Silvio, L., Davies, G.W. and Bonfield, W. Surface Topography and HA Filler Volume Effect on Primary Human Osteoblasts In Vitro, *J. Mater. Sci. Mater. Med.*, 2000: **11**: 805–810.
43. Dennis, J.E., Haynesworth, S.E., Young, R.G. and Caplan, A.I. Osteogenesis in Marrow-derived Mesenchymal Cell Porous Ceramic Composites Transplanted Subcutaneously: Effect of Fibronectin and Laminin on Cell Retention and Rate of Osteogenic Expression, *Cell Transplant.*, 1992: **1**: 23–32.
44. Goshima, J., Goldberg, V.M. and Caplan, A.I. The Osteogenic Potential of Culture-expanded Rat Marrow Mesenchymal Cells Assayed In Vivo in Calcium Phosphate Ceramic Blocks, *Clin. Orthop. Relat. Res.*, 1991: **262**: 298–311.
45. Chehroudi, B., McDonnell, D. and Brunette, D.M. The Effects of Micromachined Surfaces on Formation of Bonelike Tissue on Subcutaneous Implants as Assessed by Radiography and Computer Image Processing, *J. Biomed. Mater. Res.*, 1997: **34**: 279–290.
46. den Braber, E.T., de Ruijter, J.E., Smits, H.T., Ginsel, L.A., von Recum, A.F. and Jansen, J.A. Effect of Parallel Surface Microgrooves and Surface Energy on Cell Growth, *J. Biomed. Mater. Res.*, 1995: **29**: 511–518.
47. Wojciak-Stothard, B., Curtis, A.S., Monaghan, W., McGrath, M., Sommer, I. and Wilkinson, C.D. Role of the Cytoskeleton in the Reaction of Fibroblasts to Multiple Grooved Substrata, *Cell Motil. Cytoskeleton.*, 1995: **31**: 147–158.
48. O'Brien, F.J., Harley, B.A., Yannas, I.V. and Gibson, L.J. The Effect of Pore Size on Cell Adhesion in Collagen-GAG Scaffolds, *Biomaterials*, 2005: **26**: 433–441.
49. Mahmood, J., Takita, H., Ojima, Y., Kobayashi, M., Kohgo, T. and Kuboki, Y. Geometric Effect of Matrix Upon cell Differentiation: BMP-induced Osteogenesis Using a New Bioglass with a Feasible Structure, *J. Biochem. (Tokyo)*, 2001: **129**: 163–171.
50. Meyer, U., Meyer, T. and Jones, D.B. Attachment Kinetics, Proliferation Rates and Vinculin Assembly of Bovine Osteoblasts Cultured on Different Pre-coated Artificial Substrates, *J. Mater. Sci. Mater. Med.*, 1998: **9**: 301–307.
51. Petrovic, L., Schlegel, A.K., Schultze-Mosgau, S. and Wiltfang, J. Different Substitute Biomaterials as Potential Scaffolds in Tissue Engineering, *Int. J. Oral Maxillofac. Implants*, 2006: **21**: 225–231.

Downloaded from jba.sagepub.com at Universitats-Landesbibliothek on October 28, 2011

3.5 Improvement of the cell-loading efficiency of biomaterials by inoculation with stem cell-based microspheres, in osteogenesis

[5] **Langenbach, F.**, Naujoks, C.[#], Laser, A., Kelz, M., Kersten-Thiele, P., Berr, K., Depprich, R., Kubler, N., Kogler, G., and H andschel, J. (2012). Improvement of the cell-loading efficiency of biomaterials by inoculation with stem cell-based microspheres, in osteogenesis. J Biomater Appl *26*, 549-564.

Impact Factor: 2,246

Durchschnittlicher Impact Faktor des Forschungsgebietes:

- Biomedical Enginnering:
    - 1,579; Rang 22 von 70 Zeitschriften
-
- Materials Science, Biomaterials:
- 2,246 Rang 13 von 25 Zeitschriften

Mein Anteil an der Publikation:

- Versuche: 35%
- schriftliche Arbeit: 90%

Journal of Biomaterials Applications
http://jba.sagepub.com/

Improvement of the Cell-loading Efficiency of Biomaterials by Inoculation with Stem Cell-based Microspheres, in Osteogenesis

Fabian Langenbach, Christian Naujoks, Andrea Laser, Michael Kelz, Pia Kersten-Thiele, Karin Berr, Rita Depprich, Norbert Kübler, Gesine Kögler and Jörg Handschel

J Biomater Appl 2012 26: 549 originally published online 6 September 2010
DOI: 10.1177/0885328210377675

The online version of this article can be found at:
http://jba.sagepub.com/content/26/5/549

Published by:
SAGE
http://www.sagepublications.com

Additional services and information for *Journal of Biomaterials Applications* can be found at:

Email Alerts: http://jba.sagepub.com/cgi/alerts

Subscriptions: http://jba.sagepub.com/subscriptions

Reprints: http://www.sagepub.com/journalsReprints.nav

Permissions: http://www.sagepub.com/journalsPermissions.nav

Citations: http://jba.sagepub.com/content/26/5/549.refs.html

>> Version of Record - Jan 9, 2012

Proof - Sep 6, 2010

What is This?

Downloaded from jba.sagepub.com at Universitats-Landesbibliothek on January 11, 2012

Improvement of the Cell-loading Efficiency of Biomaterials by Inoculation with Stem Cell-based Microspheres, in Osteogenesis

FABIAN LANGENBACH,[1] CHRISTIAN NAUJOKS,[1,*] ANDREA LASER,[1] MICHAEL KELZ,[1] PIA KERSTEN-THIELE,[1] KARIN BERR,[1] RITA DEPPRICH,[1] NORBERT KÜBLER,[1] GESINE KÖGLER[2] AND JÖRG HANDSCHEL[1]

[1]*Department for Cranio- and Maxillofacial Surgery Heinrich-Heine-University Düsseldorf, Moorenstraase 5 40225 Düsseldorf, Germany*

[2]*Institute for Transplantation Diagnostics and Cell Therapeutics Heinrich-Heine-University, Düsseldorf, Moorenstrasse 5 40225 Düsseldorf, Germany*

ABSTRACT: In critical-size bone defects, autologous or allogenic cells are required in addition to compatible biomaterials for the successful defect healing. State of the art inoculation methods of biomaterials are based on the application of cell suspensions to the biomaterial. However, only less amounts of cells can be applied and sufficient adhesion to the material is required. Therefore, it was investigated whether the advantages of stem cell-based microspheres and insoluble collagenous bone matrix (ICBM) scaffolds can be combined which can lead to an advancement in cell seeding on biomaterials. Microspheres were produced from unrestricted somatic stem cells from human umbilical cord blood and were mounted on ICBM scaffolds. Following the incubation with osteogenic or control medium, the constructs were analyzed histologically after 3, 7, 14, and 28 days. Alizarin Red S and von Kossa staining revealed microsphere

*Author to whom correspondence should be addressed.
E-mail: christian.naujoks@med.uni-duesseldorf.de
Figures 3 and 4 appear in color online: http://jba.sagepub.com

0885-3282/12/05 0549–16 $10.00/0 DOI: 10.1177/0885328210377675
© The Author(s), 2010. Reprints and permissions:
http://www.sagepub.co.uk/journalsPermissions.nav

Downloaded from jba.sagepub.com at Universitats-Landesbibliothek on January 11, 2012

mineralization after 3 days in osteogenic and after 14 days in control medium. Meanwhile, a time-dependent increase in tissue, growing out of the microspheres, was detected. Our results provide evidence that microsphere–ICBM constructs are promising candidates for approaches of bone regeneration. They allow the transfer of substantially high numbers of cells in partially mineralized constructs.

KEY WORDS: biocompatibility, bone tissue engineering, scaffold, stem cell, mineralization.

INTRODUCTION

Bone defects that are caused by trauma or tumor resection often need to be reconstructed in order to restore functionality and form. Yet, the repair of such defects remains difficult leaving clinicians struggling with severe problems. The choice for a suitable technique is difficult since there is a wide range of artificial and natural scaffolds available, including metals [1,2], cements [3], polymers [4–6], decalcified bone matrix [7], and others.

Beside the choice for a natural or a synthetic material, the question arises whether in addition to these scaffolds osteogenic cells are included or not [8]. The applicability of cells is indeed difficult as they need to be immunocompatible. For the healing of critical-size defects, the application of cell-scaffold constructs or autologous bone transplants is essential. As the amount of autologous bone is restricted and the use of autologous transplants is associated with the risk of comorbidity [9,10], artificial or biological scaffolds combined with cells are promising alternatives [8,11].

Various *in vitro* and *in vivo* studies were performed to evaluate the cell behavior on a number of artificial or biological scaffold materials [12–14]. One biomaterial with promising characteristics and a superior biocompatibility *in vitro* over deproteinized bovine bone (BioOss), β-tricalciumphosphate scaffolds, and collagen sponges is insoluble collagenous bone matrix (ICBM) [14,15]. Furthermore, ICBM showed good biocompatibility *in vivo* and to bone formation when implanted with predifferentiated human unrestricted somatic stem cells (USSCs) [16].

Multipotent USSCs are isolated from human umbilical cord blood and are able to differentiate in cells of all three germ layers [17]. Furthermore, the immunological characterization of these cells at the José Carreras Stem Cell Bank (Düsseldorf) allows HLA-matching. Notwithstanding recent findings that indicate HLA-matching is not mandatory, USSCs are tolerated by host immune system [18–20]. A basically different approach that does not require the use of a scaffold is

Downloaded from jba.sagepub.com at Universitats-Landesbibliothek on January 11, 2012

available with the application of microsphere technology. Microspheres are produced by combining approximately 1.8×10^5 stem cells within a single sphere. The main advantage of this technique is that an extracellular matrix is built by the cells themselves, which resembles *in vivo* conditions more closely than those present in monolayer cultures [21,22]. When USSCs are used for the microspheres, they can be osteogenically differentiated, resulting in strong mineralization of the sphere after 1 week.

In this study we apply microsphere technique with ICBM scaffolds to investigate whether the combination of both techniques shows synergistic effects. Earlier, we demonstrated that the use of a combination of dexamethasone, ascorbic acid, and β-glycerol phosphate (DAG) appears to be more potent in inducing osteogenic differentiation than stimulation with BMP-2 alone [23]; thus the application of DAG is the method of choice in this study. We found that microspheres that were seeded on ICBM scaffolds mineralized and at the same time allowed cells to migrate to the periphery. Interestingly, only those cells that were present in the microsphere led to mineralization, whereas none of the cells which migrated into the periphery promoted any mineralization process.

MATERIALS AND METHODS

Culture of USSCs and Preparation of Microspheres

USSCs were kindly provided by the José Carreras Stammzellbank, Heinrich-Heine-University Düsseldorf, Germany. The cells were isolated from cord blood with the informed consent of the mother and subsequently cultivated according to a standardized protocol published by Kögler et al. [17]; meanwhile, they were also available as GMP grade [24]. Briefly, Ficoll (Biochrom) gradient centrifugation was used to isolate the mononuclear cell fraction. Cells were plated out at $5–7 \times 10^6$ cells/mL on T25 culture flasks (Costar) in low glucose Dulbecco's Modified Eagle Medium (DMEM) (Cambrex), supplemented with 30% Fetal Calf Serum (Pan Biotech), dexamethasone (10^{-7} M; Sigma–Aldrich), penicillin (100 U/mL; Grünenthal), streptomycin (100 mg/mL; Hefa-pharm), and ultraglutamine (2 mM; Cambrex). For the following expansion of the cells, dexamethasone was left out from the medium formulation. Cells were incubated in a humidified atmosphere at 37°C in 5% CO_2. The cells were split when confluency reached 80% by detaching the cells with 0.25% trypsin (Lonza) and replating them in the ratio 1 : 3.

Microspheres were produced as described by Langenbach et al. [22]. Briefly, cells of a well-characterized USSC line (female) were detached

Downloaded from jba.sagepub.com at Universitats-Landesbibliothek on January 11, 2012

from the plate, centrifuged, and resuspended in normal growth medium (1 Mio Cells/mL). A microsphere-assembly-unit was prepared by filling 60 μL solution consisting of 2% agarose (Biozyme) in DMEM (without any supplements) into 96-well plates. Subsequently, each well was filled with 180 μL (1.8×10^5 cells) of the cell suspension. Due to the concave surface of the hydro-gel (caused by capillary actions), the cells congregated at the center of the well and formed a sphere within 1 day.

Preparation and Inoculation of ICBM

Slices (1 cm thick) of bovine femur spongiosa were defatted by three washing steps (24 h each) with Chloroform–Methanol solution (3 : 1; Merck). After a washing step in aqua dest for 30 min, the slices were bleached with H_2O_2 (3%; Merck) for 15 min and were washed again in aqua dest. The bone was demineralized by three washing steps with 0.5 M HCl (Merck) for 90 min respectively. Disks with a diameter of 10 mm and a height of 5 mm were cut and incubated in 4 M Guanidine–HCl/50 mM Tris-HCl (pH 7.0) (Merck) for 16 h at 4°C. The cylinders were incubated with 50 mM Tris-HCl (pH 7.0)/0.15 M NaCl (Merck) for 4 h at 4°C and were washed once more with aqua dest for 30 min. For sterilization, the ICBMs were incubated in 70% ethanol (Merck) and washed three times in PBS. Dry ICBMs were placed in 12-well plates and 2 mL normal growth medium or normal growth medium supplemented with DAG (100 nM dexamethasone, 50 μM ascorbic acid, and 10 mM β-glycerophosphate; all from Sigma) was added. Each ICBM was inoculated with five microspheres. In this process, the microspheres sink into the ICBM and remain in the pores of the spongiosa scaffold. The specimens were incubated at 37°C in a humidified atmosphere with 5% CO_2 and medium was changed every 3 days.

Histology

After 3, 7, 14, and 28 days, four constructs of each treatment group were fixated in 4% formalin and incubated over night at 4°C. The scaffolds were dehydrated in increasing ethanol concentrations for 1 day per concentration and were subsequently incubated two times for 1 day in xylol (Merck). The samples were embedded in the low-temperature embedding system, Technovit 9100 (Heraeus Kulzer), according to the manufacturer's protocol. Briefly, the specimens were pre-infiltrated with Xylol/Technovit 9100 basic solution (stabilized) followed by pre-infiltration in stabilized basic solution (containing catalyst 1) and by

Downloaded from jba.sagepub.com at Universitats-Landesbibliothek on January 11, 2012

pre-infiltration in destabilized basic solution (containing catalyst 1) each for 1 day at 4°C. For the final infiltration, the samples were incubated for 3 days at 4°C in infiltration solution (basic solution (destabilized)) with catalyst 1 and PMMA). The final embedding solution consisted of 90% solution A and 10% solution B and was mixed immediately prior to the polymerization. The specimens were placed in the polymerization mold and the mixed embedding solution was added carefully. For the polymerization of the specimens, the airtight closed molds were stored at −4°C for 24 h, transferred to 4°C for 1 h and finally stored at room temperature (RT).

Sectioning and Deacrylation

Sections (8 μm) were prepared with an electronic rotary microtome (Hyrax M55, Carl Zeiss MicroImaging GmbH). The sections were stretched on superfrost plus slides, which had been precoated with a mixture of two parts ponal-solution (2% in aqua dest) and one part poly-L-lysine-solution (0.01%) for 10 min. The sections were covered with polyethylene foil and pressed with a slide-press for 12 h at 50°C.

The slides were deacrylated by incubation with 2-methoxyethylacetate (Sigma) two times for 20 min at RT, followed by incubation in xylol two times for 5 min. After rehydration in decreasing ethanol concentrations, the slides were ready for histochemical staining.

Histological Stainings

The hemalaum-eosin (H/E) staining was used to stain nuclei blue, cytoplasm red, and intercellular substance pink. The deacrylated and rehydrated sections were incubated in Mayer's hemalaum solution (Merck) for 3 min and were subsequently exposed to 0.1% HCl for 2 s. After washing with aqua dest, the sections were stained with Giemsa's azur eosin methylene blue solution (Merck) for 2 min and washed again.

For the Alizarin Red S staining, the sections were incubated in 2% Alizarin Red S (pH: 4.5) and washed in aqua dest. Alizarin Red S stains divalent cations like calcium and magnesium, whereas von Kossa staining is specific for calcium only. Calcium ions are replaced by silver ions, which are reduced to metallic silver under the influence of light. Rehydrated sections were incubated with silver nitrate solution (5%) and exposed to daylight for 15 min. After washing with aqua dest for 5 min, the sections were incubated in sodiumthiosulfate solution (2%). After washing with aqua dest for 5 min, nuclei were stained with nuclear fast red solution.

Downloaded from jba.sagepub.com at Universitats-Landesbibliothek on January 11, 2012

In order to demonstrate the nuclei more clearly, cells were stained with the DNA intercalating dye Bisbenzimide (Hoechst 33342). The sections were incubated with bisbenzimide (20 μg/mL aqua dest) in the dark and washed three times with aqua dest for 5 min.

RESULTS

Cellular Distribution Inside the ICBM

H/E staining was performed to localize the microsphere (approximately 0.9 mm in diameter) in the scaffold and to investigate the outgrowth of cells out of the microspheres (Figure 1). A time-dependent

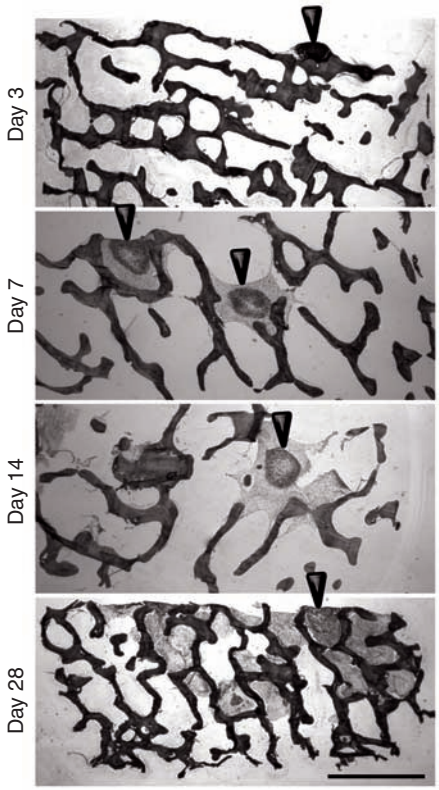

Figure 1. Microsphere–ICBM constructs were incubated for 3, 7, 14, or 28 days in DAG and were stained with H/E. The microspheres are visible as densely packed cell structures (see arrow) (bar: 2 mm).

Downloaded from jba.sagepub.com at Universitats-Landesbibliothek on January 11, 2012

increase in the amount of tissue, derived from the cells that grew out of the microspheres, was found. The shape of the microsphere remained visible in the newly formed tissue, due to a denser cellular network compared to the outgrown cells (arrows in Figure 1). Cells growing out of the microsphere were found to fill up spaces between the microsphere and the trabeculae of the spongiosa as well as spaces between adjacent trabeculae. Furthermore, the cells grew alongside the trabeculae in a thin cell layer.

In order to demonstrate the nuclei more clearly, the cells were stained with the DNA intercalating dye bisbenzimide (Figure 2). It was found that the amount of stained nuclei decreased with time of incubation inside the microsphere. Furthermore, the numbers of nuclei in the

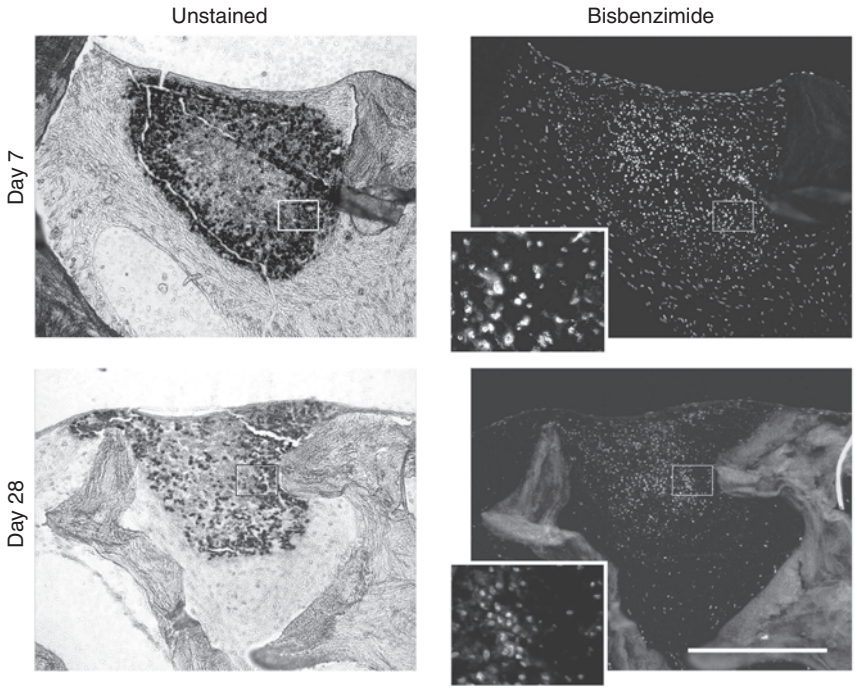

Figure 2. Nuclear distribution inside the microspheres after 7 and 28 days osteogenic differentiation with DAG. In the unstained specimens the shape of the microsphere can be seen and in the bisbenzimide stained specimens the nuclear distribution can be detected. The magnified inlay shows the reduction of the number of nuclei in the periphery of the microsphere, after 28 days (bar: 0.5 mm).

Downloaded from jba.sagepub.com at Universitats-Landesbibliothek on January 11, 2012

periphery of the microspheres had decreased compared to the center after 28 days in DAG-treated microspheres (inlay in Figure 2).

Mineralization of Microspheres

An overview of microsphere mineralization is given in Table 1. Alizarin Red S was used to demonstrate mineralization in the tissue (Figures 3 and 4, middle column). It was found that osteogenically differentiated microspheres start to mineralize after 3 days in culture and were completely mineralized after 28 days (Figure 3). Interestingly, also the control microspheres mineralized spontaneously after 14 days in culture (Figure 4). Thereby, the localizations of the mineralization showed different starting points of mineralization inside of the microspheres. Whereas the mineralization in the control microspheres started from the center, the microspheres in osteogenic medium mineralized from their periphery to the interior of the sphere. Mineralization of the cells that grew out of the microspheres could not be detected at any time in both cultures (Figures 3 and 4).

Since Alizarin Red S stain detects not only calcium in calcium phosphate but also calcium-binding proteins and proteoglycans [25], a von Kossa stain was used in addition (Figures 3 and 4, right columns). The von Kossa staining, however, is also not specific for calcium phosphate as it detects also anions like carbonate and sulfate [26]. Therefore it is suggested that Alizarin Red staining is used in combination with von Kossa staining. The chronological sequence in the mineralization-process was similar to that observed in the Alizarin Red S staining. In Figure 3, the mineralization of DAG incubated microspheres is visible at day 3 as brown/dark staining of the tissue. Again, the mineralization in the control groups is visible after 14 days (Figure 4). However, von Kossa staining also did not confirm mineralization of the outgrown tissue.

Table 1. Mineralization inside the microscope.

	Intensity					
	Alizarin Red S		von Kossa		Localization	
	Control	DAG	Control	DAG	Control	DAG
Day 3	–	+	–	+	–	Peripheral
Day 7	–	++	–	++	–	Peripheral
Day 14	++	++	++	++	Central	Peripheral
Day 28	+++	+++	+++	++	Complete	Complete

+, weak mineralization; ++, moderate mineralization; and +++, strong mineralization.

Downloaded from jba.sagepub.com at Universitats-Landesbibliothek on January 11, 2012

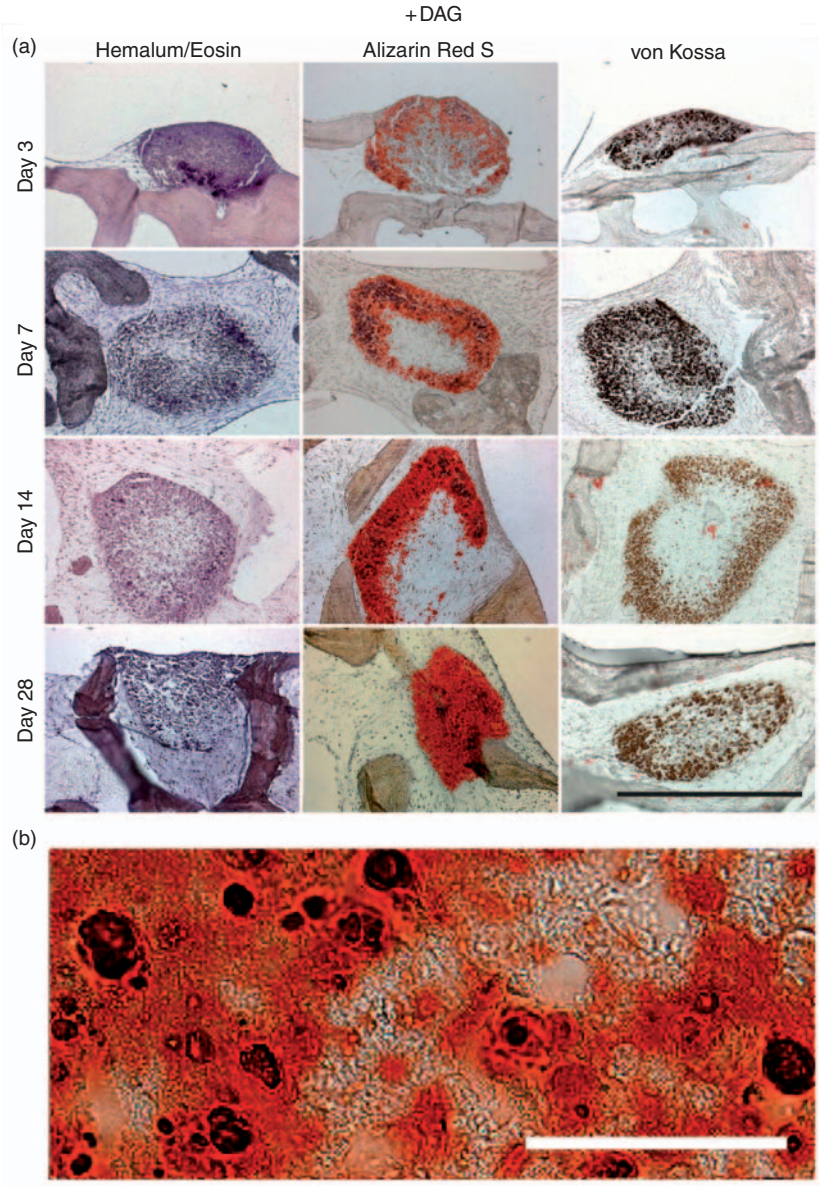

Figure 3. (a) Microsphere–ICBM constructs were incubated for 3, 7, 14, or 28 days in DAG medium and were stained with H/E (left column), Alizarin Red S (middle column) and von Kossa (right column). The microspheres are visible as densely packed cell structures (bar: 1 mm). (b) Magnification of an Alizarin Red stained mineralized microsphere after 14 days (bar: 0.1 mm).

Downloaded from jba.sagepub.com at Universitats-Landesbibliothek on January 11, 2012

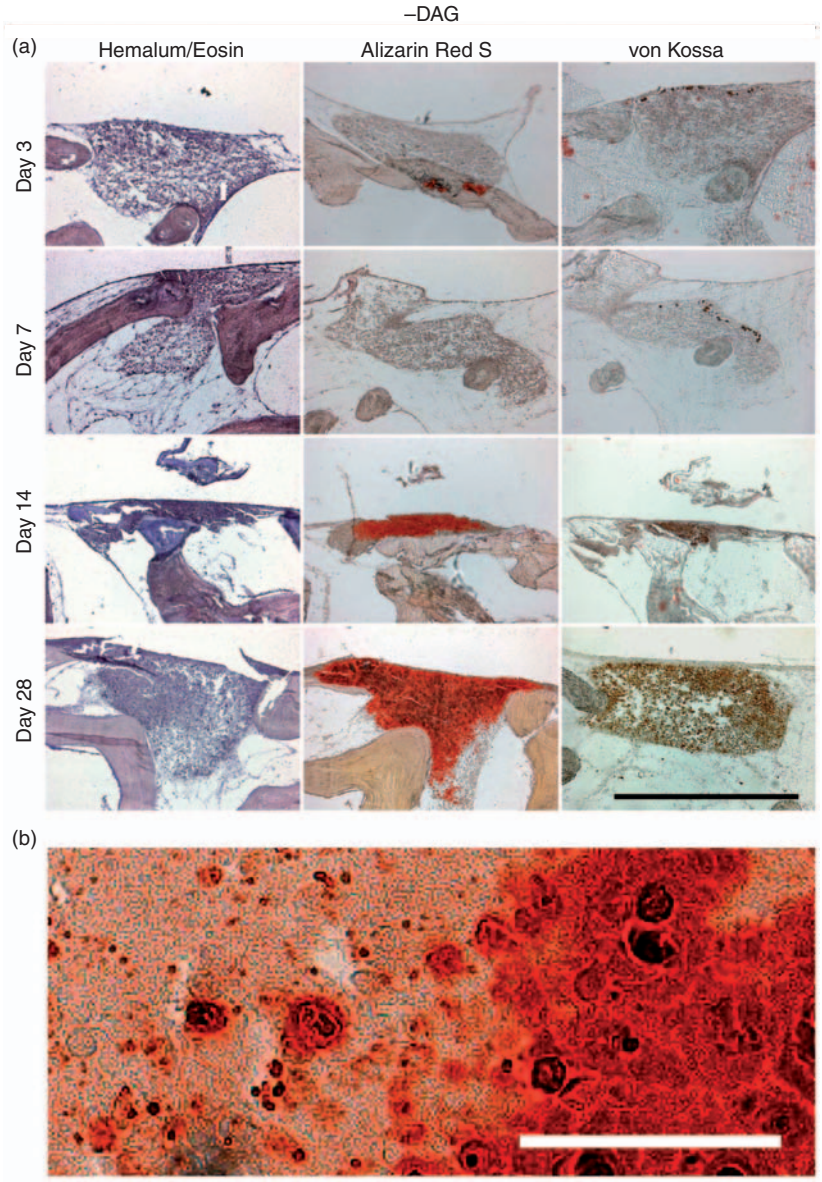

Figure 4. (a) Microsphere–ICBM constructs were incubated for 3, 7, 14, or 28 days in control medium and were stained with H/E (left column), Alizarin Red S (middle column), and von Kossa (right column). The microspheres are visible as densely packed cell structures (bar: 1 mm). (b) Magnification of an Alizarin Red stained mineralized microsphere after 14 days (bar: 0.1 mm).

Downloaded from jba.sagepub.com at Universitats-Landesbibliothek on January 11, 2012

DISCUSSION

Due to the superior characteristics of ICBM for bone tissue engineering and the advantages of the microsphere technology, these two techniques were used in combination. The main advantage of microspheres lies in their ability to synthesize extracellular matrix, thereby sharing more characteristics with the *in vivo* situation, compared to monolayer culture techniques. Furthermore, microspheres were shown to mineralize within a few days and therefore they rapidly gain stability [22].

A time-dependent increase in the amount of tissue, which consists of cells that were grown out of microspheres, was found, albeit a dense cellular meshwork, indicating that the shape of the microspheres remained visible. The cells that had grown out of the microspheres partially filled the regions between the microsphere and the trabeculae of the spongiosa as well as the spaces between the adjacent trabeculae.

At the beginning of the incubation, cells are inhomogenously distributed over the complete scaffolds. However, longer the scaffold–microsphere constructs are incubated, more cells proliferate and more parts of the scaffolds are colonized with cells. Using more microspheres which are more homogenous distributed in the scaffold could improve the uniformity of the cell distribution in the scaffold and accelerate the filling of the scaffold with cells.

It was found that the mineralization of the tissue was restricted to the microspheres. A reason for the absence of tissue mineralization outside of the microspheres could be the lower cell density in the periphery. Wilson et al. demonstrated that during cell proliferation, osteogenic differentiation is restricted or inhibited and that higher seeding densities resulted in increased bone formation *in vivo* [27]. Furthermore, low cell seeding densities led to a lower proportion of osteocalcin positive tissue compared to higher cell seeding densities [28]. Additionally, as a consequence of high cell densities, the expression of the important osteogenic regulatory factor RUNX2 (runt related nuclear transcription factor 2) as well as the transcription of osteonectin (secreted protein, acidic, cystein rich – SPARC) was up-regulated *in vitro* [29].

The spontaneous differentiation of cells inside the microsphere supports the hypothesis that high cell densities support osteogenesis. Another reason for the spontaneous differentiation may be the intercommunication of the cells and the interaction of the cells with the extracellular matrix [22]. The cells interact with the ECM via integrins on the cell surface. These integrins bind to the ECM proteins and signal bi-directionally across the plasma membrane. Thereby, they

Downloaded from jba.sagepub.com at Universitats-Landesbibliothek on January 11, 2012

influence many important cellular processes, like proliferation, migration, and gene expression [30,31]. The *de novo* synthesis and deposition of ECM proteins by mesenchymal stem cells were shown to change the chemical identity of the substrate materials as well as the integrin expression and signal transduction to influence osteogenesis [32]. It was demonstrated that the adhesion to collagen type I initiates the mitogen-activated protein kinase (MAPK) cascade. The MAPK cascade plays a critical role in the osteogenic differentiation by activating the RUNX2 transcription activator [33,34].

Another evidence for the importance of ECM proteins in osteogenic differentiation was previously provided by our group [15]. The expression of osteonectin, a matrix associated protein influences the synthesis of ECM proteins [35], as well as of collagen type I by USSC on different biomaterials, was investigated. We found an increased expression of osteonectin on collagen type I sponges, compared to other biomaterials. Knockout studies in mice provided evidence for the functional relation between collagen type I and osteonectin. Collagen type I production was significantly reduced in osteonectin knockout mice [36] and osteonectin deposition was significantly down regulated in collagen type I deficient mice [37]. In addition, we found that an increase in expression of collagen type I correlated with an increase in expression of osteonectin. The contact of microspheres to ICBM, however, is not the reason for the spontaneous differentiation. Since in a previous work [22] mineralization was detected in control microspheres which were grown without ICBM scaffold, it is unlikely that mineralization is induced by the ICBM in this study.

Differences in the starting points of microsphere mineralization can be explained by different levels of accessibility of the cells to osteogenic stimuli. The control microspheres start to differentiate spontaneously from the center of the microsphere, where they reach highest cell densities and probably the highest amount of self-synthesized osteogenic stimuli.

In contrast, in the DAG-treated group, the osteogenic stimulation is mainly provided by the DAG in the medium. Furthermore, the osteogenic stimulation of the cells in the center of the microspheres depends on a sufficient transfer of the medium to the center of the microsphere. Presumably, a lack of diffusion, caused by the tight cell layers in the periphery of the microsphere, accounts for the differences in mineralization.

Comparing cell-seeding strategies, which use the application of cell suspensions or rely on the colonization by cells of a cellular monolayer

Downloaded from jba.sagepub.com at Universitats-Landesbibliothek on January 11, 2012

on which a biomaterial is placed, the cell transfer through microspheres represents an advancement. In earlier experiments, we demonstrated that the amount of cells that could be applied on an ICBM was restricted when cell suspensions were used for inoculation [15]. When a cell suspension of 2×10^5 cells was applied on ICBM, with the same size used in this study ($\sim 0.4\,cm^3$), only about 0.5×10^5 cells adhered to the scaffolds. Compared to this, 1.8×10^5 cells were applied to an ICBM with the implantation of a single microsphere. In this study 9×10^5 cells were added per ICBM; however, more than 10 microspheres can be implanted per ICBM. Using this technique, a 40-fold higher cell load on a single ICBM is feasible, compared to inoculation with cell suspensions. In future experiments, we could try to further improve the presented constructs by using more microspheres with a smaller size. This could contribute to a more uniform cell distribution inside the microspheres that could be advantageous for the use *in vivo*. Furthermore, the positive effects of the extracellular matrix could unfold their potential at more places inside the scaffold, and also the mineralization would be more homogenously distributed.

CONCLUSION

ICBM is an excellent carrier for considerably high amounts of cells and is therefore a promising means for approaches for bone regeneration. With the help of microspheres, cell numbers that can be added to biomaterials exceed by far the numbers in current applications using cell suspensions. Furthermore, the application of microspheres accelerates the mineralization of the biomaterial–cell construct and in addition resembles *in vivo* conditions more than in current applications. Therefore the combination of microspheres with ICBM has substantial advantages available for highly efficient engineering of cell–biomaterial constructs.

ACKNOWLEDGMENTS

Fabian Langenbach was supported by a DFG grant (HA 3228/2-1). The authors thank Prof. Dr G. Kögler, José Carreras Stammzellbank of the Heinrich-Heine-University, Düsseldorf, Germany, for providing USSCs. We thank Petra Scholtysek for her contribution to this manuscript.

Downloaded from jba.sagepub.com at Universitats-Landesbibliothek on January 11, 2012

REFERENCES

1. McKee, M.D. and Nanci, A. Osteopontin: An Interfacial Extracellular Matrix Protein in Mineralized Tissues, *Connect. Tissue Res.*, 1996: **35**: 197–205.
2. Walker, P.S. and Gold, B.L. The Tribology (Friction, Lubrication and Wear) of All-metal Artificial Hip Joints 1971, *Clin. Orthop. Relat. Res.*, 1996: S4–S10.
3. Kurashina, K., Kurita, H., Kotani, A., Takeuchi, H. and Hirano, M. In Vivo Study of a Calcium Phosphate Cement Consisting of Alpha-tricalcium Phosphate/Dicalcium Phosphate Dibasic/Tetracalcium Phosphate Monoxide, *Biomaterials*, 1997: **18**: 147–151.
4. Lewis, G. Properties of Acrylic Bone Cement: State of the Art Review, *J. Biomed. Mater. Res.*, 1997: **38**: 155–182.
5. Rokkanen, P.U. Bioabsorbable Fixation Devices in Orthopaedics and Traumatology, *Ann. Chir. Gynaecol.*, 1998: **87**: 13–20.
6. Middleton, J.C. and Tipton, A.J. Synthetic Biodegradable Polymers as Orthopedic Devices, *Biomaterials*, 2000: **21**: 2335–2346.
7. Tuli, S.M. and Gupta, K.B. Bridging of Large Chronic Osteoperiosteal Gaps by Allogeneic Decalcified Bone Matrix Implants in Rabbits, *J. Trauma*, 1981: **21**: 894–898.
8. Handschel, J., Wiesmann, H.P., Depprich R., Kubler, N.R. and Meyer, U. Cell-based Bone Reconstruction Therapies – Cell Sources, *Int. J. Oral Maxillofac. Implants*, 2006: **21**: 890–898.
9. Yazar, S., Lin, C.H. and Wei, F.C. One-stage Reconstruction of Composite Bone and Soft-tissue Defects in Traumatic Lower Extremities, *Plast. Reconstr. Surg.*, 2004: **114**: 1457–1466.
10. Damien, C.J. and Parsons, J.R. Bone Graft and Bone Graft Substitutes: A Review of Current Technology and Applications, *J. Appl. Biomater.*, 1991: **2**: 187–208.
11. Meyer, U., Wiesmann, H.P., Berr, K., Kubler, N.R. and Handschel, J. Cell-based Bone Reconstruction Therapies – Principles of Clinical Approaches, *Int. J. Oral Maxillofac. Implants*, 2006: **21**: 899–906.
12. Hallab, N.J., Bundy, K.J., O'Connor, K., Clark, R. and Moses, R.L. Cell Adhesion to Biomaterials: Correlations Between Surface Charge, Surface Roughness, Adsorbed Protein, and Cell Morphology, *J. Long Term Eff. Med. Implants*, 1995: **5**: 209–231.
13. Depprich, R., Ommerborn, M., Zipprich, H. et al. Behavior of Osteoblastic Cells Cultured on Titanium and Structured Zirconia Surfaces, *Head Face Med.*, 2008: **4**: 29.
14. Handschel, J., Berr, K., Depprich, R. et al. Compatibility of Embryonic Stem Cells with Biomaterials, *J. Biomater. Appl.*, 2009: **23**: 549–560.
15. Naujoks, C., Langenbach, F., Berr, K. et al. Biocompatibility of Osteogenic Predifferentiated Human Cord Blood Stem Cells with Biomaterials and the Influence of the Biomaterial on the Process of Differentiation, *J. Biomater. Appl.*, 2010 (Epub ahead of print).

Downloaded from jba.sagepub.com at Universitats-Landesbibliothek on January 11, 2012

16. Handschel, J., Naujoks, C., Langenbach, F. et al. Comparison of Ectopic Bone Formation of Embryonic Stem Cells and Cord Blood Stem Cells In Vivo, *Tissue Eng. Part A*, 2010 (Epub ahead of print).
17. Kögler, G., Sensken, S., Airey, J.A. et al. A New Human Somatic Stem Cell from Placental Cord Blood with Intrinsic Pluripotent Differentiation Potential, *J. Exp. Med.*, 2004: **200**: 123–135.
18. Kögler, G. (2009). The Unrestricted Somatic Stem Cell (USSC) from Cord Blood for Regenerative Medicine, In: Meyer, U., Meyer, T., Handschel, J. and Wiesmann, H.P. (eds), *Fundamentals of Tissue Engineering and Regenerative Medicine*, Berlin, Heidelberg, Springer-Verlag, pp. 167–176.
19. van den Berk, L.C., Jansen, B.J., Siebers-Vermeulen, K.G., et al. Mesenchymal Stem Cells Respond to TNF but do not Produce TNF, *J. Leukoc. Biol.*, 2010: **87**: 281–289.
20. Winter, M., Wang, X.N., Daubener, W. et al. Suppression of Cellular Immunity by Cord Blood-derived Unrestricted Somatic Stem Cells is Cytokine Dependent, *J. Cell Mol. Med.*, 2008: **13**: 2465–2475.
21. Handschel, J.G., Depprich, R.A., Kubler, N.R., Wiesmann, H.P., Ommerborn, M. and Meyer, U. Prospects of Micromass Culture Technology in Tissue Engineering, *Head Face Med.*, 2007: **3**: 4.
22. Langenbach, F., Naujoks, C., Kersten-Thiele, P.V. et al. Osteogenic Differentiation Influences Stem Cell Migration out of Scaffold Free Microspheres, *Tissue Eng. Part A*, 2009: **16**: 759–766.
23. Handschel, J., Berr, K., Depprich, R.A. et al. Induction of Osteogenic Markers in Differentially Treated Cultures of Embryonic Stem Cells, *Head Face Med.*, 2008: **4**: 10.
24. Aktas, M., Radke, T.F., Strauer, B.E., Wernet, P. and Kogler, G. Separation of Adult Bone Marrow Mononuclear Cells Using the Automated Closed Separation System Sepax, *Cytotherapy*, 2008: **10**: 203–211.
25. Bonewald, L.F., Harris, S.E., Rosser, J. et al. Von Kossa Staining Alone is not Sufficient to Confirm that Mineralization In Vitro Represents Bone Formation, *Calcif. Tissue Int.*, 2003: **72**: 537–547.
26. Wang, Y.H, Liu, Y., Maye, P. and Rowe, D.W. Examination of Mineralized Nodule Formation in Living Osteoblastic Cultures Using Fluorescent Dyes, *Biotechnol. Prog.*, 2006: **22**: 1697–1701.
27. Wilson, C.E., Dhert, W.J., Van Blitterswijk, C.A., Verbout, A.J. and De Bruijn, J.D. Evaluating 3D Bone Tissue Engineered Constructs with Different Seeding Densities Using the AlamarBlue Assay and the Effect on In Vivo Bone Formation, *J. Mater. Sci. Mater. Med.*, 2002: **13**: 1265–1269.
28. Holy, C.E., Shoichet, M.S. and Davies, J.E. Engineering Three-dimensional Bone Tissue In Vitro Using Biodegradable Scaffolds: Investigating Initial Cell-seeding Density and Culture Period, *J. Biomed. Mater. Res.*, 2000: **51**: 376–382.
29. Bitar, M., Brown, R.A., Salih, V., Kidane, A.G., Knowles, J.C. and Nazhat, S.N. Effect of Cell Density on Osteoblastic Differentiation and Matrix Degradation of Biomimetic Dense Collagen Scaffolds, *Biomacromolecules*, 2008: **9**: 129–135.

Downloaded from jba.sagepub.com at Universitats-Landesbibliothek on January 11, 2012

30. Hervy, M., Hoffman, L. and Beckerle, M.C. From the Membrane to the Nucleus and Back Again: Bifunctional Focal Adhesion Proteins, *Curr. Opin. Cell Biol.*, 2006: **18**: 524–532.
31. Schwartz, M.A. and Assoian, R.K. Integrins and Cell Proliferation: Regulation of Cyclin-dependent Kinases via Cytoplasmic Signaling Pathways, *J. Cell. Sci.*, 2001: **114**: 2553–2560.
32. Kundu, A.K., Khatiwala, C.B. and Putnam, A.J. Extracellular Matrix Remodeling, Integrin Expression, and Downstream Signaling Pathways Influence the Osteogenic Differentiation of Mesenchymal Stem Cells on Poly(lactide-co-glycolide) Substrates, *Tissue Eng. Part A*, 2009: **15**: 273–283.
33. Xiao, G., Jiang, D., Thomas, P. et al. MAPK Pathways Activate and Phosphorylate the Osteoblast-specific Transcription Factor, Cbfa1, *J. Biol. Chem.*, 2000: **275**: 4453–4459.
34. Franceschi, R.T. and Xiao, G. Regulation of the Osteoblast-specific Transcription Factor, Runx2: Responsiveness to Multiple Signal Transduction Pathways, *J. Cell Biochem.*, 2003: **88**: 446–454.
35. Bradshaw, A.D., Graves, D.C., Motamed, K. and Sage, E.H. SPARC-null Mice Exhibit Increased Adiposity Without Significant Differences in Overall Body Weight, *Proc. Natl. Acad. Sci. U.S.A.*, 2003: **100**: 6045–6050.
36. Francki, A., Bradshaw, A.D., Bassuk, J.A., Howe, C.C., Couser, W.G. and Sage, E.H. SPARC Regulates the Expression of Collagen Type I and Transforming Growth Factor-beta1 in Mesangial Cells, *J. Biol. Chem.*, 1999: **274**: 32145–32152.
37. Iruela-Arispe, M.L., Vernon, R.B., Wu, H., Jaenisch, R. and Sage, E.H. Type I Collagen-deficient Mov-13 Mice do not Retain SPARC in the Extracellular Matrix: Implications for Fibroblast Function, *Dev. Dyn.*, 1996: **207**: 171–183.

Downloaded from jba.sagepub.com at Universitats-Landesbibliothek on January 11, 2012

3.6 Comparison of ectopic bone formation of embryonic stem cells and cord blood stem cells in vivo

[6] Handschel, J., Naujoks, C.[#], **Langenbach, F.**, Berr, K., Depprich, R.A., Ommerborn, M.A., Kubler, N.R., Brinkmann, M., Kogler, G., and Meyer, U. (2010). Comparison of ectopic bone formation of embryonic stem cells and cord blood stem cells in vivo. Tissue Eng Part A *16*, 2475-2483.

Impact Factor: 4,636

Durchschnittlicher Impact Faktor des Forschungsgebietes:

- Cell & Tissue Engineering:
    - 3,388 Rang 5 von 13 Zeitschriften

Mein Anteil an der Publikation:

- Versuche: 35%
- schriftliche Arbeit: 35%

TISSUE ENGINEERING: Part A
Volume 16, Number 8, 2010
© Mary Ann Liebert, Inc.
DOI: 10.1089/ten.tea.2009.0546

Comparison of Ectopic Bone Formation of Embryonic Stem Cells and Cord Blood Stem Cells *In Vivo*

Jörg Handschel, M.D., D.D.S., Ph.D.,[1] Christian Naujoks, M.D.,[1] Fabian Langenbach, M.Sc.,[1] Karin Berr, Ph.D.,[1] Rita A. Depprich, M.D., D.D.S., Ph.D.,[1] Michelle A. Ommerborn, D.M.D., Ph.D.,[2] Norbert R. Kübler, M.D., D.D.S., Ph.D.,[1] Matthias Brinkmann, M.D.,[3] Gesine Kögler, M.D., Ph.D.,[4] and Ulrich Meyer, M.D., D.D.S., Ph.D.[1]

Cell-based reconstruction therapies promise new therapeutic opportunities for bone regeneration. Unrestricted somatic stem cells (USSC) from cord blood and embryonic stem cells (ESCs) can be differentiated into osteogenic cells. The purpose of this *in vivo* study was to compare their ability to induce ectopic bone formation *in vivo*. Human USSCs and murine ESCs were cultured as both monolayer cultures and micromasses and seeded on insoluble collagenous bone matrix (ICBM). One week and 1, 2, and 3 months after implanting the constructs in immune-deficient rats, computed tomography scans were performed to detect any calcification. Subsequently, the implanted constructs were examined histologically. The radiological examination showed a steep increase in the mineralized bone-like tissue in the USSC groups. This increase can be considered as statistically significant compared to the basic value. Moreover, the volume and the calcium portion measured by computed tomography scans were about 10 times higher than in the ESC group. The volume of mineralization in the ESC group increased to a much smaller extent over the course of time, and the control group (ICBM without cells) showed almost no alterations during the study. The histological examinations parallel the radiological findings. Cord blood stem cells in combination with ICBM-induced ectopic bone formation *in vivo* are stronger than ESCs.

Introduction

Loss of bone due to tumor surgery or trauma is still a clinical challenge in modern reconstructive surgery. The repair of bone defects still poses a significant problem for many clinicians. In the early decades of bone reconstruction, surgeons used artificial tissue substitutes containing metals, ceramics, and polymers to maintain skeletal function.[1] These artificial materials enabled surgeons to restore the form and—to some extent—the function of defective bones. Nevertheless, these artificial materials have specific disadvantages, and therefore surgeons were encouraged to develop alternative approaches, including cell-based devices. Transplantation of autografts is a frequently used treatment strategy in routine clinical practice and has become the gold standard in reconstructive bone surgery, despite donor-site morbidity and donor shortage.[2]

Modern cell-based bone reconstruction techniques may offer new therapeutic opportunities for the repair of bone damaged by disease or injury. Generally, the combination of scaffolds, bioactive factors, and living cells provides a surgically implantable product for use in tissue regeneration and functional restoration.[3–5] Numerous attempts have been undertaken with varying success to restore bone defects using different biomaterials alone[6–11] or in combination with bioactive cytokines such as bone morphogenetic protein (BMP)-7, BMP-2, or BMP-2 mutants.[12,13] Cell-based strategies in bone tissue engineering use different cell sources, including autologous cells as well as allogenic and xenogenic cells.[14–17] There are some reports that use totipotent embryonic stem cells (ESCs) in tissue engineering of bone.[18,19]

ESCs are routinely derived from the inner cell mass of blastocysts and represent pluripotential embryonic precursor cells that give rise to all cell types in the developing organism. ESCs have historically been maintained in coculture with mitotically inactive fibroblasts.[20–22] This coculture system is unnecessary for murine ESCs if the medium is supplemented with leukemia inhibitory factor (LIF).[23,24] By definition, ESCs have the potential to differentiate into osteogenic cells under selective culture conditions. Specifically,

Departments of [1]Cranio- and Maxillofacial Surgery and [2]Operative and Preventive Dentistry and Endodontics, Heinrich Heine University of Düsseldorf, Düsseldorf, Germany.
Institutes of [3]Clinical Radiology and Nuclear Medicine and [4]Transplantation Diagnostics and Cell Therapeutics, Heinrich Heine University of Düsseldorf, Düsseldorf, Germany.

it has been shown by us and various investigators that ESCs can differentiate into osteoblast-like cells.[18,19,25–27] A mixture of dexamethasone, ascorbic acid, and β-glycerophosphate (DAG) is a good candidate for initiating osteogenic differentiation.[20,25–27] The osteoinductive potential of ESCs was demonstrated in a previous animal study in rats. ESCs were able to promote ectopic bone formation *in vivo* when they were used with demineralized bone.[28]

A few years ago another promising cell source was established by Kögler and colleagues.[29,30] These stem cells were derived from umbilical cord blood; have the ability to develop into mesodermal, endodermal, and ectodermal cells; and were subsequently termed human unrestricted somatic stem cells (USSCs). These CD45 and human leukocyte antigen (HLA) class II negative stem cells display proliferative capacity *in vitro* without spontaneous differentiation. It is possible to expand the cells to 10^{15} cells without losing pluripotency. *In vitro* a differentiation into osteoblasts, chondroblasts, adipocytes, and hematopoietic and neural cells is possible using specific stimuli. Like with ESCs, DAG is an adequate stimulus to initiate osteogenic differentiation of USSCs. Compared to ESCs, USSCs do not show any immunological rejection and have fewer ethical and legal restrictions. So USSCs are much closer to clinical practice than ESCs; for example, hematopoietic cells from cord blood are already used in the therapy of hematopoietic and genetic disorders.[31]

Beside cells, biomaterials are another prerequisite when filling bone lesions. An important feature of an ideal scaffold will be its cytocompatibility with the cells intended for implantation. Up to now a large number of bone substitutes have been studied as scaffold material for applications in tissue engineering.[32] Deproteinized bovine bone (Bio Oss®), β-tricalcium phosphate (Cerasorb®), polylactic/polyglycolic acid copolymer, and insoluble collagenous bone matrix (ICBM) are commonly used as scaffold materials. Recently, we studied the cytocompatibility of various biomaterials with ESCs. The results show that ICBM, followed by β-tricalcium phosphate, is most suitable for bone tissue engineering regarding cell proliferation and phenotype.[33] Commonly, tissue engineering of bone is performed using cells coaxed with scaffolds. Yet, there is still controversy concerning the use of artificial scaffolds as against the use of a natural matrix. Therefore, new approaches called micromass technology have been invented to overcome these problems by avoiding the need for scaffolds. Technically, cells are dissociated and the dispersed cells are then reaggregated into cellular spheres. Moreover, the micromass technology approach enables investigators to transfer a very large number of cells to scaffolds, the method used in this study. Importantly, since the newly formed tissue is devoid of any artificial material, it more closely resembles the *in vivo* situation (review in Handschel *et al*.[34]).

Regarding our previous results and the findings mentioned in the literature, the purpose of this *in vivo* study was to investigate the bone formation in various constructs containing USSCs (with and without micromass technology), ESCs, and ICBM.

Materials and Methods

Cell culture of ESCs and USSCs

Feeder-independent murine ESCs were derived from the inner cell mass of blastocysts extracted from C57BL/6 mice. The ESCs were kindly provided by K. Pfeffer (Institute for Microbiology, Heinrich Heine University, Germany). The cells were tested to be positive for the stem cell marker Pouf1 (alias Oct4) and Foxd3[35] (data not shown). A total number of 1.5×10^6 cells per Petri dish (10 cm in diameter) were cultured in Dulbecco's modified Eagle's medium (DMEM). The medium was supplemented with 5 mM glutamine, 100 U/mL penicillin, 100 μg/mL streptomycin, 50 μM 2-mercaptoethanol, and 15% fetal calf serum. The cells were incubated in a humidified atmosphere at 37°C in 8% CO_2 and were split every second day.

USSCs were kindly provided by Gesine Kögler (José Carreras Cord Blood Bank, Heinrich Heine University, Germany). The cells were isolated from cord blood with informed consent of the mother, as described by Kögler and colleagues.[30] Briefly, the mononuclear cell fraction of the cord blood, isolated by Ficoll (Biochrom) gradient centrifugation, was plated out at 5 to 7×10^6 cells/mL on T25 culture flasks (Costar) in low-glucose DMEM (Cambrex), supplemented with 30% fetal calf serum, dexamethasone (10^{-7} M; Sigma-Aldrich), penicillin (100 U/mL; Grünenthal), streptomycin (100 mg/mL; Hefa-pharma), and ultraglumatine (2 mM; Cambrex). Cells were incubated in a humidified atmosphere at 37°C in 5% CO_2 and were split when confluency reached 80%. For the further expansion of the cells, the dexamethasone was left out of the medium.

USSC microspheres were prepared in a microsphere assembly bioreactor that was prepared by filling 60 μL solution consisting of 2% agarose in DMEM (without any supplements) into 96-well plates. USSCs were detached from the plates, centrifuged, and resuspended in the normal growth medium (1 m cells/mL). One hundred eighty microliters of cell suspension consisting of 180,000 cells was added on top of the solidified agarose hydrogel, and the cultures were incubated over night. Due to the concave surface of the hydrogel (caused by capillary action) the cells congregate in the center of the well and form a sphere.

Osteogenic differentiation of ESCs and USSCs as well as preparation and differentiation of USSC microspheres

Three days before inoculation of the ICBM scaffolds, osteogenic differentiation of ESC and USSC cultures was initiated. Osteogenic differentiation of USSCs was performed by adding DAG (0.1 μM dexamethasone, 50 μM ascorbic acid, and 10 mM β-glycerophosphate; all from Sigma) to the normal growth medium, as mentioned earlier.[36] Before the osteogenic differentiation of ESCs the cells were incubated for 1 day with the normal growth medium lacking LIF and were subsequently cultured in the normal growth medium lacking LIF but supplemented with DAG.

To initiate osteogenic differentiation in the microspheres, the old medium was replaced by 160 μL normal growth medium containing DAG in the above-mentioned concentrations. Subsequently, the microspheres were cultured for 3 days with a change of medium after 2 days.

Preparation of ICBM and inoculation with USSCs and ESCs

One-centimeter-thick slices of bovine femur spongiosa were defatted in three washing steps (24 h each) with chlo-

roform methanol solution (3:1; Merck). After initial washing in distilled water for 30 min, the slices were bleached with H_2O_2 (Merck) for 15 min and were washed again in distilled water. Washing the slices three times for 90 min in 0.5 M HCl (Merck) was used for demineralization. Cylinders with a diameter of 6 mm and a height of 5 mm were cut and incubated in 4 M Guanidin-HCl/50 mM Tris-HCl (pH 7.0) (Merck) for 16 h at 4°C. The slices were incubated with 50 mM Tris-HCl (pH 7.0)/0.15 M NaCl (Merck) for 4 h at 4°C and were washed once more with distilled water for 30 min.

After 3 days of osteogenic differentiation of the ESC and USSC cultures, the cells were detached from the plates and 80,000 cells were added on each ICBM cylinder. After an additional 3 days with osteoinductive medium, the ICBMs were implanted into rats. Inoculation of the ICBMs with USSC microspheres was performed by studding ICBMs with seven microspheres. The microspheres were implanted into the pores of the matrix evenly all over its surface and were incubated for 3 days in osteoinductive medium, before they were implanted into the rats.

Animals and surgical procedure

To avoid any immunogenic reactions 31 male immunocompromised rats (Rowett Nude [RNU] rats) were used. All animals were aged 2 to 3 months and treated in accordance with the guidelines of the local authorities (Bezirksregierung Düsseldorf). Four transplants were implanted into each rat. The four transplants were randomly inserted into a muscle bag paravertebrally. Two muscles bags were created on each side of the spine. Figure 1 illustrates the surgical procedure. All surgical procedures were performed under general anesthesia. The following transplants were used:

1. ICBM + osteogenically differentiated USSCs that were seeded on the biomaterial 3 days before implantation
2. ICBM + osteogenically differentiated USSC microspheres that were seeded on the biomaterial 3 days before implantation
3. ICBM + osteogenically differentiated ESCs that were seeded on the biomaterial 3 days before implantation
4. ICBM without cells (control group)

Animals were euthanized 1 month (eight animals), 2 months (eight animals), 3 months (eight animals), and 4 months (seven animals) after implantation. The study was approved by the local ethics committee.

Radiological examination

One week after transplantation and 1, 2, 3, and 4 months later, computed tomography (CT) was performed in the anesthetized rats. Examinations were performed with a 64-row Multi-Detector-CT (Somatom Sensation Cardiac 64; Siemens Medical Solutions). Unenhanced scans were performed covering the entire rat body using 100 kV and 200 mAs. Slice collimation was 64×0.6 mm with a reconstructed slice width of 1 mm and a reconstruction interval 0.5 mm. On the basis of these CT scans the volume of any mineralization in each transplant was determined using dedicated commercial software (Siemens Medical Solutions). Using a threshold of 150 HU, volumetry of calcium containing tissue was performed semiautomatically. This investigation was performed by a blinded researcher (M.B.). Statistical analysis was done using SPSS 17.0. To detect any statistically significant differences the Kruskal–Wallis test and the Wilcoxon test were performed. A *p*-value below 5% was regarded as statistically significant.

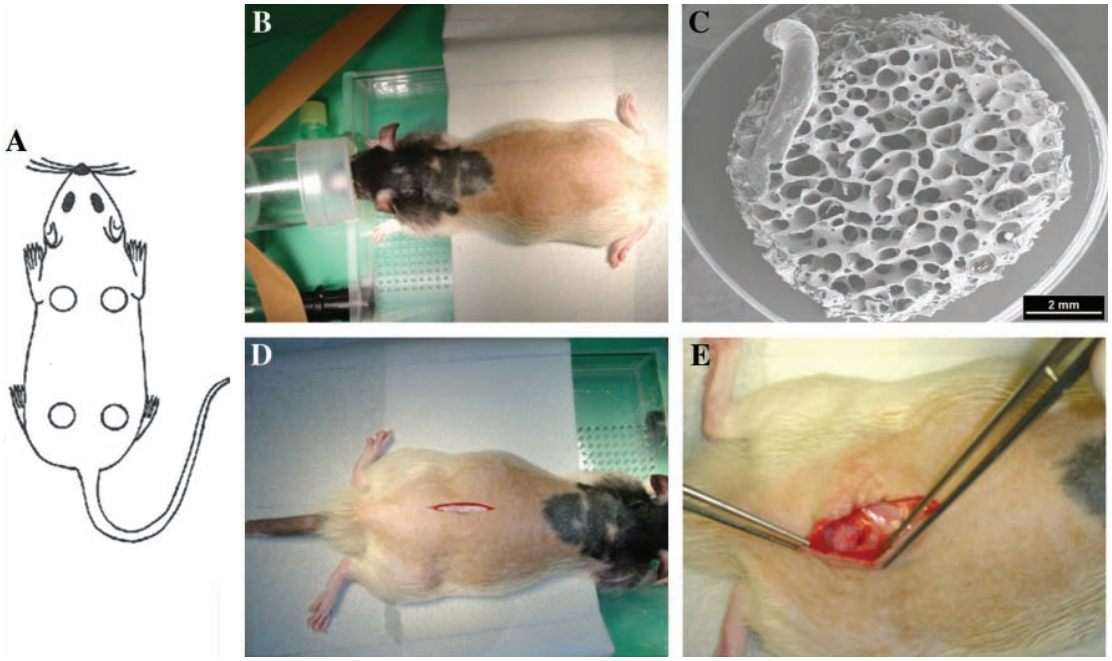

FIG. 1. The site of implantation (**A, E**), the surgical approach (**D**), the clinical setting (**B**), and a scanning electron microscopy micrograph of a transplant (**C**) are shown. Insoluble collagenous bone matrix has large interconnecting pores. Color images available online at www.liebertonline.com/ten.

Table 1. Laboratory Parameters

Time after implantation	*Hemoglobin (g/dL)*	*Lymphocytes (10^3/mm^3)*	*Granulocytes (10^3/mm^3)*	*CRP (mg/dL)*
1 week	13.31 + 1.52	0.51 + 0.35	2.3 + 0,69	<0.1
2 months	13.9 + 1.74	0.83 + 0.30	5.15 + 5.38	<0.1
3 months	14.2 + 0.58	0.59 + 0.27	2.21 + 0.50	<0.1
4 months	13.0 + 1.42	0.47 + 0.19	4.00 + 3.95	<0.1
Physiological values	11.10–18.00	1.2 + 3.2	1.2–6.8	<0.1

CRP, c-reactive protein.

Histological examination

After explantation all transplants were fixed in paraformaldehyde and embedded in paraffin. Sections of each sample were stained with hematoxylin–eosin or alizarin red as mentioned in the literature. Briefly, slides were washed in distilled water for 3 min, then stained with hemalum for 3 min, treated for 2 s with HCl, washed again, then stained for 2 min with eosin, washed again, and then treated with increasing ethanol concentrations up to 100%. Before the slides were finally covered with entellan, they were incubated in xylene. The slides were stained with alizarin red (mixture of 0.5 g alizarin red and 5 mL 0.28% NH_3 with 45 mL distilled water [pH 6.4]). Before the slides were finally covered with entellan they were incubated in xylene. To investigate the quantity of mineralized tissue in each sample, the mineralized area in each slide (red) was determined by a blinded researcher using image analyzer software. Statistical analysis was done using SPSS 17.0. To detect any statistically significant differences the Kruskal–Wallis test and the Wilcoxon test were performed. A *p*-value below 5% was regarded as statistically significant.

Measurement of sprouting distance

To evaluate if osteogenic differentiation of the microspheres influenced the capability of cells to migrate out of the microsphere into the surrounding area (or the scaffold), an *in vitro* cell outgrowth experiment was used. After 1 and 5 days microspheres were washed with phosphate-buffered saline and transferred into 24-well tissue culture plates, including 500 µL normal growth medium per well. After 5 days of incubation, the microspheres were formalin fixed and stained with hemalum/eosin, inside the well plates.

The outgrowth capability was evaluated by measuring the distances from the center of the microsphere to the most distant cells. Mean values and standard deviation were measured at eight predefined angles (Fig. 4a) per microsphere, in three independent experiments each with four to six microspheres.

Results

No animal showed any signs of inflammation during the study. In particular, none of the laboratory parameters showed any pathological values with the exception of the lymphocyte cell count (Table 1), which can be attributed to the relative lymphocyte deficiency of the rats.

The radiological examination of the mineralized volumes revealed that there was a cell-dependent degree of mineralization. Figures 2a and 3 show that until 1 week after transplantation no signs of mineralization could be detected. However, after 1 month a steep increase in the transplants with USSCs (both the monolayer group, $187.6 \pm 13\,mm^3$, and the micromass group, $151.3 \pm 15\,mm^3$) was observed, whereas only minimum mineralization in the ESC group and the (cell-free) control group was detected (see Fig. 2). Although there was a statistically significant difference between both USSC groups and the ESC and control group ($p < 0.001$), the USSC groups did not differ considerably from each other. During the course of the study the mineralized volume in the ESC group increased and the control

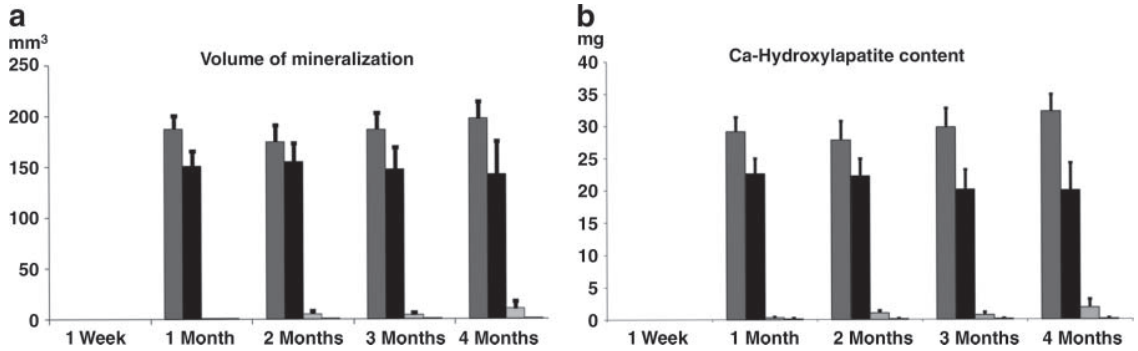

FIG. 2. (**a**) Volume of newly mineralized tissue as defined by semiautomatic assessment using computed tomography (CT). The mean and standard error are shown. Statistically significant differences are mentioned in the text: dark-grey, unrestricted somatic stem cell (USSC) monolayer (group 1); black, USSC micromass (group 2); light grey, embryonic stem cell (ESC) (group 3); grey, no cells (control; group 4). (**b**) Newly mineralized hydroxylapatite by semiautomatic assessment using CT. The mean and standard error are shown. Statistically significant differences are mentioned in the text: dark grey, USSC monolayer (group 1); black, USSC micromass (group 2); light-grey, ESC (group 3); grey, no cells (control; group 4).

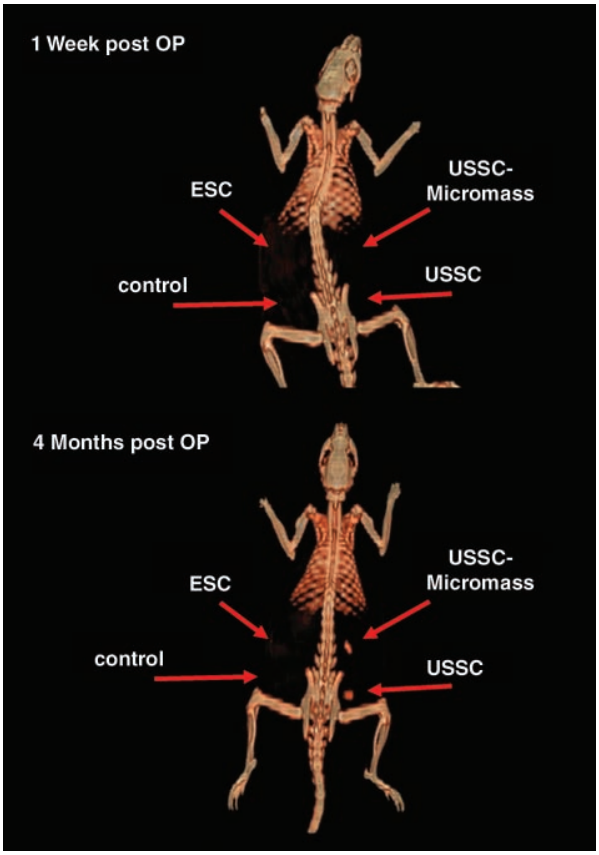

FIG. 3. CTs of a rat 1 week and 4 months after implantation. Note: there is no mineralization detectable on the ESC and control side, whereas the USSCs obviously induced ectopic mineralizations. Post OP, postoperation. Color images available online at www.liebertonline.com/ten.

group remained at very low levels. In contrast, there was no additional increase in the USSC groups (Fig. 2a).

The measurement of the calcium content is similar to the volume measurement with the exception that the USSC monolayer group (group 1) showed significantly higher values than the USSC micromass group (group 2) ($p < 0.05$). However, both USSC groups exceeded the other two groups significantly ($p < 0.001$). The ESC group reached only 10% of the values of the USSC groups after 4 months (Fig. 2b).

Histological analysis demonstrated a bone-like tissue formation and the results confirmed these radiological findings. Particularly the alizarin-red-stained sections of the transplants showed a dependence of the mineralization on the type of transplanted cells. The quantity of the alizarin-red-stained sections in Figure 5 shows that the transplants seeded with USSCs are significantly more mineralized than transplants with ESCs or transplants without cells (control). Further, the significant differences were shown in Figure 6. Analog with the measurement of the calcium content, the USSC monolayer group (group 1) reached a significantly different level to ESCs 1 month earlier than the USSC micromass group.

The measurement of the sprouting distance out of the micromass could explain the difference between the USSC monolayer group and the USSC micromass group. In this experiment a significant decrease in the mean outgrowth distance of cells out of osteogenically differentiated microspheres compared to control microspheres was evident. Figure 4b shows the significant differences in the incubation-dependant decrease in outgrowth distances of cells from the microspheres. Further, a time-dependent reduction in outgrowth distances was observed after 5 days in the control group and the osteogenically differentiated group. DAG treatment induced a significant (evaluated by Student's *t*-test) decrease in outgrowth distance from day 1 to 5 ($p < 0.0005$). In this period, the mean outgrowth distance

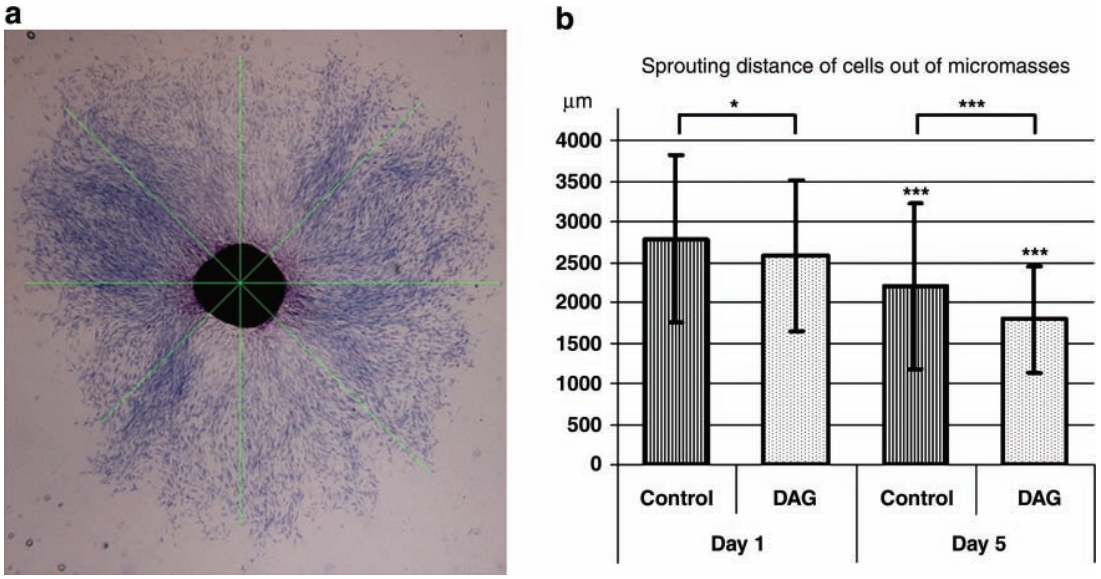

FIG. 4. (**a**) The sprouting distances are measured from the centers of the micromasses to the most distant cells at predefined angles. (**b**) Incubation-dependent decrease in outgrowth distances of cells from microspheres. The figure shows the mean values ± standard deviation of three independent experiments. Student's *t*-test was used to generate *p*-values (*$p < 0.05$, ***$p < 0.0005$) for comparison with the respective values of day 1. Significant differences between DAG-treated and control microspheres are also shown. Color images available online at www.liebertonline.com/ten.

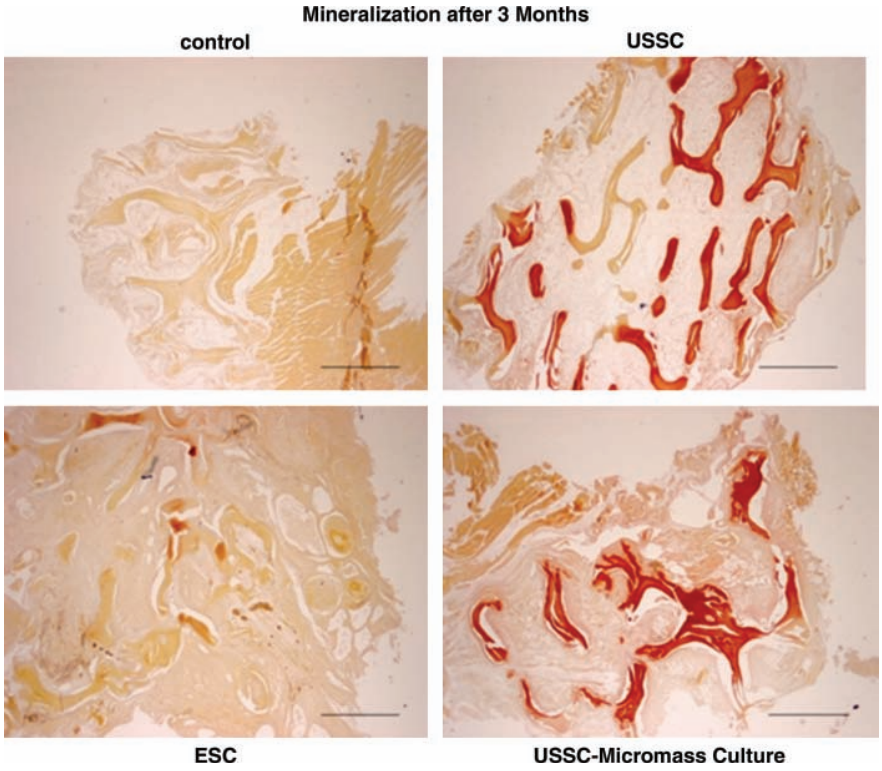

FIG. 5. Histological sections stained with alizarin red 3 months after implantation. Mineralized areas of the bone-like tissue are stained red. Scale bars indicate 1 mm. Color images available online at www.liebertonline.com/ten.

declined to 69% of the mean distance in the DAG group and to 79% in the control group.

Discussion

Tissue engineering and regenerative medicine therapies have now gained entrance to all medical specialties. Today's situation, reflecting the current state of clinical use, is one that is characterized by efforts to introduce new treatment options as well as to establish clinical standards for recently performed therapies.[3] The two main components of an extracorporal tissue-engineered hybrid construct are the cells and the scaffold material. Possible sources of cells for tissue engineering are autologous, allogenic, and xenogenic cells. Each category can be subdivided according to whether the cells are in a more or less differentiated stage. Whereas mature cells (e.g., osteoblasts) and mesenchymal stem cells are used in autologous transplants, ESCs and USSCs are currently used for allogenic transplantations. Therefore, our efforts are focused on establishing transplants with these cell lines. In a previous study the biocompatibility of ESCs and various scaffolds was tested, revealing that ICBM showed the best results.[33] ESCs are the major representative cell line of pluripotential cells. These cells were first isolated and grown in culture more than 25 years ago.[21,37] ESCs exhibit two remarkable features in culture. First, they represent pluripotential embryonic precursor cells that may differentiate into any cell type in the embryo. A second feature of ESCs is that they can be propagated indefinitely as a stable self-renewing cell population. Recently, we have demonstrated that ESCs can be differentiated into osteogenic cells.[33] Nevertheless, the use of ESCs in tissue engineering and regenerative medicine involves some risks. When undifferentiated ESCs are transplanted into severely combined immunodeficient mice, they frequently form teratomas.[38] This risk must be eliminated before implantation in humans.

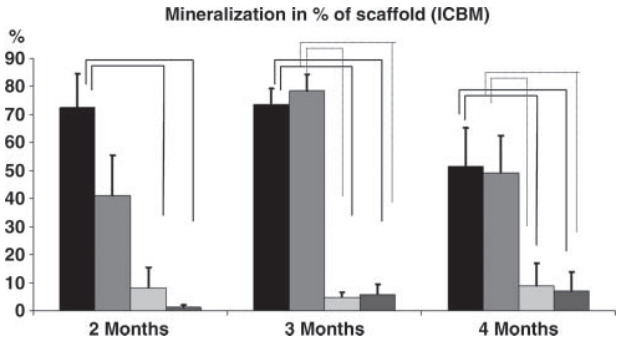

FIG. 6. Area of newly mineralized tissue in the alizarin red staining. The mean and standard error are shown. Statistically significant differences ($p < 0.001$) are shown as lines between the bars: black, USSC monolayer (group 1); grey, USSC micromass (group 2); light grey, ESC (group 3); dark grey, no cells (control; group 4).

Since 2004[30] USSCs have been increasingly attracting interest in tissue engineering.[30,39–42] They can be differentiated into a huge variety of cell types, including chondroblasts, adipocytes, osteoblasts, and hematopoietic and neural cells, for example, astrocytes and neurons.[30]

This animal trial has yielded interesting results regarding bone tissue engineering. First, transplanted cells do induce ectopic bone-like mineralization *in vivo*. One must recall that the cell–scaffold constructs were implanted in muscle bags and had no connections to the skeleton. Thus, osteoblasts of rats (hosts) are presumably not involved in the process of mineralization, at least in the initial phase.

Second, the various cell lines promote mineralization to an unequal extent. Human USSCs outperform murine ESCs regarding the induction of ectopic mineralization. The values of the USSC transplants were in part about 10 times higher than the values of ESCs. The absolute values of ESC-induced mineralization were confirmed by a recently published experiment.[28] We can only speculate why ESCs have lower potential in ectopic bone formation in our study.[43] A possible reason is that the ESCs are much more influenced by local factors in the implantation site. Probably the myogenic environment in the muscle leads to a brake in the osteogenic differentiation of the cells as shown by Golob and colleagues.[44] This supports our thesis that due to an incomplete osteogenic differentiation, a break is possible after implantation due to incomplete epigenetic silencing of genes that may be prone to myogenic differentiation. Further, USSCs show a similar fibroblast morphology and have many similarities to mesenchymal stem cells.[30] Recently, Gentleman *et al.* thoroughly compared MSCs in their osteogenic potential to ESCs and the former were found to have osteogenic gene expression several orders of magnitude above ESCs.[45] These findings are in agreement with our results. Another reason for the disparity in bone formation between ESCs and USSCs may be the different culture conditions. In accordance with the published standard protocols ESCs were cultured with 15% FBS,[46] whereas the USSCs were cultured with 30% FBS.[30] Another reason for the lower osteogenesis in the ESC group might be the different stage of differentiation of the two cell lines. ESCs are in a less differentiated stage than the USSCs and so might need a longer period of osteogenic stimulation. Nevertheless, both cell lines achieved the same osteogenic stimulation. In addition, it seems that the kind of pretreatment (USSC monolayer vs. USSC micromass) does also influence the outcome. In this experiment the USSC spheres, which are cultivated in an osteogenic medium, induce mineralization to a lesser extent than the USSC monolayer cells.

The reason for the different performance of USSC micromass in our study could be the boundary mineralization of the spheres. As we were able to show in a preliminary experiment, the process of mineralization starts at the boundary of the microsphere. This may prevent sufficient diffusion of DAG medium to the cells in the center of the spheres. As shown in the sprouting experiment, cell migration out of the USSC microspheres is diminished by osteogenic induction. Thus, fewer cells than in the monolayer group (group 1) were able to participate in the mineralization process of the transplants.

As we wanted to compare microspheres and monolayer cultures and keep the experiment comparable, we decided to reduce the osteogenic stimulation to a minimum period of time. This short period of osteogenic stimulation may also be the reason for the fact that we observed only low osteogenesis on ESCs. However, both cell lines achieved the same osteogenic stimulation.

Moreover, the applied cell count on the scaffold and the cell survival on the scaffold may be the reason for the differences in the above-mentioned results regarding the osteogenic differentiation. Even though we did not measure the cell count before and after implantation, we were able to show in a preliminary experiment that ESCs and USSCs show the same characteristics regarding cell attachment and cell proliferation on ICBM *in vitro*.[47]

In our study we compared human USSCs and murine ESCs, which might be a point of criticism. Due to the special legal restrictions for research with human ESCs, we considered using murine ESCs. Even if there are certain differences between human and murine ESCs, these two cell types share fundamental characteristics. For example, Sato *et al.* demonstrated that the two pluripotent stem cells have a common core molecular program.[48] Further, the protocols for the osteogenic differentiation of human and murine ESCs are similar. For both cell types DAG is used for osteogenic differentiation toward the osteogenic lineage, resulting in differentiation into osteogenic cells. Because of these similarities we decided to use murine ESCs instead of human ESCs.

USSCs seem to be compatible candidates for bone tissue engineering. Some authors report less immunogenicity in USSCs than in bone-marrow-derived stem cells and that they can be used even in non-HLA-matched patients.[49,50] Moreover, the transplantation of HLA-matched USSCs into patients with leukemia is already a treatment option currently in use.[51,52] Therefore, the clinical use of USSC-based bone transplants is also conceivable.

Another advantage of USSCs over mesenchymal stem cells (e.g., bone-marrow-derived or adipose-tissue-derived stem cells) is the absence of explanting morbidity.

An additional advantage over ESCs is ethical inoffensiveness and the absence of legal concern in many countries.[53]

Conclusions

USSCs rather than ESCs are promising candidates for bone tissue regeneration and—in combination with ICBM—do induce ectopic bone formation. Future experiments should address immunogenity, side effects, and, of course, the up-sizing of the constructs to bring USSC-based constructs nearer to clinical use.

Acknowledgments

We are very grateful to Prof. Dr. K. Pfeffer, Institute für Microbiology at Heinrich Heine University of Düsseldorf, who provided the murine ESCs. Fabian Langenbach is supported by a grant from the German Research Community (DFG) (HA 3228/2-1). The work of Prof. Kögler is supported by the DFG Grant KO2119/6-1.

Disclosure Statement

All authors agree to disclose any commercial associations that might create a conflict of interest in connection with this article. All authors declare that there are no competing interests regarding the interpretation or presentation of the above-mentioned data or results.

References

1. Binderman, I., and Fin, N. Bone substitutes organic, inorganic, and polymeric: cell material interactions. In:

Yamamuro, T., Hench, L., and Wilson, J., eds. CRC Handbook of Bioactive Ceramics. Boca Raton, FL: CRC Press, 1990, pp. 45–51.
2. Damien, C.J., and Parsons, J.R. Bone graft and bone graft substitutes: a review of current technology and applications. J Appl Biomater **2,** 187, 1991.
3. Handschel, J., Simonowska, M., Naujoks, C., Depprich, R.A., Ommerborn, M.A., Meyer, U., and Kübler, N.R. A histomorphometric meta-analysis of sinus elevation with various grafting materials. Head Face Med **5,** 12, 2009.
4. Tuan, R.S., Boland, G., and Tuli, R. Adult mesenchymal stem cells and cell-based tissue engineering. Arthritis Res Ther **5,** 32, 2003.
5. Vacanti, C.A., and Vacanti, J.P. Bone and cartilage reconstruction with tissue engineering approaches. Otolaryngol Clin North Am **27,** 263, 1994.
6. Kasaj, A., Reichert, C., Gotz, H., Rohrig, B., Smeets, R., and Willershausen, B. *In vitro* evaluation of various bioabsorbable and nonresorbable barrier membranes for guided tissue regeneration. Head Face Med **4,** 22, 2008.
7. Cohen, S.R., Holmes, R.E., Meltzer, H.S., Levy, M.L., and Beckett, M.Z. Craniofacial reconstruction with a fast resorbing polymer: a 6- to 12-month clinical follow-up review. Neurosurg Focus **16,** E12, 2004.
8. Handschel, J., Wiesmann, H.P., Stratmann, U., Kleinheinz, J., Meyer, U., and Joos, U. TCP is hardly resorbed and not osteoconductive in a non-loading calvarial model. Biomaterials **23,** 1689, 2002.
9. Holmes, R.E., Cohen, S.R., Cornwall, G.B., Thomas, K.A., Kleinhenz, K.K., and Beckett, M.Z. MacroPore resorbable devices in craniofacial surgery. Clin Plast Surg **31,** 393, 2004.
10. Thaller, S.R., Hoyt, J., Borjeson, K., Dart, A., and Tesluk, H. Reconstruction of calvarial defects with anorganic bovine bone mineral (Bio-Oss) in a rabbit model. J Craniofac Surg **4,** 79, 1993.
11. Velich, N., Nemeth, Z., Hrabak, K., Suba, Z., and Szabo, G. Repair of bony defect with combination biomaterials. J Craniofac Surg **15,** 11, 2004.
12. Kubler, N.R., Wurzler, K.K., Reuther, J.F., Sieber, E., Kirchner, T., and Sebald, W. [Effect of different factors on the bone-forming properties of recombinant BMPs]. Mund Kiefer Gesichtschir **4 Suppl 2,** S465, 2000.
13. Terheyden, H., Knak, C., Jepsen, S., Palmie, S., and Rueger, D.R. Mandibular reconstruction with a prefabricated vascularized bone graft using recombinant human osteogenic protein-1: an experimental study in miniature pigs. Part I: prefabrication. Int J Oral Maxillofac Surg **30,** 373, 2001.
14. Meyer, U., and Wiesmann, H.P. Tissue engineering: a challenge of today's medicine. Head Face Med **1,** 2, 2005.
15. Puricelli, E., Ulbrich, L.M., Ponzoni, D., and Filho, J.J. Histological analysis of the effects of a static magnetic field on bone-healing process in rat femurs. Head Face Med **2,** 43, 2006.
16. Handschel, J., Wiesmann, H.P., Depprich, R., Kubler, N.R., and Meyer, U. Cell-based bone reconstruction therapies—cell sources. Int J Oral Maxillofac Implants **21,** 890, 2006.
17. Yamaguchi, M., Hirayama, F., Murahashi, H., Azuma, H., Sato, N., Miyazaki, H., Fukazawa, K., Sawada, K., Koike, T., Kuwabara, M., Ikeda, H., and Ikebuchi, U. *Ex vivo* expansion of human UC blood primitive hematopoietic progenitors and transplantable stem cells using human primary BM stromal cells and human AB serum. Cytotherapy **4,** 109, 2002.
18. Heng, B.C., Cao, T., Stanton, L.W., Robson, P., and Olsen, B. Strategies for directing the differentiation of stem cells into the osteogenic lineage *in vitro*. J Bone Miner Res **19,** 1379, 2004.
19. zur Nieden, N.I., Kempka, G., Rancourt, D.E., and Ahr, H.J. Induction of chondro-, osteo- and adipogenesis in embryonic stem cells by bone morphogenetic protein-2: effect of cofactors on differentiating lineages. BMC Dev Biol **5,** 1, 2005.
20. Bielby, R.C., Boccaccini, A.R., Polak, J.M., and Buttery, L.D. *In vitro* differentiation and *in vivo* mineralization of osteogenic cells derived from human embryonic stem cells. Tissue Eng **10,** 1518, 2004.
21. Evans, M.J., and Kaufman, M.H. Establishment in culture of pluripotential cells from mouse embryos. Nature **292,** 154, 1981.
22. Burt, R.K., Verda, L., Kim, D.A., Oyama, Y., Luo, K., and Link, C. Embryonic stem cells as an alternate marrow donor source: engraftment without graft-versus-host disease. J Exp Med **199,** 895, 2004.
23. Chambers, I. The molecular basis of pluripotency in mouse embryonic stem cells. Cloning Stem Cells **6,** 386, 2004.
24. Smith, A.G., Heath, J.K., Donaldson, D.D., Wong, G.G., Moreau, J., Stahl, M., and Rogers, D. Inhibition of pluripotential embryonic stem cell differentiation by purified polypeptides. Nature **336,** 688, 1988.
25. Chaudhry, G.R., Yao, D., Smith, A., and Hussain, A. Osteogenic cells derived from embryonic stem cells produced bone nodules in three-dimensional scaffolds. J Biomed Biotechnol **2004,** 203, 2004.
26. Depprich, R., Zipprich, H., Ommerborn, M., Naujoks, C., Wiesmann, H.P., Kiattavorncharoen, S., Lauer, H.C., Meyer, U., Kübler, N.R., and Handschel, J. Osseointegration of zirconia implants compared with titanium: an *in vivo* study. Head Face Med **4,** 30, 2008.
27. Buttery, L.D., Bourne, S., Xynos, J.D., Wood, H., Hughes, F.J., Hughes, S.P., Episkopou, V., and Polak, J.M. Differentiation of osteoblasts and *in vitro* bone formation from murine embryonic stem cells. Tissue Eng **7,** 89, 2001.
28. Kahle, M., Wiesmann, H., Berr, K., Depprich, R.A., Kübler, N.R., Naujoks, C., and Handschel, J. Ectopic bone formation with embryonic stem cells in rats. J Mater Sci Mater Med 2009.
29. Kögler, G. The unrestricted somatic stem cell (USSC) from cord blood for regenerative medicine. In: Meyer, U., Meyer, T., Handschel, J., and Wiesmann, H.P., eds. Fundamentals of Tissue Engineering and Regenerative Medicine. Berlin, Heidelberg: Springer-Verlag, 2009, pp. 167–176.
30. Kögler, G., Sensken, S., Airey, J.A., Trapp, T., Muschen, M., Feldhahn, N., Liedtke, S., Sorg, R.V., Fischer, J., Rosenbaum, C., Greschat, S., Knipper, A., Bender, J., Degistirici, O., Gao, J., Caplan, A.I., Colletti, E.J., Almeida-Porada, G., Müller, H.W., Zanjani, E., and Wernet, P. A new human somatic stem cell from placental cord blood with intrinsic pluripotent differentiation potential. J Exp Med **200,** 123, 2004.
31. Benito, A.I., Diaz, M.A., Gonzalez-Vicent, M., Sevilla, J., and Madero, L. Hematopoietic stem cell transplantation using umbilical cord blood progenitors: review of current clinical results. Bone Marrow Transplant **33,** 675, 2004.
32. Wiesmann, H.P., Joos, U., and Meyer, U. Biological and biophysical principles in extracorporal bone tissue engineering. Part II. Int J Oral Maxillofac Surg **33,** 523, 2004.
33. Handschel, J., Berr, K., Depprich, R., Naujoks, C., Kubler, N.R., Meyer, U., Ommerborn, M., and Lommns, L. Compatibility of embryonic stem cells with biomaterials. J Biomater Appl **23,** 549, 2009.
34. Handschel, J.G., Depprich, R.A., Kubler, N.R., Wiesmann, H.P., Ommerborn, M., and Meyer, U. Prospects of micromass culture technology in tissue engineering. Head Face Med **3,** 4, 2007.

35. Baharvand, H., Ashtiani, S.K., Taee, A., Massumi, M., Valojerdi, M.R., Yazdi, P.E., Moradi, S.Z., and Farrokhi, A. Generation of new human embryonic stem cell lines with diploid and triploid karyotypes. Dev Growth Differ **48,** 117, 2006.
36. Depprich, R., Ommerborn, M., Zipprich, H., Naujoks, C., Handschel, J., Wiesmann, H.P., Kübler, N.R., and Meyer, U. Behavior of osteoblastic cells cultured on titanium and structured zirconia surfaces. Head Face Med **4,** 29, 2008.
37. Martin, G.R. Isolation of a pluripotent cell line from early mouse embryos cultured in medium conditioned by teratocarcinoma stem cells. Proc Natl Acad Sci U S A **78,** 7634, 1981.
38. Aleckovic, M., and Simon, C. Is teratoma formation in stem cell research a characterization tool or a window to developmental biology? Reprod Biomed Online **17,** 270, 2008.
39. Degistirici, O., Jager, M., and Knipper, A. Applicability of cord blood-derived unrestricted somatic stem cells in tissue engineering concepts. Cell Prolif **41,** 421, 2008.
40. Markov, V., Kusumi, K., Tadesse, M.G., William, D.A., Hall, D.M., Lounev, V., Carlton, A., Leonard, J., Cohen, R.J., Rappaport, E.F., and Saitta, B. Identification of cord blood-derived mesenchymal stem/stromal cell populations with distinct growth kinetics, differentiation potentials, and gene expression profiles. Stem Cells Dev **16,** 53, 2007.
41. Penolazzi, L., Lambertini, E., Tavanti, E., Torreggiani, E., Vesce, F., Gambari, R., and Piva, R. Evaluation of chemokine and cytokine profiles in osteoblast progenitors from umbilical cord blood stem cells by BIO-PLEX technology. Cell Biol Int **32,** 320, 2008.
42. Penolazzi, L., Pocaterra, B., Tavanti, E., Lambertini, E., Vesce, F., Gambari, R., and Piva, R. Human osteoclasts differentiated from umbilical cord blood precursors are less prone to apoptotic stimuli than osteoclasts from peripheral blood. Apoptosis **13,** 553, 2008.
43. Francastel, C., Schubeler, D., Martin, D.I., and Groudine, M. Nuclear compartmentalization and gene activity. Nat Rev Mol Cell Biol **1,** 137, 2000.
44. Golob, J.L., Paige, S.L., Muskheli, V., Pabon, L., and Murry, C.E. Chromatin remodeling during mouse and human embryonic stem cell differentiation. Dev Dyn **237,** 1389, 2008.
45. Gentleman, E., Swain, R.J., Evans, N.D., Boonrungsiman, S., Jell, G., Ball, M.D., Shean, T.A., Oyen, M.L., Porter, A., and Stevens, M.M. Comparative materials differences revealed in engineered bone as a function of cell-specific differentiation. Nat Mater **8,** 763, 2009.
46. Handschel, J., Berr, K., Depprich, R.A., Kubler, N.R., Naujoks, C., Wiesmann, H.P., Ommerborn, M., and Meyer, U. Induction of osteogenic markers in differentially treated cultures of embryonic stem cells. Head Face Med **4,** 10, 2008.
47. Naujoks, C., Langenbach, F., Berr, K., Depprich, R., Kubler, N., Meyer, U., Handschel, J., and Kögler, G. Biocompatibility of osteogenic pre-differentiated human cord blood stem cells with biomaterials and the influence of the biomaterial on the process of differentiation. J Biomater Appl 2010 Mar 5 [Epub ahead of print].
48. Sato, N., Sanjuan, I.M., Heke, M., Uchida, M., Naef, F., and Brivanlou, A.H. Molecular signature of human embryonic stem cells and its comparison with the mouse. Dev Biol **260,** 404, 2003.
49. Bradstock, K.F., Hertzberg, M.S., Kerridge, I.H., Svennilson, J., McGurgan, M., Huang, G., Antonenas, V., and Gottlieb, D.J. Unrelated umbilical cord blood transplantation for adults with haematological malignancies: results from a single Australian centre. Intern Med J **36,** 355, 2006.
50. Kleen, T.O., Kadereit, S., Fanning, L.R., Jaroscak, J., Fu, P., Meyerson, H.J., Kulchycki, L., Slivka, L.F., Kozik, M., Tary-Lehmann, M., and Laughlin, M.J. Recipient-specific tolerance after HLA-mismatched umbilical cord blood stem cell transplantation. Transplantation **80,** 1316, 2005.
51. Ishimura, M., Ohga, S., Nomura, A., Toubo, T., Morihana, E., Saito, Y., Nishio, H., Ide, M., Takada, H., and Hara, T. Successful umbilical cord blood transplantation for severe chronic active Epstein-Barr virus infection after the double failure of hematopoietic stem cell transplantation. Am J Hematol **80,** 207, 2005.
52. Bachanova, V., and Weisdorf, D. Unrelated donor allogeneic transplantation for adult acute lymphoblastic leukemia: a review. Bone Marrow Transplant **41,** 455, 2008.
53. Handschel, J., Meyer, U., and Wiesmann, H.P. Embryonic stem cell use. In: Meyer, U., Meyer, T., Handschel, J., and Wiesmann, H.P., eds. Fundamentals of Tissue Engineering and Regenerative Medicine. Berlin, Heidelberg: Springer-Verlag, 2009, pp. 159–166.

Address correspondence to:
Christian Naujoks, M.D.
Department for Cranio- and Maxillofacial Surgery
Heinrich Heine University of Düsseldorf
Moorenstr. 5 (Geb. 18.73)
Düsseldorf D-40225
Germany

E-mail: christian.naujoks@med.uni-duesseldorf.de

Received: August 7, 2009
Accepted: February 2, 2010
Online Publication Date: April 20, 2010

3.7 Effects of dexamethasone, ascorbic acid and β -glycerophosphate in the osteogenic differentiation of stem cells

[7] **Langenbach, F.**, Naujoks, C.# Berr, K., Smeets, R., Depprich, R., Stamm, T., Schwartz, F., Kubler, N.R. and Handschel, J. (2012). Effects of dexamethasone, ascorbic acid and β-glycerophosphate in the osteogenic differentiation of stem cells. Stem Cells Reviews and Reports. Revision Submitted (22. May 2012)

Impact Factor: 3,766

Durchschnittlicher Impact Faktor des Forschungsgebietes:

- Cell & Tissue Engineering:
    - 3,388 Rang 7 von 13 Zeitschriften

- Cell Biology:
    - 3,376, Rang 75 von 178 Zeitschriften

Mein Anteil an der Publikation:

- schriftliche Arbeit: 90%

Effects of dexamethasone, ascorbic acid and β -glycerophosphate in the osteogenic differentiation of stem cells

Langenbach, F.[1], Naujoks, C.[1,#], Berr, K.[1], Depprich, R.[1], Stamm, T.[2], Schwartz, F.[3], Kubler, N.R.[1] and Handschel, J.[1]

[1] Heinrich-Heine University, Cranio and M axillofacial Surgery, Moorenstr. 5, 40225 Düsseldorf, Germany, [2]University of Münster, Outpatient Clinic of Orthodontics, Waldeyerstr. 30, 48149 M ünster, Germany; [3]Heinrich-Heine University, Department of Oral Surgery, Heinrich Heine University, 40225, Düsseldorf, Germany

[#]Corresponding Author

Abstract

Understanding the principals behind how culture supplements drive particular stem cells into the osteogenic lineage is important to improving protocols for osteogenic tissue engineering. This review describes the effects of dexamethasone, ascorbic acid and β-glycerophosphate on intracellular signaling cascades that lead to osteogenic differentiation of stem cell of the bone marrow stromal cell (BMSCs) population. Moreover, osteogenic differentiation markers are described, including extracellular markers, and c ellular as well as intracellular signs of differentiation. In this context a special focus is laid on t he differences between dystrophic and b one specific mineralization. We concluded that dexamethasone (Dex) is not sufficient to induce osteogenesis and that its role seems rather to be as an enhancer for the activity of Runx2, by regulating TAZ and MKP1. In this process, Runx2 needs previous activation by ascorbic acid (Asc) and β-glycerophosphate (β-Gly) mediated phosphorylation. Moreover, it seems that the osteogenic response to these factors requires basic expression of Runx2 and BMP.

Keywords: **dexamethasone; ascorbic acid; beta-glycerophosphate; autocrine BMP signaling; basic Runx2 expression; TAZ (transcriptional co-activator with PDZ-binding motif); homeodomain proteins; differentiation markers; mineralization**

Introduction

Bone defects can occur because of congenital factors or originate from causes such as trauma, infection, tumor resection and osteoporosis. Furthermore, defects of the cranio- and maxillofacial skeletal system caused by tooth loss and ag e-related atrophy of the jaw are a significant clinical problem. To attain and preserve quality of life, it is necessary to reconstruct or regenerate these bone defects in order to recover aesthetics and restore functionality. Despite the significant morbidity from donor site procedures and quantitative limitations, the use of autologous bone grafts is still the gold standard for tissue repair [1]. Modern cell-based bone r econstruction therapies may offer new therapeutic opportunities and tissue engineering represents a more biologically-oriented approach to heal tissue defects [2]. Using cells, scaffolds and growth factors, customized tissue-engineered constructs can be grown *in vitro* and implanted later [3]. Stem cells from several tissues are promising candidates for bone tissue engineering. However, there are only a few cell types that are able to form heterotopic bone and many cell types that are able to form mineralized tissue. Many studies report that skeletal stem cells (SSC) from bone m arrow and unr estricted somatic stem cells (USSC) from umbilical cord blood are able to establish a hem atopoietic

microenvironment (HME) and to form bone after implantation [4-6]. Definitive evidence that USSC cultures are not a mixture of cord blood cells, of which some are able of osteogenic differentiation and others are able to differentiate into hematopoietic cells, was provided by Wernet et al., [7]. They revealed the three germ layer differentiation potential by lentiviral labeling of single USSCs. In contrast, there is little evidence for the ability of stem cells from other sources than bone marrow and cord blood (e.g. adipose tissue, dental pulp and periodontal ligament) to support hematopoiesis [4]. For general information on the delicate differences between stem cells and the uncertainties about the definition of mesenchymal stem cells, please refer to the comment of Bianco et al. [8]. Furthermore, we recommend the review of Robey about "Cell Sources for Bone Regeneration", which highlights the importance of SSC in osteogenic tissue engineering [4]. In this context, it is important to note that the culture conditions for the expansion of stem cells, and especially of stem cells in the bone marrow stromal cell (BMSCs) population, are important for the success of osteogenic tissue engineering. Prolonged culture of BMSCs can deplete the SSC pool or lead to over-dilution of SSCs in the heterogeneous BMSC population [4, 9].

In the last decade, different approaches for the differentiation of stem cells into the osteogenic lineage have evolved. Recently, Roberts et al. [10] screened for optimal combinations of several osteoinductive agents, Vater et al. [11] reviewed the different culture media for the differentiation of BMSC and lately Dalle Cabonare et al. [12] explained the role of the master osteogenic transcription factor Runx2. Even if the treatment of confluent layers of cells with combinations of dexamethasone (Dex), ascorbic acid (Asc) and β-glycerophosphate (β-Gly) is the most frequently used method, there is no review of the precise mechanisms by which these reagents push stem cells into the osteogenic lineage. In this review, latest findings concerning the underlying mechanisms in osteogenic differentiation of BMSC cultures under the influence of Dex, Asc and (β-Gly) (the combination is frequently called DAG) , are described.

Differentiation markers *in vitro*

The most prominent marker for the successful osteogenic differentiation of a cell population *in vitro* is the mineralization of the extracellular matrix (ECM). At the beginning of osteogenic differentiation, a proliferative burst is initiated, followed by the formation of mineralized nodules. This mineralization is routinely investigated by histological staining with Alizarin Red S or von Kossa. However, since Alizarin Red S staining detects calcium in calcium/phosphate (Ca/P) as well as in calcium-binding proteins and proteoglycans and von Kossa staining is not specific for calcium phosphate, as it also detects anions such as carbonates and sulfates, Bonewald et al. [13] suggested using these staining techniques in combination [14]. Recently, our group adapted a protocol of a commercially available detection kit that uses a hydroxyalpatite-specific fluorescence dye for histological staining [15]. Even though these methods are suitable for detecting mineralization, they cannot distinguish between different Ca/P minerals. Lammers et al. [16] therefore demonstrated how a complex set of methods can be used to determine the mineral content of a sample. They used:

- quantitative wavelength-dispersive X-ray spectroscopy (WDX) to determine whether a bone-specific Ca/P ratio is present in the sample
- transmission electron microscopy (TEM) for the characterization of hydroxylapatite specific crystal growth

- selected area electron diffraction (SAED)analysis to compare diffraction patterns
- Raman spectroscopy to compare the phosphate-oxygen bond of different calcium-phosphates.

One of these methods is particularly important for distinguishing between dystrophic mineralization, a product of cell death, and active mineralization of the matrix, and t herefore for avoiding false positive results for osteo- specific mineralization. With TEM, one can distinguish between oriented hydroxylapatite specific needle shaped crystal growth and unorganized Ca/P depositions (such as amorphous Ca/P).

If time-dependent differences for *in vitro* and *in vivo* mineralization need to be investigated, xylenol orange and calcein blue can be added t o the living animal or the growing cell culture [17]. Colorimetric assays for detection of calcium are used to quantify progresses in matrix mineralization.

Before stem cells of the BMSC population differentiate into cells that are able to build up mineral nodules, they undergo a complex differentiation cascade. In this process, the cells change their shape from fibroblastoid to cuboidal, and produce a bone-like ECM. This matrix is mainly composed of collagen type I (Col1), and several bone-specific proteins, and is a pr erequisite for successful mineralization. Bone matrix proteins such as osteocalcin (OC) serve as primary nucleators for the mineralization of the ECM [18]. This protein has a *γ*–carboxy-glutamate residue that plays a role as the primary nucleator of mineralization by bridging with a calcium ion [19]. Therefore, this protein is a typical marker of osteogenic differentiation. Another prominent but less specific marker is osteopontin (OPN). Beck and K necht reported that OPN is up-regulated by increased inorganic phosphate levels in osteoblasts but also in several other cell types and i s one of the earliest matrix secretion events by osteoblasts during bone remodeling [20]. There are two peaks in the expression of OPN during osteogenic differentiation of osteoblasts, the first during the proliferation of the cells (about 25% of maximal levels) and a s econd that begins at the onset of mineralization, achieving peak levels of expression during mineralization [21]. Recently McKee et al, described how OPN potentially acts as an adhesion promoter between older and newer bone, or to ‘prime’ the bone surface for subsequent cell adhesion and/or cell signaling events, or to regulate early stages of the mineralization process [22].

Many studies use Col1 and alkaline phosphatase (ALP) as early markers in the osteogenic differentiation of various cell types; however, the transcription of these markers varies between the different cell lines. Some stem cell lines and also finally committed cells already express high levels of ALP [23-24] and Col1 [25-26], so that a further increase in the expression of these markers may not be necessary. Another possible reason is that there might be cells that only recapitulate certain developmental processes of osteogenic differentiating cells (osteoprogenitors or BMSC), may not respond to osteogenic factors with the up-regulation of ALP and C ol1. Furthermore, a large body of evidence demonstrates that the expression of Col1 is not significant or is only slightly increased during osteogenic differentiation by dexamethasone (Dex), ascorbic acid (Asc) and bet a-glycerophosphate (b-Gly) [25-26]. ALP is a membrane-bound enzyme that makes inorganic phosphate available for its incorporation into minerals by the hydrolyzation of phosphate esters [27]. However, even though ALP induction is a key event in the differentiation of osteoblasts, the detection of ALP is not an indicator for osteogenic commitment, since cells of other organs and tissues such as

liver, kidney and adipose tissue are also ALP positive. This might lead to confusing results when ALP is the only measure of osteogenic differentiation.

Earlier stages in osteogenesis can be investigated by the detection of bone-specific transcription factors. Initial events in the osteogenic differentiation of stem cells of the BMSC population are attributed to early intracellular signaling and transcriptional events. Several mechanisms have been found to induce osteogenic differentiation. In one mechanism, bone morphogenic proteins (BMPs) stimulate Smad proteins and the MAPK signaling pathway, which stimulate osteogenic transcription factors including Runx2. This transcription factor is a key regulator in the osteogenic differentiation and induces the transcription of several osteogenic markers, such as Col1, OC, osterix and bone sialoprotein (BSP), by binding to their promoters [28-29]. In another mechanism, Runx2 can induce osteogenic differentiation after MAP/ERK-transduced extracellular interactions between cellular integrins and ECM proteins [30-34]. Although osteogenic differentiation can be induced without the addition of BMP2, autocrine BMP2 production is necessary for the function of Runx2 [35]. According to Phimphilai et al., BMPs and Runx2 cooperatively interact to stimulate osteoblast gene expression [35]. However, since different pathways are activated and temporal differences in the response of several cell types are possible, these two mechanisms need to be taken into account when early signs of osteogenic differentiation processes are investigated. For example, Salasznyk et al assayed the phosphorylation of Runx2 [34], Phimphilai et al. checked for the phosphorylation of SMADs [35] and Li et al. tested for the phosphorylation of ERK in the MAP/ERK pathway [36]. Activation of these pathways resulted in the activation of Runx2 transcription. Lately, TAZ (transcriptional co-activator with PDZ-binding motif), which is the essential co-activator of Runx2 and is therefore important in the early fate decision of stem cells of the BMSC population, has been used to detect early signs of osteogenic differentiation (later described in more detail).

Even though Runx2 is an essential factor for osteogenic differentiation, its expression does not increase in the maturation of osteoblasts after an initial onset of expression. Therefore, only the appearance of Runx2 transcripts is useful for detecting early commitment to the osteoblastic phenotype [28]. Pregizer et al. showed that the increase in OC expression was correlated with a decrease in Runx2 expression in osteoblasts. Measurement of OC and Runx2 expression is therefore an effective way to follow the development of the osteoblast phenotype [37]. However, even though Runx2 is the transcription factor that induces the expression of OC, the presence of Runx2 does not lead to an expression of OC at the beginning of the osteogenic differentiation of osteoblasts. Pregizer et al. found that the initial transcriptional silence of OC on day 4 of differentiation of osteoblasts was attributable to a post-translational block in recruiting Runx2 to the OC promoter [37]. Four days later, this block was relieved and Runx2 gained access to the promoter of OC. Another important transcription factor that is critical in osteoblast differentiation is osterix. Osterix acts downstream of Runx2 to induce differentiation of pre-osteoblasts into fully functional osteoblasts [29]. In fact, osterix has a Runx2 responsive element in its promoter [38] and can thus serve as an early marker for Runx2 activity.

In conclusion, ON, OC, OPN, BSP, mineralization and cell morphology are suitable extracellular markers for both the detection of osteoblastic differentiation and observation of bone morphology (see Table 1). For the above-mentioned reasons, Col1 and ALP are also suitable as marker of

Table 1 Differentiation markers in vitro and their suitability in osteogenesis studies

Localization	Marker	Function	Detection Method	Suitability for the	
				detection of osteoblastic differentiation	observation of bone morphology
Extracellular	Collagen type 1	Main constituent of the ECM	IHC, WB, qRT-PCR, Masson Goldner, birefringence measurement	↘	↑
	Osteonectin	Early constituent of the ECM.	IHC, WB, qRT-PCR	↑	↑
	Osteocalcin	Mineralization and calcium ion homeostasis; Binds to collagen and serves as nucleator for HA cristalization	IHC, WB, qRT-PCR	↑	↑
	Osteopontin	Early constituent of the ECM. Regulation of osteoclast activity	IHC, WB, qRT-PCR	↑	↑
	Bone Sialoprotein	Serves as nucleator for HA cristalization; Regulation of osteoclast activity	IHC, WB, qRT-PCR	↑	↑
	Alkaline Phosphatase	Hydrolyzation of phosphate esters for the utilization of inorganic phopsphate	IHC, WB, qRT-PCR, ELISA	→	↑
	BMP2	Osteogenic transforming growth factor	IHC, WB, qRT-PCR, ELISA	↗	↘
	Mineralization	Mechanical stability and storage of nutrients	Alizarin Red S, Von Kossa, Osteolmage, xylenol orange, calcein, Toluidin Blue, Masson Goldner	↑	↑
	columnar or cuboidal shaped cells	Ideal shape for osteoid deposition	Masson Goldner, H/E	↗	↗
Intracellular	Runx2	Crucial Transcription Factor in osteogenic differentiation	IHC, WB, qRT-PCR	↘	↗
	Osterix	Transcription factor downstream of Runx2	IHC, WB, qRT-PCR	↑	↗
	BMP2	Growth factor for bone formation and osteogenic differentiation	IHC, WB, qRT-PCR, ELISA	↑	↑
	TAZ	Upregulated in response to Dex. Coactivator of Runx2	IHC, WB, qRT-PCR	↑	↗
	ERK phosphorylation	Response to extracellular signals by MAP/ERK signaling. Phosphorylates Runx2	WB	→	↓
	SMAD 1, 5 and 8 phosphorylation	Respond to BMP signaling. Translocate to the nucleus to regulate osteogenic gene expression.	WB	↑	↓

Abbreviations: HA: hydroxyapatite; ECM: extracellular Matrix IHC: Immunohistochemistry; WB: Western Blot; qRT-PCR: quantitative real time PCR; ELISA: Enzyme Linked Immunosorbent Assay; ↑: excellent ;↗:good; →: restricted; ↘: less suitable; ↓: unqualified

osteoblastic differentiation and obs ervation of bone morphology but need t o be us ed cautiously. Osterix, BMP2, TAZ, ERK- and SMAD-phosphorylation are good intracellular markers for osteoblastic differentiation (Table 1). Due to massive posttranscriptional modifications of Runx2, the mRNA expression of Runx2 is only suitable for detection of an early commitment. Detection of ERK and SMAD-phosphorylation is

difficult and impractical in observations of bone morphology.

The function of dexamethasone, ascorbic acid and β-glycerophosphate

Dexamethasone

At least three weeks period of continuous treatment of a confluent monolayer of cells with Dex, in combination with β-Gly and Asc, is required for osteogenic differentiation [39], demonstrating that the differentiation process does not start with an initial event that is sufficient of itself to induce a complete osteogenic commitment, but that Dex, Asc and β-Gly orchestrate several regulatory mechanisms over a period of time. Several approaches have been undertaken in order to elucidate the function of Dex, which have often resulted in conflicting findings attributable to differences in the differentiation state and the osteogenic potential of the cells. Moreover, the precise mechanism of Dex is not fully understood due to the contradictory effects of Dex *in vitro* and *in vivo* and to the differing effects of Dex depending on its concentration. Endogenous glucocorticoid (GC) signaling is required for normal bone volume and architecture in bone formation *in vivo*, and it has therefore been suggested that endogenously expressed GCs may have an anabolic effect on skeletal metabolism and bone formation *in vivo* [27, 40]. However, the continued application of the GC Dex in the treatment of autoimmune and inflammatory diseases is often accompanied by severe side effects on the skeleton, since it induces osteoporosis by impairing osteoblast activity [41].

Since Tenenbaum and Heersche [42] demonstrated in 1985 that the optimal concentration of Dex in osteogenesis of chick periosteum cells was 100nM, this concentration has been used in many approaches for the differentiation of cells. In a study of Walsh et al. [43], observations on BMSCs of 30 human donors has provided evidence that the physiological level of Dex (10nM) is the optimal concentration for mineralized nodule formation. A review by Seong et al. [44] noted that both concentrations have been used at similar frequencies in research articles. Due to the negative effects of 100nM of Dex in some reports, and due to the fact that Walsh et al. used human BMSCs in contrast to Tennenbaum and Heersche, who used chick periosteum cells, we recommend a physiological level of 10nM of Dex.

Dex regulates Runx2 via activation of TAZ

The precise mechanisms of how Dex induces osteogenesis *in vitro* remained unclear until recent findings elucidated the regulatory mechanisms of Dex on the function of Runx2 via the activity of the beta catenin-like molecule TAZ (transcriptional co-activator with PDZ-binding motif) [45] (see Figure 1). TAZ contains a coiled-coil C-terminal domain that recruits core components of the transcriptional machinery and a specific domain that binds to the Pro-Pro-X-Tyr motif (where X is any amino acid) of Runx2 [46-47]. Interestingly, in rat and murine BMSC, TAZ co-activates Runx2-dependent gene transcription while repressing peroxisome-proliferator-activated receptor gamma (PPARγ)-dependent gene transcription, a critical transcription factor for adipogenic differentiation [45, 47]. Hong et al. demonstrated that the expression of TAZ is increased in response to Dex in rat BMSCs and suggested that TAZ is involved in the signaling pathway of Dex [45]. Zebrafish that were TAZ-depleted revealed absence of bone formation, providing further evidence for the importance of TAZ in osteoblast differentiation [47]. It seems that TAZ is a crucial factor in the fade decision of

stem cells of the BMSC population, and that the key event by which Dex induces osteogenesis is the up-regulation of TAZ expression.

Dex regulates Runx2 via activation of MKP-1

Another mechanism by which Dex further induces osteogenesis is the modulation of Runx2 phosphorylation via the mitogen-activated protein kinase (MAPK) phosphatase (MKP-1) (Figure 1). In fact, Dex has been shown to increase MKP-1 expression, leading to the de-phosphorylation of Serine 125 of Runx2 and to enhance Runx2 trans-activation in Runx2 transfected primary dermal fibroblasts and BMSC from rats. It was demonstrated that the de-phosphorylation of Runx2 played a crucial role in osteogenic differentiation and late-stage mineralization processes [27]. It seems that Dex and Runx2 synergistically induce OC and BSP expression, as well as mineral deposition. Both the timing of Dex administration and concentration have significant effects on mineralization and differentiation [48]. The osteogenic response to Dex may, at least in part, require the presence of Runx2, which is probably the reason for the contradictory results concerning the function of Dex *in vitro*. Therefore, one can hypothesize that cells with different expression levels of Runx2 have variable sensitivity to Dex induced osteogenic differentiation. Cells without an inherent osteogenic differentiation potential, with very little or no endogenous Runx2, are therefore probably less susceptible to or incapable of Dex-induced osteogenesis.

Phosphorylation states regulate Runx2 activity

Interestingly, it seems that both the de-phosphorylation of the serine125 of Runx2 and the phosphorylation of other serines lead to increased activity and gene expression of osteogenic genes [27, 49]. However, in the case of Dex, only the de-phosphorylation of Runx2 has positive effects on osteogenic gene expression. By contrast, previous findings have demonstrated that several factors and events, such as contact with Col1 or extracellular inorganic phosphate, leads to Runx2 activation by phosphorylation. This divergence is explained by different phosphorylation sites, specifically the stimulatory phosphorylation sites in the proline-serine-threonine (PST)-rich domain of the C-terminal region of Runx2 and the stimulatory de-phosphorylation site Serine125 in the N-terminal runt domain [27, 50]. Further information on how the addition of Asc and inorganic phosphate results in ERK phosphorylation-mediated Runx2 phosphorylation will be described below. In addition to the multiple phosphorylation sites, cell type-, species- and isoform-specific differences in Runx2 expression may account for differences in the responsiveness of Runx2 to Dex and other stimuli. There is evidence that states of Runx2 phosphorylation alter the interaction with accessory factors that orchestrate Runx2 function. Several mechanisms have been shown to further regulate Runx2 function. Gaur et al. [51] demonstrated that the canonical WNT pathway promotes bone formation through beta-catenin/TCF1(T cell factor 1)-mediated activation of Runx2. The transcription factor TCF1 mediates WNT activation by binding to its responsive element in the promoter of the *Runx2* gene. Gaur et al. concluded that the WNT/TCF1 pathway contributes to bone formation through Runx2 activation, which drives osteogenic differentiation [51]. A further mechanism that regulates Runx2 activity is BMP signaling, which has been shown to be required for Runx2-dependent induction of the osteoblast phenotype. Phimphilai et al. have determined that autocrine BMP production is necessary for Runx2 to be

active and that there is a cooperatively interaction between BMPs and Runx2 [35].

Runx2/BMP interaction is important for the osteogenic differentiation

Binding of BMPs to their receptors elicits phosphorylation of Smads 1, 5 and 8. These Smads complex with Smad4 and translocate into the nucleus where they regulate gene expression of the osteogenic transcription factors Runx2, osterix and the MSX/DLX homeodomain proteins [52-54], as well as transcriptional co-activators such as p300, CBP and P/CAF [29, 55-56]. Afzal et al. [56] found a Smad-interacting domain (SMID) in Runx2, which overlaps with the nuclear matrix targeting signal (NMTS). The Smad-Runx2 interaction is an important component in the Runx2 activity that regulates

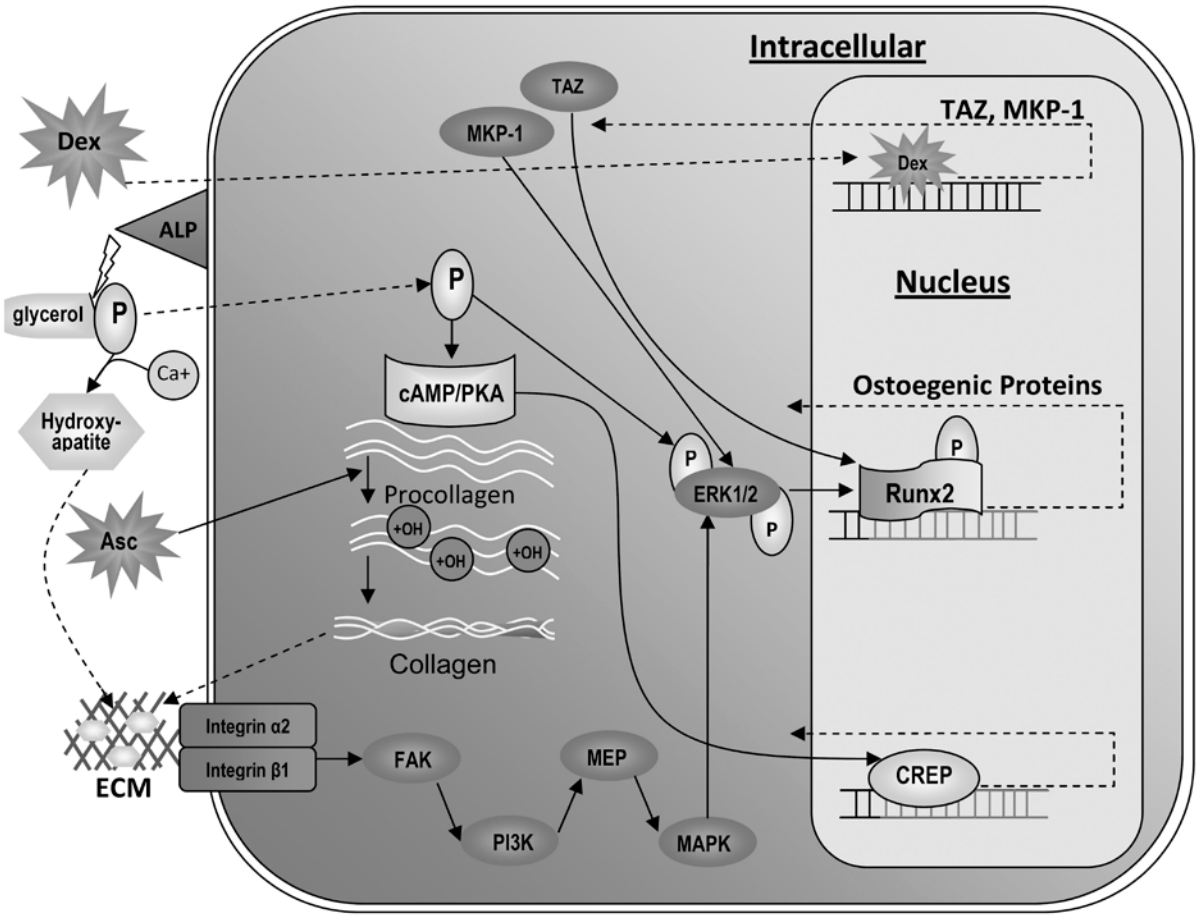

Figure 1: Dexamethasone (Dex) induces the osteogenic differentiation of stem cells by increasing the expression of transcription of the Runx2 co-activator TAZ. Additionally, Dex treatment induces the expression of the gene encoding MKP-1 (a component of the MAPK signaling pathway), which dephosphorylates and thereby activates the key transcription factor Runx2 via ERK signaling. The addition of ascorbic acid (Asc) facilitates osteogenic differentiation by increasing secretion of collagen type I (Col1), resulting in increased binding of $\alpha_2\beta_1$integrins to Col1. This leads to the phosphorylation of ERK1/2 in the MAPK signaling pathway, and a subsequent translocalization of P-ERK1/2 to the nucleus where it activates Runx2 by phosphorylation. β-glycerophosphate (β-Gly) is cleaved by ALP and facilitates osteogenic differentiation by being the source of phosphate for hydroxylapatatite, by phosphorylating ERK1/2 and by activating the Protein Kinase C (PKC) pathway, which activates Runx2. Interrupted arrows = translocalization, solid arrows = regulation. Abbreviations: TF = Transcription Factor, +OH = hydroxylation

osteogenic differentiation. BMP-mediated regulation of Runx2 involves the binding and release of the homeodomain (HD) protein DLX5 to Runx2. During osteoblast proliferation, OC gene expression is repressed by the HD protein Msx2 [54] by interacting with histone deacetylases [57] or inhibiting *trans*-activating factors [58] and Runx2 itself [54]. At the onset of differentiation, Msx2 is released from the chromatin of OC and Dlx3, and Dlx5 is recruited with Runx2. In this process, Dlx3 is bound to the HD binding site in the promoter region of OC. Later in osteogenic differentiation, i.e., during matrix mineralization, Dlx3 is replaced by Dlx5. Interestingly, the increase in Dlx5 binding to the promoter is associated with an increase in RNA polymerase II. From these results, Hassan et al. concluded "that multiple HD proteins in osteoblasts constitute a regulatory network that mediates development of the bone phenotype through the sequential association of distinct HD proteins with promoter regulatory elements." Further evidence for the BMP2/Runx2 interaction is provided by the finding that inhibition of BMP signaling disrupts the ability of Runx2 to stimulate osteoblast differentiation in mice, leading to the suggestion that autocrine BMP production is necessary for Runx2 activity in murine stem cells of the BMSC population [35].

Several osteogenic factors only have osteogenic effects when acting in combination with other factors [10]. Continuous treatment of BMSC with Dex augments chondrogenic, adipogenic and osteogenic differentiation [59], leading to the suggestion that Dex has no direct effect on osteogenic differentiation, but promotes differentiation in combination with other factors such as Asc and b-Gly.

Ascorbic Acid

Asc facilitates osteogenic differentiation by increasing col1 secretion

Asc is required as a cofactor for enzymes that hydroxylate proline and lysine in pro-collagen (Figure 1) [11]. Hydroxylated pro-collagen can readily assume a triple-helical conformation, resulting in a secretion that is six-fold faster than non-helical collagen [60]. In the absence of Asc, proline cannot be hydroxylated and collagen chains are not able to form a proper helical structure [60]. Therefore, the role of Asc in osteogenic differentiation is mainly attributed to the secretion of Col1 into the ECM. Jaiswal et al., [61] determined that the best results for osteogenic differentiation of human BMSCs is achieved at a concentration of 50µM ascorbic acid-2-phosphate, a more stable analogue of Asc under standard culture conditions. Xiao et al. proposed a model to explain the role of ECM in the induction and maintenance of osteoblast differentiation: "(1) Osteoblasts must be in contact with a collagen-containing ECM before they can differentiate. (2) Osteoblasts bind to this ECM via interactions between Col1 and $\alpha_2\beta_1$ integrins. (3) Integrin ligand binding activates MAPK and related pathways that transduce signals to the nucleus. (4) Runx2 is phosphorylated and activated by MAPK, thereby allowing it to stimulate osteoblast differentiation by increasing transcription of osteoblast marker genes such as OC" [28, 32]. This was demonstrated by the absence of osteogenesis in pre-osteoblast cultures treated with collagenase, as well as in cultures in which $\alpha_2\beta_1$integrin was suppressed [62-63]. The importance of the ECM is further highlighted by the finding that the ECM proteins Col1 and vitronectin are sufficient to induce osteogenic differentiation of BMSC cultures [30], and that unrestricted somatic stem cells (USSC) from human cord blood undergo osteogenic differentiation in

spheroid microtissues due to contact between cells and to the ECM, without the addition of Dex, Asc and β-Gly [15, 64].

Cellular interaction with ECM proteins leads to enhanced Runx2 activity

However, the precise mechanism of this MAPK/ERK-mediated activation of Runx2 remained unclear until the classic theory of MAP kinase action, namely that phosphorylation events are distinct from changes in gene expression, was revealed by virtue of the discovery finding that nuclear kinases interact directly with the chromatin of target genes [36, 65]. Specifically, ECM interaction activates the MAP kinase pathway, leading to accumulation of P-ERK in the nucleus. Together with Runx2, it associates with OC and BSP genes to induce osteoblast-specific gene expression. The proximal promoter of OC has two osteoblastic *cis*-acting elements (OSE2a and OSE2b), which are the targets of Runx2 and are both necessary for the expression of OC [36, 66]. Immunofluorescence laser confocal microscopy and ChiP analyses have revealed that P-ERK, together with Runx2, selectively binds to these regions. A comparable mechanism was found for the regulation of BSP expression [36].

However, regardless of peak protein levels and DNA binding activity at the early stages of differentiation, binding of Runx2 to its genomic targets is blocked. Different mechanisms have been attributed to this block and the later release of Runx2. Bialek et al. demonstrated that Twist proteins have an anti-osteogenic function that is mediated by the Twist box, which interacts with the Runx2 DNA-binding domain to inhibit its function [67]. As mentioned above, Runx2 is both negatively and positively regulated by Dlx3, DLX5 and MSX2.

Many osteoblast genes, such as OC, OPN, BSP and Col1, contain functional HD regulatory elements that are regulated by Runx2 in combination with Dlx3 and Dlx5 [54]. For example, Dlx5 binds to a HD protein-binding site upstream of the two Runx2 binding sites of BSP [68-69]. Whereas Runx2 is constitutively bound to the BSP promoter in the presence and absence of Asc, Dlx5 only binds to its HD-binding site in differentiated osteoblasts that have been treated with Asc. Total Dlx5 protein levels are similar in differentiated osteoblasts and controls, and thus an increased affinity of Dlx5 to the chromatin of BSP can be attributed to ascorbic acid-induced intracellular signaling.

Beta-Glycerophosphate

Treatment with β-Gly can result in non-osteogenic dystrophic mineralization

β-Gly plays an important role in the osteogenic differentiation of stem cells of the BMSC population. Nevertheless, its use for the osteogenic differentiation of stem cells and osteoblasts has led to many false positive results. Besides expression of some surface markers one of the minimal prerequisites that a cell has to fulfill to be announced as mesenchymal stem cells is the capability of osteogenic, adipogenic and chondrogenic differentiation. When cells that are incapable of an osteogenic differentiation are treated with high concentrations (>=2mM) of β-Gly they produce dystrophic mineralization or non-apatitic mineralization, which can be detected by Alizarin Red S or Von Kossa, [13]. However, detection of mineralization in confluent mono-layers by Alizarin Red S or Von Kossa is often the only evidence provided for an osteogenic differentiation potential. If positive results for adipogenic and chondrogenic differentiation are observed for the same cells, then these cells are falsely declared as “mesenchymal stem cells (MSC)”.

β-Gly serves as phosphate source for bone mineral and induces osteogenic gene expression by ERK phosphorylation

Despite being the source of phosphate needed to produce the hydroxylapatite mineral, $Ca_{10}(PO_4)_6(OH)_2$, recent findings have shown that inorganic phosphate (Pi) acts as an intracellular signaling molecule to regulate the expression of many osteogenic genes, including OPN [70-71] and BMP2 [72] (Figure 1). For this regulation, phosphate enters the cell and influences cell function. The activation of the ERK signaling pathway by Pi is biphasic and is mediated by two independent phosphorylations of ERK separated by a time interval of several hours. Only after the second phosphorylation ERK exerts its function on the osteogenic gene expression. Inhibition of ERK completely inhibits OPN expression [71] and the increase in BMP-2 mRNA in response to Pi [72]. This shows that ERK signaling is necessary for Pi mediated increased BMP2 expression. In addition to the ERK-mediated increase in BMP2 expression, Tada et al. [72], also demonstrated that Pi increases BMP2 expression by activation of the cyclic-AMP/protein-kinase-A pathway. Interestingly, they also demonstrated that both pathways operate independently of each other.

Additional osteoinductive supplements

In addition to the classical stimulation with DAG, combinations of several growth factors with each other or with DAG have been shown to facilitate osteogenic differentiation *in vitro* and *in vivo*. Factors that have a positive effect on osteogenic differentiation *in vitro* and *in vivo* include vitamin D3 (vitD3), bone morphogenetic proteins, cyclic AMP (cAMP) and all-*trans*-retinoic acid (atRA). Recently Chen et al reviewed that, "following TGF-β/BMP induction, both the Smad and p38 MAPK pathways converge at the Runx2 gene to control mesenchymal pre-cursor cell differentiation." VitD3 alone is not able to induce osteogenesis, but can enhance osteogenic differentiation. [73-74]. cAMP is a potent stimulant of the protein kinase A (PKA) signaling pathway [75-76], which can stimulate the expression of osteogenic markers and induces mineralization *in vitro.* For general information about roles of parathyroid hormones in bone remodeling please refer to the review of Lombardi et al.[77].In most reports, positive effects of all-*trans*-retinoic-acid are reported only in combination with BMP2 [78]. The precise mechanisms of the effects of atRA are largely unknown and are cell and species specific treatment of BMSC with FGF increases the proliferation of osteogenic cells and exerts positive osteogenic effects by inducing Runx2 activity after ERK phosphorylation [79], but also leads to the abrogation of the ability to form HME *in vivo* [9].

Conclusion

To summarize, both basic levels of Runx2 and autocrine production of BMP seems to be important for the osteogenic differentiation of stem cells of the BMSC population. It appears that TAZ (transcriptional co-activator with PDZ-binding motif) is a crucial factor in the fade decision of MSCs and that the key event by which Dex induces osteogenesis is the up-regulation of TAZ expression. TAZ binds to Runx2 in the nucleus where it regulates osteoblastic differentiation by recruiting core components of the transcriptional machinery. Additionally, Dex induces osteogenic differentiation of BMSCs by increasing the transcription of the gene encoding MKP-1 (a component of the MAPK signaling pathway), which de-phosphorylates and thereby activates Runx2. The addition of ascorbic acid facilitates osteogenic differentiation by increasing the secretion of collagen type I, resulting in an increased binding of

$\alpha_2\beta_1$integrins to Col1. This in turn leads to the phosphorylation of ERK1/2 in the MAPK signaling pathway and s ubsequent trans-localization of P-ERK1/2 to the nucleus, where it binds to Runx2 and induces gene expression of osteogenic proteins. β-Gly facilitates osteogenic differentiation by being the source of phosphate for hydroxyapatite, phosphorylating ERK1/2, activating cAMP/PKA and BMP-2 signaling.

Acknowledgments

This review was supported in part by the Deutsche Forschungsgemeinschaft (DFG) grant HA 3228/3-1.

Conflict of Interests

The authors declare no potential conflicts of interest.

References

1. Sasso, R. C., LeHuec, J. C., Shaffrey, C. (2005) Iliac crest bone graft donor site pain after anterior lumbar interbody fusion: a prospective patient satisfaction outcome assessment. *J Spinal Disord Tech*, 18 Suppl(S77-81.

2. Meyer, U., Wiesmann, H. P., Berr, K., Kubler, N. R., Handschel, J. (2006) Cell-based bone reconstruction therapies-principles of clinical approaches. *Int J Oral Maxillofac Implants*, 21(6), 899-906.

3. Schulze, M., Tobiasch, E. (2011) Artificial Scaffolds and Mesenchymal Stem Cells for Hard Tissues. *Advances in biochemical engineering/biotechnology*,

4. Robey, P. G. (2011) Cell sources for bone regeneration: the good, the bad, and the ugly (but promising). *Tissue Eng Part B Rev*, 17(6), 423-430.

5. Kogler, G., Sensken, S., Airey, J. A., et al. (2004) A new human somatic stem cell from placental cord blood with intrinsic pluripotent differentiation potential. *J Exp Med*, 200(2), 123-135.

6. Handschel, J., Naujoks, C., Langenbach, F., et al. (2010) Comparison of ectopic bone formation of embryonic stem cells and cord blood stem cells in vivo. *Tissue Eng Part A*, 16(8), 2475-2483.

7. Mackie, E. J., Tatarczuch, L., Mirams, M. (2011) The skeleton: a multi-functional complex organ. The growth plate chondrocyte and endochondral ossification. *Journal of Endocrinology*, 211(2), 109-121.

8. Bianco, P., Robey, P. G., Simmons, P. J. (2008) Mesenchymal stem cells: revisiting history, concepts, and assays. *Cell Stem Cell*, 2(4), 313-319.

9. Sacchetti, B., Funari, A., Michienzi, S., et al. (2007) Self-renewing osteoprogenitors in bone marrow sinusoids can organize a hematopoietic microenvironment. *Cell*, 131(2), 324-336.

10. Roberts, S. J., Chen, Y., Moesen, M., Schrooten, J., Luyten, F. P. (2011) Enhancement of osteogenic gene expression for the differentiation of human periosteal derived cells. *Stem Cell Research*, 7(2), 137-144.

11. Vater, C., Kasten, P., Stiehler, M. (2011) Culture media for the differentiation of mesenchymal stromal cells. *Acta biomaterialia*, 7(2), 463-477.

12. Dalle Carbonare, L., Innamorati, G., Valenti, M. T. (2011) Transcription Factor Runx2 and its Application to Bone Tissue Engineering. *Stem cell reviews*,

13. Bonewald, L. F., Harris, S. E., Rosser, J., et al. (2003) von Kossa staining alone is not sufficient to confirm that mineralization in vitro represents bone formation. *Calcif Tissue Int*, 72(5), 537-547.

14. Langenbach, F., Naujoks, C., Laser, A., et al. (2012) Improvement of the cell-loading efficiency of biomaterials by inoculation with stem cell-based microspheres, in osteogenesis. *J Biomater Appl*, 26(5), 549-564.

15. Langenbach, F., Berr, K., Naujoks, C., et al. (2011) Generation and differentiation of microtissues from multipotent precursor cells for use in tissue engineering. *Nat Protoc*, 6(11), 1726-1735.

16. Lammers, L., Naujoks, C., Berr, K., et al. (2012) Impact of DAG stimulation on mineral synthesis, mineral structure and osteogenic differentiation of human cord blood stem cells. *Stem Cell Res*, 8(2), 193-205.

17. Wang, Y. H., Liu, Y., Maye, P., Rowe, D. W. (2006) Examination of mineralized nodule formation in living osteoblastic cultures using fluorescent dyes. *Biotechnol Prog*, 22(6), 1697-1701.

18. Termine, J. D., Kleinman, H. K., Whitson, S. W., Conn, K. M., McGarvey, M. L., Martin, G. R. (1981) Osteonectin, a bone-specific protein linking mineral to collagen. *Cell*, 26(1 Pt 1), 99-105.

19. Nagata, T., Bellows, C. G., Kasugai, S., Butler, W. T., Sodek, J. (1991) Biosynthesis of bone proteins [SPP-1 (secreted phosphoprotein-1, osteopontin), BSP (bone sialoprotein) and SPARC (osteonectin)] in association with mineralized-tissue formation by fetal-rat calvarial cells in culture. *Biochem J*, 274 (Pt 2)(513-520.

20. Beck, G. R., Jr., Knecht, N. (2003) Osteopontin regulation by inorganic phosphate is ERK1/2-, protein kinase C-, and proteasome-dependent. *The Journal of biological chemistry*, 278(43), 41921-41929.

21. Lian, J. B., Stein, G. S. (1995) Development of the osteoblast phenotype: molecular mechanisms mediating osteoblast growth and differentiation. *The Iowa orthopaedic journal*, 15(118-140.

22. McKee, M. D., Pedraza, C. E., Kaartinen, M. T. (2011) Osteopontin and wound healing in bone. *Cells Tissues Organs*, 194(2-4), 313-319.

23. Riekstina, U., Cakstina, I., Parfejevs, V., et al. (2009) Embryonic stem cell marker expression pattern in human mesenchymal stem cells derived from bone marrow, adipose tissue, heart and dermis. *Stem Cell Rev*, 5(4), 378-386.

24. Ali, N. N., Rowe, J., Teich, N. M. (1996) Constitutive expression of non-bone/liver/kidney alkaline phosphatase in human osteosarcoma cell lines. *Journal of bone and mineral research : the official journal of the American Society for Bone and Mineral Research*, 11(4), 512-520.

25. Franceschi, R. T., Iyer, B. S., Cui, Y. (1994) Effects of ascorbic acid on collagen matrix formation and osteoblast differentiation in murine MC3T3-E1 cells. *J Bone Miner Res*, 9(6), 843-854.

26. Ogston, N., Harrison, A. J., Cheung, H. F., Ashton, B. A., Hampson, G. (2002) Dexamethasone and retinoic acid differentially regulate growth and differentiation in an immortalised human clonal bone marrow stromal cell line with osteoblastic characteristics. *Steroids*, 67(11), 895-906.

27. Phillips, J. E., Gersbach, C. A., Wojtowicz, A. M., Garcia, A. J. (2006) Glucocorticoid-induced osteogenesis is negatively regulated by Runx2/Cbfa1 serine phosphorylation. *J Cell Sci*, 119(Pt 3), 581-591.

28. Ducy, P., Zhang, R., Geoffroy, V., Ridall, A. L., Karsenty, G. (1997) Osf2/Cbfa1: a transcriptional activator of osteoblast differentiation. *Cell*, 89(5), 747-754.

29. Nakashima, K., Zhou, X., Kunkel, G., et al. (2002) The novel zinc finger-containing transcription factor osterix is required for osteoblast differentiation and bone formation. *Cell*, 108(1), 17-29.

30. Kundu, A. K., Khatiwala, C. B., Putnam, A. J. (2009) Extracellular matrix remodeling, integrin expression, and downstream signaling pathways influence the osteogenic differentiation of mesenchymal stem cells on poly(lactide-co-glycolide) substrates. *Tissue Eng Part A*, 15(2), 273-283.

31. Franceschi, R. T., Xiao, G., Jiang, D., Gopalakrishnan, R., Yang, S., Reith, E. (2003) Multiple signaling pathways converge on the Cbfa1/Runx2 transcription factor to regulate osteoblast differentiation. *Connect Tissue Res*, 44 Suppl 1(109-116.

32. Xiao, G., Gopalakrishnan, R., Jiang, D., Reith, E., Benson, M. D., Franceschi, R. T. (2002) Bone morphogenetic proteins, extracellular matrix, and mitogen-activated protein kinase signaling pathways are required for osteoblast-specific gene expression and differentiation in MC3T3-E1 cells. *J Bone Miner Res*, 17(1), 101-110.

33. Boudreau, N. J., Jones, P. L. (1999) Extracellular matrix and integrin signalling: the shape of things to come. *Biochem J*, 339 (Pt 3)(481-488.

34. Salasznyk, R. M., Klees, R. F., Williams, W. A., Boskey, A., Plopper, G. E. (2007) Focal adhesion kinase signaling pathways regulate the osteogenic differentiation of human mesenchymal stem cells. *Exp Cell Res*, 313(1), 22-37.

35. Phimphilai, M., Zhao, Z., Boules, H., Roca, H., Franceschi, R. T. (2006) BMP signaling is required for RUNX2-dependent induction of the osteoblast phenotype. *J Bone Miner Res*, 21(4), 637-646.

36. Li, Y., Ge, C., Franceschi, R. T. (2010) Differentiation-dependent association of phosphorylated extracellular signal-regulated kinase with the chromatin of osteoblast-related genes. *Journal of bone and mineral research : the official journal of the American Society for Bone and Mineral Research*, 25(1), 154-163.

37. Pregizer, S., Baniwal, S. K., Yan, X., Borok, Z., Frenkel, B. (2008) Progressive recruitment of Runx2 to genomic targets despite decreasing expression during osteoblast differentiation. *Journal of cellular biochemistry*, 105(4), 965-970.

38. Nishio, Y., Dong, Y., Paris, M., O'Keefe R, J., Schwarz, E. M., Drissi, H. (2006) Runx2-mediated regulation of the zinc finger Osterix/Sp7 gene. *Gene*, 372(62-70.

39. Song, I. H., Caplan, A. I., Dennis, J. E. (2009) In vitro dexamethasone pretreatment enhances bone formation of human mesenchymal stem cells in vivo. *Journal of orthopaedic research : official publication of the Orthopaedic Research Society*, 27(7), 916-921.

40. Swarthout, J. T., Tyson, D. R., Jefcoat, S. C., Jr., Partridge, N. C. (2002) Induction of transcriptional activity of the cyclic adenosine monophosphate response element binding protein by parathyroid hormone and epidermal growth factor in osteoblastic cells. *Journal of bone and mineral research : the official journal of the American Society for Bone and Mineral Research*, 17(8), 1401-1407.

41. Canalis, E., Delany, A. M. (2002) Mechanisms of glucocorticoid action in bone. *Annals of the New York Academy of Sciences*, 966(73-81.

42. Tenenbaum, H. C., Heersche, J. N. (1985) Dexamethasone stimulates osteogenesis in chick periosteum in vitro. *Endocrinology*, 117(5), 2211-2217.

43. Walsh, S., Jordan, G. R., Jefferiss, C., Stewart, K., Beresford, J. N. (2001) High concentrations of dexamethasone suppress the proliferation but not the differentiation or further maturation of human osteoblast precursors in vitro: relevance to glucocorticoid-induced osteoporosis. *Rheumatology*, 40(1), 74-83.

44. Seong, J. M., Kim, B. C., Park, J. H., Kwon, I. K., Mantalaris, A., Hwang, Y. S. (2010) Stem cells in bone tissue engineering. *Biomedical materials*, 5(6), 062001.

45. Hong, D., Chen, H. X., Xue, Y., et al. (2009) Osteoblastogenic effects of dexamethasone through upregulation of TAZ expression in rat mesenchymal stem cells. *J Steroid Biochem Mol Biol*, 116(1-2), 86-92.

46. Kanai, F., Marignani, P. A., Sarbassova, D., et al. (2000) TAZ: a novel transcriptional co-activator regulated by interactions with 14-3-3 and PDZ domain proteins. *The EMBO journal*, 19(24), 6778-6791.

47. Hong, J. H., Hwang, E. S., McManus, M. T., et al. (2005) TAZ, a transcriptional modulator of mesenchymal stem cell differentiation. *Science*, 309(5737), 1074-1078.

48. Mikami, Y., Omoteyama, K., Kato, S., Takagi, M. (2007) Inductive effects of dexamethasone on the mineralization and the osteoblastic gene expressions in mature osteoblast-like ROS17/2.8 cells. *Biochemical and biophysical research communications*, 362(2), 368-373.

49. Shui, C., Spelsberg, T. C., Riggs, B. L., Khosla, S. (2003) Changes in Runx2/Cbfa1 expression and activity during osteoblastic differentiation of human bone marrow stromal cells. *Journal of bone and mineral research : the official journal of the American Society for Bone and Mineral Research*, 18(2), 213-221.

50. Franceschi, R. T., Xiao, G. (2003) Regulation of the osteoblast-specific transcription factor, Runx2: responsiveness to multiple signal transduction pathways. *Journal of cellular biochemistry*, 88(3), 446-454.

51. Gaur, T., Lengner, C. J., Hovhannisyan, H., et al. (2005) Canonical WNT signaling

promotes osteogenesis by directly stimulating Runx2 gene expression. *J Biol Chem*, 280(39), 33132-33140.

52. Lee, M. H., Javed, A., Kim, H. J., et al. (1999) Transient upregulation of CBFA1 in response to bone morphogenetic protein-2 and transforming growth factor beta1 in C2C12 myogenic cells coincides with suppression of the myogenic phenotype but is not sufficient for osteoblast differentiation. *Journal of cellular biochemistry*, 73(1), 114-125.

53. Lee, M. H., Kim, Y. J., Kim, H. J., et al. (2003) BMP-2-induced Runx2 expression is mediated by Dlx5, and TGF-beta 1 opposes the BMP-2-induced osteoblast differentiation by suppression of Dlx5 expression. *The Journal of biological chemistry*, 278(36), 34387-34394.

54. Hassan, M. Q., Javed, A., Morasso, M. I., et al. (2004) Dlx3 transcriptional regulation of osteoblast differentiation: temporal recruitment of Msx2, Dlx3, and Dlx5 homeodomain proteins to chromatin of the osteocalcin gene. *Molecular and cellular biology*, 24(20), 9248-9261.

55. Sierra, J., Villagra, A., Paredes, R., et al. (2003) Regulation of the bone-specific osteocalcin gene by p300 requires Runx2/Cbfa1 and the vitamin D3 receptor but not p300 intrinsic histone acetyltransferase activity. *Molecular and cellular biology*, 23(9), 3339-3351.

56. Afzal, F., Pratap, J., Ito, K., et al. (2005) Smad function and intranuclear targeting share a Runx2 motif required for osteogenic lineage induction and BMP2 responsive transcription. *J Cell Physiol*, 204(1), 63-72.

57. Mehra-Chaudhary, R., Matsui, H., Raghow, R. (2001) Msx3 protein recruits histone deacetylase to down-regulate the Msx1 promoter. *The Biochemical journal*, 353(Pt 1), 13-22.

58. Zhou, Y. L., Lei, Y., Snead, M. L. (2000) Functional antagonism between Msx2 and CCAAT/enhancer-binding protein alpha in regulating the mouse amelogenin gene expression is mediated by protein-protein interaction. *The Journal of biological chemistry*, 275(37), 29066-29075.

59. Oshina, H., Sotome, S., Yoshii, T., et al. (2007) Effects of continuous dexamethasone treatment on differentiation capabilities of bone marrow-derived mesenchymal cells. *Bone*, 41(4), 575-583.

60. Franceschi, R. T., Iyer, B. S. (1992) Relationship between collagen synthesis and expression of the osteoblast phenotype in MC3T3-E1 cells. *J Bone Miner Res*, 7(2), 235-246.

61. Jaiswal, N., Haynesworth, S. E., Caplan, A. I., Bruder, S. P. (1997) Osteogenic differentiation of purified, culture-expanded human mesenchymal stem cells in vitro. *J Cell Biochem*, 64(2), 295-312.

62. Xiao, G., Wang, D., Benson, M. D., Karsenty, G., Franceschi, R. T. (1998) Role of the alpha2-integrin in osteoblast-specific gene expression and activation of the Osf2 transcription factor. *J Biol Chem*, 273(49), 32988-32994.

63. Franceschi, R. T., Iyer, B. S., Cui, Y. (1994) Effects of ascorbic acid on collagen matrix formation and osteoblast differentiation in murine MC3T3-E1 cells. *Journal of bone and mineral research : the official journal of the American Society for Bone and Mineral Research*, 9(6), 843-854.

64. Langenbach, F., Naujoks, C., Kersten-Thiele, P. V., et al. (2010) Osteogenic differentiation influences stem cell migration out of scaffold-free microspheres. *Tissue Eng Part A*, 16(2), 759-766.

65. Pokholok, D. K., Zeitlinger, J., Hannett, N. M., Reynolds, D. B., Young, R. A. (2006) Activated signal transduction kinases frequently occupy target genes. *Science*, 313(5786), 533-536.

66. Frendo, J. L., Xiao, G., Fuchs, S., Franceschi, R. T., Karsenty, G., Ducy, P. (1998) Functional hierarchy between two OSE2 elements in the control of osteocalcin gene expression in vivo. *The Journal of biological chemistry*, 273(46), 30509-30516.

67. Bialek, P., Kern, B., Yang, X., et al. (2004) A twist code determines the onset of osteoblast differentiation. *Developmental cell*, 6(3), 423-435.

68. Roca, H., Phimphilai, M., Gopalakrishnan, R., Xiao, G., Franceschi, R. T. (2005) Cooperative interactions between RUNX2 and homeodomain protein-binding sites are critical for the osteoblast-specific expression of the bone

sialoprotein gene. *The Journal of biological chemistry*, 280(35), 30845-30855.

69. Franceschi, R. T., Ge, C., Xiao, G., Roca, H., Jiang, D. (2009) Transcriptional regulation of osteoblasts. *Cells, tissues, organs*, 189(1-4), 144-152.

70. Foster, B. L., Nociti, F. H., Jr., Swanson, E. C., et al. (2006) Regulation of cementoblast gene expression by inorganic phosphate in vitro. *Calcified tissue international*, 78(2), 103-112.

71. Fatherazi, S., Matsa-Dunn, D., Foster, B. L., Rutherford, R. B., Somerman, M. J., Presland, R. B. (2009) Phosphate regulates osteopontin gene transcription. *J Dent Res*, 88(1), 39-44.

72. Tada, H., Nemoto, E., Foster, B. L., Somerman, M. J., Shimauchi, H. (2011) Phosphate increases bone morphogenetic protein-2 expression through cAMP-dependent protein kinase and ERK1/2 pathways in human dental pulp cells. *Bone*, 48(6), 1409-1416.

73. Maehata, Y., Takamizawa, S., Ozawa, S., et al. (2006) Both direct and collagen-mediated signals are required for active vitamin D3-elicited differentiation of human osteoblastic cells: roles of osterix, an osteoblast-related transcription factor. *Matrix Biol*, 25(1), 47-58.

74. Fromigue, O., Marie, P. J., Lomri, A. (1997) Differential effects of transforming growth factor beta2, dexamethasone and 1,25-dihydroxyvitamin D on human bone marrow stromal cells. *Cytokine*, 9(8), 613-623.

75. Siddappa, R., Martens, A., Doorn, J., et al. (2008) cAMP/PKA pathway activation in human mesenchymal stem cells in vitro results in robust bone formation in vivo. *Proc Natl Acad Sci U S A*, 105(20), 7281-7286.

76. Tintut, Y., Parhami, F., Bostrom, K., Jackson, S. M., Demer, L. L. (1998) cAMP stimulates osteoblast-like differentiation of calcifying vascular cells. Potential signaling pathway for vascular calcification. *The Journal of biological chemistry*, 273(13), 7547-7553.

77. Lombardi, G., Di Somma, C., Rubino, M., et al. (2011) The roles of parathyroid hormone in bone remodeling: prospects for novel therapeutics. *Journal of endocrinological investigation*, 34(7 Suppl), 18-22.

78. Cowan, C. M., Aalami, O. O., Shi, Y. Y., et al. (2005) Bone morphogenetic protein 2 and retinoic acid accelerate in vivo bone formation, osteoclast recruitment, and bone turnover. *Tissue engineering*, 11(3-4), 645-658.

79. Xiao, G., Jiang, D., Gopalakrishnan, R., Franceschi, R. T. (2002) Fibroblast growth factor 2 induction of the osteocalcin gene requires MAPK activity and phosphorylation of the osteoblast transcription factor, Cbfa1/Runx2. *The Journal of biological chemistry*, 277(39), 36181-36187.

3.8 Scaffold-free microtissues: differences to monolayer cultures and their potential in bone tissue engineering.

[8] **Langenbach, F.**, Naujoks, C.[#] Smeets, R., Berr, K., Depprich, R., Kubler, N.R. and Handschel, J. (2012). Scaffold-free microtissues: differences to monolayer cultures and their potential in bone tissue engineering. Clin Oral Invest. Accepted (23. May 2012)

Impact Factor: 2,25

Durchschnittlicher Impact Faktor des Forschungsgebietes:

- Dentistry, Oral Surgery & Medicine:
    - 1,345 Rang 14 von 77 Zeitschriften

Mein Anteil an der Publikation:

- schriftliche Arbeit: 90%

Scaffold-free microtissues: differences from monolayer cultures and their potential in bone tissue engineering

Fabian Langenbach[1], Christian Naujoks[1,#], Ralf Smeets[2], Karin Berr[1], Rita Depprich[1], Norbert Kübler[1], Jörg Handschel[1]

[1]Heinrich-Heine University, Cranio and M axillofacial Surgery, Moorenstr. 5, 40225 Düsseldorf, Germany [2]University Medical Center Hamburg Eppendorf, Oral and Maxillofacial Surgery, Martinistr.52, 20246 Hamburg, Germany

[#]Corresponding Author

Abstract:

Objectives: Cell-based therapies for bone augmentation after tooth loss and for the treatment of periodontal defects improve healing defects. Usually, osteogenic cells or stem cells are cultivated in two-dimensional (2D) primary cultures, before they are combined with scaffold materials, even though this means a l oss of the endogenous three-dimensional (3D) microenvironment for the cells. Moreover, the use of single-cell suspensions for the inoculation of scaffolds or for the direct application into an area of interest have the disadvantages of low initial cell numbers and s usceptibility to unwanted cellular distribution, respectively.

Materials and Methods: We addressed the question whether an a lternative to monolayer cultures, namely 3D microtissues, have the potential to improve osteogenic tissue engineering and its clinical outcome.

Results: By contrast, to monolayer cultures osteogenic differentiation of 3D microtissues is enhanced by mimicking *in vivo* conditions. It seems that the osteogenic differentiation in microtissues is enhanced by strong integrin-ECM(extracellular matrix) interaction and by stronger autocrine BMP2 signaling. Moreover, microtissues are less prone to wash out by body fluids and allow the precise administration of large cell numbers.

Conclusion: Microtissue cultures have closer characteristics with cells in vivo and t heir enhanced osteogenic differentiation makes scaffold-free microtissues a promising concept in osteogenic tissue engineering.

Clinical Relevance: Microtissues are particularly suitable for tissue engineering because they improve seeding efficiency of biomaterials by increasing the cell load of a scaffold. This results in accelerated osteogenic tissue formation and could contribute to earlier implant stability in mandibular bone augmentation.

Key words: osteogenic tissue engineering, cellular aggregates, spheroids, 3D cell culture

Background

The already high number of patients that need therapy for the treatment of critical-size bone defects will further increase in the future due to the rising age of the population. Scaffold materials that are used to bridge defects need t o be combined with osteogenic cells to guarantee successful healing of the defect. Bone defects after trauma, infection, tumor resection and osteoporosis, as well as defects of the cranio- and maxillofacial skeletal system caused by tooth loss and a ge-related atrophy of the jaw, are major clinical problems. Frequently, conventional methods for bone tissue regeneration, such as transplantation of autologous bone grafts, are not possible due to restricted availability of the bone or significant morbidity of the donor site [*1*]. Furthermore, there are significant disadvantages of alternative bone-filling materials, including infection and insufficient osseointegration. As an

alternative, tissue engineering-based bone reconstruction therapies promise new therapeutic opportunities [*2*]. With the combination of scaffolds and growth factors, cellular customized tissue-engineered bone grafts (TEBG) could be grown *in vitro* and implanted [*3*]. For a detailed review about bone regeneration by stem cell and tissue engineering in general please refer to the review of Z. Y. Zhang et al. [*4*] and for a review especially of the oral and maxillofacial region please refer to the work of Z. Zhang [*5*]. Besides the significant progress in the field of bone tissue engineering and the already high potential of stem cell-based bone tissue engineering applications [*4*], findings about the importance of cell-cell and cell-matrix contacts in three–dimensional (3D) cell cultures [*6*] have highlighted potentialities to further improve osteogenic tissue engineering. As a result, several 3D culture systems for multipotent stem cells and osteoblastic cells have been developed, which have led to the discovery of improved osteoblast differentiation in 3D- compared to 2D-cultures [*7-12*]. As a consequence, massive research has been performed to combine 3D-culture technologies with osteogenic tissue engineering. In the literature, these cell aggregates are referred to as cellular spheroids, micromasses, microspheres or microtissues, the last being used in this review.

Methods for the production of microtissues and their advantages in different applications

Microtissue technology for osteogenic tissue engineering emerged from three different research fields, all dealing with cell agglomerates of different kinds of cells. For almost 20 years, the potential of multicellular spheroids as a 3D *in vitro* culture system, has been used to study tumor biology. According to Kunz-Schughart et al., [*13*] “the growth of tumor cells as three-dimensional multicellular spheroids in vitro has led to important insights in tumor biology, since properties of the *in vivo* tumor such as proliferation or nutrient gradients can be studied under controlled conditions.” Another research field dealing with microtissues or agglomerated cells is cartilage engineering. Chondrocytes are propagated in cell culture and are re-aggregated into microtissues [*14*]. This results in the formation of cartilage-like tissues by the addition of chondrogenic factors. Moreover, the chondrogenic differentiation of multipotent stem cells, like mesenchymal stem cells from human cord blood, is routinely performed by their agglomeration and the addition of chondrogenic factors [*15*]. The third research field dealing with cellular microtissues is developmental biology, where embryoid bodies (EB) are formed from embryonic stem cells (ESC). All three methods provided deep insight into the complexity but also into the potential of 3D cell cultures for bone tissue engineering. Spheroid culture in tumor biology provided knowledge about borders that are set to the technique by limited diffusion of nutrients and gases. Agglomerates in cartilage engineering demonstrated the potential of microtissues in the directed differentiation of tissue progenitors and multipotent stem cells. At last, microtissues in developmental biology provided evidence that pluripotent stem cells differentiate spontaneously into cells of different germ layer, just because of their culture in spheroids.

Several methods have been developed for the production of 3D tissues. In cartilage engineering multipotent stem cells, for example from adipose tissue or bone marrow, and cartilage-derived chondrocytes have been agglomerated by the addition of defined cell numbers to centrifuge tubes and centrifugation for a few minutes (Fig 1A) [16, 17]. With this method, a pellet is generated that can be transferred into culture vessels,

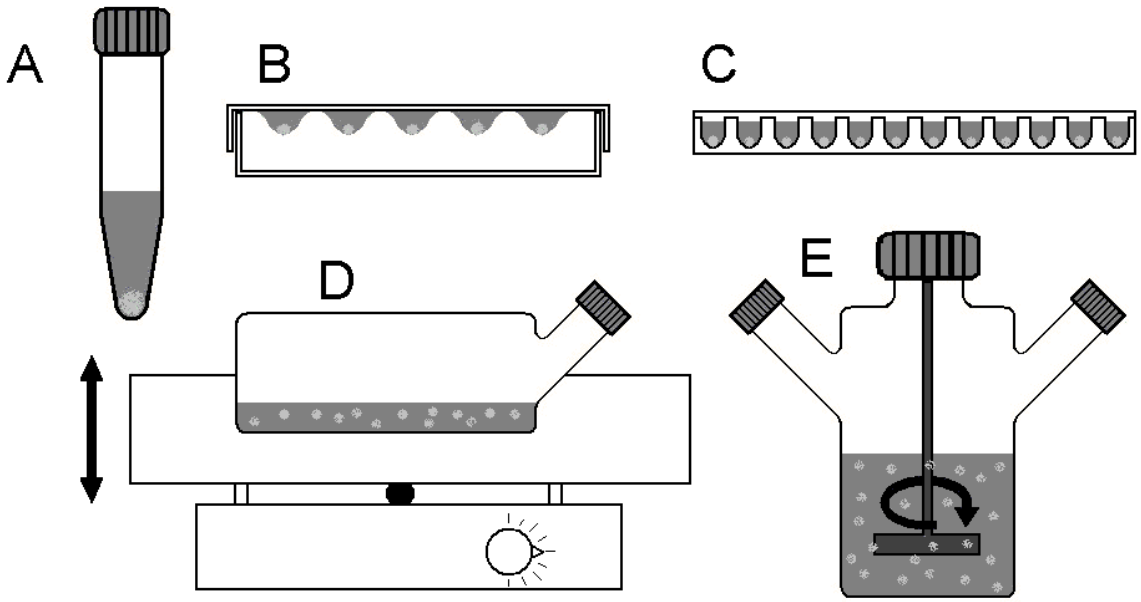

Figure 1: Techniques for the production of microtissues. Generation of:large microtissues by centrifugation in tubes (A), small microtissues and e mbryoid bodies for example from single cell clones in hanging drops (B), microtissues in variable but defined sizes on non-adherent conical culture plates (C) microtissues with random sizes in gyratory shakers (D) and spinner flask (E).

which provide a better medium supply than the centrifuge tube. Embryoid body formation for the differentiation of ESC can be achieved by using non-adherent plane culture surfaces or the hanging drop method (Fig 1B) [*18-20*]. Both methods are suitable for generating EB by the attachment of single cells to each other. However, only the hanging drop method allows the generation of EBs from single cell clones. A cell suspension is diluted until only one c ell per drop of medium is left, that is then placed on the surface of a culture plate that is then turned upside down. The surface tension of the medium holds the drop in position and the cell or the EB floats in the medium. On the contrary, on non-adherent plane culture surfaces EBs may consist of single cell clones or EBs that have attached to one another. In the study of tumor biology, microtissues have been produced via spinner flasks (Fig 1E) or gyratory shakers (Fig 1D). The constant stirring of the medium in the flask and the flow in the vessel on a gyratory shaker prevents tumor cell lines, e.g., from hepatoma, from attaching to surfaces [*21, 13*]. The agglomeration of cells on non-adherent concave or conical culture surfaces either uses available commercial non-adherent 96-well plates or are produced by preparation of 96-well plates with agarose medium (Fig 1C) [*22-24, 7, 25*]. The agarose medium technique uses the capillary action of the liquid, which creates a c oncave surface when it becomes solid. According to Hildebrandt and c olleagues [*24*], the most effective and convenient technique for generating microtissues from human bone marrow, compared to the rotation culture and hanging drop technique, is the cultivation of cell suspensions in non-adherent 96-well plates. Non-adherent 96-well plates offered best spheroid formation efficiencies and t he size was best controllable in dependency of the cell numbers seeded per well. For further information on the advantages and disadvantages of different spheroid culture techniques, including aggregate formation efficiency, homogeneity of the aggregates and their viability please refer to the work of Hildebrandt and colleagues [*24*].

Different cell-cell and cell-extracellular-matrix contacts in monolayer cultures and 3D cultures lead to diverse cellular behavior

As already described by Handschel and colleagues in their review of micromass technology in 2007 [*26*], the basic principle and the advantages of multicellular spheres is the contact of cells between one another and to the extracellular matrix (ECM). In contrast to monolayer cultures where cells are only connected to neighboring cells in two dimensions, a 3D interaction between cells is present in microtissues. This results in differences between localizations as well as the numbers of cell-to-cell contacts, resulting in altered cellular responsiveness and gene transcription profiles [*6*]. Cukierman et al. provided evidence that even terminal differentiated cells like fibroblasts have higher proliferation rates than cells in monolayer cultures [*27*]. Moreover, cells are able to change their shape and behavior upon specific cell signals only when they are cultured in 3D, as demonstrated by Weaver et al for human breast cancer cells [*28*]. Compared to monolayer cultures the gene expression profile of liver cells in 3D is much closer to the expression of cells *in vivo* [*29*]. In a review of Zhang et al. [*5*], the importance of the ECM in the development of scaffold materials was highlighted. By referring to the work of Stevens and George [*30*], they explained that “an ideal scaffold for bone regeneration should be designed based on the constituents and micro- and macrostructure of the native ECM”.

According to Kelm and Fussenegger [*31*], advances in microtissue production have highlighted the potential of scaffold-free cell aggregates in maintaining tissue-specific functionality, supporting seamless integration of implants into host tissues. In microtissues cells are connected to ECM proteins in all dimensions, whereas in 2D cultures, the cells only have contact with ECM-proteins that are deposited between the culture vessel and themselves. The ECM consists of proteins such as collagens, elastin and laminin and has several functions in tissues and organs. Among tissue-specific mechanical properties and the transduction of mechanical forces, the ECM influences cellular functions while being simultaneously influenced by the cells [*6*]. ECM proteins exert their function on cells by interacting with integrins on the cell surface. These receptors specifically bind to motifs located on ECM proteins, i.e. the amino acid sequence RGD of fibronectin [*32*] and the sequence GFOGER of many collagens [*33-35*]. Upon binding of cellular integrins, a signaling feedback pathway initiates integrin receptor clustering at the plasma membrane and focal adhesion-associated protein recruitment in osteoblasts [*35, 36*]. Biggs and Dalby discussed that, focal adhesions emerge as diverse protein networks that provide structural integrity and dynamically link the ECM to the intracellular actin cytoskeleton, directly facilitating cell migration and spreading through continuous regulation and dynamic reinforcement [*35*].

Growth factors and culture supplements that induce or facilitate osteogenic differentiation

The most frequently used method for the osteogenic differentiation of stem cells is incubation with a combination of dexamethasone, ascorbic acid and β-glycerophosphate (DAG). It seems that dexamethasone induces osteogenic differentiation by upregulating the beta catenin-like molecule TAZ (transcriptional co-activator with PDZ-binding motif), which interacts with the master osteogenic transcription factor Runx2 [*37-39*]. Moreover, dexamethasone modulates Runx2 activity by upregulating the mitogen-activated protein kinase (MAPK) phosphatase (MKP-1), which leads to the de-phosphorylation of a specific

serine of Runx2 and enhanced Runx2 trans-activation [*40*]. Ascorbic acid contributes to osteogenic differentiation through its role as a co-factor in the hydroxylation of pro-collagen, which then forms collagen that is secreted into the ECM. Collagen is a major protein of the bone matrix [*41*] and promotes osteogenic differentiation of stem cells [*42, 43*]. The phosphate of β-glycerophosphate has two important functions in osteogenesis. First, it is incorporated into the bone mineral hydroxylapatite (HA), $Ca_{10}(PO_4)_6(OH)_2$, and second, it phosphorylates extracellular signal related kinase (ERK) which leads to the expression of many osteogenic genes [*44, 45*].

In addition to the classical stimulation with DAG, combinations of several growth factors with each other or with DAG have been shown to facilitate osteogenic differentiation *in vitro* and *in vivo*. Factors that have a positive effect on osteogenic differentiation include vitamin D3 (vitD3), bone morphogenetic proteins (BMPs) and cyclic AMP (cAMP). BMPs induce osteogenic differentiation via binding to their cell surface receptor, resulting in the phosphorylation and complexation of several SMAD molecules, which then trans-locate into the nucleus where they induce gene expression and activate Runx2 [*39, 46*]. Furthermore, BMPs utilize other signaling cascades such as the MAPK cascades and the phosphatidyl-inositol 3-kinase (PI3K) pathway [*47*]. Fibroblast growth factor (FGF) is a potent factor for the enhancement of osteogenic differentiation. It acts via inactivation of IGF1 and TGF-beta signaling, resulting in enhanced differentiation of mesenchymal stem cells (MSCs), and by an activating phosphorylation of Runx2 after ERK1/2 phosphorylation [*48*]. Vitamin D3 acts via binding to its vitD3-responsive element (VDRE) in osteogenic genes such as osteocalcin [*49*]. cAMP induces osteogenic differentiation by binding to the cAMP response element-binding protein (CREP) which then promotes the expression of the BMP target genes ID-2 and ID-4, resulting in an autonomous stimulation of osteogenesis and a paracrine signaling of BMP2 [*50*].

Enhanced osteogenic differentiation of microtissues compared to monolayers and probable reasons for this difference

Compared to monolayer cultures, there is an accelerated osteogenic differentiation of cells in microtissues. Whereas mineralized bone nodule formation is first detected after one week [*51, 52*] to two weeks [*53*] in monolayer cultures, bone nodules are already present after 3 days in spheroid cultures (Fig. 2c) [*54, 23, 11, 55*]. Prior to the formation of bone nodules (see arrows in Fig 2), multipotent stem cells or osteoblast precursors undergo a complex differentiation process, in which the cells change their architecture from a fibroblastoid to a cuboidal shape and start to produce a bone-like ECM. The bone ECM is mainly composed of collagen type I and several bone-specific proteins, which are a prerequisite for the initiation of mineralization. Specific bone matrix proteins like osteopontin are primary nucleators for the mineralization [*56*]. Thus, one probable reason for the accelerated mineralization is the enhanced secretion of bone-specific ECM.

Wang and colleagues provided insight into the molecular regulation processes of commercial MSCs (Cambrex, USA) during osteogenesis in spheroids [*57*]. They demonstrated that markers maintaining the stemcellness were downregulated and that the osteogenic transcription factor Runx2 was upregulated in spherical microtissues [*57*]. From these findings, they concluded that it was probable that 3D microtissue cultures affected the cell condition, which became sensitive to switching into another cell lineage, resulting in increased osteogenic differentiation. Even more interesting than the enhanced osteogenic

differentiation of microtissues in osteogenic medium is the spontaneous differentiation of microtissues from human unrestricted somatic stem cells (USSC) of cord blood [*54*]. It was demonstrated that the first mineral nodules were present after 5 days in microtissues in normal growth medium [*54*] (Fig 2b1). Lammers and c olleagues compared the mineralization in microtissues from USSC that were incubated in osteogenic medium with microtissues incubated in standard growth medium with histological staining, scanning electron microscopy (SEM), quantitative wavelength-dispersive X-ray spectroscopy (WDX), transmission electron microscopy (TEM), selected area electron diffraction (SAED) and Raman spectroscopy [*55*]. Analysis of the samples with WDX enables for the detection of the element composition of a sample. This analysis showed that mineral nodules of DAG microtissues and control microtissues mainly consisted of calcium phosphate and oxygen. Moreover, the calculated calcium phosphate ratios for both groups were slightly lower (Ca/P: 1.52 – 1.62) than that of HA (Ca/P: 1.67). One explanation that was provided was the substitution of Ca by magnesium (Mg) in the mineral. Furthermore, a substitution of PO_4^{3-} by HPO_4^{2-} in the crystal structure of the

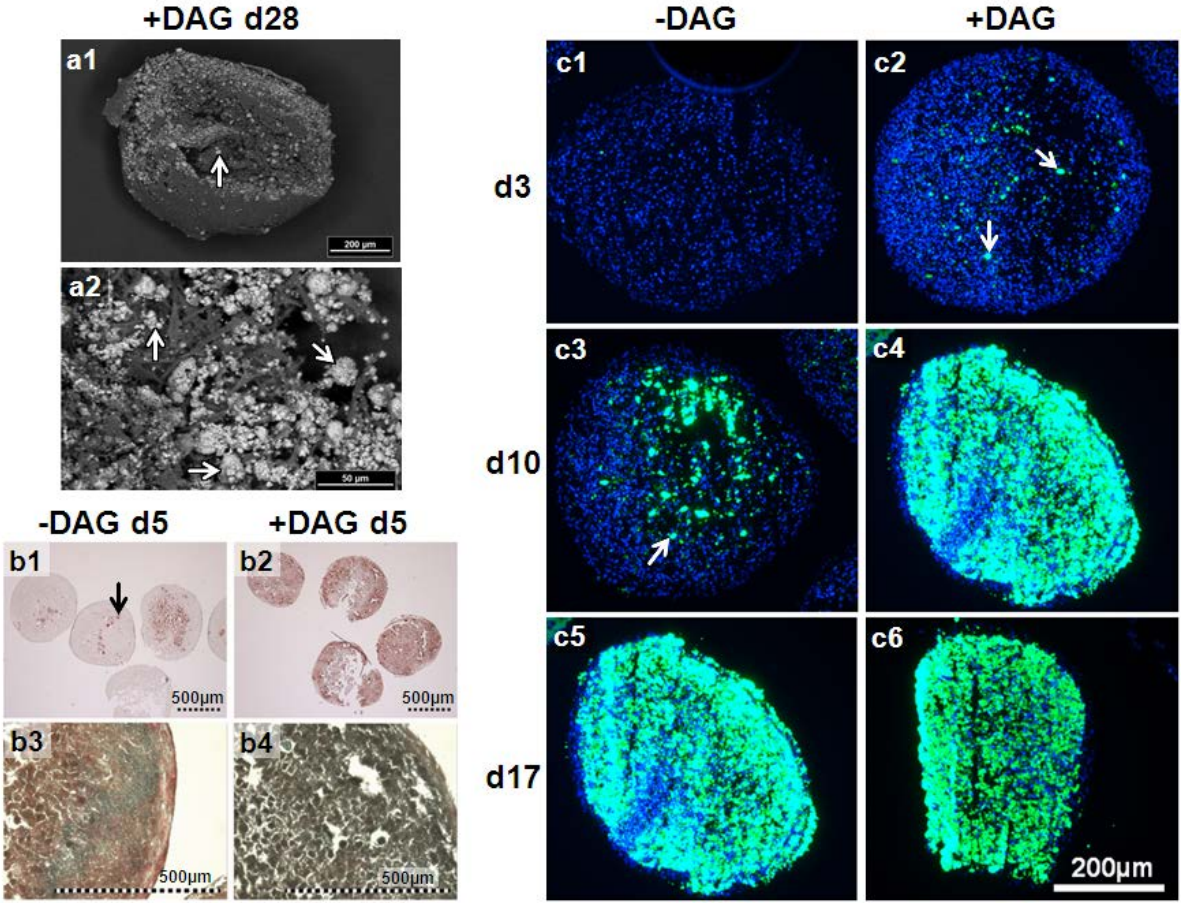

Figure 2: Mineralization of microtissues. (a1) Scanning electron microscopic image of a microtissue cross-section. (b1) Bone nodules can be det ected between the cells of the microtissue (white arrows). Alizarin red S staining (b1-b2) and Masson Goldner staining (b3-b4) of USSC microspheres, incubated withor without DAGfor 5 days. Calcium is stained dark red (b1-b2); extracellular matrix is green and cytoplasm is red (b3-b4). Figure b1-b4 is a modification of Fig 2 o f Langenbach et al.(http://online.liebertpub.com/doi/abs/10.1089/ten.TEA.2009.0131?url_ver=Z39.88-2003&rfr_id=ori:rid:crossref.org&rfr_dat=cr_pub%3dpubmed) [*54*]. OsteoImage staining of microtissues with or without DAG after 3, 10 and 17 days. White arrows in DAG microtissues after three days (c2) indicate early mineralization.

mineral would result in a positive charge of the molecule which would be compensated by leaving out a Ca ion. Indications for such a substitution, which results in a so-called calcium deficient HA, were provided by Raman spectroscopy. In Raman spectroscopy, the oscillation of the P-O-binding of the PO_4^{3-} group of calcium phosphate results in a characteristic peak at 960 cm^{-1}. Shoulders and broadening of this peak indicated phosphate groups in which the length of the P-O-bonding was affected, such as HPO_4^{2-}, which provided further explanations for the low Ca/P ratio. From further analysis of the crystal growth pattern with TEM, Lammers et al identified the mineral composition of the samples. They found that the minerals in both groups had similarities with native bone; however, there were differences in the composition of the diverse calcium-phosphate(Ca/P) minerals in the two groups. It was concluded that the mineral of the control group mainly consisted of calcium-deficient-HA (CDHA) with an amorphous mineral fraction (ACP), while the mineral formed in the osteogenic medium group mainly consisted of ACP, octa-calciumphosphate, magnesium-whitlockite, CDHA and HA. Even though HA is the predominant mineral in bone, several other forms of apatitic minerals are present. As early as in 1987, Legros et al. [*58*] demonstrated that the mineral of bone samples, regardless of species (rat or bovine) or age, was found to be a calcium-deficient apatite containing both CO_3^{2-} and $HPCO_4^{2-}$ ions in the crystal lattice. Furthermore, they showed that the Ca/P ratio increased with age from 1.51 in newborn rats, which was the same ratio as that in microtissues of Lammers et al. [*55*], to 1.69 in adults.

Currently, there is no literature about the precise mechanisms that drive this enhanced and spontaneous differentiation. However, there is some evidence showing that contact with ECM proteins plays an essential role. Integrins transduce extracellular signals via a molecule called focal adhesion kinase (FAK), a protein that is constitutively associated with the β-integrin subunit [*59*]. FAK itself functions as an initiator of multiple signaling cascades. After the activating phosphorylation of FAK, signaling cascades are initiated that regulate the synthesis of osteospecific proteins. How important these mechanisms of ECM-protein induced and integrin→FAK-mediated signaling are in the osteogenic differentiation of stem cells and in osteoblasts was explained by Xiao and colleagues: "(1) Osteoblasts must be in contact with a collagen-containing ECM before they can differentiate. (2) Osteoblasts bind to this ECM via interactions between Col1 and α2β1 integrins. (3) Integrin ligand binding activates MAPK and related pathways that transduce signals to the nucleus. (4) Runx2 is phosphorylated and activated by MAPK, thereby allowing it to stimulate osteoblast differentiation by increasing transcription of osteoblast marker genes such as OCN" [*42, 60*]. A large body of evidence for this theory has been provided by experiments, which have demonstrated that blocking of α2β1 integrins as well as treating cell cultures with collagenase suppresses osteogenic differentiation [*61, 62*]. The other way round, the contact of human MSCs with compartments of the ECM (vitronectin and Col1) is sufficient to induce osteogenic differentiation [*43, 51*] and the expression of osteogenic transcription factors like osteonectin [*63*]. Moreover, this upregulation is correlated with an increase in the expression of collagen type I. It is suggested that contact with the ECM secreted by the cells themselves lead to the above mentioned integrin→FAK-mediated activation of osteogenic transcription factors.

Another inducer of osteogenic differentiation processes may be the high cell density inside the microtissues. It is well known that osteogenic differentiation *in vitro* requires

high cell densities and that osteogenic differentiation is restricted during cell proliferation [*64*]. This is supported by the findings of Bitar et al., who demonstrated that the expression of the osteogenic transcription factor Runx2 was upregulated as a consequence of higher cell densities [*65*]. Moreover, Jähn et al. showed that the transformation of the osteoblast phenotype *in vitro* into a more mature stage could be achieved more rapidly in 3D culture and that dense monolayers elicited more mature osteoblasts than low-density seeded monolayers, while hOB cells in pellets seemed to have transformed even further along the osteoblast lineage [*66*].

Recently, Kabiri et al. [*67*] found that autocrine BMP signaling may be responsible for increased osteogenic differentiation of cellular aggregates. They found an approximately 30-fold upregulation in BMP2 expression after one week of culture. This increase was not accompanied by increased upregulation of osteonectin, osteopontin, ALP, Runx2 and Collagen type I on the same day, but led to an increase in these factors after 14 days of culture when BMP-2 levels had already returned to basal expression levels. Interestingly, the increase in BMP2 expression was not dependent on the osteogenic medium, it also increased 25-fold in control medium compared to 2D cell cultures. These findings provide further evidence that osteogenic differentiation of stem cells is initiated by the contact of cells with one another and to the ECM that surrounds the cells. Phimphilai et al. found that autocrine BMP2 production is necessary for the function of Runx2 and that Runx2 and BMP2 cooperatively interact to stimulate osteoblast gene expression [*68*]. It has been demonstrated earlier that murine pre-osteoblast cell lines and marrow stromal cells produce basal levels of BMPs that are essential for osteogenic differentiation [*69*]. Bone marrow aspirates contain an inherent osteogenic cell population, called skeletal stem cells (SSC), that is, with exception to some neo- and prenatal cells (e.g. from cord blood) the only cell type that is able to form bone including a hematopoietic microenvironment [*70-72*]. As SSCs, and presumably also USSC are inherently osteogenic, 3D culture is probably enough to initiate osteogenic differentiation. In this process, the activating phosphorylation of Runx2 by ERK after interaction of the cell with collagens, cell-cell contacts and growth factors in the extracellular space, are sufficient triggers for the differentiation.

Apoptosis of osteoblasts in vivo is an important factor to control the number of osteoblasts that are involved in new bone formation inside bone remodeling units. In this process, some osteoblasts are entombed within the matrix as osteocytes but the majority die by apoptosis [*73*]. Currently, there are controversial results of whether stem cells undergo apoptosis in microtissues that are incubated under standard medium conditions. Kelm and colleagues [*74*] demonstrated massive apoptotic processes inside microtissues of mouse, rat and human MSCs by TUNEL assays and immunohistochemical detection of caspases. Furthermore, Hildebrandt and colleagues [*24*] found reduced viability per diameter in control microtissues. By contrast, Lammers and colleagues found no apoptosis, but spontaneous osteogenic differentiation of USSCs [*55*]. Whether these differences are caused by different cell lines or standard culture conditions remain unclear. Whereas Lammers and colleagues used a very high concentration of fetal calve serum (FCS), i.e. 30%, Kelm only used 10% FCS [*74*]. Interestingly, apoptosis was suppressed in cultures of Kelm and colleagues that were exposed to osteogenic medium. This is again supported by Hildebrandt and colleagues [*24*], who demonstrated relatively constant viability per diameter in treated osteogenic microtissues. Thus, it is probable that there is a strong

correlation between the suppression of apoptosis and osteogenic differentiation. Kelm hypothesized that in an environment lacking the appropriate biological cues for maintaining their undifferentiated state, MSCs have to differentiate for sustained survival or otherwise undergo apoptosis [*74*]. This can be regarded as a "biological safety switch" to prevent adverse effects of MSCs in ectopic organs. From this point of view, it is probable that USSCs, which have a higher multipotent plasticity compared to MSCs from bone marrow, are able to compete with cues provided in microtissues by differentiating into the osteogenic lineage.

Current and probable applications for microtissues in osteogenic tissue engineering

Recently, Altmann et al. concluded that the 3D culture of osteoblasts or MSCs, which are both known to require 3D microenvironments for proper adhesion, growth, aggregation and/or tissue-specific differentiation, provides a promising tool for *in vitro* pre-conditioning into a mature osteoblast phenotype for applications in bone augmentation and hard tissue regeneration [*75*].

In previous works we and others have demonstrated that microtissues of osteoblasts or USSCs can be osteogenic differentiated while maintaining the ability to let cells divide and migrate to the surrounding tissue [*76, 54*]. This characteristic is extremely important when microtissues are implanted *in vivo*, in case of gaps that need to be colonized by osteogenic cells. It was found that the optimal differentiation time for microtissues is three to five days in order to maintain outgrowth capability. The cells that migrate out of the microtissues probably derive from the cells of the surface of the microtissues, which migrate and divide. In another study, these results were transferred to a model for the enhanced inoculation and osteogenic differentiation of scaffolds [*25*]. It was shown that microtissues of USSCs could be implanted into insoluble collagenous bone matrix scaffolds (ICBM) where they mineralized after a short time and allowed cells to migrate to the surrounding scaffold material. In this process, they partially filled spaces between the microtissues and the scaffold material, as well as spaces between adjacent trabeculae of the spongiosa. Compared to inoculation with cell suspensions a 40-fold higher cell load on a single ICBM is feasible [*25*].

According to Ferrera et al., subcutaneous implantation in nude mice led to a high rate of success in progression throughout differentiation of implants (12 of 12), independent of donor age and gender (25 to 73 years of age). This offers the possibility of implanting structures at different and controlled stages of osteogenic progression [*76*]. Furthermore, microtissues allow the precise administration of large numbers of cells into a specific area and have the advantage of strong rigidity that prevents dissociation of the cells inside the tissue [*23*]. Kelm and Fussenegger stated that microtissues are not as susceptible to wash-out as single cells due to their larger size, and are significantly more adhesive than monolayer cultures or single cells because of increased ECM production [*77, 78*]. This characteristic is of particular importance in approaches that combine implant materials with stem cells that have not been pre-incubated with a scaffold. Multicellular complexes that reside at the implantation site could improve the stability of the implant-to-tissue contact, in contrast to single cells that are applied as suspensions. Moreover, there is a potential use of microtissues combined with membranes in the healing of periodontal defects. According to Berahim and colleagues, a periodontal defect could be filled by migrating cells that derive from the division of cells in microtissues that were

previously seeded on membranes [*79*]. The washing away of the spheres and the cells by crevicular fluid could be prevented combining of membrane-facilitated guided tissue regeneration with microtissues. Finally, the suitability of microtissues for osteogenic tissue engineering was demonstrated in a previous work from our group. ICBM scaffolds implanted with microtissues were shown to mediate ectopic bone formation upon implantation in rat muscle bags, whereas scaffolds implanted without cells did not lead to bone formation [*22*].

To conclude, microtissue technology provides better *in vivo*-like conditions for stem cells and osteoblasts than monolayer cultures, accompanied by improved osteogenic differentiation. Microtissue technology can improve seeding efficiency of biomaterials by increasing the cell load of a scaffold and are less prone to wash out than single cells. This results in accelerated osteogenic tissue formation and therefore could contribute to earlier implant stability in mandibular bone augmentation. Moreover, microspheres hold promise for facilitated, accelerated and improved generation of tissue-engineered bone and stem cells to support the healing of periodontal defects.

Conflict of Interests:

The authors declare that they have no conflict of interest.

Acknowledgements

This review was supported in part by the Deutsche Forschungsgemeinschaft (DFG) grant HA 3228/3-1

References

1. Sasso RC, LeHuec JC, Shaffrey C (2005) Iliac crest bone graft donor site pain after anterior lumbar interbody fusion: a prospective patient satisfaction outcome assessment. J Spinal Disord Tech 18 Suppl:S77-81

2. Meyer U, Wiesmann HP, Berr K, Kubler NR, Handschel J (2006) Cell-based bone reconstruction therapies-principles of clinical approaches. Int J Oral Maxillofac Implants 21 (6):899-906

3. Petite H, Vandamme K, Monfoulet L, Logeart-Avramoglou D (2011) Strategies for improving the efficacy of bioengineered bone constructs: a perspective. Osteoporos Int 22 (6):2017-2021

4. Zhang ZY, Teoh SH, Hui JH, Fisk NM, Choolani M, Chan JK (2012) The potential of human fetal mesenchymal stem cells for off-the-shelf bone tissue engineering application. Biomaterials 33 (9):2656-2672

5. Zhang Z (2011) Bone regeneration by stem cell and tissue engineering in oral and maxillofacial region. Front Med 5 (4):401-413

6. Abbott A (2003) Cell culture: biology's new dimension. Nature 424 (6951):870-872

7. Burns JS, Rasmussen PL, Larsen KH, Schroder HD, Kassem M (2010) Parameters in three-dimensional osteospheroids of telomerized human mesenchymal (stromal) stem cells grown on osteoconductive scaffolds that predict in vivo bone-forming potential. Tissue engineering Part A 16 (7):2331-2342

8. Muraglia A, Corsi A, Riminucci M, Mastrogiacomo M, Cancedda R, Bianco P, Quarto R (2003) Formation of a chondro-osseous rudiment in micromass cultures of human bone-marrow stromal cells. J Cell Sci 116 (Pt 14):2949-2955

9. Trojani C, Weiss P, Michiels JF, Vinatier C, Guicheux J, Daculsi G, Gaudray P, Carle GF, Rochet N (2005) Three-dimensional culture and differentiation of human osteogenic cells in an injectable hydroxypropylmethylcellulose hydrogel. Biomaterials 26 (27):5509-5517

10. Boehrs J, Zaharias RS, Laffoon J, Ko YJ, Schneider GB (2008) Three-dimensional culture environments enhance osteoblast differentiation. J Prosthodont 17 (7):517-521

11. Kale S, Biermann S, Edwards C, Tarnowski C, Morris M, Long MW (2000) Three-dimensional cellular development is essential for ex vivo formation of human bone. Nat Biotechnol 18 (9):954-958

12. Tortelli F, Cancedda R (2009) Three-dimensional cultures of osteogenic and chondrogenic cells: a tissue engineering approach to mimic bone and cartilage in vitro. Eur Cell Mater 17:1-14

13. Kunz-Schughart LA, Kreutz M, Knuechel R (1998) Multicellular spheroids: a three-dimensional in vitro culture system to study tumour biology. Int J Exp Pathol 79 (1):1-23

14. Meyer U, Wiesmann HP, Libera J, Depprich R, Naujoks C, Handschel J (2012) Cartilage defect regeneration by ex vivo engineered autologous microtissue - preliminary results. In Vivo 26 (2):251-257

15. Arufe MC, De la Fuente A, Mateos J, Fuentes I, De Toro FJ, Blanco FJ (2011) Analysis of the chondrogenic potential and secretome of mesenchymal stem cells derived from human umbilical cord stroma. Stem Cells Dev 20 (7):1199-1212

16. Estes BT, Diekman BO, Gimble JM, Guilak F (2010) Isolation of adipose-derived stem cells and their induction to a chondrogenic phenotype. Nat Protoc 5 (7):1294-1311

17. Kafienah W, Al-Fayez F, Hollander AP, Barker MD (2003) Inhibition of cartilage degradation: a combined tissue engineering and gene therapy approach. Arthritis Rheum 48 (3):709-718

18. Keller GM (1995) In vitro differentiation of embryonic stem cells. Curr Opin Cell Biol 7 (6):862-869

19. Potter SW, Morris JE (1985) Development of mouse embryos in hanging drop culture. Anat Rec 211 (1):48-56

20. Wobus AM, Wolf E, Beier HM (2000) Embryonic stem cells and nuclear transfer strategies. Present state and future prospects. Cells Tissues Organs 166 (1):1-5

21. Kelm JM, Timmins NE, Brown CJ, Fussenegger M, Nielsen LK (2003) Method for generation of homogeneous multicellular tumor spheroids applicable to a wide variety of cell types. Biotechnol Bioeng 83 (2):173-180

22. Handschel J, Naujoks C, Langenbach F, Berr K, Depprich RA, Ommerborn MA, Kubler NR, Brinkmann M, Kogler G, Meyer U (2010) Comparison of ectopic bone formation of embryonic stem cells and cord blood stem cells in vivo. Tissue Eng Part A 16 (8):2475-2483

23. Langenbach F, Berr K, Naujoks C, Hassel A, Hentschel M, Depprich R, Kubler NR, Meyer U, Wiesmann H-P, Kogler G, Handschel J (2011) Generation and differentiation of microtissues from multipotent precursor cells for use in tissue engineering. Nat Protocols 6 (11):1726-1735

24. Hildebrandt C, Buth H, Thielecke H (2011) A scaffold-free in vitro model for osteogenesis of human mesenchymal stem cells. Tissue Cell 43 (2):91-100

25. Langenbach F, Naujoks C, Laser A, Kelz M, Kersten-Thiele P, Berr K, Depprich R, Kubler N, Kogler G, Handschel J (2012) Improvement of the cell-loading efficiency of biomaterials by inoculation with stem cell-based microspheres, in osteogenesis. J Biomater Appl 26 (5):549-564

26. Handschel JG, Depprich RA, Kubler NR, Wiesmann HP, Ommerborn M, Meyer U (2007) Prospects of micromass culture technology in tissue engineering. Head Face Med 3:4

27. Cukierman E, Pankov R, Stevens DR, Yamada KM (2001) Taking cell-matrix adhesions to the third dimension. Science 294 (5547):1708-1712

28. Weaver VM, Petersen OW, Wang F, Larabell CA, Briand P, Damsky C, Bissell MJ (1997) Reversion of the malignant phenotype of human breast cells in three-dimensional culture and in vivo by integrin blocking antibodies. J Cell Biol 137 (1):231-245

29. Sivaraman A, Leach JK, Townsend S, Iida T, Hogan BJ, Stolz DB, Fry R, Samson LD, Tannenbaum SR, Griffith LG (2005) A microscale in vitro physiological model of the liver: predictive screens for drug metabolism and enzyme induction. Curr Drug Metab 6 (6):569-591

30. Stevens MM, George JH (2005) Exploring and engineering the cell surface interface. Science 310 (5751):1135-1138

31. Kelm JM, Fussenegger M (2004) Microscale tissue engineering using gravity-enforced cell assembly. Trends Biotechnol 22 (4):195-202

32. Garcia AJ (2005) Get a grip: integrins in cell-biomaterial interactions. Biomaterials 26 (36):7525-7529

33. Heino J, Huhtala M, Kapyla J, Johnson MS (2009) Evolution of collagen-based adhesion systems. Int J Biochem Cell Biol 41 (2):341-348

34. Barczyk M, Carracedo S, Gullberg D (2010) Integrins. Cell Tissue Res 339 (1):269-280

35. Biggs MJ, Dalby MJ (2010) Focal adhesions in osteoneogenesis. Proc Inst Mech Eng H 224 (12):1441-1453

36. Lim JY, Dreiss AD, Zhou Z, Hansen JC, Siedlecki CA, Hengstebeck RW, Cheng J, Winograd N, Donahue HJ (2007) The regulation of integrin-mediated osteoblast focal adhesion and focal adhesion kinase expression by nanoscale topography. Biomaterials 28 (10):1787-1797

37. Gaur T, Lengner CJ, Hovhannisyan H, Bhat RA, Bodine PV, Komm BS, Javed A, van Wijnen AJ, Stein JL, Stein GS, Lian JB (2005) Canonical WNT signaling promotes osteogenesis by directly stimulating Runx2 gene expression. J Biol Chem 280 (39):33132-33140

38. Hong JH, Hwang ES, McManus MT, Amsterdam A, Tian Y, Kalmukova R, Mueller E, Benjamin T, Spiegelman BM, Sharp PA, Hopkins N, Yaffe MB (2005) TAZ, a transcriptional modulator of mesenchymal stem cell differentiation. Science 309 (5737):1074-1078

39. Hong D, Chen HX, Xue Y, Li DM, Wan XC, Ge R, Li JC (2009) Osteoblastogenic effects of dexamethasone through upregulation of TAZ expression in rat mesenchymal stem cells. J Steroid Biochem Mol Biol 116 (1-2):86-92

40. Phillips JE, Gersbach CA, Wojtowicz AM, Garcia AJ (2006) Glucocorticoid-induced osteogenesis is negatively regulated by Runx2/Cbfa1 serine phosphorylation. J Cell Sci 119 (Pt 3):581-591

41. Franceschi RT, Iyer BS (1992) Relationship between collagen synthesis and ex pression of the osteoblast phenotype in MC3T3-E1 cells. J Bone Miner Res 7 (2):235-246

42. Xiao G, Gopalakrishnan R, Jiang D, Reith E, Benson MD, Franceschi RT (2002) Bone morphogenetic proteins, extracellular matrix, and mitogen-activated protein kinase signaling pathways are required for osteoblast-specific gene expression and differentiation in MC3T3-E1 cells. J Bone Miner Res 17 (1):101-110

43. Kundu AK, Khatiwala CB, Putnam AJ (2009) Extracellular matrix remodeling, integrin expression, and downstream signaling pathways influence the osteogenic differentiation of mesenchymal stem cells on poly(lactide-co-glycolide) substrates. Tissue Eng Part A 15 (2):273-283

44. Fatherazi S, Matsa-Dunn D, Foster BL, Rutherford RB, Somerman MJ, Presland RB (2009) Phosphate regulates osteopontin gene transcription. J Dent Res 88 (1):39-44

45. Tada H, Nemoto E, Foster BL, Somerman MJ, Shimauchi H (2011) Phosphate increases bone morphogenetic protein-2 expression through cAMP-dependent protein kinase and ERK1/2 pathways in human dental pulp cells. Bone 48 (6):1409-1416

46. Afzal F, Pratap J, Ito K, Ito Y, Stein JL, van Wijnen AJ, Stein GS, Lian JB, Javed A (2005) Smad function and intranuclear targeting share a Runx2 motif required for osteogenic lineage induction and BMP2 responsive transcription. J Cell Physiol 204 (1):63-72

47. Payne KA, Meszaros LB, Phillippi JA, Huard J (2010) Effect of phosphatidyl inositol 3-kinase, extracellular signal-regulated kinases 1/2, and p38 mitogen-activated protein kinase inhibition on osteogenic differentiation of muscle-derived stem cells. Tissue Eng Part A 16 (12):3647-3655

48. Ito T, Sawada R, Fujiwara Y, Tsuchiya T (2008) FGF-2 increases osteogenic and chondrogenic differentiation potentials of human mesenchymal stem cells by inactivation of TGF-beta signaling. Cytotechnology 56 (1):1-7

49. Maehata Y, Takamizawa S, Ozawa S, Kato Y, Sato S, Kubota E, Hata R (2006) Both direct and collagen-mediated signals are required for active vitamin D3-elicited differentiation of human osteoblastic cells: roles of osterix, an osteoblast-related transcription factor. Matrix Biol 25 (1):47-58

50. Siddappa R, Martens A, Doorn J, Leusink A, Olivo C, Licht R, van Rijn L, Gaspar C, Fodde R, Janssen F, van Blitterswijk C, de Boer J (2008) cAMP/PKA pathway activation in human mesenchymal stem cells in vitro results in robust bone formation in vivo. Proc Natl Acad Sci U S A 105 (20):7281-7286

51. Salasznyk RM, Williams WA, Boskey A, Batorsky A, Plopper GE (2004) Adhesion to Vitronectin and Collagen I Promotes Osteogenic Differentiation of Human Mesenchymal Stem Cells. J Biomed Biotechnol 2004 (1):24-34

52. Levi B, Nelson ER, Brown K, James AW, Xu D, Dunlevie R, Wu JC, Lee M, Wu B, Commons GW, Vistnes D, Longaker MT (2011) Differences in osteogenic differentiation of adipose-derived stromal cells from murine, canine, and human sources in vitro and in vivo. Plast Reconstr Surg 128 (2):373-386

53. Zhang W, Deng ZL, Chen L, Zuo GW, Luo Q, Shi Q, Zhang BQ, Wagner ER, Rastegar F, Kim SH, Jiang W, Shen J, Huang E, Gao Y, Gao JL, Zhou JZ, Luo J, Huang J, Luo X, Bi Y, Su Y, Yang K, Liu H, Luu HH, Haydon RC, He TC, He BC (2010) Retinoic acids potentiate BMP9-induced osteogenic differentiation of mesenchymal progenitor cells. PLoS One 5 (7):e11917

54. Langenbach F, Naujoks C, Kersten-Thiele PV, Berr K, Depprich RA, Kubler NR, Kogler G, Handschel J (2010) Osteogenic differentiation influences stem cell migration out of scaffold-free microspheres. Tissue Eng Part A 16 (2):759-766

55. Lammers L, Naujoks C, Berr K, Depprich R, Kubler N, Meyer U, Langenbach F, Luttenberg B, Kogler G, Wiesmann HP, Handschel J (2012) Impact of DAG stimulation on mineral synthesis, mineral structure and osteogenic differentiation of human cord blood stem cells. Stem Cell Res 8 (2):193-205

56. Nagata T, Bellows CG, Kasugai S, Butler WT, Sodek J (1991) Biosynthesis of bone proteins [SPP-1 (secreted phosphoprotein-1, osteopontin), BSP (bone sialoprotein) and SPARC (osteonectin)] in association with mineralized-tissue formation by fetal-rat calvarial cells in culture. Biochem J 274 (Pt 2):513-520

57. Wang W, Itaka K, Ohba S, Nishiyama N, Chung UI, Yamasaki Y, Kataoka K (2009) 3D spheroid culture system on micropatterned substrates for improved differentiation efficiency of multipotent mesenchymal stem cells. Biomaterials 30 (14):2705-2715

58. Legros R, Balmain N, Bonel G (1987) Age-related changes in mineral of rat and bovine cortical bone. Calcif Tissue Int 41 (3):137-144

59. Leong L, Hughes PE, Schwartz MA, Ginsberg MH, Shattil SJ (1995) Integrin signaling: roles for the cytoplasmic tails of alpha IIb beta 3 in the tyrosine phosphorylation of pp125FAK. J Cell Sci 108 (Pt 12):3817-3825

60. Ducy P, Zhang R, Geoffroy V, Ridall AL, Karsenty G (1997) Osf2/Cbfa1: a transcriptional activator of osteoblast differentiation. Cell 89 (5):747-754

61. Xiao G, Wang D, Benson MD, Karsenty G, Franceschi RT (1998) Role of the alpha2-integrin in osteoblast-specific gene expression and activation of the Osf2 transcription factor. J Biol Chem 273 (49):32988-32994

62. Franceschi RT, Iyer BS, Cui Y (1994) Effects of ascorbic acid on collagen matrix formation and osteoblast differentiation in murine MC3T3-E1 cells. Journal of bone and mineral research : the official journal of the American Society for Bone and Mineral Research 9 (6):843-854

63. Naujoks C, Langenbach F, Berr K, Depprich R, Kubler N, Meyer U, Handschel J, Kogler G (2011) Biocompatibility of osteogenic predifferentiated human cord blood stem cells with biomaterials and the influence of the biomaterial on the process of differentiation. J Biomater Appl 25 (5):497-512

64. Holy CE, Shoichet MS, Davies JE (2000) Engineering three-dimensional bone tissue in vitro using biodegradable scaffolds: investigating initial cell-seeding density and culture period. J Biomed Mater Res 51 (3):376-382

65. Bitar M, Brown RA, Salih V, Kidane AG, Knowles JC, Nazhat SN (2008) Effect of cell density on osteoblastic differentiation and matrix degradation of biomimetic dense collagen scaffolds. Biomacromolecules 9 (1):129-135

66. Jahn K, Richards RG, Archer CW, Stoddart MJ (2010) Pellet culture model for human primary osteoblasts. Eur Cell Mater 20:149-161

67. Kabiri M, Kul B, Lott WB, Futrega K, Ghanavi P, Upton Z, Doran MR (2012) 3D mesenchymal stem/stromal cell osteogenesis and autocrine signalling. Biochem Biophys Res Commun 419 (2):142-147

68. Phimphilai M, Zhao Z, Boules H, Roca H, Franceschi RT (2006) BMP signaling is required for RUNX2-dependent induction of the osteoblast phenotype. J Bone Miner Res 21 (4):637-646

69. Abe E, Yamamoto M, Taguchi Y, Lecka-Czernik B, O'Brien CA, Economides AN, Stahl N, Jilka RL, Manolagas SC (2000) Essential requirement of BMPs-2/4 for both osteoblast and osteoclast formation in murine bone marrow cultures from adult mice: antagonism by noggin. J Bone Miner Res 15 (4):663-673

70. Robey PG (2011) Cell sources for bone regeneration: the good, the bad, and the ugly (but promising). Tissue Eng Part B Rev 17 (6):423-430

71. Sacchetti B, Funari A, Michienzi S, Di Cesare S, Piersanti S, Saggio I, Tagliafico E, Ferrari S, Robey PG, Riminucci M, Bianco P (2007) Self-renewing osteoprogenitors in bone marrow sinusoids can organize a he matopoietic microenvironment. Cell 131 (2):324-336

72. Bianco P, Robey PG, Simmons PJ (2008) Mesenchymal stem cells: revisiting history, concepts, and assays. Cell Stem Cell 2 (4):313-319

73. Jilka RL (2007) Molecular and cellular mechanisms of the anabolic effect of intermittent PTH. Bone 40 (6):1434-1446

74. Kelm JM, Breitbach M, Fischer G, Odermatt B, Agarkova I, Fleischmann BK, Hoerstrup SP (2012) 3D Microtissue Formation of Undifferentiated Bone Marrow Mesenchymal Stem Cells Leads to Elevated Apoptosis. Tissue engineering Part A 18 (7-8):692-702

75. Altmann B, Steinberg T, Giselbrecht S, Gottwald E, Tomakidi P, Bächle-Haas M, Kohal RJ (2011) Promotion of osteoblast differentiation in 3D biomaterial micro-chip arrays comprising fibronectin-coated poly(methyl methacrylate) polycarbonate. Biomaterials 32 (34):8947-8956

76. Ferrera D, Poggi S, Biassoni C, Dickson GR, Astigiano S, Barbieri O, Favre A, Franzi AT, Strangio A, Federici A, Manduca P (2002) Three-dimensional cultures of normal human osteoblasts: proliferation and differentiation potential in vitro and upon ectopic implantation in nude mice. Bone 30 (5):718-725

77. Kelm JM, Lorber V, Snedeker JG, Schmidt D, Broggini-Tenzer A, Weisstanner M, Odermatt B, Mol A, Zund G, Hoerstrup SP (2010) A novel concept for scaffold-free vessel tissue engineering: self-assembly of microtissue building blocks. J Biotechnol 148 (1):46-55

78. Kelm JM, Fussenegger M (2010) Scaffold-free cell delivery for use in regenerative medicine. Adv Drug Deliv Rev 62 (7-8):753-764

79. Berahim Z, Moharamzadeh K, Rawlinson A, Jowett AK (2011) Biologic interaction of three-dimensional periodontal fibroblast spheroids with collagen-based and synthetic membranes. J Periodontol 82 (5):790-797

4 Fazit und Ausblick

Die Kombination aus Mikrogeweben und/oder Zellsuspensionen mit ICBM bietet hervorragende Eigenschaften für das osteogene Tissue Engineering. Die demineralisierte Spongiosa mit anhaftenden osteogen differenzierten USSC bildet bestmöglich eine Entwicklungsstufe der desmalen Ossifikation ab; nämlich Osteoid mit auskleidenden Osteoblasten. Dabei sind die Vorteile von ICBM die hervorragende Biokompatibilität und die spongiöse Struktur. Aufgrund der Flexibilität und geringen Festigkeit der ICBM-Gerüste eignen sich diese besonders für die Regeneration und den Aufbau von formgebenden, nicht Lasten tragenden Knochen. Bei der Verwendung von ICBM in den meisten anderen Fällen, müssen Knochendefekte bis zur vollständigen Mineralisierung geschient werden.

Die Besiedelung von ICBM Gerüsten mit Mikrogeweben anstelle von Zellsuspensionen bildet eine Weiterentwicklung zum klassischen Verfahren der Zell/Biomaterial Kombination. Die Verwendung von Mikrogeweben erlaubt die Kultivierung von Zellen in 3D und dadurch eine bessere Vergleichbarkeit mit *in vivo* Bedingungen, die schnelle osteogene Differenzierung und die Ablagerung von knochentypischem Biomineral wie CDHA, ACP, HA und weiteren Calciumphosphat-Verbindungen. Zudem ermöglicht die Verwendung von Mikrogeweben den Transfer von großen Zellzahlen an genau definierte Orte. Mit der Fähigkeit zur ektopen Knochenbildung *in vivo* bilden ICBM/Mikrogewebe-Konstrukte einen höchst vielversprechenden Ansatz zur Rekonstruktion von großen Knochendefekten.

Die Ergebnisse des Tierversuchs lassen vermuten, dass es weitere Verbesserungsmöglichkeiten für eine noch schnellere ektope Knochenbildung gibt. Gerüste nur Durch das kombinierte Beimpfen mit Mikrogeweben und Zellsuspensionen könnte die Anzahl von Zellen im Gerüst weiter erhöht werden, um eine noch schnellere osteogen Differenzierung zu bewirken. Zudem könnte durch die Verwendung eines Bioreaktors die Kultur *in vitro* verkürzt und optimiert werden. Zusätzlich bestehen verschiedene Möglichkeiten durch Wachstumsfaktoren die Heilung zu verbessern. Zum Beispiel könnte durch die Zugabe von VEGF (vascular endothelial growth factor) das Einwachsen von Blutgefäßen zu beschleunigt und mittels BMP2 und Parathormon die Einheilung des TEKT in den Knochen verbessert werden.

Zur Spezifizierung der Mechanismen hinter der verbesserten und spontanen osteogenen Differenzierung in Mikrogeweben könnten mittels Antikörpern die Interaktion mit der EZM blockiert oder verantwortliche Signalwege (MAPK-, ERK- oder PI3K-Signalweg) mittels Chemikalien inhibiert werden. Neben den Fortschritten in der Materialwissenschaft ist das Wissen über Grundlegende Strukturen, die zur verbesserten Osteogenese in dreidimensionalen Zellkulturen führen, wichtig für die Weiterentwicklung des osteogenen Tissue Engineering. Durch gezieltes Ansprechen verantwortlicher Signalwege kann

vermutlich die Zellkultur verbessert, Zeit gespart und dam it letztendlich die Therapie von Knochendefekten optimiert werden. Dabei darf jedoch nicht aus den Augen verloren werden, dass durch die unzähligen Variationsmöglichkeiten der Einzelkomponenten ein perfektes TEKT nur sehr schwer erreichbar ist. Irgendwann müssen die aktuell besten Einzelkomponenten für ein TEKT identifiziert und der nächste Schritt hin zur Anwendung im Patienten unternommen werden.

Danksagung

Mein außerordentlicher Dank gilt Herrn PD Dr. Dr. Handschel für die Betreuung dieser Arbeit, die ohne sein Engagement nicht möglich gewesen wäre. Er unterstützte mich mit vielen Tipps und Anregungen und hatte immer ein offenes Ohr für meine Fragen. Außerdem möchte ich mich für das große Vertrauen und die gewährten Freiheiten, sowie für seine weitreichende Förderung sehr herzlich bedanken.

Mein besonderer Dank gilt Herrn Prof. Kübler für seine wissenschaftlichen Ratschläge, die Bereitstellung seines Labors, Materialien und Reagenzien sowie für die zwischenzeitliche Finanzierung meiner Stelle.

Bei Herrn Prof. Klein möchte ich mich herzlich für die Hilfe beim Anerkennungsverfahren meines FH-Studiums und für die Betreuung und Begutachtung meiner Arbeit bedanken.

Frau Dr. Berr danke ich für ihre wissenschaftliche Unterstützung bei Planung, Durchführung und Auswertung von Versuchen sowie für die Hilfe bei der Anfertigung von Publikationen.

Ich bedanke mich bei den Herren Prof. Wiesmann, Prof. Meyer und Dr. Dr. Naujoks für ihre Vorarbeiten bei der Mikrogewebe Technik. Bei Prof. Meyer und Dr. Dr. Naujoks bedanke ich mich zusätzlich für ihre wissenschaftlichen Anregungen.

Für die freundschaftliche Arbeitsatmosphäre und ständige Hilfsbereitschaft möchte ich bei meinen Kolleginnen Andrea Hassel, Marianne Hölbling und Dorothee Köhler, sowie meiner ehemaligen Kollegin Julia Hartmann und meinem ehemaligen Kollegen Michael Hentschel bedanken.

Danke an alle Mitarbeiter in der Klinik für Kiefer- und Plastische Gesichtschirurgie.

Ich bedanke mich bei Frau Prof. Kögler für die Bereitstellung der USSC, für die Zusammenarbeit in den DFG Projekten und für ihre wissenschaftlichen Ratschläge.

Weiterhin danke ich meinen Eltern für all Das, was mich zu einem Menschen mit Vertrauen in seine eigenen Stärken und Fähigkeiten gemacht hat und für alle Eigenschaften die sie mir mitgegeben haben, welche mich zur Erstellung dieser Arbeit befähigt haben.

Abschließend möchte ich mich mit vollem Herzen bei meiner Frau und meinen Kindern für ihre Geduld und Unterstützung in jeglicher Hinsicht bedanken.

Eidesstattliche Erklärung

Ich versichere an Eides statt, dass die Dissertation von mir selbstständig ohne unzulässige fremde Hilfe unter Betrachtung der „Grundsätze zur Sicherung guter wissenschaftlicher Praxis der Heinrich-Heine Universität Düsseldorf“ erstellt worden ist. Diese Dissertation wurde in der vorgelegten oder einer ähnlichen Form noch bei keiner anderen Institution eingereicht und es wurden bisher keine erfolglosen Promotionsversuche von mir unternommen.

Lebenslauf

Fabian Langenbach

Addresse: Siegburger Str. 43,
53757 Sankt Augustin

Geburtsort und -Tag: 26.12.1982 in Siegburg, Deutschland

Familienstatus: Verheiratet, zwei Kinder (geboren Juli 2009 und Juni 2011)

Nationalität: Deutsch

WISSENSCHAFTLICHE KARRIERE:

Promotionsstudent der Mathematisch-Naturwissenschaftlichen-Fakultät, Fach Biology, Heinrich-Heine Universität Düsseldorf	**seit Apr. 2009**
Wissenschaftlicher Mitarbeiter der Klinik für Kiefer und Plastische Gesichtschirurgie, Uniklinik Düsseldorf	**seit Mär. 2008**
Abschluss zum **Master of Science in Biology with Biomedical Sciences** (Note: 1,5) Thema der **Master These:** "Adipose Tissue Derived Stromal Cells Contribute Myogenic Proteins to Myotubes" (Note: 1,0) Erstellt am Universitätsklinikum Bonn, Physiologie II, Prof. Dr. med. Anton Wernig (Betreuer)	**Feb. 2008**
Abschluss zum **Bachelor of Science in Biology** (Note: 1,7) Thema der **Bachelor These:** "Toxicology of Environmental Samples from the Perspective of Biodefense" (Note: 1,0). Erstellt am Deutschen Zentrum für Luft und Raumfahrt, Abteilung für Luft und Raumfahrtmedizin Dr. Christa Baumstark-Khan (Betreuerin)	**Jul. 2005**
Auslandsstudium: Høgskolen i Nord Trøndelag", Levanger, Norwegen	**Jul. – Dez. 2004**
Abschluss zum **Biologisch-Technischen Assistenten (BTA),** Rheinischen Akademie e.V. Köln (Note: 2,1)	**Jun. 2002**

JOBS

Wissenschaftliche Hilfskraft bei Caesar (Center of Advanced European Study and Research), Dentale Zellbiologie, Bonn	**Jan. 2006 – Feb. 2007**
Wissenschaftliche Hilfskraft in der Biochemie der FH Bonn-Rhein-Sieg	**Sep. 2005 – Jan. 2006**

EHRENÄMTER

Sachkundiger Bürger im Jugendhilfeausschuss der Stadt Sankt Augustin	**seit Sep 2010**
Sachkundiger Bürger im Ausschuss für Schule, Bildung und Weiterbildung, der Stadt Sankt Augustin	**Sep. 2009 – Aug. 2010**

WEITERBILDUNGEN:

Antrags- und Projektmanagement	**Apr. 2011**
Tierversuchskurs	**Jan. 2009**
Gruppenleiterkurs: Gentechnisches Arbeiten in Gentechnischen Anlagen	**Nov. 2008**
Grundlagen Marketing und Management	**Jul. 2006**

PRÄSENTATIONEN:

„Evaluation der osteogenen Differenzierung von Mikromassen aus Nabelschnurstammzellen". **Langenbach F**, Naujoks C, Depprich R, Handschel J; 21. Mai 2009; *59. Jahrestagung der Arbeitsgemeinschaft für Kieferchirurgie*, Wiesbaden, Deutschland

"Cells grow out of osteogenic differentiated cellular-microspheres". **Langenbach F**, Naujoks C, Depprich R, Kübler N, Handschel J; 24.Mai – 27. Mai, 2009; *19th International Conference on Oral and Maxillofacial Surgery*, Shanghai, China

„Charakterisierung osteogen differenzierter Mikromassen aus pluripotenten Stammzellen". **Langenbach F**, Naujoks C, Kersten-Thiele P, Kübler, Depprich, Handschel J; 03. – 06.Juni, 2009; 59. *Kongress der Deutschen Gesellschaft für Mund- Kiefer- und Gesichtschirurgie Wien, Österreich*

„Evaluierung der osteogenen Potenz von zellulären Mikromassen in Kombination mit einem klinischen Knochenersatzmaterial". **Langenbach F**, Laser A, Naujoks C, Depprich R, Kübler N, Handschel J: 13.-14. Mai, 2010; *60. Jahrestagung der Arbeitsgemeinschaft für Kieferchirurgie*, Bad Homburg, Deutschland

"Strong upregulation of osteogenic genes in stem cell microspheres compared to differentiated monolayer cultures and superior cell loading efficiency of biomaterials by inoculation with microspheres". **Langenbach F**, Naujoks C, Kelz M, Kübler NR, Kögler G, Handschel J; 13. – 17. September 2010; *20th Congress for the European Association of Cranio-Maxillo-Facial Surgery,* Brügge, Belgien

„Unterschiede im Gentranskriptionsprofil zwischen 2D- und 3D-Zellkulturen während der osteogenen Differenzierung". **Langenbach F**, Naujoks C, Berr K, Depprich R, Kübler NR, Handschel J; 02. – 03. Juni, 2011; *61. Jahrestagung der Arbeitsgemeinschaft für Kieferchirurgie*, Bad Homburg, Deutschland

POSTER:

"Effects of Combustion Generated Nanoparticles on Bacterial SOS Response Controlled Gene Expression". **Langenbach F**, Huxoll R, Baumstark-Khan C, et al.; 1. – 4. May 2005 *Nanoparticle Workshop: Combustion Generated Nanoparticles and Their Health Effects: Molecular and Cellular Basics*, Bonn, Deutschland

„Comparative Gene-Expression-Analysis between Monolayer-Cultures and 3D Microsphere Cultures of Human Unrestricted Somatic Stem Cells during Osteogenesis". **Langenbach F**, Naujoks C, Kübler NR, Handschel J; 11. – 14. Juni, 2010 *3rd International Congress on Stem Cells and Tissue Formation,* Dresden, Deutschland

"Differences in the gene transcription profiles of monolayer cultures and 3D microsphere-cultures of human unrestricted somatic stem cells (USSC) during osteogenesis". **Langenbach F**, Naujoks C, Berr K, , Kübler NR, Handschel J; 12. – 15. Oktober, 2011; *Bone-Tec 2011 International Bone Tissue Engineering Congress,* Hannover, Deutschland